N° :______

THESE DE DOCTORAT

DEVELOPMENT AND RESISTANCE TO FIRE OF INTUMESCENT SILICONE BASED COATING - FIRE PROTECTION OF STEEL IN SIMULATED FIRE

Présentée et soutenue publiquement à

L'UNIVERSITE DES SCIENCES ET TECHNOLOGIES DE LILLE

pour obtenir le grade de

DOCTEUR

Spécialité : Molécule et Matière Condensée

par

Bastien Gardelle

Ingénieur ENSCL

Thèse dirigée par

Prof. Serge Bourbigot et Prof. Sophie Duquesne

Soutenue le 29 Octobre 2013 devant la Commission d'Examen composée de :

Dir. Recherche CNRS J.M Lefebvre	Université Lille 1	Président du jury
Prof. G. Camino	Politecnico di Torino	Rapporteur
Dr. Habil. B. Schartel	BAM	Rapporteur
Dr. P. Vandereecken	Dow Corning	Examinateur
Prof. S. Bourbigot	ENSCL	Directeur de thèse
Prof. S. Duquesne	ENSCL	Co-directeur de thèse

AKNOWLEDGMENTS

The work presented in this manuscript has been carried out in the laboratory UMET headed by Alexandre Legris in the team "Ingénierie des Systèmes Polymères" managed by Dr. Jean-Marc Lefebvre. I would like to first thank them for welcoming me and for giving me the opportunity to work on this interesting and innovative project.

I specially would like to express my gratitude to Prof. Sophie Duquesne and Prof. Serge Bourbigot who supervised me during these three years. They provided me with an unbelievable scientific and moral support that I could ever have desired. Their expertise, their patience and guidance experienced during the whole period of the PhD, combined with their exceptional continuous and stimulating participation, kept me highly motivated and enthusiastic.

During the entire PhD, I was able to take advantage of a partnership with Dow Corning company. I particularly would like to acknowledge Dr.Patrick Vandereecken for generous scientific and technical contribution in the field of silicone.

I would like to acknowledge Prof. Jean Marc Lefebvre who has agreed to chair this jury as well as Prof. Giovanni Camino and Dr. Bernhard Schartel for having accepted to take of their time and to bring their expertise as examiners to assess this manuscript.

I extend these thanks to the team of the NMR reseach centre of Lille 1, especially Bertrand Revel, Bertrand Doumert and Grégory Tricot for their time and patience training me on the NMR techniques and for their kindness.

I also sincerely thank all the of the current and former member of the laboratory UMET-ISP for their help and friendship over the last three years. I especially would like to thank Pierre for his impressive technical support and his "personality". To my labmates whom I have become friendly Antoine, Andréa, Clémence, Aurore, Fabienne, Brigitte, Mathieu, Carmen, Gaëlle, Michel, Séverine, Mathilde, Maude, Ghassan, Marion, Nicolas, Marianne, Franck, Gwenaëlle, Pauline.

Finally, I would like to thank my family, my mother, my father, my sister, and my brother for their invaluable support as well as my friends, especially Anne-Lise.

Contents

List of Figures

List of Tables

Abbreviations

C30B	Modified organoclay
CP	Cross-polarization
DTG	Derivative thermogravimetric
EG	Expandable Graphite
EPMA	Electron probe micro analysis
FTIR	Fourier Transformed Infra-Red spectroscopy
GCC	Ground calcium carbonate
MAS	Magic Angle Spinning
NMR	Nuclear Magnetic Resonance
PhS	Phenyl silicone
SEM	Scanning electron microscopy
RTV	Room temperature vulcanized
TEM	Transmission electron microscopy
TGA	Thermogravimetric analysis
TGA-FTIR	Thermogravimetric analysis - Fourier transformation infrared
WAXS	Wide-angle x-ray scattering
XRD	X-ray Diffraction
XRF	X-ray fluorescence

General Introduction

Nowadays, the material mainly used in building is steel. However, structural steel loses a significant part of its load carrying ability when its temperature exceeds 500°C. In case of fire prevention of the structural collapse of a building is paramount to ensure the safe evacuation of people, and is a prime requirement of building regulations in many countries. To meet those requirement the development of fire protective systems are thus required.

Intumescent coatings constitute one of the oldest and one of the most efficient ways to protect a substrate against fire. They have the ability to expand when heated upon a critical temperature leading to the formation of thick insulative foam limiting heat transfer between the flame and the substrate. These coatings are designed to perform under severe conditions and to maintain the substrate integrity when exposed to high temperature.

Most of intumescent coatings are organic based and therefore exhibit some disadvantages. The main ones are their low weatherability properties and a potential toxicity and opacity of smokes emitted during their thermal degradation. Silicone resins are known to exhibit excellent ageing properties and low toxicity and opacity of smokes. Even if, the use of pure silicone as protective coating against fire has never been studied, these resins seem to be good candidates for the protection of steel structures against fire. This approach will be considered in this work.

The aim of this project is thus to develop an intumescent silicone based coating for the fire protection of substrates that could be used in the building industry.

This manuscript will be divided into four parts.

The **first chapter of this PhD** reviews regulation and standards concerning the protection of metallic structures, and describes the different passive fireproofing materials existing for steel protection. Then, the development of innovative coatings for the protection of steel against fire will be discussed.

The **second chapter** deals with the development of silicone intumescent coatings based either on high cross-linked silicon resin or on room temperature vulcanized (RTV) silicone rubber. Both coatings exhibit drawbacks, such as low viscosity at high temperature for the first one and low expansion behavior for the second one.

To overcome those drawbacks, the **third chapter** is devoted to the investigation of the resistance to fire on steel of RTV silicone rubber containing expandable graphite in fire scenarios. Even if those systems exhibit high fire performance, the mechanical properties of the char is too low to apply thick silicone intumescent coating.

That is why in the **fourth chapter,** the development of high cross-linked RTV silicone rubber added with expandable graphite for the fire protection of steel in hydrocarbon fire scenarios, using thick silicone coatings, is described.

The manuscript is based on the following papers. As a consequence, all the details concerning the experimental techniques will not be described. Moreover, only, the main results will be presented in this manuscript. If you need further information please refer to the papers reported in Appendix 2.

- Patent: PROTECTING SUBSTRATES AGAINST DAMAGE BY FIRE – Inventors: B.Gardelle, S.Duquesne, P.Vandereecken and S.Bourbigot - filed in March 2012 - In Revision
- B. Gardelle, S. Duquesne, V. Rerat, S. Bourbigot, Thermal degradation and fire performances of intumescent silicone based coating, **Polymer for Advanced Technologies -** Vol 24, p62-69, (2013)
- B. Gardelle, S. Duquesne, P. Vandereecken, S. Bourbigot, Fire performance of curable silicone based coatings, **ACS book Fire and Polymers VI: New Advances in Flame Retardant Chemistry and Science -** Vol 1118, p205-221, 2012
- B. Gardelle, S. Duquesne, P. Vandereecken, S. Bourbigot, Characterization of the carbonization process of expandable graphite/silicone formulations in a simulated fire, **Polymer Degradation and Stability -** Vol 98, p1052-1063, May 2013
- B. Gardelle, S. Duquesne, P. Vandereecken, S. Bourbigot, Mode of action of organoclay on the fire performance of intumescent silicone based coating, **Progress organic coating,** Accepted - 2013
- B. Gardelle, S. Duquesne, P. Vandereecken, S.Bellayer, S. Bourbigot, Resistance to fire of curable silicone/Expandable graphite based coating: effect of the catalyst. **European Polymer Journal,** In press - 2013
- S.Bourbigot, B.Gardelle, S.Duquesne - Intumescent silicone-based coatings for the fire protection of carbon fiber reinforced composites - **International Association for Fire Safety Science - Submitted -** 2013.

N.B.: The silicone matrix used and experimental techniques (not presented in the papers) are summarized in the Appendix 1.

Chapter I: State of the art

I-1 Introduction

In recent decades, disastrous accidents caused by fire have reminded people of its risks in industrial buildings and equipment. The aim of this chapter is to make an overview of the different fire scenarios, of the nature of substrates which have to be protected and the ways to protect them.

As we will see in this first part, among the different fire protection systems, intumescent coatings appear to be attractive candidates. Thus, in a second part of this chapter, intumescence process will be fully investigated, from its mode of action to its critical parameters and its limitations. This part will show that the main limitations of intumescent paints are due to their organic characters. As a consequence, in the last part, a discussion on the use of silicone resins as an alternative to organic paints for fire protection will be done.

I-2 Passive Fire Protection

Resistance to fire or passive fire protection evaluates the capacity of a material to keep its integrity and/or its functionality in a fire scenario. In most of the cases, the materials used in building are steel, wood or composites. On all those substrates, passive fire protection systems are based on insulative systems designed to prevent heat transfer from the fire to the structure being protected. To apply a coating, called fire protective coating, is the easiest way to improve fire resistance. This work focuses on the steel fire protection.

I-2.1 Steel fire protection

Steel is a material used worldwide in the construction of bridges or buildings and is present on several markets such as marine and offshore platforms. Structural steel is usually the first choice of architects and engineers for framework of single and multi-store buildings. It offers maximum design flexibility and is widely used as an architectural feature in its own right. It has the advantage of being a noncombustible material. However, steel exhibits high heat conductivity and in case of fire, temperature raises up rapidly through the structure. Consequently, both the yield stress and elastic modulus of steel, the two most important material properties in determining the load-carrying capacity, decrease considerably with increasing temperatures (Figure 1)[1].

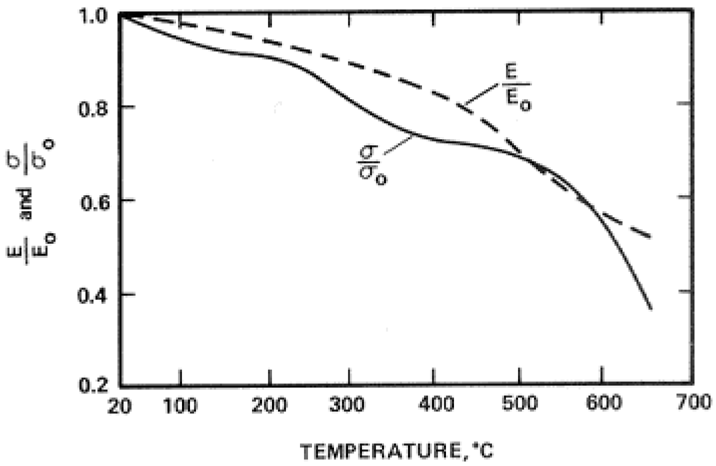

Figure 1 : Effect of temperature on elastic modulus (E) and yield stress (σ) of steel with E0 and σ0 the modulus of elasticity and the yield stress at ambient temperature

Steel begins to lose most of its structural properties between 470 and 500°C[2]. Around 600°C, the yield stress and elastic modulus have fallen by at least 40% compared to the room temperature values, which could cause the collapse of the structure. It is because of this relatively low failure temperature that the protection of metallic materials against fire is an important issue in the construction industry. Indeed, prevention of the structural collapse of the building is paramount to ensure the safe evacuation of people from the building, and is a requirement of building regulations in many countries.

These regulations also depend on the size of the surface to be protected. Small building, from which occupants can escape rapidly in a case of fire, may not require any special protection against collapse. In larger building, the time required for the complete evacuation of occupants is longer. In this case, collapse has to be delayed by providing a higher level of structural fire protection in order to ensure the safety of occupants. In particular, the collapse of the twin towers in New York, on the 11th September 2001, is one of the most important accidents demonstrating the importance of the fire protection of steel structures. Indeed, it was demonstrated that the towers did not collapse because of the impact of the planes, but because of the progressive heating of the steel which was not sufficiently protected against fire and which reached its failure temperature rapidly[3]. This and other tragic disasters caused by fire have made fire protection standards and regulation more and more severe.

Fire protective coatings target performances can be classified in two main categories. The first one, measured in terms of time (1h, 2h) consists in the increase of the fire resistance, as defined by ASTM E119 for building or by ASTM E1529 or UL1709 for hydrocarbon fire tests. The second category of performance is the reducing of the flame spread of the combustible substrate, such as wood and composite, as measured by the flame spread index ASTM E84 in the USA[4].

In the case of steel protection, required levels of protection are normally specified in terms of time and temperature on the basis of one or more criteria. It can vary from few minutes for airplane applications for example to several hours for building applications. The duration is established by a time rating which is determined by testing, in accordance with an approved standard. Some of the more commonly specified test standards[5] are listed in Table 1 and presented in (Figure 2).

Table 1 : Usual test standards established by differents countries

Standard	Country	Dedscription
ASTM E119	USA	Cellulosic or wood fire, used since 1903
ISO 834 (standard time/temp.curve)	International	Cellulosic or wood fire (similar to ASTME119)
DIN 4102	Germany	Cellulosic or wood fire (similar to ASTME119)
BS 476	U.K	Hydrocarbon fire
UL1709	USA	Hydrocarbon fire; developed in the early 1970's

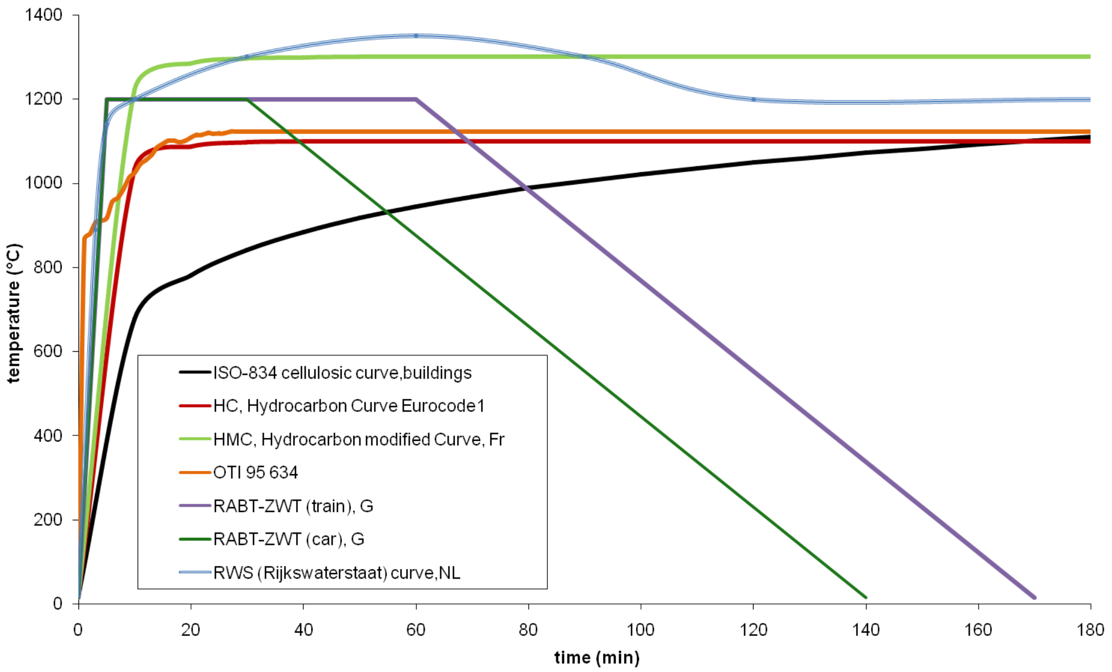

Figure 2: Standard fire tests curves

The cellulosic fire curve (ISO834 or ASTM E119) simulates the rate of temperature increase observed in a residential building fire where the main sources of combustion fuel (such as papers and furniture) are cellulosic in nature. This fire curve is characterized by a relatively slow temperature rise to around 927 °C in one hour. However, this slow heating rate is not relevant for hydrocarbon fire scenario. Indeed, the burning rates for certain material such as petrol or chemical are well in excess than those of cellulosic materials. That is why hydrocarbon fire scenario (B5476 and UL1709) has been developed. The hydrocarbon test curve mimics the rapid temperature rise seen when a hydrocarbon fuel, such as oil, burns. The temperature reaches 1100°C in 5 minutes. The UL1709 hydrocarbon fire test curve was developed by the Mobil Company in the early 1970's and adopted by a number of organizations and in particular by the Underwriters laboratories[6].

In all of these different fire scenarios, the critical temperature is an essential parameter. Critical temperature of steel, for example, is defined as the temperature at which only 60% of the original strength remains, which corresponds to its imminent failure under full design loads. For regular reinforcing steel, the temperature of 500°C has been officially adopted as a standard for normally loaded structure components. This temperature is of 400°C for highly loaded system, since the steel loses a substantial proportion of its strength at above 500°C. Consideration must be given to the whole range of condition in which the fire protection is required to resist during its service life: weather condition, ultraviolet rays, corrosive environment and physical-mechanical service conditions. In order to comply with this severe fire regulation, different passive fire proofing materials and fire stops barrier have been developed and will be discussed in the following section.

I-2.2 Passive Fireproofing Materials

Traditional fireproofing coatings are cementitious coatings, fibrous materials, fire protective panels, ceramic coatings and intumescent coatings[7, 8].

Cementitious coatings are based on Portland cement, magnesium oxychloride cement, vermiculite, gypsum, and other minerals[4]. Fibrous fillers, supplementary binders and density or rheology controlling additives are typically mixed with water on site and applied by spraying during steel construction at thicknesses of 3 cm or more. Some of these coatings can be applied onto flammable substrates by the use of rollers and/or a moving belt. These coatings can provide fire protection from one-half to several hours by water release and thermal insulation effects. They are low cost and easy to apply, and some are resistant to weather exposure. However, because of their weight, thickness and poor esthetics, they limit architectural design. Thus, building designers avoid them for visually exposed steel. On the other hand, they may also be dislodged in a violent fire.

On the other hand, fibrous materials such as boars or blankets of mineral wool and ceramics fibers can also be used. They are mainly used as passive fireproofing systems when thermal insulation is an additional requirement. Inorganic binders that do not burn out during the initial stages of the fire are recommended. As ceramic fiber is more expensive than mineral wool, they are often used in combination. However, the main drawback is that fibrous materials easily absorb water and that is why they are only recommended for internal use except where they can be effectively clad with metal sheeting.

Fire protective panels are produced with various types of materials from different fire resistant classes. Panels may consist of a metallic cladding, often stainless steel, cementitious boards... These panels may resist cellulosic or hydrocarbon fires as required. They are generally fixed to structural members with steel binding wire or bolted to supported frame (Figure 3). However, to reach high insulative properties, very thick material is used. Consequently, it increases significantly the weight of the structure and modifies its architecture.

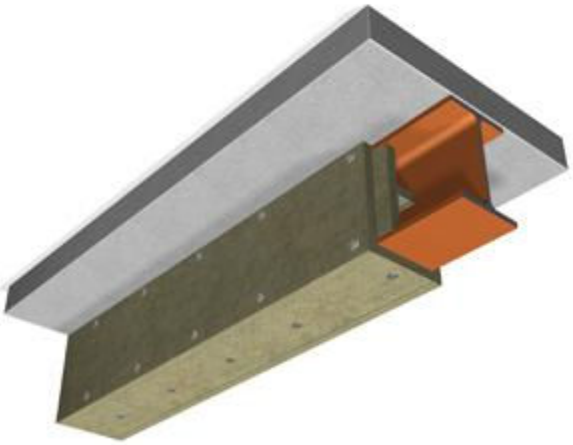

Figure 3: Fire protective panels fixed on steel structure[9]

Some coatings, such as Al_2O_3–TiO_2, ZrO_2, and other ceramic thermal barrier coatings are used, for example in aerospace, electronics and biomedical applications, and may be applied usually to metal substrates by plasma/high-velocity oxygen flame spraying [10]. Recent research discloses a related ceramifying coating material, suitable for protecting cables at high temperature, using an inorganic phosphate, which is exemplified by ammonium polyphosphate, as part of the ceramifying system along with a mineral silicate exemplified by talc, mica, or clay[11]. On the other hand, we recently reported the use of ceramic precursor - polysilazane - based coating for steel protection against fire. The purpose of this work was to form a ceramic of low thermal conductivity at high temperature which could protect a substrate in fire scenario[12]. The performance of the polysilazane coating was improved incorporating a fire retardant, namely aluminium trihydroxide, in the formulation but the performance of such coating was limited compared to commercial coating for the fire protection.

Finally, intumescent materials can also be used. They are classified as either thick or thin film intumescent coatings. Depending on the fire scenario - hydrocarbon or cellulosic - one kind of intumescent coating has to be used. For cellulosic fire (ISO834), thin intumescent coating will be used. These films were introduced as early as the 1930's and are generally available as solvent or water based systems. They typically use thermoplastic acrylic based resin system, they respond rapidly and intumesce quickly when exposed to a cellulosic fire environment. More than one hour protection can be achieved using between 1 and 3 mm thick coating. Coatings protecting against hydrocarbon fires (UL1709) are typically two-component (usually epoxy) solvent-free systems applied at 3-5 mm per coat often through separate heated lines with an in-line static mixer at the spray tip. These coatings are usually used in offshore platform and so, are exposed to corrosive environment. The steel surface is prepared by an abrasive blast, and then an anticorrosive primer must be applied. This solution for the fire protection exhibits several advantages such as a low weight, a possibility to be applied indoor or outdoor, a low thickness which enables to preserve the architecture of the structure. Thus, it appears as an interesting approach and that is why it has been used in this work.

The following part will thus describe in details what is an intumescent coating and the limitation of conventional intumescent coatings.

I-3 Fire protection based on Intumescent coating

I-3.1 The intumescent concept

In 1971, Vandersall[13] published a paper describing the history and critical element of intumescent coatings. This concept is well described in the literature and can be simply resumed in the process below (Figure 4).

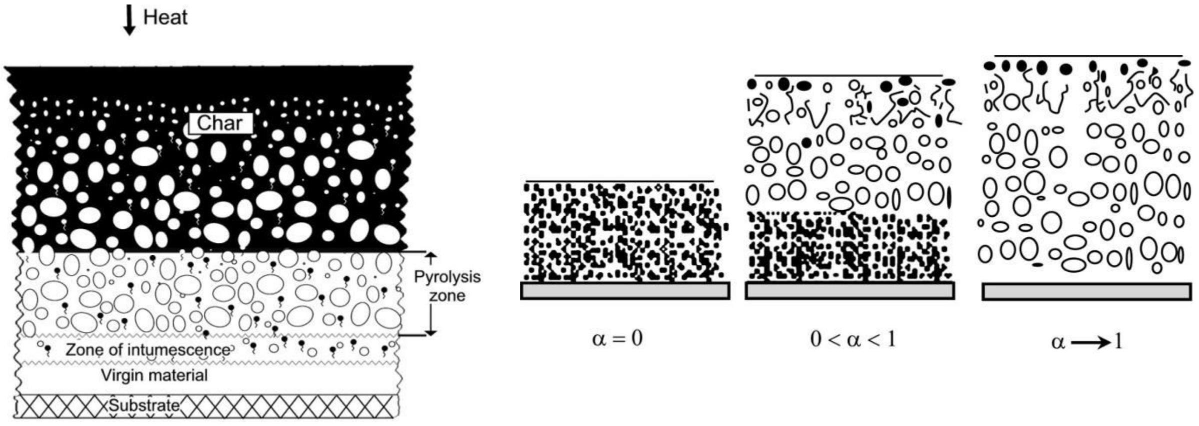

(a)

(b)

Figure 4: Schematic view of an intumescent coating with its different zones (a) and its development as a function of the conversion degree α (b)

When exposed to high temperature, these coatings have the properties to swell to thick insulative foam[4, 13]. The intumescence process results from a combination of charring and foaming at the surface of the substrate. The charred layer acts thus as a physical barrier which slows down heat and mass transfer between gas and condensed phase.

The formation of an intumescent char is a complicated process involving several critical aspects: rheology (expansion phase, viscoelasticity of char), chemistry (charring) and thermophysics (limitation of heat and mass transfer)[14]. Indeed, at high temperature, the surface of the material begins to melt and is converted into a highly viscous liquid. Simultaneously, endothermic reactions occur leading to the release of gases which are trapped in this viscous fluid. The resulting material is composed of high expanded foam sometimes up to many times its original thickness. This expanded carbonaceous char acts as an insulative barrier between the fire and the substrate and so protects it[14-16].

Figure 5 illustrates a typical char obtained from an intumescent coating after fire exposure. It consists in a multi-cellular layer. The size and size distribution of the alveolus play an active role in the performance of the coating[4, 17]. This layer of char absorbs a large part of the heat generated by the fire, thus maintaining the temperature of the substrate below the critical limit for a certain period of time.

Figure 5 : Typical char obtained at high temperature (expansion about 2800%)

To obtain intumescence phenomenon, coatings are mostly based on the combination of a char-forming material, an acid source and a blowing agent embedded in a binder resin[4, 18]:

- Char forming material is a carbon-rich polyhydric compound. Polyhydric alcohols are mostly used. The number of carbon will influence the amount of char formed whereas the number of hydroxyls will determine the rate of char formation.
- The acid source is an inorganic acid, either free but more often formed in situ from precursor upon heating.
- Blowing agents are usually halogenated or nitrogenated compounds, which release large quantities of non-flammable gases in a given range of temperature.

Examples of the components from the different categories are shown in Table 2 [19, 20]

Table 2: Examples of components playing a role in intumescent coatings[19, 20]

Inorganic acid source	Carbonisation compounds	Foaming compounds
-Acids (phosphoric, boric, sulphuric) -Ammonium salts (phosphate, polyphosphate) -Melamine phosphate or polyphosphate -Organophosphorous compounds (alkyl phosphate, haloalkyl phosphate)	-Starch -Sorbitol -Pentaerythritol -Polyurethane -Phenol-formaldehyde resins	-Chlorinated paraffins -Melamine

Some compounds can play several roles during the intumescence process. For example, melamine phosphate can play the role of blowing agent and acid source.

The presence of each compound in an intumescent formulation does not ensure intumescent behavior of a material. Indeed, the choice of the matrix is also important. In particular, its thermal degradation pathway and its rheological behavior at high temperature are decisive[21]. In fact, a series of chemical and physical processes must occur in an appropriate sequence, while the temperature increases, to produce the intumescent phenomenon.

Numerous papers describe the chemical mechanism leading to the intumescence phenomenon[13, 14, 19]. They show that, at first, the acid source breaks down to yield a mineral acid. Then, this acid takes part in the dehydration of the carbonization agent to yield the carbon char, and finally the blowing agent decomposes to yield gaseous products. The latter cause the char to swell and hence provide an insulating multicellular protective layer. This shield limits the heat transfer from the substrate to the heat source.

There is potentially a large choice of compounds from which formulating intumescent systems. However, only a few compounds are used in practice and they have mostly been selected empirically. The inorganic acid is very often phosphoric acid in the form of an ammonium salt (APP – ammonium polyphosphate or MPP, Melamine Polyphosphate). Recent study highlights the benefits to use boric acid and ammonium polyphosphate to improve fire performance of intumescent coating, explained by the formation of a borophosphate at high temperature[22]. Pentaerythritol (PER) and its oligomers are traditional polyhydric compounds while polyurethane or suitable epoxy resins are examples of char precursors. Melamine (Mel) is commonly used as blowing agents. All of the ingredients are important because they interact with each other to achieve the desired overall performance.

Other than this traditional APP/Mel/PER coating, expandable graphite (EG) appears to be a 'particular' intumescent additive known to impart fire retardancy to various materials[23]. EG is a graphite intercalation compound in which sulfuric acid and/or nitric acid are inserted between the carbon layers (Figure 6a). When exposed to heat, exfoliation of the graphite occurs, i.e. expansion along c-axis of the crystal structure by about hundred times. The material generated in that way is a puffed-up material of low density with a ''worm'' like structure (Figure 6b).

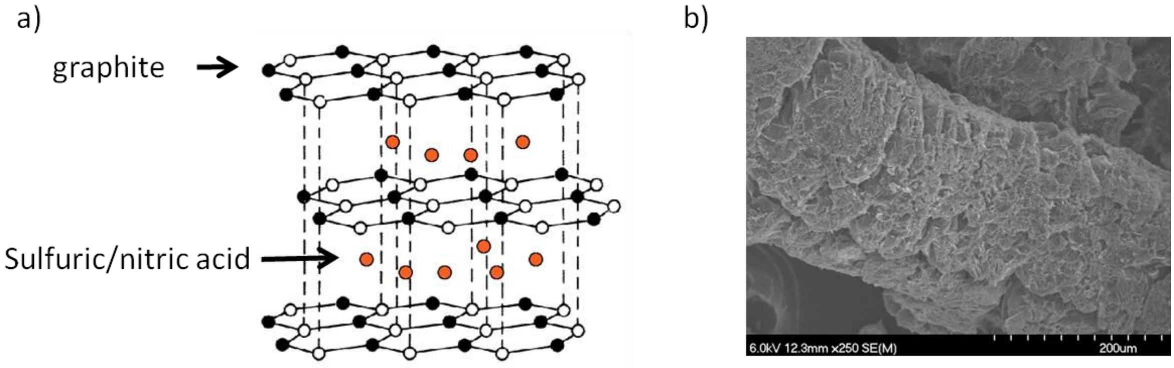

Figure 6 : Structure of EG and b) SEM pictures of worms from EG

For recent decades, more and more papers have been dealing with the use of expandable graphite in intumescent based coatings. This particular intumescent additive increases the fire performance and anti-oxidant properties of the coatings[4, 24, 25]. However, in the above mentioned studies, expandable graphite is incorporated into complex organic intumescent based formulations. It is noteworthy that in those organic intumescent based coating, EG decreases considerably the cohesion of the char[25] which is one of the key parameters for intumescent coating to ensure high insulative properties.

As described previously, intumescent coating acts as a heat barrier limiting the heat transfer between the fire and the substrate. Several physical parameters have to be taken into account to develop efficient intumescent coating and to explain its mode of action. The physical properties are therefore described in the next section.

I-3.2 Physical properties of intumescent coatings

In order to determine the parameters governing the fire performance of an intumescent structure, we firstly consider an expanded structure exposed to a heat flux $\dot{q}''$ (Figure 7) coated on steel plate (thickness e).

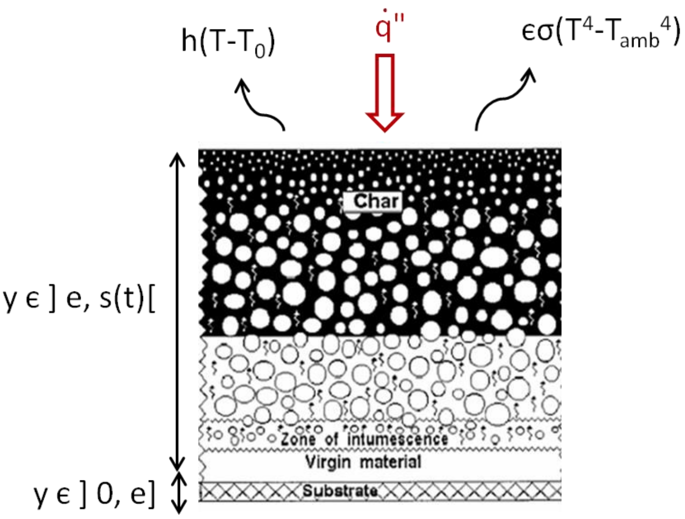

Figure 7: Schematic expanded structure exposed to an external heat flux

The effective flux received by the material and the heat diffusion in the material are respectively described by the equation 1 and 2.

$$\dot{q}''_{eff} = A\dot{q}'' + h(T_{inf} - T) + \epsilon\sigma(T^4_{amb} - T^4) \qquad \text{Equation 1}$$

$$y \in]e, s(t)[, \rho c_p \frac{\partial T}{\partial t} = \nabla.(k\nabla T) + Q \qquad \text{Equation 2}$$

In equation 1, A is the absorptivity assuming to be 1, h is the convective coefficient, T_{inf} is the temperature of surrounding air (300 K), T_{amb} is the temperature of the surrounding (300 K), ϵ is the emissivity (0.9) and σ is the Stephan - Boltzmann constant.

In equation 2, s(t) describes the swelling of the coating depending on the time, c_p is the heat capacity, ρ is the density, k is the thermal conductivity, T is the temperature and t is the time. During the intumescence process and the degradation of the material, heterogeneous reactions (solid/gas), involving the destruction of the condensed phase with the evolution of gases and formation of char occur. It corresponds to the source term Q which depends on the degradation kinetics parameters and on the heat of decomposition of the intumescent material.

According to those equations, the most important parameters of the expanded char affecting its thermal insulation performance seem to be its ability to **expand** and its thermo physical properties such as **thermal conductivity and stability**. Moreover, the mechanical properties of the intumescent char is also a parameter to be taken into account. Indeed, to ensure good insulative properties, the expanded structure has to exhibit good **mechanical properties** and adhesion with the substrate to be protected. Those properties are detailed herein after.

I-3.2.1 Mechanical properties of intumescent chars

Mechanical strength of the char is a key parameter to ensure its integrity in case if a fire scenario. This factor is significant because in such a scenario, char destruction can proceed not only by means of ablation and heterogeneous surface burning, but also by means of an external influence such as wind, mechanical action of the fire or convective air flows.

Mechanical properties of intumescent chars depend both on the chemical structure and on the porosity of the char[26]. Moreover, physical structure data (such as thickness of the walls in the char cap, micro-density of the char) have also to be taken into account. Depending on the fire scenario, mechanical properties of the intumescent char is the main parameter to take into consideration. In hydrocarbon fire scenario, this property is more important since the conditions are more severe than in cellulosic fire scenario.

To ensure the good cohesion of the char, several additives can be incorporated to the intumescent formulation such as mineral fibres[16], organo-clay[27, 28], ceramic precursor... These compounds might react with the inorganic acid source to form a dense ceramic on the top of the intumescent char[22].

On the other hand, different methods have been developed to evaluate the mechanical properties of intumescent char. Reshetnikov et al. used a "Structurometer ST-1", developed at the Moscow State Food Academy, to measure the force required to destroy a char[26]. The samples were first pyrolysed and then a destructive force was applied to the sample. It was concluded that one of the main factors influencing the mechanical properties is the char porosity: the smaller the pore size the better the char strength. However, the mechanical properties of the char are investigated at ambient temperature which may not be representative of its behaviour at high temperature. A similar method was developed in our laboratory at Lille University[29] in recent years, using Thermal Scanning Rheometer. The main interest of this approach is that mechanical properties of the char are evaluated at high temperature. However, the measurement cannot be carried out at higher temperature than 500°C due to experimental limitations. A new method was develop during this project to overcome those drawbacks and will be detailed further in the manuscript.

I-3.2.2 Thermal conductivity and diffusivity

According to the equation 1, heat conductivity is one of the parameters governing the performance of an expanded structure in terms of insulation.

Very few articles in the literature deal with the measurement of thermal conductivity at high temperature of material. J.E.J Stagg determined thermal conductivities of intumescent char at high temperature by numerical simulation[17]. He evaluated thermal conductivity from ambient temperature to 1200K and its dependence with the porosity of the material. He calculated that thermal conductivity of intumescent char material varies from 0.1 W/m.K. to 0.4 W/m.K. from ambient temperature to 600°C, suggesting the heat insulative properties of these materials. He showed that the thermal conductivity of an intumescent structure is directly linked to its morphology. Indeed, at elevated temperature, radiation across pores causes significant augmentation of the apparent thermal conductivity. If the pore size is relatively small compared to the length scale on which temperature varies throughout the char and since the interior of the pore is a blackbody, then it may readily be shown that the additional heat flux due to radiated heat is given approximately by $4\varphi\delta\sigma\frac{\partial T}{\partial y}$, where δ is the pore size, φ is the porosity, σ is the Stefan–Boltzmann constant and $\frac{\partial T}{\partial y}$ is the temperature gradient in the direction of heat transfer. If k is the effective thermal conductivity without radiation enhancement, then the additional radiative heat flux may be conflated into a total effective thermal conductivity, given approximately by the Equation 3:

$$k_{tot} = k + 4\varphi\delta\sigma T^3 \qquad \text{Equation 3}$$

This highlights the fact that the char has to be composed of small size and homogenous pores to ensure the lowest thermal conductivity at high temperature. However, even if he determined thermal conductivity versus temperature by numerical simulation and found good fit with experimental data obtained on the char (after expansion), all the data are obtained on an expanded structure and not during the expansion of the material.

On the other hand, the other important parameter when dealing with heat transfer is the thermal diffusivity α (eq. 4) which depends on the thermal conductivity k, the density ρ, and the specific heat capacity c_p.

$$\alpha = \frac{k}{\rho . c_p} \qquad \text{Equation 4}$$

It describes the ability of a material to conduct heat (k) compared to store it ($\rho . c_p$) and must therefore be considered. In a material with high thermal diffusivity, heat moves rapidly through and its insulative properties will thus be decreased.

I-3.2.3 Expansion

Intumescent coatings upon heating swell to a thick insulative foam (with appropriate thermal properties described in the last section) to protect a substrate against fire source. The thickness of this expanded structure has to be taken into account, such as its swelling velocity.

Recently, Bourbigot et al. have demonstrated that the insulative performance of intumescent coating is increased by its high swelling velocity and high expansion[30, 31]. The onset temperature of the swelling process has also to be considered. It has to occur at low temperature.

As a conclusion, several parameters have to be taken into account in order to ensure high insulative properties of an intumescent char. The main ones are: high expansion, high swelling velocity, high mechanical properties and low heat conductivity and diffusivity. To meet all these parameters and thus to ensure high fire performance, classical intumescent paints have very complex formulations. These materials are typically organic-based and therefore present some limitations. This will be discussed in the following part.

I-3.3 Limitation of classical organic intumescent coating

We have shown that depending on the fire scenario, different organic intumescent based coatings are used. One kind of matrix is used for one fire scenario: acrylic for cellulosic, and epoxy for hydrocarbon fire scenario. The intumescent process is mainly due to chemical reaction and viscosity phenomenon occurring during the thermal degradation. The thermal constrain plays therefore an active role on the intumescence development. Depending on the thermal stress and the heating rate, the foam structure and properties are significantly different[32].

Moreover, due to their organic composition, they exhibit some disadvantages. Firstly, these coatings are usually not weatherable[33]. Jimenez et al. studied the ageing of an epoxy intumescent coating, by immersing it for 1 month in water and in salted water. At first, they showed that immersion in distilled water for 1 month implied a slight decrease of the protective properties. At the extreme surface of the coating, APP turns into polyphosphoric acid, which, combined with the mechanical erosion effect of water, is dissolved/detached in water. Secondly, the coatings immersed for 1 month in the salted water bath exhibited very poor protection of the steel plates, and no intumescence was observed. They explain this phenomenon by the migration of sodium and chloride into the matrix. The sodium reacts with the polyphosphates to substitute ammonium species, preventing the release of ammonia during burning and thus preventing the char swelling. The low weatherability of the intumescent coating is due to the presence of ammonium polyphosphate which is used in most commercial intumescent coatings. That is why, for outdoor applications, a protective topcoat is needed.

Secondly, organic additives undergo exothermic decomposition when heated which reduces the thermal insulating value of the system. Moreover, the coating releases organic gases (potentially toxic and opaque) which are undesirable in a closed fire environment[34].

Thirdly, the resulting carbonaceous char in some cases has a low structural integrity (namely in the case of acrylic based system) and the coating cannot withstand the mechanical stress induced by a fire.

Finally, even if the use of intumescence for the fire protection is well known and efficient, it exhibits some drawbacks. That is why some alternatives have to be found and the development of hybrid "organic-inorganic" intumescent coating are more and more studied.

I-4 Resistance to fire of hybrid "organic-inorganic" based coating

For recent decades, some papers have been published on the use of copolymers epoxy-silicone in the field of resistance to fire[16, 35]. Akzo Nobel International Coating company was the first to fill a patent dealing with the use of a copolymer epoxy-siloxane for the fire protection in hydrocarbon fire scenario[36]. They showed that the use of siloxane provides good fire protection and can, in the absence of fibers (such as silicate fibers or carbon fibers), produce chars with better adhesive and cohesive strength than known commercial intumescent coatings. Wang et al[35]. evidenced that the use of the combination of epoxy and self-cross-linked silicone acrylate led to an increase of crosslinking degree of the polymer binder in intumescent coating. This could significantly improve compactness of coating and slow down permeation of water and migration of fire retardant additives, which resulted in an improvement in the corrosion resistance of the coating. The interaction of the fire retardant additives with the mixed binder led to the formation of a foam structure of char layer. Self cross-linked acrylate was beneficial to increase intumescent rate of coating and to form a better foam structure of char layer. Those studies highlight the potential of hybrid "organic-inorganic" coating in the field of fire protection.

However, all these matrices contain a large amount of organic compounds and the limitations concerning smoke opacity and toxicity explained in the last section should be quite similar. Moreover, the intumescent system used is composed of ammonium polyphosphate and therefore could cause the same problem regarding weatherability.

That is why we have selected silicone as resin to develop intumescent coating. Our idea was to develop a coating that, when exposed to fire, leads to the formation of an inorganic expanded structure. In that frame, the use of silicone resin appears to be very interesting since, depending on the conditions, silicone can lead to the formation of silica when degraded.

The following part of this chapter will thus detail the different types and properties of such resins.

I-5 Silicone

I-5.1 Structures and synthesis

Silicones are polymers whose backbones consist of alternating Si-O bonds with the general formula illustrated in Figure 8.

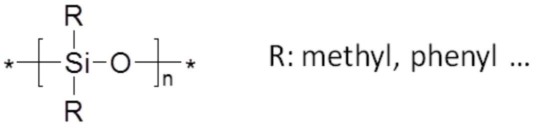

Figure 8: General formula of silicone

Silicon resins are generally characterized by their structure using the D, T, Q system. The main chain unit is called D and refers to the two oxygen atoms bonded to the silicon atom. In a similar way, T and Q units can be defined relatively to the number of oxygen atoms linked to the silicon one (Figure 9).

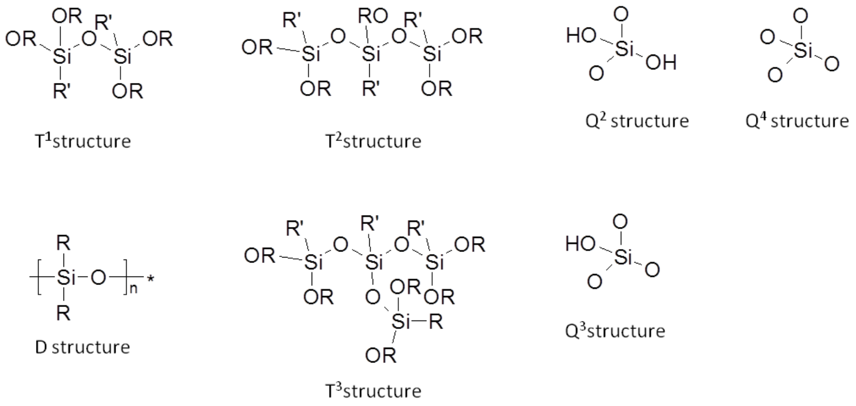

Figure 9: Schematics presentation of D, Ti and Qi silicone structures

They are obtained by a three-step synthesis: chlorosilane synthesis, chlorosilane hydrolysis and polymerisation/polycondensation.

Chlorosilane synthesis: nowadays, silicones are obtained commercially (± 850,000 t/y) from chlorosilanes prepared following the direct process of Rochow[37] and using silicon metal obtained from the reduction of sand at high temperature (Figure 10) and methyl chloride obtained by condensation of methanol with hydrochloric acid (Figure 11).

$$SiO_2 + 2\,C \longrightarrow Si + 2\,CO$$

Figure 10: Reaction of the sand reduction

$$CH_3OH + HCl \xrightarrow{cat} CH_3Cl + H_2O$$

Figure 11: Formation of methyl chloride

The reaction giving chlorosilanes takes place in a fluidized bed of silicon metal powder with a stream of methylchloride usually at temperatures of 250 to 350°C and at pressures of 1 to 5 bars. A mixture of different silanes is obtained containing mainly the dimethyldichlorosilane (Figure 12). The reaction is exothermic and has a yield of 85 to 90%. A copper-based catalyst is used.

$$xCH_3Cl + Si \longrightarrow (CH_3)_2SiCl_2 + \text{others silanes}$$

Figure 12: Formation of chlorosilane

Chlorosilane hydrolysis: polydimethylsiloxanes are obtained by the hydrolysis of dimethydichlorosilane in the presence of excess water (Figure 13).

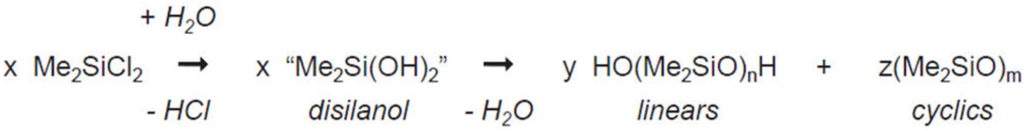

$$x\ Me_2SiCl_2 \xrightarrow[-\,HCl]{+\,H_2O} x\ \text{“}Me_2Si(OH)_2\text{”} \xrightarrow[-\,H_2O]{} y\ HO(Me_2SiO)_nH + z(Me_2SiO)_m$$

Figure 13: Formation of linears and cyclic silicone by hydrolysis

Polymerization/condensation: the linear and cyclic oligomers obtained by hydrolysis of the dimethyldichlorosilane have too short chains for most applications. They must be condensed (linears) or polymerised (cyclics) to give macromolecules of sufficient length[38].

The above polymers are all linear apart from the cyclics, but these are also made up of difunctional units, called ‘D’. We can distinguish three main kinds of silicone resins: branched silicone resin, high temperature vulcanized (HTV) silicone rubber and low temperature vulcanized (RTV) silicone rubber. Branched polymers or resins can be prepared if, during hydrolysis, a certain amount of T or Q units are included, which will allow the formation of a 3D silica network. This can be described if we consider the hydrolysis of the methyltrichlorosilane in the presence of trimethylchlorosilane (Figure 14):

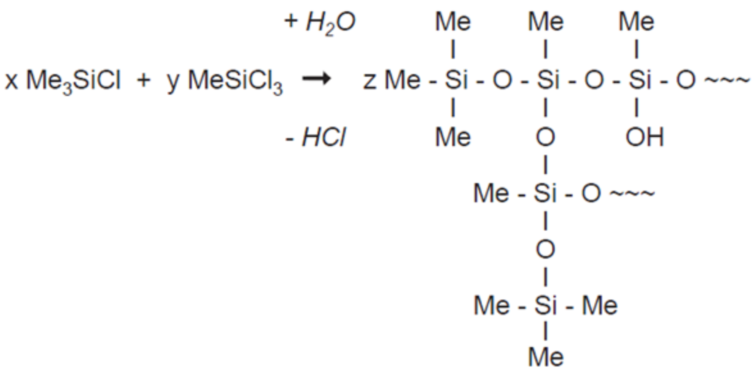

Figure 14: Formation silicone resin composed of tri-dimensional network

Silicone polymers are easily transformed into a three-dimensional network and into an elastomer (silicone rubber) via cross-linking reaction. This reaction allows the formation of chemical bonds between adjacent chains. This polymer is available in different forms from liquid to cross-linked rubber. The rubbers can be found in two main classes[39]: one cross-linked by polyaddition (HTV), and another by polycondensation (RTV).

For poly-addition, cross-linking of silicone rubber is achieved using vinyl endblocked polymers which react with the SiH groups from functional oligomers. This reaction is catalyzed by Pt or Rh metal complex[39] as illustrated in Figure 15[37] and occurs at high temperature.

$$\sim\sim\sim \mathrm{OMe_2Si\text{-}CH{=}CH_2 + H\text{-}SiR_3} \xrightarrow{\text{cat}} \sim\sim\sim \mathrm{OMe_2Si\text{-}CH_2\text{-}CH_2\text{-}SiR_3}$$

Figure 15 : Polyaddition reaction

Silicones prepared via the poly-condensation method are used to make sealants that find applications in original equipment manufactories for glazing sealing windows and doors for either residential or public buildings. They are also used as building component providing a barrier against severe environments such as humidity or dust[40]. These products are ready to use and require no mixing: cross-linking starts when the product is exposed to moisture. Most silicone sealants are formulated from a reactive polymer prepared from an hydroxy-polydimethylsiloxane and a large excess of methyltrietoxysilane. The polycondensation reaction is illustrated in Figure 15.

$$\mathrm{HO{-}(Me_2SiO)_x{-}H} \quad + \mathrm{exc.\ MeSi(OAc)_3}$$

$$\xrightarrow{\text{-2AcOH}} \mathrm{(AcO)_2MeSiO(Me_2SiO)_xOSiMe(OAc)_2}$$

Figure 16 : Poly-condensation reaction

I-5.2 Silicone properties

The simultaneous presence of 'organic' groups attached to an 'inorganic' backbone gives to silicones a combination of unique properties and allows their use in sealants and adhesives compositions in different field such as aerospace (for high thermal stability), electronics (for their electrical resistance), medical (for their excellent biocompatibility) and building (for their capability to seal materials of various nature, and their good resistance to weathering)[39]. They have the properties to exhibit very low thermal conductivity and to release quantity of toxic gases during their degradation compare to classical organic compound[41, 42]. The most common used silicones are the PDMS terminated with trimethylsilyloxy groups, whose structure is described in Figure 17.

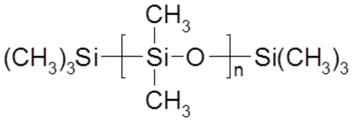

$(CH_3)_3Si-[Si(CH_3)_2-O]_n-Si(CH_3)_3$

Figure 17: PDMS terminated trimethylsilyloxy groups

Physical and thermal properties of silicone depend mainly on their cross linked density and on the R group (Figure 8). Linear PDMS tends to decompose in one step in nitrogen flow without residue, whereas branched PDMS degrades in several steps. Char yield increases with the branched rate [43]. Thermal degradation of branched silicone depends also on the presence of phenyl in the side group. It was shown that the polysiloxanes with phenyl side group show higher thermal stability than those with methyl groups[43].

Thus it was shown that, because of its excellent thermal stability, its fire properties including low heat of combustion and low rate of heat release compared to conventional organic polymers [42, 44] and its good weatherability, silicone seems to be a good candidate to substitute organic intumescent coating for the fire protection.

I-5.3 Resistance to fire of silicone based coating

Silicone coatings used for the fire protection are poorly reported in the literature. Beigbeder et al. evaluated the fire protective performance of PDMS/Carbone nanotube based coating onto aluminium plate. They showed that in convective/radiative heating test, this kind of coating exhibited improved properties compared to virgin aluminum. This effect was attributed to the high adsorption of the PDMS chains onto carbon nanotube mostly triggered by CH-π interactions between the methyl group from PDMS and the π-electron-rich surface of the carbon nanotube leading to the formation of a cohesive structure when burning [45].

Silicone resin with dispersed carbon nanotubes were then introduced by Nanocyl's (ThermoCyl) to give fire protection to a wide variety of substrates, such as plastics, cables, textiles, foams, metals, and wood [46]. This coating, with a thickness of 100 µm, appears to be effective in certain fire scenarios. However, these silicone based coatings are also not intumescent and have limited fire performance for the steel protection in fire scenario[47].

I-6 Conclusion

In this first chapter, we have evidenced the necessity of the fire protection of building structures composed of steel. The most used systems for the protection of these substrates in fire scenario are intumescent paints. The insulative properties of these coatings are governed by several parameters such as: (i) high expansion, (ii) high swelling velocity, (iii) high mechanical properties and (iv) low heat conductivity. Nowadays, all the intumescent materials are organic based. Nevertheless, they exhibit several drawbacks. Among them,(i) they usually exhibit poor aging properties; (ii) organic components undergo exothermic decomposition which reduces the thermal insulative value of the system,(iii) the coating releases organic gases (potentially toxic) which are undesirable in a closed fire environment and (iv) one kind of intumescent paint must be dedicated to a given fire scenario.

Due to its excellent thermal/weatherability properties, silicone was thus selected as a good alternative binder for intumescent coatings. **The challenge of this work is to develop an intumescent coating based on silicone resin which exhibits better fire performance than classic organic intumescent paint in various fire scenarios (cellulosic and hydrocarbon fire) and to determine the critical parameters governing its fire performance.**

Chapter II: Development of new silicone based coating for the steel fire protection

II-1 Introduction

The aim of this chapter is to evaluate the potential of the silicone based coating for the fire protection of steel. We have shown that three kinds of silicone matrix can be distinguished: high cross-linked silicone resin, room temperature vulcanized (RTV) silicone rubber and high temperature vulcanized (HTV) silicone rubber. In this chapter, two systems are studied. The first one is based on a high cross-linked silicone matrix and the second one is a RTV silicone sealant.

In a first part, the fire resistance of phenyl silicone coating (a high cross-linked silicone matrix) is evaluated using two lab-scale tests that have been developed in the Lab: one based on the Torch Test (radiative/convective heating scenario) and the other on a heat radiator test (radiative heating scenario).

Moreover, as previously mentioned, it is recognized that the governing parameters[48] for intumescent coating to get efficient heat barrier performance are its expansion and its low thermal conductivity (formation of a dense and porous char). Those parameters will thus be examined for this system. To determine the thermal conductivity of intumescent coating at high temperature, new protocols have been developed based on the transient plane source technology and will be described in this chapter[49]. The determination of expansion is based on visual observations.

Finally, thermal degradation of the silicone coating will be studied characterizing the gas and condensed phases in order to explain the intumescence phenomenon and thus the fire performance of silicone based coatings.

This first part is based on the following paper:

B. Gardelle, S. Duquesne, V. Rerat, S. Bourbigot, Thermal degradation and fire performances of intumescent silicone based coating, **Polymer for Advanced Technologies -** Vol 24, p62-69, (2013)

In a second part, fire performance of two silicone sealants (RTV silicone) is investigated using the torch test. Similarly to what have been done on the first part, the thermal parameters including heat conductivity and thermal diffusivity will be measured as a function of temperature and will be commented[49]. The structure of the RTV silicone based-coatings will then be investigated by ^{29}Si solid state nuclear magnetic resonance (NMR) and potential relationships between the structure and the thermal properties will be examined.

This second part is based on the following paper:

B. Gardelle, S. Duquesne, P. Vandereecken, S. Bourbigot, Fire performance of curable silicone based coatings, **ACS book Fire and Polymers VI: New Advances in Flame Retardant Chemistry and Science -** Vol 1118, p205-221, 2012

II-2 Fire performance of high cross linked silicone matrix[50]

II-2.1 Introduction

The purpose of this part is to investigate the fire resistance of phenyl silicone coating exposed to an open flame (Torch Test) and exposed to a pure radiative heating source (heat radiator test). The silicone resin used for this first study is a phenyl branched resin composed of T structure and containing 6% of hydroxyl group, hereafter called PhS.

In order to enhance the fire performance of this coating, 8% of 7081 resin modifier is added to the matrix. The modifier is a mixture of polydimethylsiloxane (PDMS) and silica coated by a silane. PDMS is known to degrade at high temperature[51] (in the same range of temperature as classical silicone resin) and should therefore play the role of blowing agent. The materials are first dissolved in ethanol and the formulations are coated on steel plates to obtain 400 +/- 50 µm dried coating (XC38, 3 mm thick). The coatings are then dried at 90°C for 1 hour. Commercial water-based intumescent paint (Nullifire S707-120 (Nullifire, England)) is used as reference in this first part. The same thickness of Nullifire is coated on the same steel plate as above.

The thermal conductivity (formation of a dense and porous char) [48] and the thermal degradation of the silicone based coating will be investigated to explain its fire protective behavior.

II-2.2 Fire performance of PhS and PhS/modifier based coating

To evaluate the insulative properties of PhS and PhS/modifier based coating, coatings are tested in torch test and heat radiator test. In both fire tests, the temperature is measured at the back side of the plate. The temperature reached at the steady state enables to evaluate the insulative properties of the coating.

In the torch test, it appears that when the modifier is added to the silicon matrix, there is a high expansion of the coating and it reaches the same fire performance as the intumescent paint. However, in pure radiative heating source, silicone based coating cracks and, consequently, exhibits low fire performances. These cracks may be due to the high vibration of Si-O bound in infrared field[52].

The main results and experimental observations are summed up in the Table 3.

Table 3: Summary of fire performance and visual observation of PhS and PhS/modifier based coating in two different fire scenarios (torch test / heat radiator test)

Coating	Torch test	Heat radiator
PhS	- Low expansion 150% - Low fire performance compared to commercial intumescent paint $T_{\text{steady state}} = 350°C$	- Low expansion 200% - Several cracks - Fire performance limited due to cracks and small expansion $T_{\text{steady state}} = 360°C$
PhS/modifier	- Large expansion 1000% - Similar fire performance as commercial intumescent paint - $T_{\text{steady state}} = 230°C$	- Large Expansion 800% - Several cracks - Fire performance limited due to cracks $T_{\text{steady state}} = 340°C$
Commercial intumescent paint (Nullifire)	- Large expansion - Good fire performance $T_{\text{steady state}} = 230°C$	- Large expansion : 800% - No cracks at the surface - Good cohesion of the char $T_{\text{steady state}} = 210°C$

In the two tests commented above, the silicone/modifier coatings exhibit an intumescent behavior whereas it is not the case of the pure silicone system. The expansion enables the formation of an insulative barrier, reducing heat transfer from the external heating source to the substrate.

As discussed in the first chapter the heat conductivity is one important parameter governing the performance of the coating in terms of heat insulation. Thermal conductivity of silicone and silicone/modifier were thus measured from ambient temperature to 600°C (Figure 18). For both materials, it varies from 0.1 to 0.35 W/m.K, depending on the temperature, and the values are in the same order of magnitude as those found in the literature[17, 48] for organic based intumescent coatings.

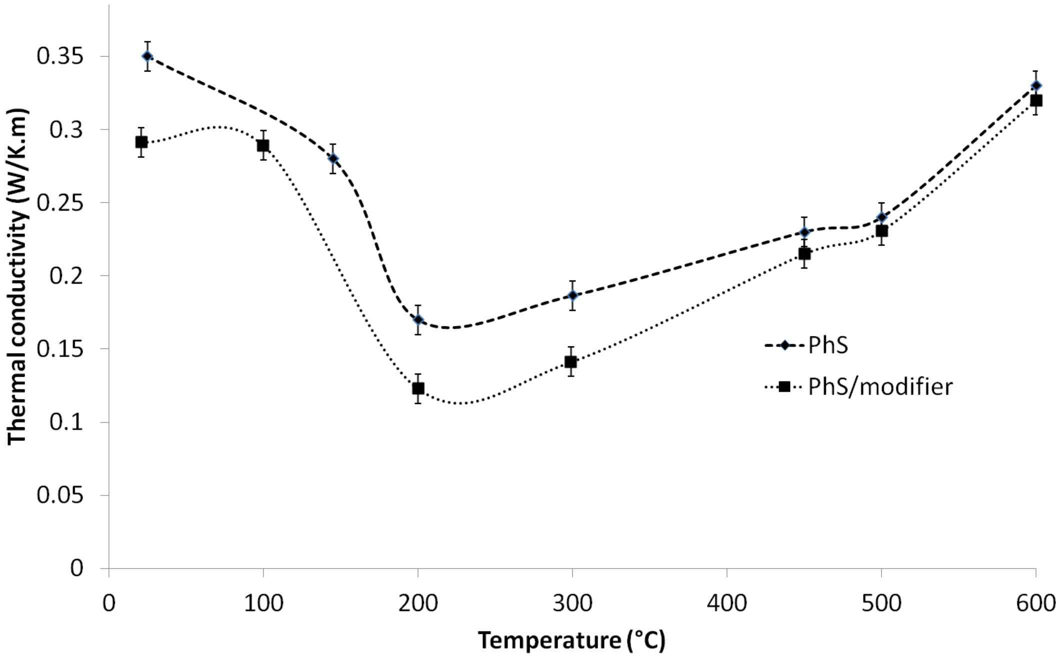

Figure 18: Thermal conductivity versus temperature for PhS and PhS/modifier

For the two silicon-based coatings, thermal conductivities are very low (lower than 0.35 W/ m.K.) but the modifier increases the expansion of the coating during the fire test creating a thicker insulative barrier. This difference in the expansion could thus explain the differences in the fire protection behavior. To highlight it, the behavior of PhS and PhS/modifier based coating in torch test is simulated by a model developed in the laboratory using Comsol Multiphysics V4.1 software[30].

II-2.3 Modeling of the fire behavior of silicone based coating in Torch Test

The aim of this part is to quantify the role of the final expansion on the insulative properties of two coating exhibiting same thermal conductivity at high temperature. At first, we consider a 400 µm coating on steel plate exposed to an open flame (described as heat flux $\dot{q}''$ and as boundary condition), as described in Figure 19.

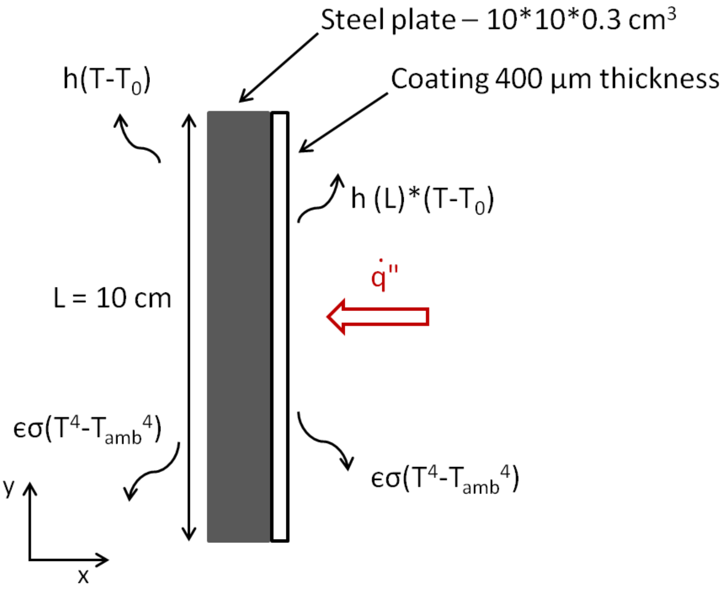

Figure 19: Schematic representation of the Torch Test

As described in the first chapter, the effective flux received by the coating and the heat diffusion are described by the following equations:

$$\dot{q}^{"}_{eff} = A\dot{q}^{"} + h(T_{inf} - T) + \epsilon\sigma(T^4_{amb} - T^4) \qquad \text{Equation 1}$$

$$y \in]e, s(t)[, \rho c_p \frac{\partial T}{\partial t} = \nabla.(k\nabla T) + Q \qquad \text{Equation 2}$$

In order to model the fire behavior of both materials, several parameters have to be quantified.

First, a heat flux $\dot{q}"$ is measured using a flux meter at different point on the face exposed to the flame.

Then, the convective coefficient h along the y direction of the plate is determined using the temperature versus time curve obtained for the virgins steel plate. The results of the convective coefficient and heat flux versus L on the top side of the steel plate are presented in Figure 20. It shows that heat flux and h coefficient present a Gaussian shape along the steel plate. This is typically the shape obtained for the heat flux considering a flame impinging a substrate[53]. One of the main parameter to take into account is the ratio H (distance burner - plate)/d (burner diameter) which reaches about 4 in our study. In this case, Singh et al. evidences that to reach the same maximum heat flux (about 70 kW/m²) the combustible fluid has a Reynolds number of about 5500. We can therefore assume that the Reynolds number of the fluid used in the Torch Test is in the same range of magnitude. As a consequence, the regime of the flame is turbulent. Due to the low emissivity of the flame, radiation is usually small compared to convection[54] and in this condition the heat transfer occurring around the flame impact is driven by forced convection explaining the value of h input in the model (higher than 20).

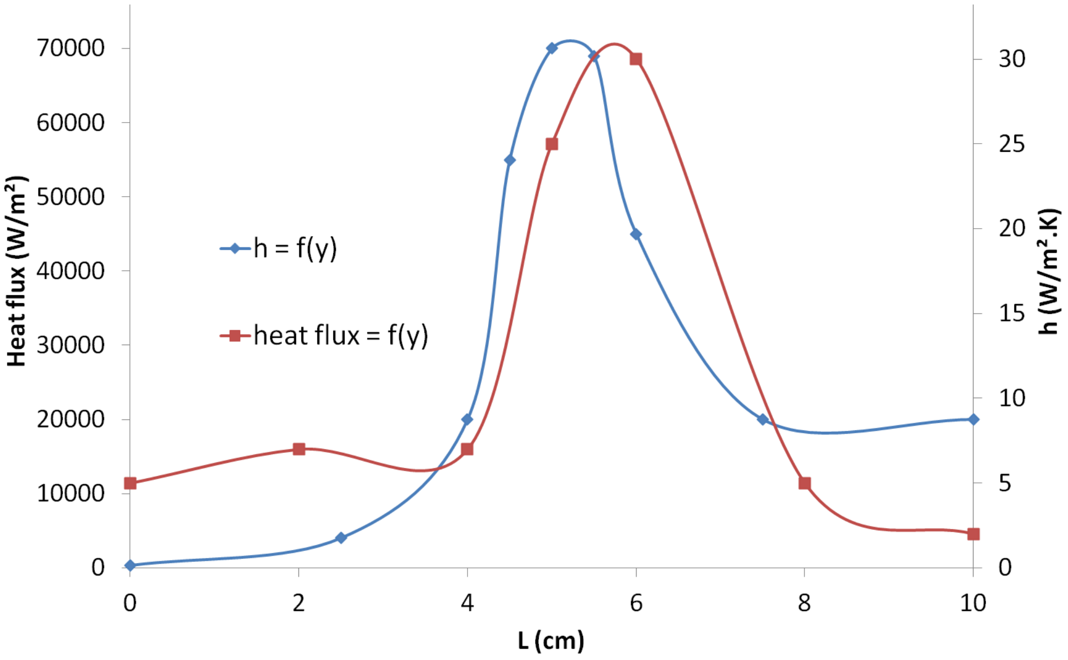

Figure 20: convective coefficient h and heat flux in y direction in the torch test condition

The next step of the modeling consists in entering in the software the values of thermal conductivity, obtained by the Hot Disk device.

The last parameter to be investigated is the expansion and swelling velocity - s(t) - of both materials. By visual observation during the fire test, the maximum of the expansion for PhS and PhS/modifier is respectively reached after 300s and 180s of fire testing. The expansion versus time curve input in the model is presented in Figure 21.

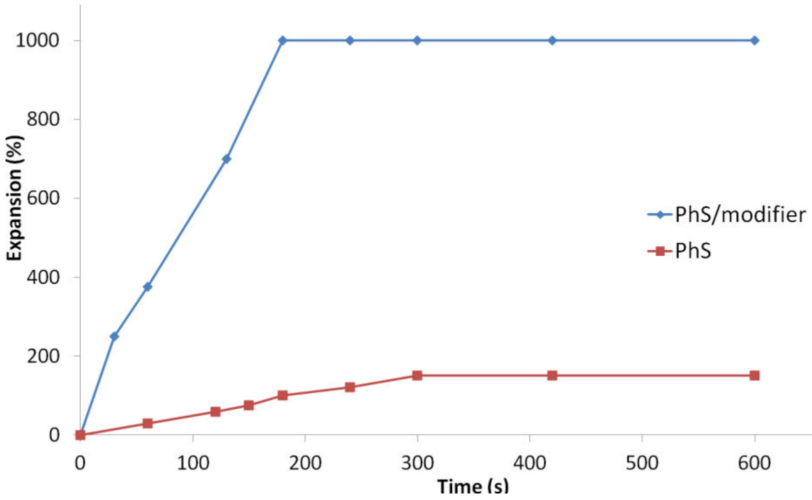

Figure 21: Expansion versus time curve of PhS and PhS/modifier estimated during the Torch Test

Due to the expansion of the coating upon heating, the boundaries of the model are not fixed during the fire test. Taking into account moving boundaries is a typical issue of heat transfer modeling. Our approach was to consider the dynamic of the problem, using the arbitrary Lagrangian-Eulerian (ALE)[30, 55] method coupled with heat transfer in the coating layer (not fixed) and the steel layer (fixed).

The governing equations and the associated boundaries conditions were solved in 2D, taking into account the dynamic of the problem using ALE method implemented in Comsol Multiphysics V.4.1 coupled with heat transfer. The expansion of the intumescent coating is expressed in the ALE frame and is well captured by the model (Figure 22).

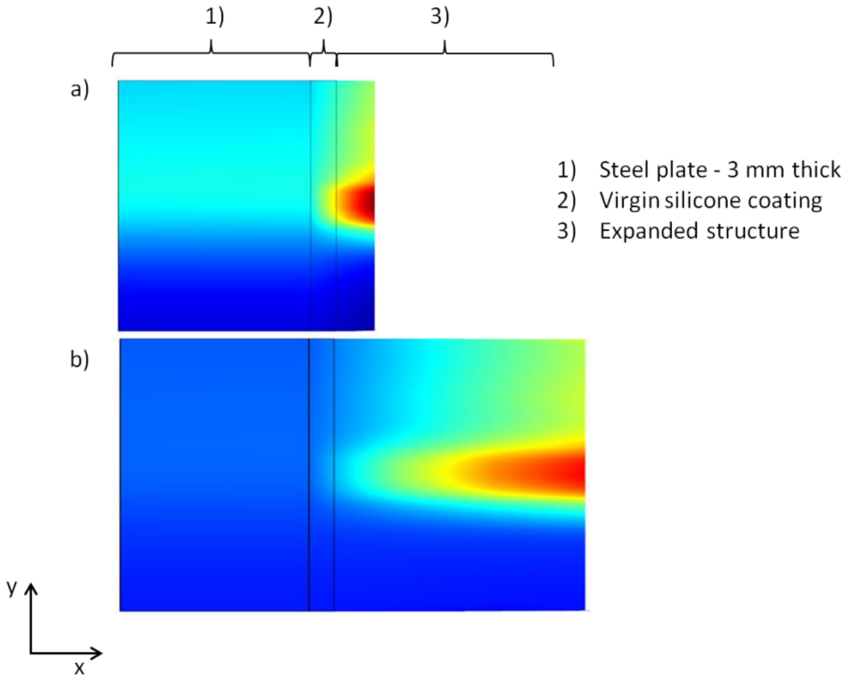

Figure 22: Simulated heat gradient in the expanding silicone structure for a) PhS and b) PhS/modifier based coating at the end of the Torch Test

Even if the model does not include all phenomena involved in intumescence, the simulated temperatures calculated at the center of the plate are in agreement with those obtained experimentally (Figure 23).

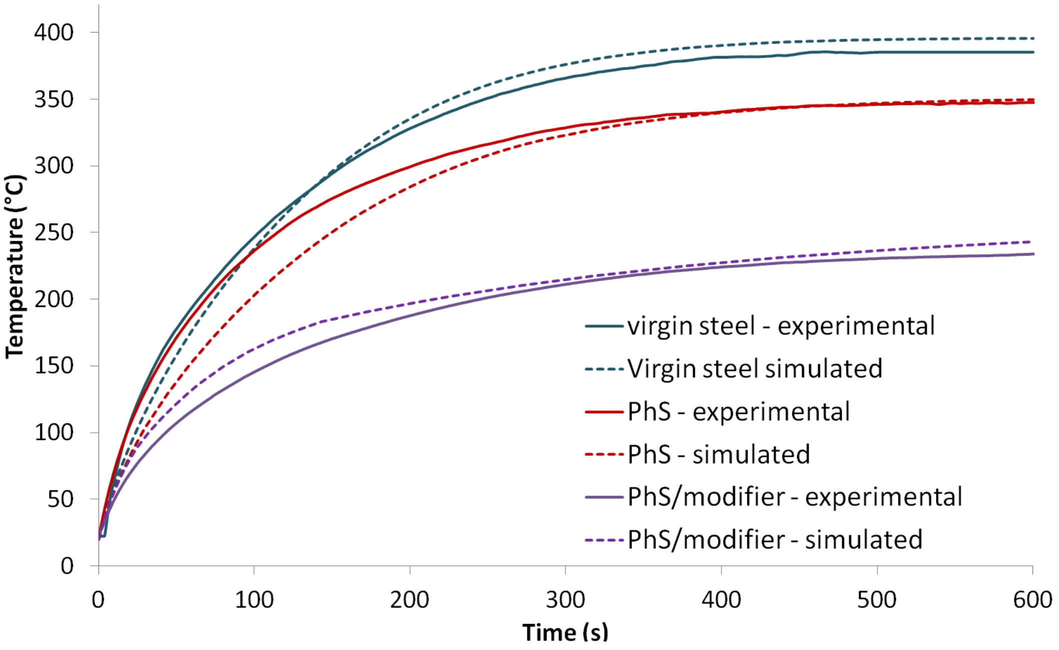

Figure 23: Temperature versus time curve of PhS and PhS/modifier obtained experimentally and simulated

An acceptable fit between both curves is obtained. In particular, the temperatures reached at the steady state are in good agreement. The difference between the simulated and the experimental curve during the first minute may be attributed to a wrong estimation of s(t). **However, it demonstrates that the difference of expansion between the two silicone coatings exhibiting similar thermal conductivity at high temperature explains their different insulative properties.**

The next step of this work was dedicated to the study of the intumescent phenomenon, and more specifically: what is the role of the modifier in the expansion phenomena?

II-2.4 Thermal degradation mechanism of PhS/modifier

TGA, ^{29}Si solid state NMR and gas phase analysis were used to investigate the thermal degradation mechanism of PhS and PhS/modifier . The results (Table 4) demonstrate that the degradation of the PhS resin occurs in two main steps, leading to tri-dimensional network composed of Q^4 structure at high temperature.

It appears that PhS and the modifier degrade at the same temperature, but the degradation rate of the modifier is much faster than that of the silicone. There is no chemical interaction between the modifier and the silicone matrix (Table 4). Thus, it is not possible to explain the differences in the expansion by a chemical reactivity between the resin and the modifier. Thus, it could be assumed that the expansion is linked to the fast degradation of the modifier.

Table 4 : Thermal conductivity measurement and analysis of the condensed and gas phase during the degradation of PhS and PhS/modifier

	Heat thermal treatment	Mass loss %-wt	^{29}Si MAS NMR	Gas released	k (W/m.K)
PhS	250°C	4.0%	T^2 and T^3 structure	Oligomers of silicone	0.18
PhS/ modifier		3.7%	D, T^2 and T^3 structures	Oligomers of silicone	0.14
PhS	600°C	29.0%	Tridimensional network-Q structures	Aromatic compounds such as benzene	0.33
PhS/ modifier		31.0%	Tridimensional network-Q structures	Oligomers of silicone from PDMS and aromatic compounds	0.32

As a consequence, those results allow us to propose that the intumescent phenomenon observed during the fire tests (and the resulting fire protective behavior) could be attributed to a rheological phenomenon. The PhS silicone coating may soften upon heating and then expands because of the fast degradation of the modifier, releasing gases. This phenomenon is pointed out by TGA[56]. The network formed at high temperature can trap the gases released by the modifier and make the coating to swell, leading to the formation of an expanded tri-dimensional network based on silica. This expanded coating has a low thermal conductivity (0.32 W/m.K.) and provides the fire protection.

In this first part, we have developed a novel intumescent paint based on silicone resin and we have shown good fire performance when the coating is exposed to an open flame. In order to validate this concept, the fire performance of PhS/modifier based coating was evaluated in a cellulosic fire scenario.

II-2.5 Fire performance of PhS/modifier in a simulated cellulosic fire

Figure 24 shows the temperature versus time curves obtained for 1 mm based coatings using a lab scale furnace test.

For virgin steel, critical temperature (500°C) is reached in 900s, whereas for PhS/modifier based coating, it is reached in 1250s. However, this critical temperature is not reached for the Nullifire steel plate, since the temperature at the end of the test is about 450°C.

Those results demonstrates that even if PhS/modifier material exhibits heat barrier properties compared to virgin steel plate, its fire performance in cellulosic fire scenario are limited compared to commercial intumescent paint.

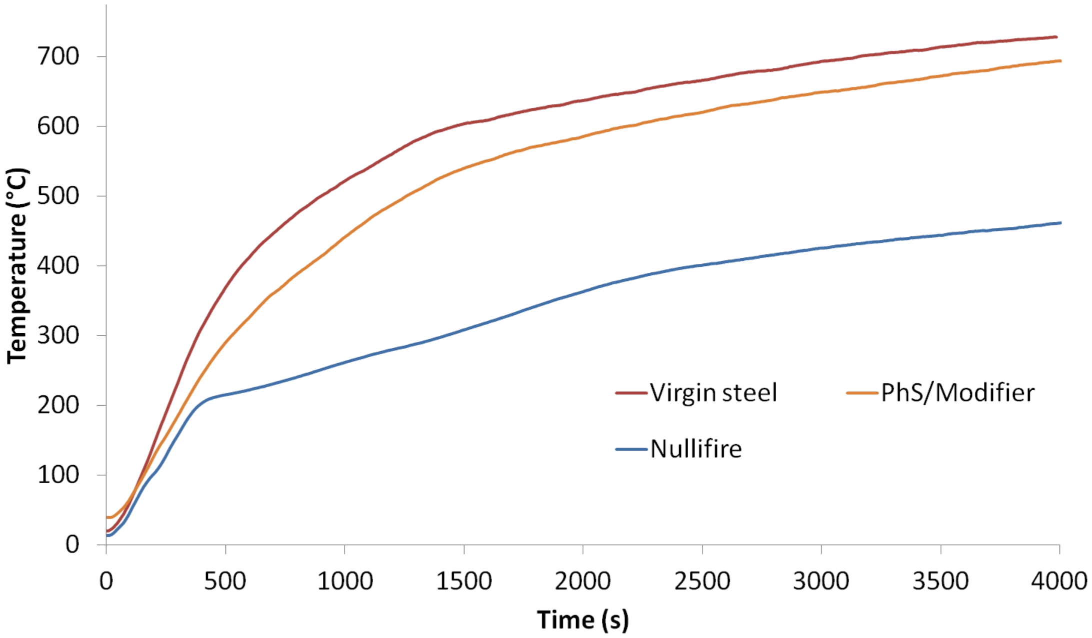

Figure 24: Temperature versus time curve of PhS/modifier and Nullifire based coating in cellulosic fire scenario

Figure 25a) shows the residue of the PhS/modifier coating after only 180s of fire testing. It highlights the fact that the coating flows from the plate during the first minute of testing. On the other hand, Figure 25b) illustrates the residue of Nullifire based coating after the furnace testing. It evidences the formation of an expanded and cohesive foam (expansion 3500%) explaining the high insulative properties in a simulated cellulosic fire.

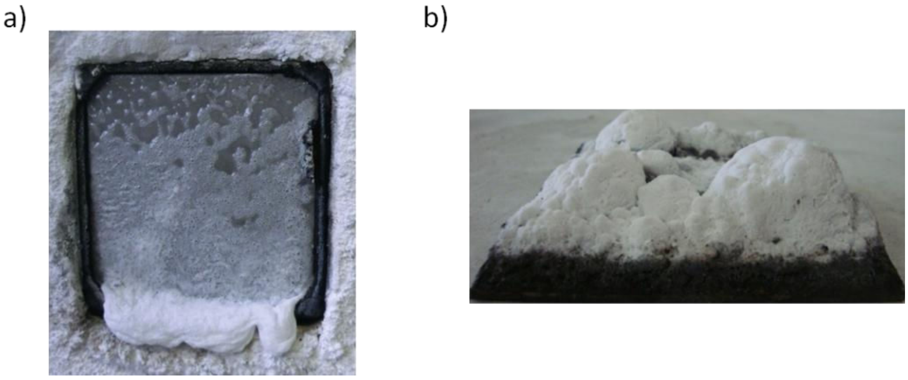

Figure 25: a) Residue after 180s testing of PhS/modifier and b) Residue at the end of the test of Nullifire based coating (test: cellulosic fire scenario)

In order to explain this phenomenon, rheological behavior of the silicone matrix was studied versus temperature. This test enables to measure the apparent complex viscosity of the silicone matrix versus temperature. Figure 26 shows the apparent complex viscosity of the silicone matrix from 20°C to 80°C and highlights a strong decrease of its viscosity at 70°C. The low viscosity of the matrix at high temperature limits considerably its use for the fire protection even if it exhibits good performance when exposed to an open flame.

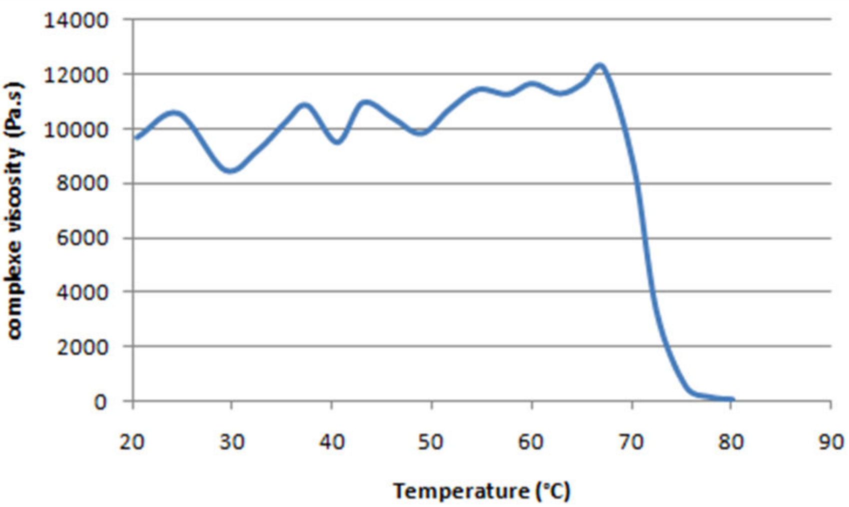

Figure 26: Apparent complex viscosity of PhS versus temperature

In order to improve the fire performances of our silicone based coating, new matrices have been tested. The fire performance of room temperature curable silicone based coatings is thus evaluated in the following part.

II-3 Fire performance of curable silicone based coating[57]

II-3.1 Introduction

In this part, the fire performance of two RTV silicone resins added with calcium carbonate is evaluated using the torch test.

The first resin, hereafter called silicone 1 (**S1**), was composed of an hydroxylated PDMS with a viscosity of 80 cS (viscosity is measured using cone/plate rheometer CP-52), a large excess of methyltrimethoxysilane (MTM) and a tin catalyst. The second, hereafter called silicone 2 (**S2**), is composed of an hydroxylated PDMS with a viscosity of 2000 cS (viscosity is measured using cone/plate rheometer CP-52), a large excess of MTM and a titanium catalyst. S1 and S2 mainly differ from their chain length, S2 having a longer chain length (Dp = 500) than S1 (Dp = 25) and thus a higher viscosity.

The two silicone matrices have been characterized by ^{29}Si solid state NMR, which evidenced that the two resins are composed of D, T^2 and T^3 structures. Deconvolution of each spectrum revealed that the crosslink density of S1 is higher than that of S2. S1 is composed of 7% of T structure whereas S2 is composed of 5% of T structure.

Calcium carbonate is incorporated in the two silicone matrices in order to increase their fire performance. Indeed, calcium carbonate has attracted more and more interest due to its availability as raw material and to its low cost. This filler is mainly used in PDMS to improve its mechanical[39] and flame retardant properties[58, 59]. Calcium carbonate also enhances thermal stability of PDMS. Upon heating, silicone containing calcium carbonate forms a ceramic-like calcium silicate residue[59] that could have a protective behavior in case of fire. Thus, 50% of ground calcium carbonate (GCC) stearic acid coated with an average particle size of 4.5µm, supplied by Dow Corning, is incorporated into the matrix to enhance its fire performance. Both formulations are applied on a 10 cm x 10 cm x 3 mm steel plate to obtain 400 ± 40 µm dried coating.

In order to fully explain the fire performance of both coatings, thermal properties such as thermal stability, thermal conductivity and diffusivity at high temperature are investigated.

II-3.2 Results and discussion

To evaluate the influence of T structures and of the silicone network on the fire performances of S1 and S2 based coating containing GCC, the fire performance of S1/GCC and S2/GCC formulations are first evaluated using the torch test.

Even if the two formulations do not exhibit an intumescent behavior upon heating (Figure 27), they have insulative properties and S2/GCC based coating shows better fire performances than S1/GCC based coating.

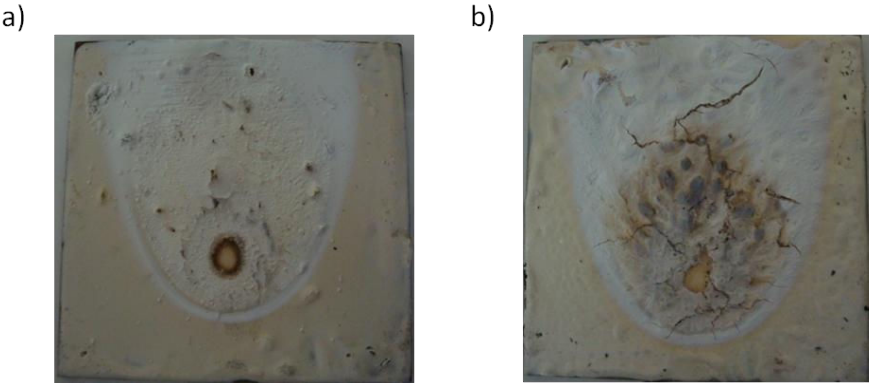

Figure 27: a) S1+50%GCC b) S2 + 50%GCC steel plate residues after torch test

In the case of intumescent materials, fire protection is due to the formation of thick insulative foam with low thermal conductivity at high temperature. In the present work, and at the opposite of the results obtained previously for high cross-linked PhS/Modifier based coating, the coatings do not swell during fire experiments. We can thus reasonably assume that the main parameters governing the fire performance are their thermal properties at high temperature, such as thermal conductivity and diffusivity. For the two formulations, those parameters were thus determined.

The heat conductivity (Figure 28) decreases from 25°C to 400°C due to the formation of some alveolus inside the material. Indeed, the heating rate in the furnace used for thermal properties measurements is very low compared to that in the torch test and therefore, it allows the material to encapsulate gases evolved during the degradation of the matrix. For S1 and S2 based material, thermal conductivities are similar and reach respectively 0.32 ± 0.02 W/K.m and 0.23 ± 0.01 W/K.m at 500°C (Figure 28), which correspond to materials exhibiting heat insulative properties.

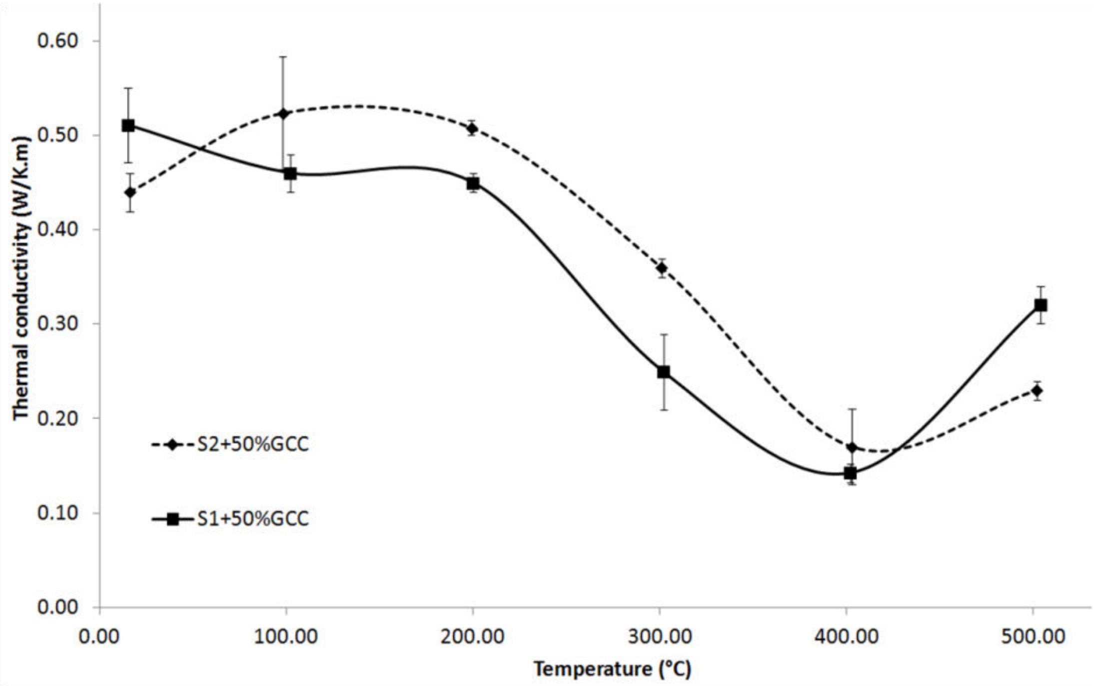

Figure 28: Thermal conductivity versus temperature for S1/GCC and S2/GCC

Thermal diffusivity describes the ability of a material to conduct heat (k) instead of storing it ($\rho.c_p$). In a material with high thermal diffusivity, heat moves rapidly through. At high temperature, thermal diffusivity of S1/GCC material is significantly higher than that of S2/GCC based material (Figure 29).

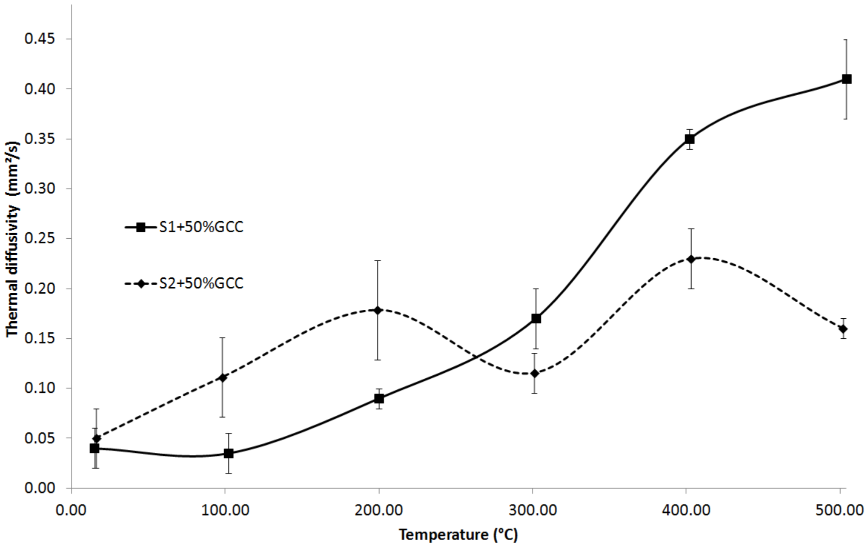

Figure 29: Thermal diffusivity versus temperature for S1/GCC and S2/GCC

The heat diffuses therefore more rapidly in S1/GCC matrix than in S2/GCC. Since the k parameter of the two materials is similar, the change of thermal diffusivity is explained by the variation of $\rho.c_p$, i.e. by a different heating storage. Heating storage of S1 is lower compared to that of S2. This strong difference of thermal diffusivity between the two materials could be due to different thermal stability. Depending on its degradation pathway, the resin exhibits morphological modification and hence different thermal properties.

The degradation of the two systems was thus investigated using TGA and solid state ^{29}Si NMR. It was concluded that GCC is incorporated into both silicone resins, but remaining silanol group are present in S1/GCC based material. This leads to a lower thermal stability, due to depolymerization reaction catalyzed by the silanol groups, occurring at low temperature (250°C). We have evidenced that the thermal conductivity of the two materials are very closed and first measurement of Cp highlights the fact that their values are also in the same order of magnitude. The difference of the thermal diffusivity could therefore be attributed to a lower density of the S1/GCC compare to S2/GCC. Finally, because of this lower thermal stability (and also because of different degradation pathway), S1/GCC has a higher thermal diffusivity than S2/GCC at high temperature. Consequently, heat moves rapidly through S1/GCC based coating leading to a lower fire performance compared to S2/GCC.

This work has evidenced that in the field of resistance to fire, methyl-silicone based coatings should not to be composed of silanol groups, in order to ensure a high thermal stability combined with appropriate thermal parameters (low heat conductivity and thermal diffusivity). In the next step of this study, the fire performance of 1 mm of S2/GCC based coating has been evaluated in cellulosic fire scenario to validate the use of such coating for the fire protection of steel structure.

II-3.3 Fire performance of RTV silicone in a simulated cellulosic fire

Figure 30 shows the temperature versus time curve of S2/GCC in cellulosic fire scenario. For this system, critical temperature is reached in 1960 s, evidencing the heat barrier properties of the coatings compared with the virgin steel. On the other hand, compared with the fire performance of a classical organic commercial intumescent paint, the heat barrier properties of S2/GCC are still limited. We have shown in the first chapter that one of the main parameters governing fire performance of coating is its swelling ability. In the case of S2/GCC material, the coating does not swell in cellulosic fire scenario and, therefore, the insulative barrier properties are limited.

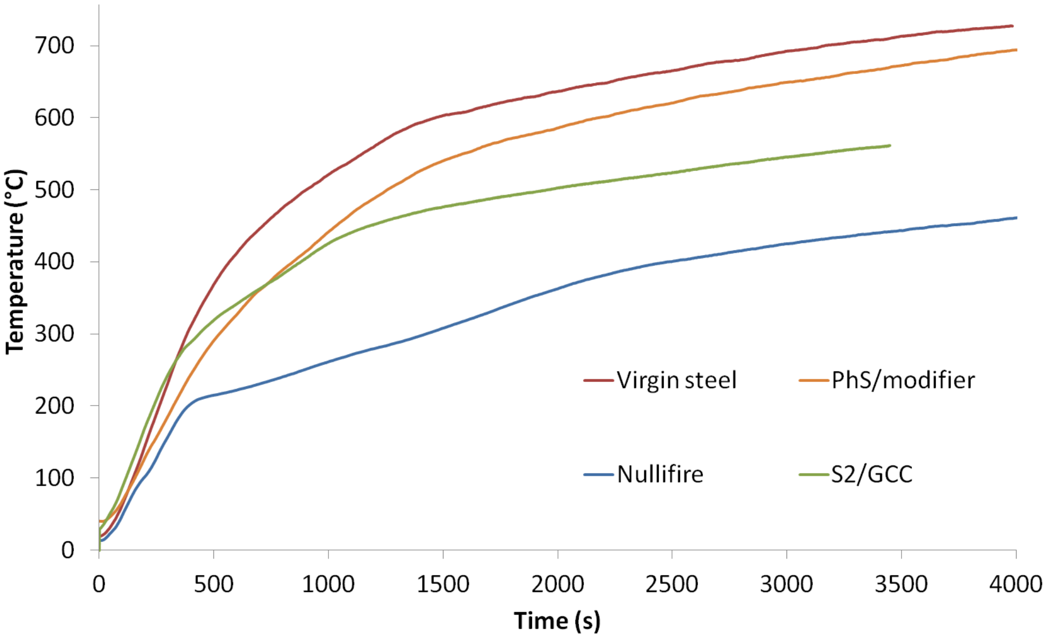

Figure 30: Temperature versus time curve of S2/GCC, PhS/modifier and Nullifire based coating in celluosic fire scenario

However, S2/GCC coating exhibits better fire performances compared to phenyl silicone/modifier based coating. In the case of phenyl silicone based coating, the material flows from the plate due to its low viscosity at high temperature whereas S2/GCC based coating exhibits a hard remaining residue after furnace testing (Figure 31). This study demonstrates that for the protection of steel against fire, RTV silicone matrix seems to be a better candidate than high cross-linked silicone resin.

Figure 31: S2/GCC residue after furnace test in cellulosic fire scenario

II-4 Conclusion

In this chapter, we have evaluated the fire performance of two main silicone based coatings.

The first silicone-based coating based on high cross-linked silicone matrix, exhibits high fire performance when exposed to an open flame. It was explain by: (i) the relative high expansion of the coating during the fire test (appropriate viscosity of the degrading material encapsulating evolving gases of the modifier) and (ii) the low thermal conductivity at high temperature. However, due to the too low viscosity of the matrix at 70°C, the intumescent coating falls off the plate in cellulosic fire scenario. The use of this system is thus clearly limited.

The second silicone coating is based on RTV silicone matrices. Experiments carried out on the Torch test evidences that methyl-silicone based coatings have to be composed of D structure without remaining silanol group to ensure a high thermal stability combined with appropriate thermal parameters (low heat conductivity and thermal diffusivity) that will lead to high fire performance. Moreover, similarly to what observed for the first system, in cellulosic fire scenario, RTV based coating evidences heat barrier properties but lower compared with those of a commercial intumescent paint. However, this system is clearly not well expanded and we showed in the first part of this chapter that one of the main parameter governing the fire performance of intumescent coating is the expansion, associated with appropriate thermal parameters including heat conductivity.

Thus, in the next chapter, we will develop new formulations based on RTV resin that allow combining expansion and thermal properties to obtain competitive fire protective coatings.

Chapter III: Resistance to fire of Silicone/Expandable graphite based coatings

III- 1.Introduction

The aim of this chapter is to develop silicone intumescent based coating exhibiting high fire performance in both cellulosic and hydrocarbon fire scenarios. We have shown in the first chapters that several parameters have to be investigated to reach high insulative properties. The combination of APP/PER/Mel is widely used as intumescent ingredients for fire protective coating. However, in recent decades, more and more papers reported the use of expandable graphite in intumescent based coatings. As we have shown in the first chapter, expandable graphite is an intrinsically intumescent additive. Due to the release of sulfuric and/or nitric acid upon heating, there is expansion of the graphite platelets. This intumescent additive increases the fire performance and anti-oxidant properties of conventional intumescent based coating[4, 24, 25] and is thus incorporated into complex intumescent formulation. The aim of this chapter is to investigate the fire performance of silicone based coating incorporating EG. The different parameters that affect the performance (expansion, thermal conductivity ...) will be investigated.

As we have evidenced in the last chapter, silicone matrix has to be composed of mainly D structures with no silanol group remaining. That is why, in this chapter, a low cross-linked RTV silicone is used. In a first part, thin silicone based coating including EG are evaluated in hydrocarbon fire scenario and the mode of action of EG is investigated.

This first part is based on the following paper:

- B. Gardelle, S. Duquesne, P. Vandereecken, S. Bourbigot, Characterization of the carbonization process of expandable graphite/silicone formulations in a simulated fire, **Polymer Degradation and Stability,** Vol 98, p1052-1063, May (2013).

For the fire protection of steel against hydrocarbon fire, thick intumescent based coatings are used - about 3-5 mm. That's why in a second step, thicker silicone based coatings are tested. In this kind of fire, the mechanical property of the char is a key parameter and have to be improved. For this, several additives can be added to the intumescent formulation such as mineral fibres [16], organo-clay [27, 28], ceramic precursor[60]. After a large screening (not presented in this manuscript), organoclay was determined as the best candidate. Thus 5% (optimum) of modified organoclay is incorporated in silicone/EG formulations.

This part is based on the following paper:

- B. Gardelle, S. Duquesne, P. Vandereecken, S.Bellayer, S. Bourbigot, Resistance to fire of intumescent silicone based coating: the role of organoclay, **Progress in organic coating -** Accepted (2013).

Finally, resistance to fire of silicone based coating is investigated in cellulosic fire.

III- 2 Resistance to fire of thin silicone/expandable graphite based coating in hydrocarbon fire scenario[61]

III- 2.1 - Introduction

In this part, fire performance of RTV silicone added with expandable graphite is evaluated in hydrocarbon fire scenario. The silicone matrix called **S3** was composed of a hydroxylated PDMS with a viscosity of 15000cs (Dp = 1000), methyltrimethoxysilane and a titanium catalyst. The silicone matrix was analyzed by ^{29}Si NMR and it highlights the formation of 3% of T structure during the crosslinking of the resin. From 5% to 25% of expandable graphite (ES350F5 from Graphitwerk Kropfmuehl (Germany) with an average grain size of 300µm) is incorporated into the silicone matrix. As previously discussed in the state of the art, the main parameters governing the fire performance of intumescent based coating are: the swelling behavior, the thermal conductivity at high temperature and a good cohesion of the char. In order to fully explain the fire performance obtained for S3+25%EG, these parameters are thus investigated on this system. Finally, the carbonization process is elucidated.

III- 2.2 Results and discussion

First of all, Figure 32 reports the temperature profiles obtained for S3/EG in a simulated hydrocarbon fire. It evidences that the times to reach critical temperatures of each formulation increases with the amount of graphite. The time to reach 500°C for the virgin steel, for S3+5%EG, S3+10%EG, S3+15%EG, S3+20%EG, S3+25%EG is respectively 250s, 385s, 580s, 690s, 740s and 810s. It therefore highlights that the heat barrier properties of S3/EG based coating increases with the amount of EG added in the coating. In classical intumescent organic based coating, if a large amount of expandable graphite is incorporated to the intumescent composition, the resulting char exhibits low mechanical properties and the char detaches from the substrate[25] leading to poor fire performance. In the case of silicone based coating, an unexpected good cohesion of the expanded char is observed.

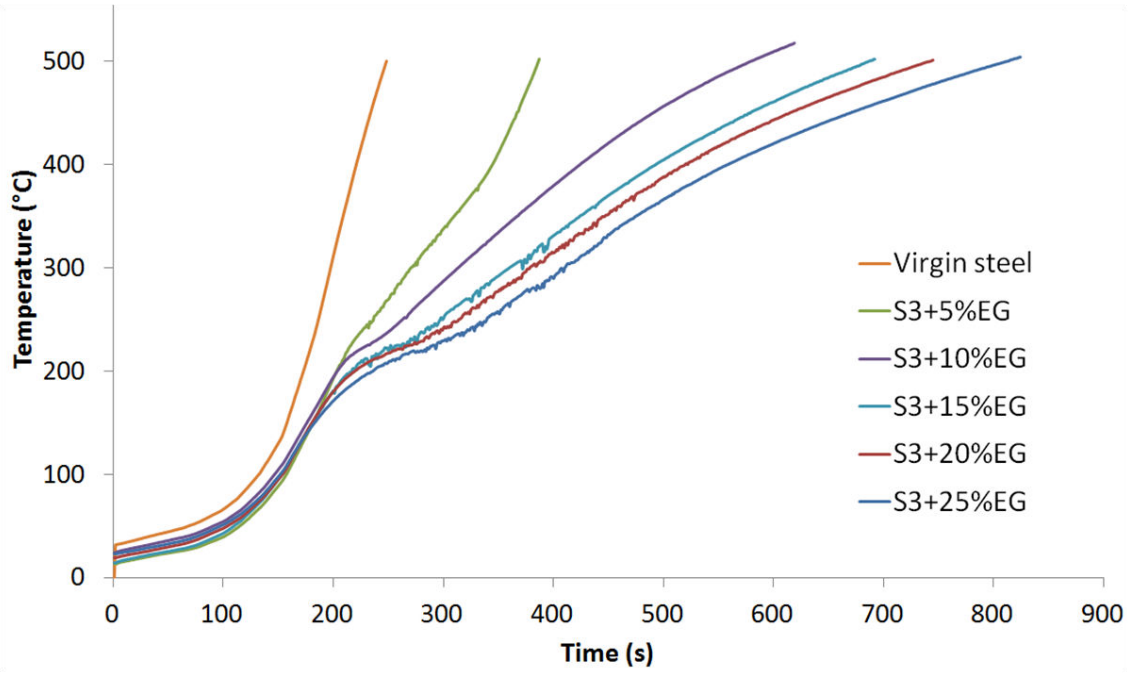

Figure 32 : Temperature versus time curve of S3 added from 5% to 25% of EG in hydrocarbon fire scenario

The best fire performance is achieved for S3 including 25%EG. In this case, silicone based coating exhibits better fire performance than commercial intumescent paint (Figure 33). Indeed, the time to reach critical temperature (500°C) for the commercial intumescent paint and S3+25%EG based coating is respectively 685s and 810s.

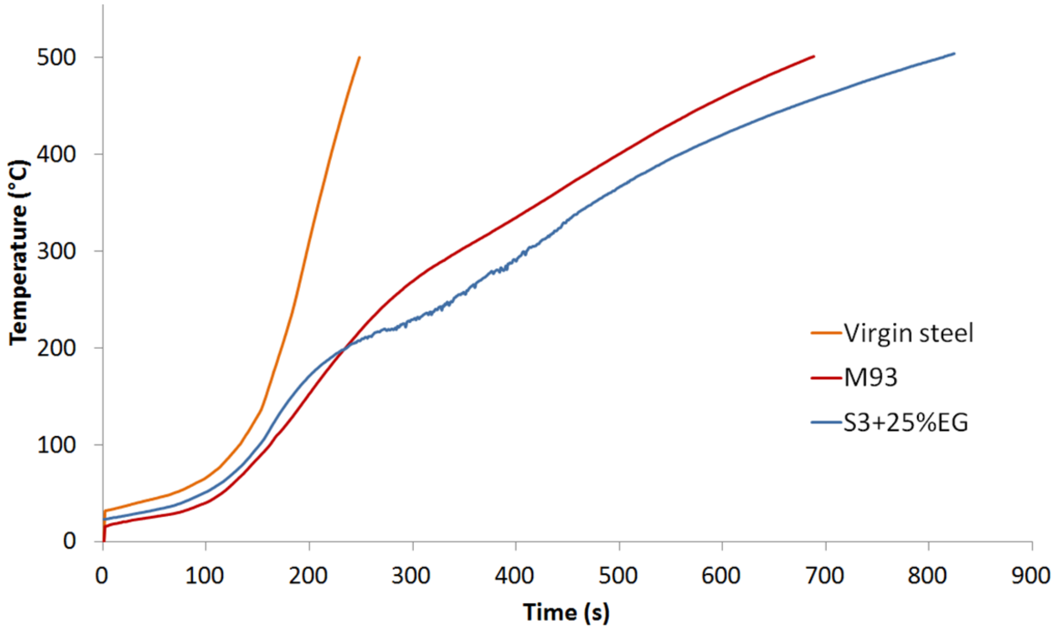

Figure 33: Temperature versus time curve of S3+25%EG and M93 based coatings in hydrocarbon fire scenario

To explain the fire performance of S3/EG based coating, several parameters are investigated: the expansion and swelling velocity, the thermal conductivity at high temperature and the characterization of the carbonization process was carried out to explain the cohesion of the char.

The expansion and swelling velocity of this formulation is first measured using two approaches: one following the expansion in the cone calorimeter test (50kW/m² external heat flux) and in second approach the furnace test experiment was stopped at different time and the expansion of the char was measured. The results are represented and compared in Figure 34.

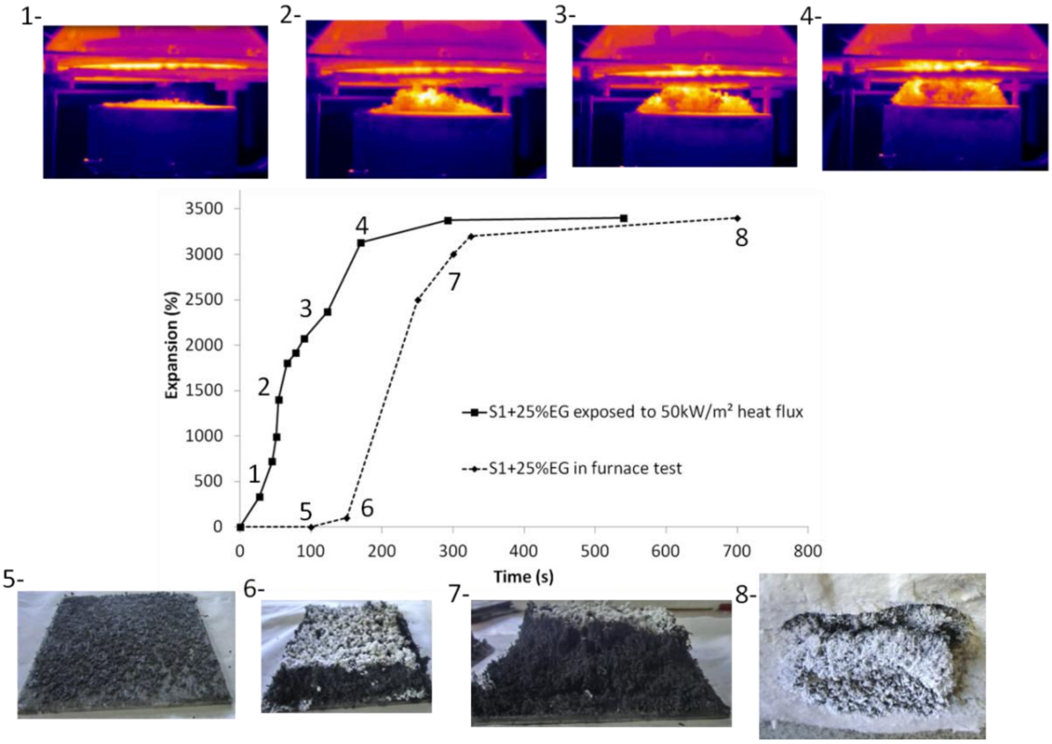

Figure 34: Swelling versus time curve measured in the furnace test and in cone calorimeter test

The expansion versus time curves evidence that the maximum of the expansion and the swelling velocity do not depend on the fire scenario (mass loss calorimeter vs. furnace test UL1709) and reach respectively 3400% and 18%/s. It demonstrates that, the swelling of the material is due to a temperature increase. The expansion phenomenon is mainly due to the expansion of graphite platelets at high temperature and therefore, the expansion rate is not affected by the fire scenario.

The maximum of the expansion and swelling rate are not the only parameters to take into account to explain the fire performance of intumescent coating. The thermal conductivity at high temperature has also to be considered. It was thus measured from ambient temperature to 500°C. To correlate, the thermal conductivity and the expansion of the material at high temperature, the expansion is measured from ambient temperature to 500°C using a third approach with a two plates rheometer[22]. The results are presented in Figure 35. The material begins to swell at 200°C due to the expansion of graphite platelets leading to the formation of an expanded structure. This expansion leads to a decrease in the thermal conductivity of the material. The maximum expansion is reached at 400°C and the thermal conductivity is minimal (0.22 W/K.m) at the same temperature. At 500°C, the expansion does not increase and therefore no significant morphology modification of the material is expected. Moreover, at this temperature, radiative heat transfer occurs inside the material. That explains the increase of the thermal conductivity at higher temperature which reaches 0.35 W/K.m at 500°C.

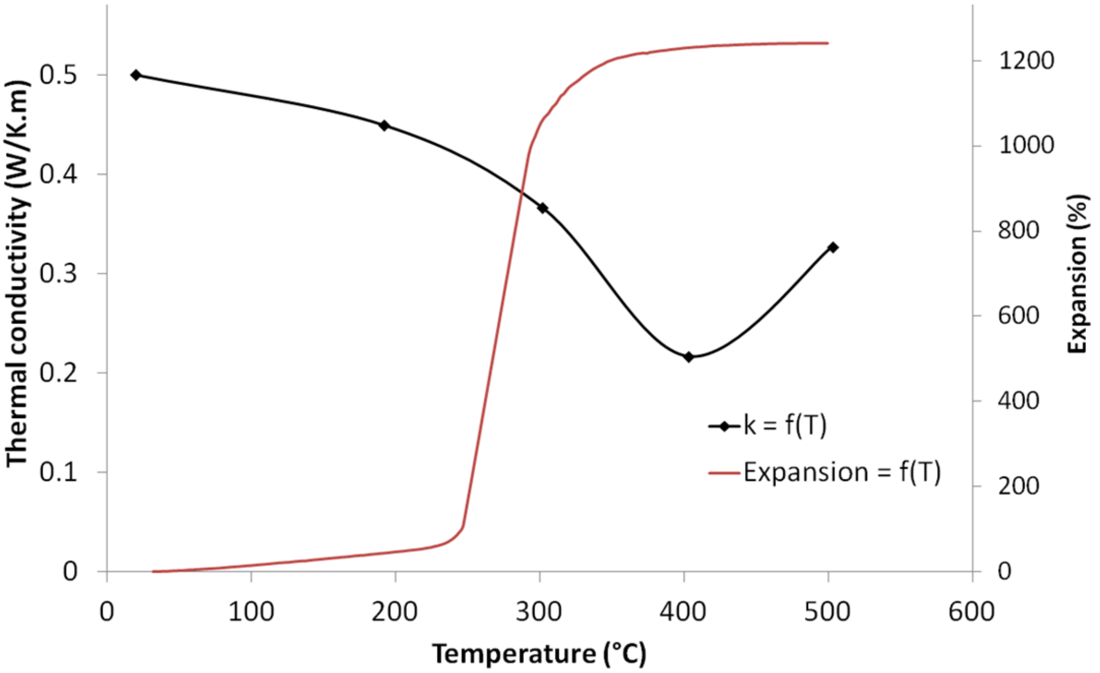

Figure 35: k = f(T) and expansion = f(T) measured in a rheometer for S3+25%EG

As a conclusion, when exposed to a fire scenario, S3+25%EG based coating exhibits high expansion rate (3400%) and velocity (18%/s) and low thermal conductivity at high temperature permitting the formation of an insulative barrier reducing heat transfer from the external heating source to the substrate.

The next step of the study was dedicated to study the carbonization process so as to explain the surprisingly good cohesion of the structure based on graphite.

The char after furnace testing is composed of two main parts that have been fully characterized. The top is composed of amorphous silica and quartz and the heart of the char is composed of graphite platelets embedded in complex silicone structure. X-ray photoelectron spectroscopy was used to highlight the evolution of the silicone matrix in a fire scenario and thus to explain the cohesion of the char. It was concluded that at high temperature, there is oxidation of the graphite platelets, as reported in the literature[62], leading to the formation of reactive group: carbonyl and hydroxyl groups. On the other hand, the silicone matrix degrades leading to the formation of SiC, T and Q structures. Because of the polar properties of Si-O bond and the presence of reactive groups onto graphite sheets, silicone structures are adsorbed onto graphite platelets (highlighted by XPS experiments) explaining the good cohesion of the char at high temperature (Figure 36). It was thus proposed that the good cohesion of the heart of the char is due to: (i) the presence of undegraded matrix; and (ii) thanks to the graphite platelets embedded in complex silicone structures.

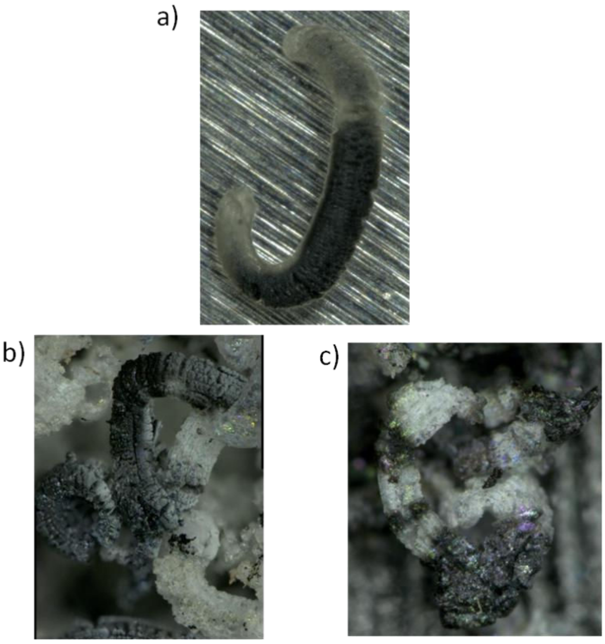

Figure 36: a), b), and c) Residues of S3 /EG after furnace testing evidencing the coating of the graphite platelets by silicone structures

In hydrocarbon fire scenario, thick intumescent based coating (about 3-5 mm) is used. The next part was thus dedicated to the evaluation of the fire resistance performance of thick S3+25%EG coating. A thickness of 1.5 mm was first investigated. Figure 37 shows the time/temperature curve of this coating in hydrocarbon fire scenario and highlights a complete loss of cohesion of the char from the plate during the first minute of the test leading to the loss of the insulative properties. The temperature thus sharply increases to reach 500°C in 490s. The picture of the char during fire experiment (Figure 37) shows the presence of some residue on the plate, the concern is thus not about its adhesion on the plate but on its cohesion during fire experiment. For 1.5 mm based coating, the expansion is too high and the cohesion is not good enough to prevent the falling down of the char during fire experiment.

.

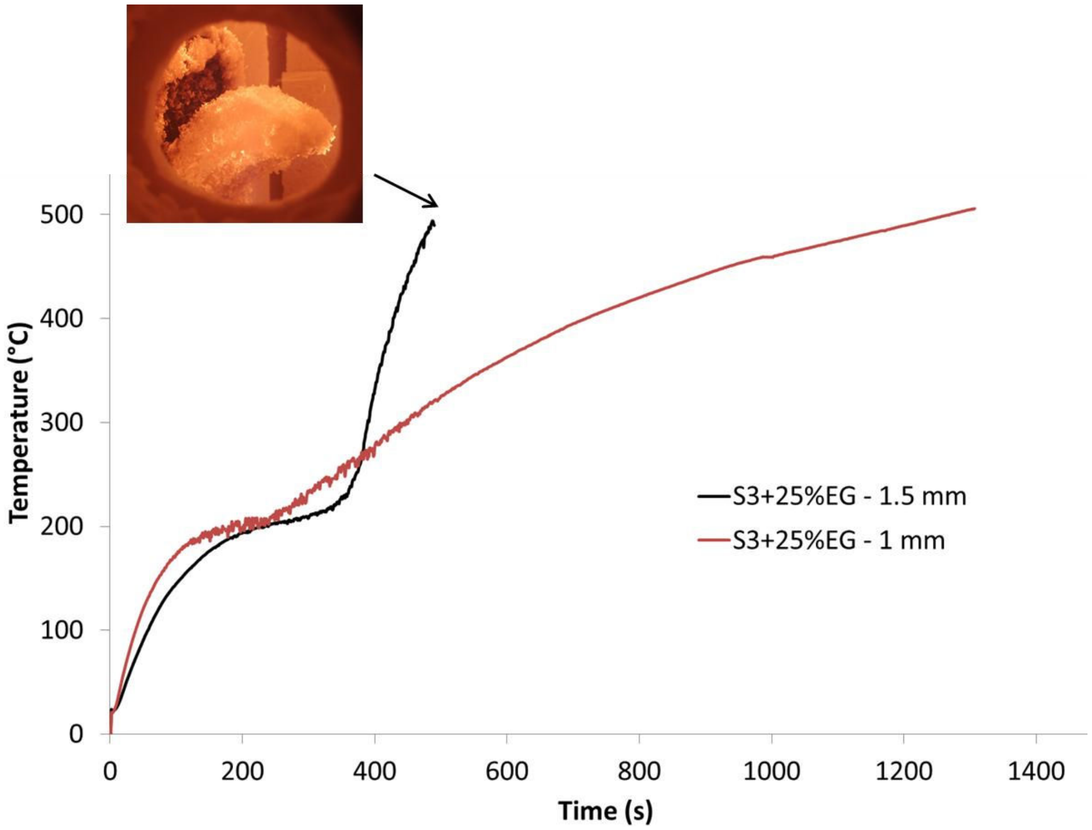

Figure 37: Temperature versus time curve of 1.5 mm S3+25%EG based coating in hydrocarbon fire scenario

In order to increase the cohesion of the char, organoclay is incorporated to the S3/EG formulation. The next step is thus dedicated to the fire performance of S3/EG/clay based coating.

III- 3 Resistance to fire of silicone/expandable graphite/clay based coatings in hydrocarbon fire scenario

III- 3.1 Introduction

The aim of this part is to evaluate the fire performance of thick (superior than 1 mm) silicone based coating in hydrocarbon fire scenario. The performances were evaluated in hydrocarbon fire scenario in the case of thick coating. The mechanical properties of the char was then investigated using a test previously developed in the lab[63]: the air jet test. In this test, 1 mm intumescent based coatings are exposed to an external heat flux (35 kW/m²) and the char is impacted by air flow (25 m/s). It is possible, by visual observation, to determine if the air jet destroys or not the intumescent char. This test gives thus good indications of the mechanical properties of the char.

Finally, the silicone/clay material was fully characterized by ^{29}Si NMR, transmission electronic microscopy (TEM), wide angle X-ray scattering (WAXS) and the chemical composition of the char was analyzed by X-ray fluorescence to better understand the effect of the organoclay.

III- 3.2 Results and discussion

Figure 38a shows the temperature versus time curve of 1.5 mm S3/EG and S3/EG/Clay based coatings.

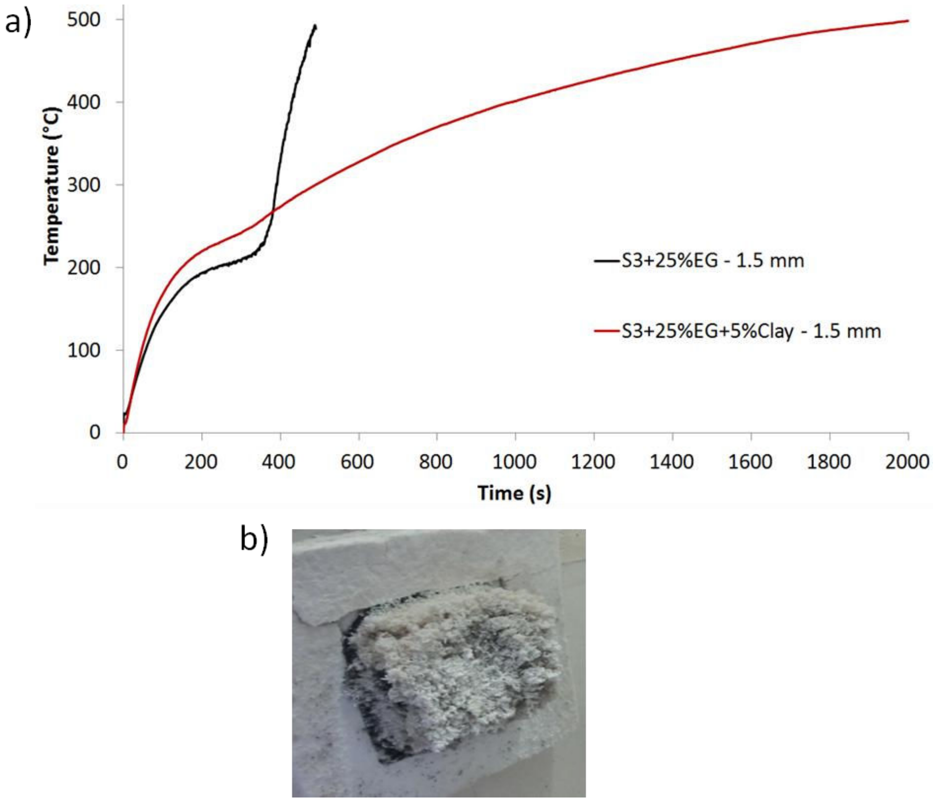

Figure 38: a) Temperature versus time curve in hydrocarbon fire scenario b) S3/EG/Clay residue after fire testing

When the clay is added to S3/EG based formulation, the char exhibits good cohesion (Figure 38b) and high fire performance - in this case, 500°C is reached in 2050s.

The mechanical properties of the two chars are investigated using the Air Jet test. It is shown that, the clay increases significantly the cohesion and the mechanical properties of the char and thus, better fire performance are achieved. This increasing of the cohesion properties of the char can be explained by (i) a decrease in the expansion rate or (ii) physical reinforcement due to the presence of the clay. Both assumptions are investigated.

The expansion ability of S3+25%+5%Clay based material is investigated using cone calorimeter test. Figure 39a) shows the expansion versus time of S3+25%EG and S3+25%EG+5%Clay when exposed to a 50kW/m² heat flux. It highlights the fact that the clay does not significantly affect the expansion ability (rate and velocity) of the S3+25%EG based material. Figure 39b) and c) show the expansion of both materials after 120s fire testing and demonstrate the similar expansion behavior of both materials.

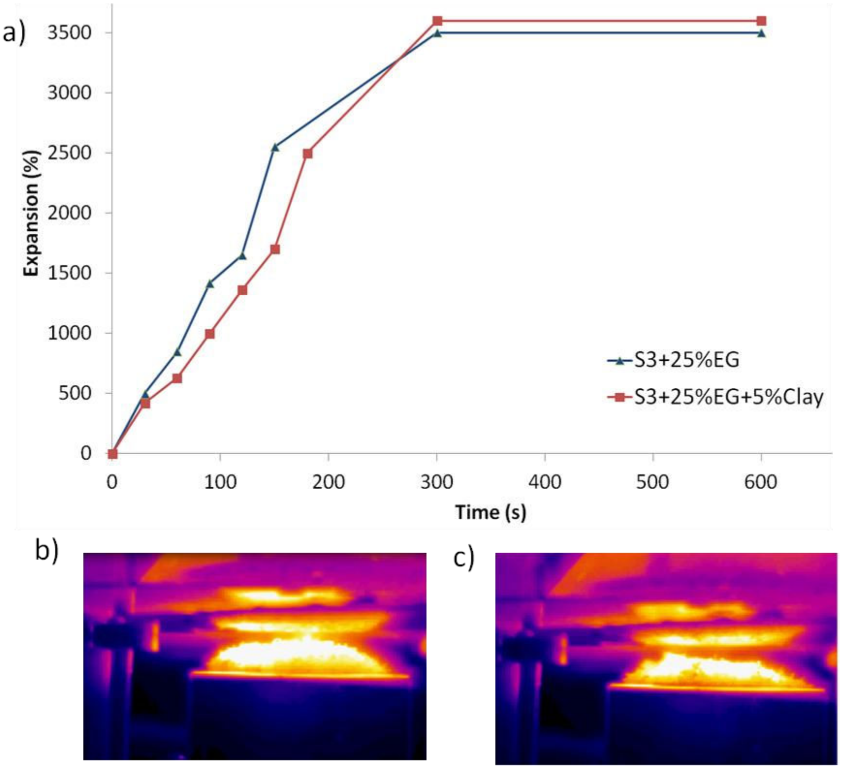

Figure 39: a) Expansion = f(t) of S3+25%EG and S3+25%EG+5%Clay exposed to 50kW/m² ; b) S3+25%EG and c)S3+25%EG+5%Clay pictures after 120s testing

It can thus be concluded that the clay does not limit the final expansion of the char. The improvement of the mechanical properties of the char should be due to physical reinforcement of the clay. To explain the mode of action of the clay, silicone matrix added with the clay was characterized using ^{29}Si solid state NMR, WAXS and TEM. These techniques enable to point out several interactions between the clay and the matrix. TEM images indicate the intercalation into some clay platelets of silicone resin as well as the presence of some tactoids. The WAXS analysis confirms and evidences an intercalation into the galleries of the clay of the resin. Moreover, solid state NMR demonstrates that chemical reaction between the hydroxyl groups of the edges of the clay and the silicone matrix occurs. Due to these interactions, the clay is dispersed in the whole part of the char. It is pointed out analysing different part of the char by X-ray fluorescence. A mechanism of action of organoclay is, thus, proposed and illustrated in Figure 40.

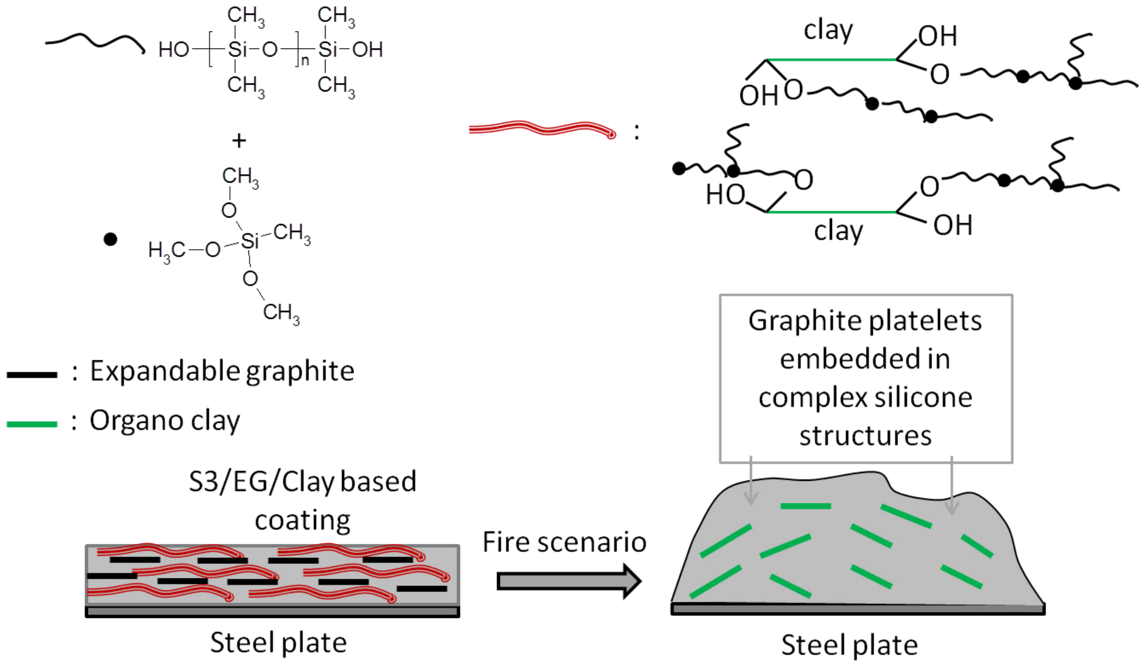

Figure 40: Mode of action of organoclay in S3+25%EG+5%Clay coating

When S3/EG/Clay based coating is exposed to hydrocarbon fire scenario, the graphite platelets expand and are embedded in a complex and cohesive silicone structure. Moreover, the clay platelets are well dispersed in the whole char and no decantation or surface migration is observed. The reinforcement of the char takes place thanks to specific reactions between the hydroxyl groups of the clay and the silicone and also, with intercalation of the silicone chains into the galleries of the clay. The char thus presents high mechanical properties and hence high fire protective behavior. In this case, it is possible to develop 1.5 mm silicone based coating exhibiting high fire performance.

However, in hydrocarbon fire scenario, the thickness of the intumescent coating used can reach 3-5 mm. The formulation containing clay was therefore tested at 3 mm. Figure 41 shows the temperature versus time obtained. During the first minutes of the test, the fire performance of 3 mm based coating is higher than that of 1.5 mm. However, the expansion of the coating is too high and the char reinforcement by the clay is not sufficient to maintain the cohesion of the whole part of the char. Consequently, a part of the char falls off during the fire test explaining the knee point at 400s for the 3 mm formulation on the temperature versus time curve. The insulative properties of S3+25%EG+5%Clay are therefore similar at 1.5 mm and 3 mm.

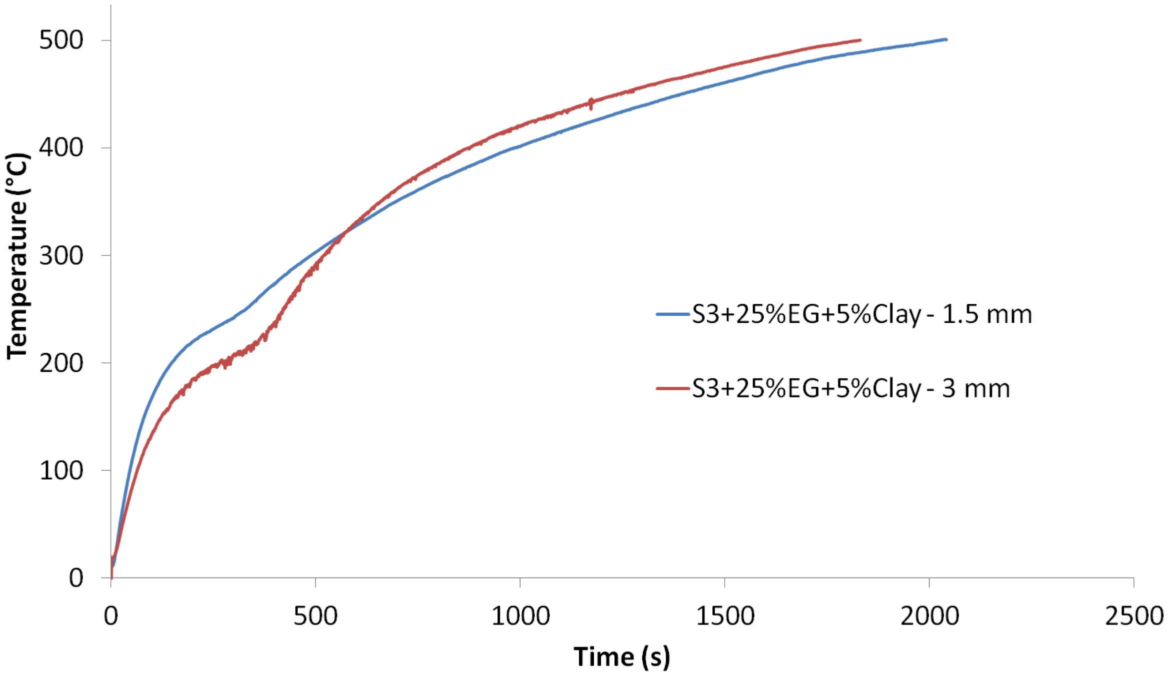

Figure 41: Temperature versus time curve of S3+25%EG+5% clay at 1.5 mm and 3 mm in hydrocarbon fire

Figure 42 b) evidences the fact that a part of the char falls down during the test for 3 mm coating.

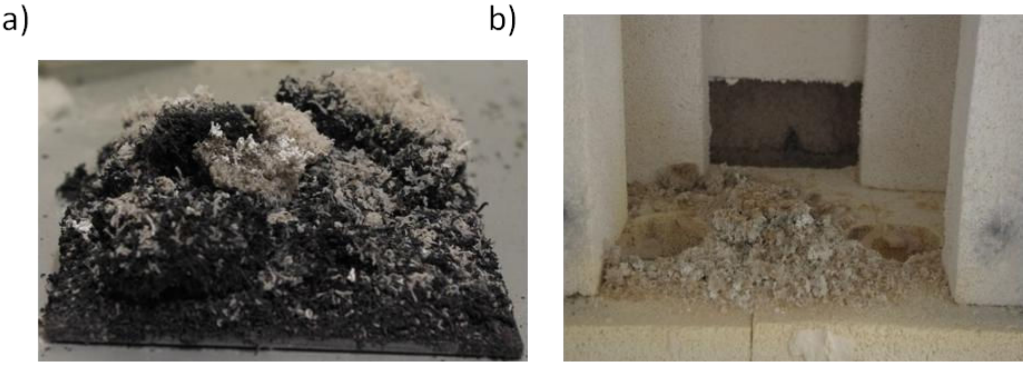

Figure 42: a) Residue of S3+25%EG+5%Clay 3 mm residue and b) inside the furnace after hydrocarbon fire

Finally, even if the mechanical properties of the char is increased adding the clay, it seems to be the limited factor for very thick intumescent coating.

After evaluating the fire protection of steel by silicone coating against simulated hydrocarbon fire, new formulations are developed for its protection in cellulosic fire.

III-4 Fire performance of silicone based coating in cellulosic fire scenario (standard ISO834)

III- 4.1 Introduction

We have shown in the second chapter that RTV silicone rubber added with calcium carbonate (GCC) exhibits insulative performance in cellulosic fire scenario. However, its performance is limited compared to that of commercial intumescent paint because of the non-swelling behavior of the coating. Moreover, in the previous part we show that EG can be used advantageously to form an expanded char structure exhibiting good cohesion. In this part, the fire performance of S3/EG added with calcium carbonate and reinforcement fillers such as clay is thus evaluated in cellulosic fire scenario.

III- 4.2 Fire properties of high loading silicone formulations

The tested formulations are summed up in the Table 5. Fire performance of 1 mm intumescent based coating is tested in cellulosic fire scenario (ISO834). An acrylic commercial intumescent paints Intuflam supplied by Lurie is used as reference.

Table 5: Silicone formulations exposed to cellulosic fire scenario

Formulations	F1	F2	F3
Silicone matrix (S3)	75%	50%	56%
Expandable graphite	25%	25%	20%
Calcium carbonate (GCC)	-	25%	20%
Clay	-	-	4%

The temperature / time curves obtained in cellulosic fire scenario are presented in Figure 43.

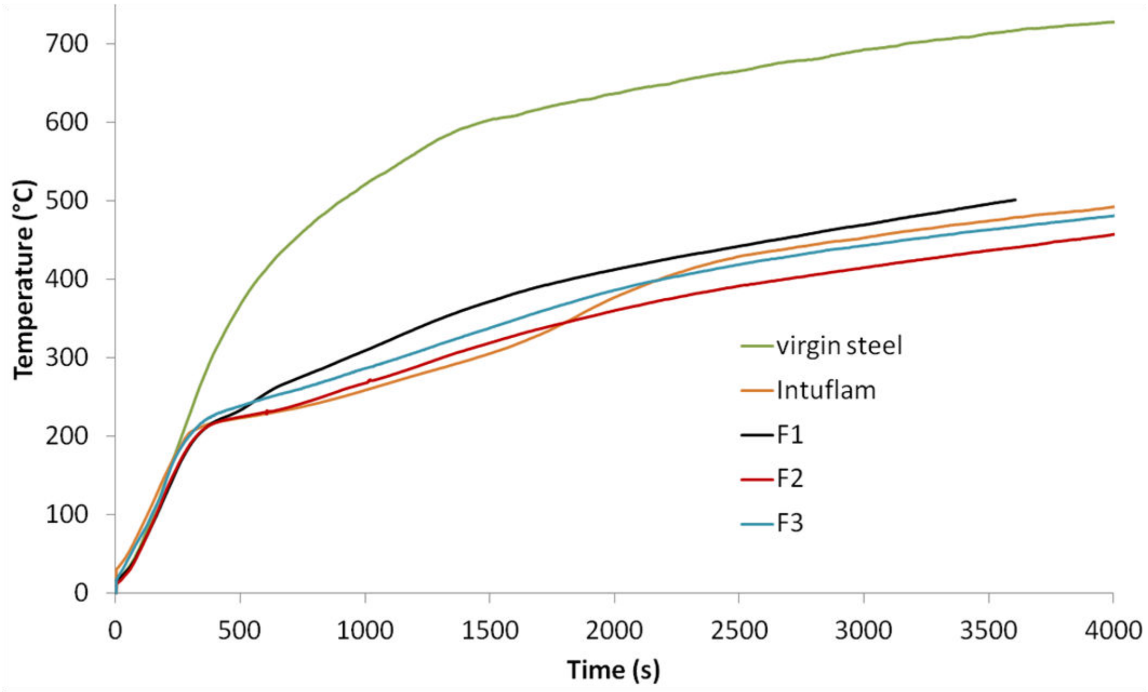

Figure 43: Temperature versus time curve of intumescent coating tested in cellulosic fire scenario

When 25% of EG is added to S3, the fire performance was limited compared with that of commercial intumescent paint. Indeed, critical temperature is reached in 3585s whereas at the end of the test (after 4000s) the temperature at the back side of Intuflam is 492°C and the critical temperature is therefore not reach for Intuflam based coating. When 25% of GCC is added to the previous formulation, silicone based coating exhibits better fire performance than the commercial intumescent paint. At the end of the test, the temperature at the back side of the plate reaches 465°C. However, the cohesion properties of the char is poor, it can be very easily removed from the plate. F2 residue after furnace test is shown in Figure 44. A high expansion (about 3500%) is observed and, as previously reported, the char is composed of a white powder at the surface and the heart remains black.

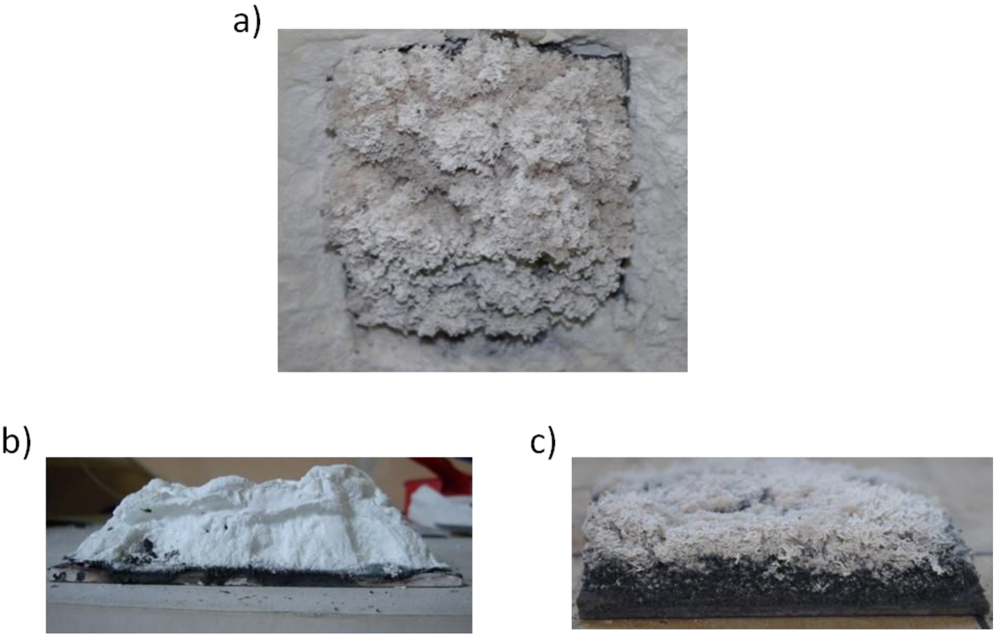

Figure 44: a) F2 residue, b) Intuflam residue and c) F3 residue after furnace test in cellulosic fire scenario

To increase the mechanical properties of the char, the amount of expandable graphite was decreased and 4% of clay was added to the S3/GCC/EG based coating. The temperature versus time curve of F3 (Figure 43) highlights that F3 based coating exhibits similar fire performance as commercial intumescent paint and is better than those of S3/EG based coating. The final temperature reaches for F3 is 470°C. F3 residue exhibits a high expansion rate (3000%), which is in the same order of magnitude as that of Intuflam based residue (Figure 44b and c). As previously observed, the F3 based residue is composed of two main parts, a white powder covers the top of the char and its heart remains black. The next step of the study was thus dedicated to study the mode of action of calcium carbonate pointing out the degradation pathway of F3 based formulation.

III- 4.3 Mode of action of calcium carbonate in cellulosic fire scenario

At First, the thermal stabilities of the silicone matrix and of the silicone matrix added with 27% of calcium carbonate (to keep the ratio silicone matrix/GCC constant) are investigated in nitrogen flow. Then, the residue of F3 after furnace test is analyzed by X-ray photoelectron spectroscopy (XPS), FTIR and XRD to propose a mode of action of F3 based coating.

III- 4.2.1 Thermal stability

First of all, thermal stability of S3, GCC and S3+27%GCC are investigated at 10 °C/min under nitrogen flow and the remaining mass versus temperature is presented in Figure

45. For virgin silicone matrix, the thermal degradation occurs in one step with a residue of 2% at 800°C. The temperature at which the degradation rate is maximum is 655°C. For, GCC, thermal degradation occurs in one step leading to a residue of 55% and the temperature maximum degradation is 745°C. When 27% of GCC is incorporated to the silicone matrix, the thermal degradation occurs in two steps, the temperature where the degradation is maximal for both steps are respectively 650°C and 750°C. The weight losses for the two steps are respectively 68% and 13%. The first step corresponds to the degradation of the silicone matrix leading to the released of cyclic oligomers of silicone and the second of carbon dioxide as we have shown in the second chapter (analyzing the gas evolved during the thermal degradation of S2+50%GCC).

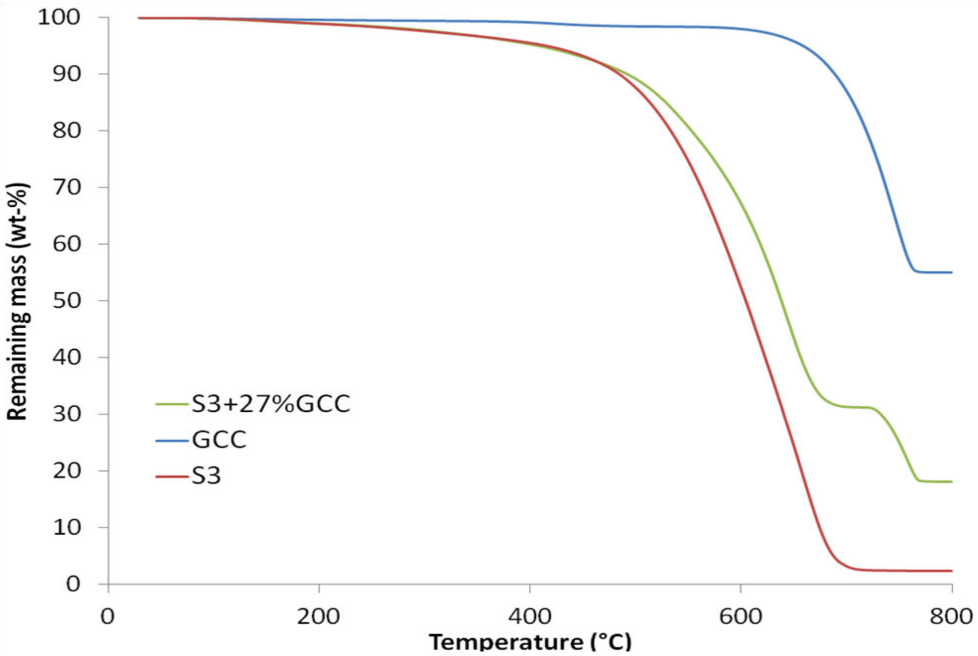

Figure 45: TGA of S3, S3+27%GCC and GCC in nitrogen flow at 10°C/min

In order to determine whether a potential increase or decrease in the thermal stability takes place between the silicone matrix and the calcium carbonate, the difference weight loss curves between experimental and calculated TG curves were computed as follows[14] :

$M_{silicone}(T)$: values of weight given by the TG curve of the silicone matrix

$M_{GCC}(T)$: values of weight given by the TG curve of the calcium carbonate

Mexp(T): values of weight given by the TG curve of the mixture (S3+27%GCC)

Mcal(T): calculated TG curve computed by linear combination between the values of weight given by the TG curve of both additives: $Mth(T) = 0.73*M_{silicone}(T) + 0.27*M_{GCC}(T)$

$\Delta(T)$: difference weight loss curve: $\Delta(T) = Mexp(T) - Mcal(T)$.

The Δ(T) curve allows us to show a potential increase or decrease in the thermal stability of the system. The Mexp (T), Mcal (T) and Δ(T) curves are presented in the Figure 46.

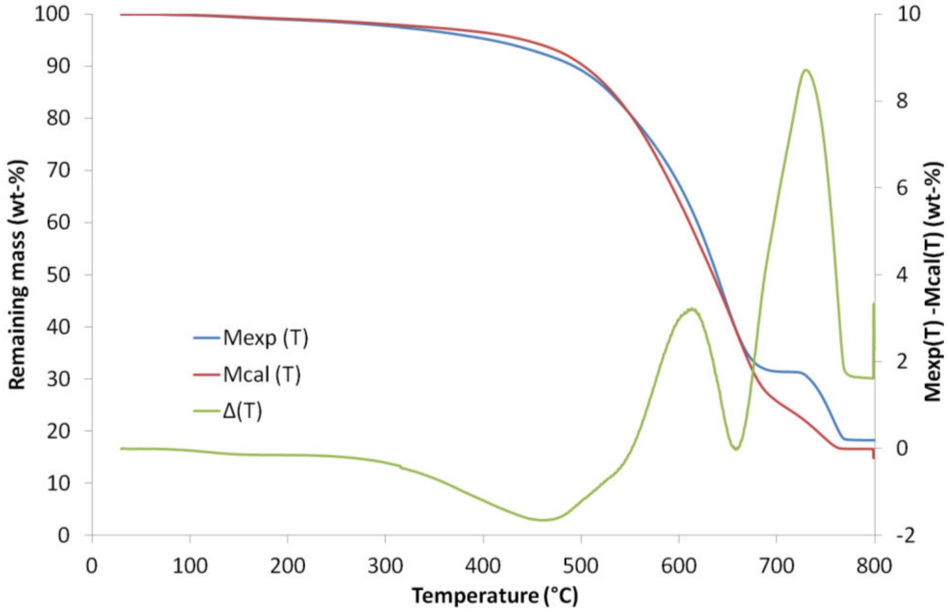

Figure 46: TGA experimental and calculated curves of S3+27%GCC in nitrogen flow at 10%C/min

The calculation of the difference weight loss curve of the silicone matrix, GCC and the mixture of the two components shows unambiguously that an interaction (physical or chemical) occurs between 650°C and 750°C leading to a stabilization of the system. In this range of temperature, the degradation of silicone matrix and of calcium carbonate occurs leading to the formation of SiOx and CaO which could react together. Hermansson et al. highlighted that at high temperature degradation products from PDMS and CaO should react together leading to calcium silicate[59] (Figure 47).

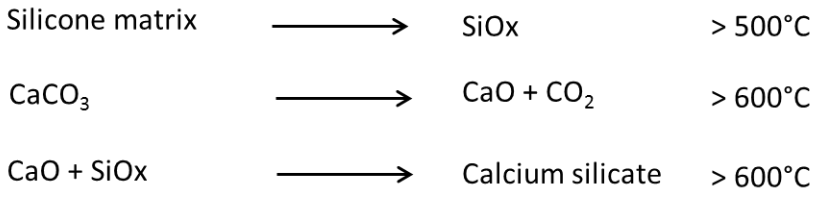

Figure 47 : Successive reactions leading to calcium silicate up to 600°C

Thermal analysis of S3 and S3+27%GCC evidences that interactions (chemical or physical) occur between the matrix and the filler leading to an increasing of the thermal stability of the system. The next part is dedicated to the characterization of the residue of F3 obtained after cellulosic fire scenario to propose a mode of action of calcium carbonate in S3/EG based coating.

III- 4.2.2 Characterization of F3 residue after cellulosic fire scenario

The top and the bulk part of the char (F3 residue) are analyzed by FTIR, XPS and XRD.

In a first step, both parts of the char are analyzed by FTIR/Attenuated total reflection (ATR) spectroscopy and the spectra are presented in Figure 48.

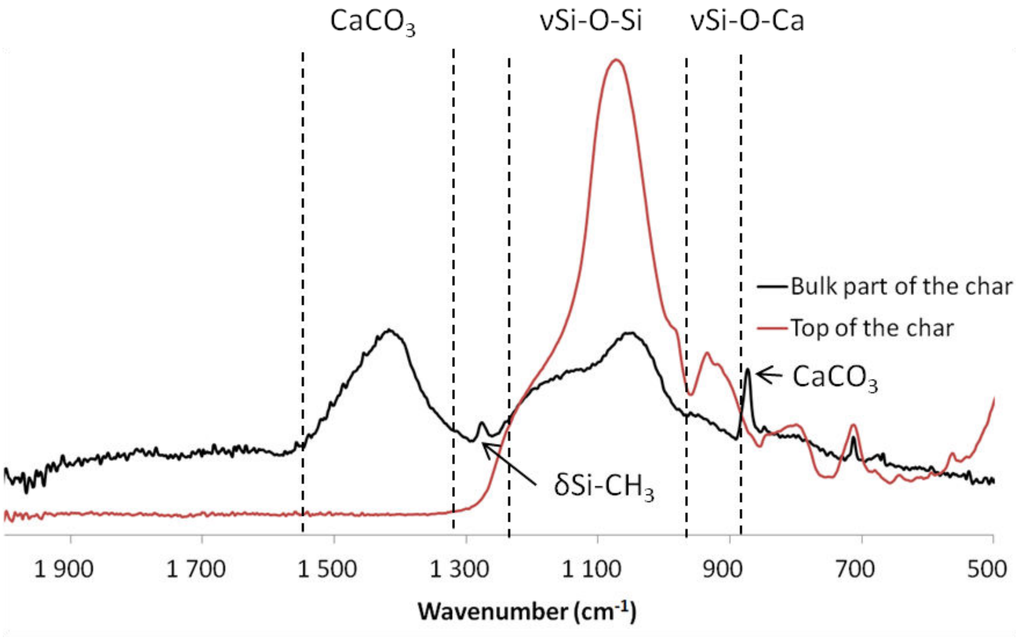

Figure 48: FTIR spectra of the top and the bulk part of the char obtained from S3/EG/GCC after cellulosic fire scenario

The spectrum of the top of the char presents two main broad bands. The first, between 1000 cm^{-1} and 1100 cm^{-1} is assigned to the stretching vibration of Si-O-Si bounds. The second around 950 cm^{-1} is characteristic of the stretching vibration of Si-O-Ca bound[64] of calcium silicate. For the bulk part of the char the same peaks as previously detailed appear and three additional bands are observed at 1420cm^{-1} ; 875 cm^{-1} (both corresponding to calcium carbonate[65]) and 1260 cm^{-1} (characterizing the bending vibration of Si-CH_3 bound from the silicone matrix).

In order to confirm the presence of calcium silicate in the char, both parts are analyzed by XPS. The survey obtained is presented in Figure 49. It shows that the char is composed of silicon, oxygen, carbon and calcium. As aluminium is not detected in the survey, we can assume that the clay is not detected. The intensity of calcium and silicon are higher for the top of the char sample than for the bulk part of the char whereas there is more carbon in the bulk than in the top of the char.

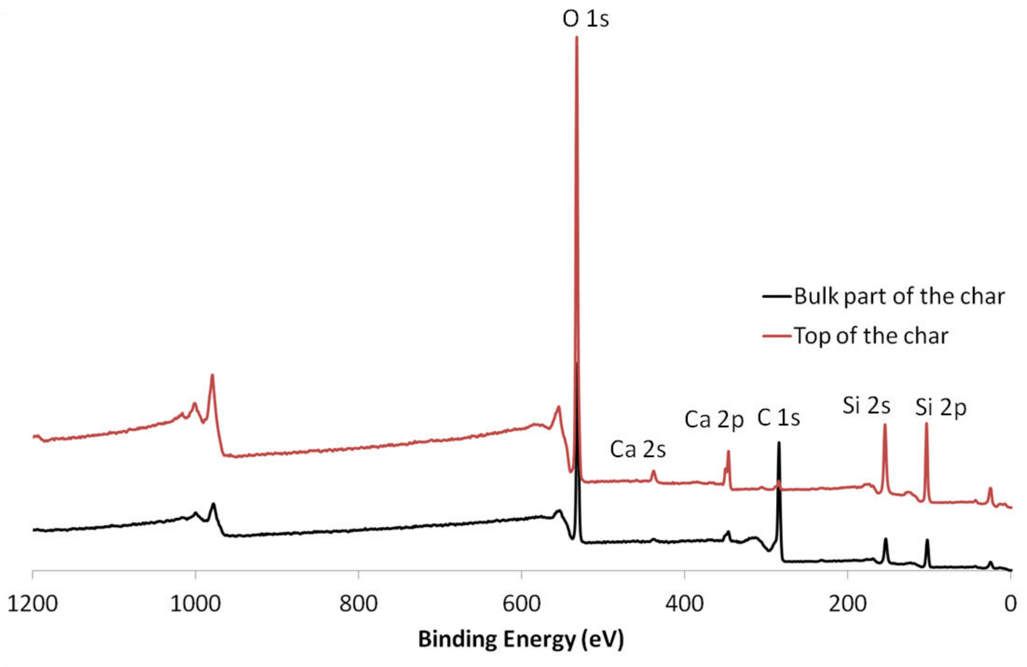

Figure 49: Survey of the bulk part and the top of the char of F3 obtained after furnace test (ISO834)

The analysis of the Ca2p spectrum highlights the presence of the calcium species with an oxidation degree of +II for the two specimens. However, the C1s spectrum (Figure 50) of the bulk part of the char demonstrates the presence of carbide species with a peak around 283 eV. The peak around 285 eV corresponds to C-C from the graphite. In the top of the char, carbon species are more oxidized since a broad peak at 289 eV is observed.

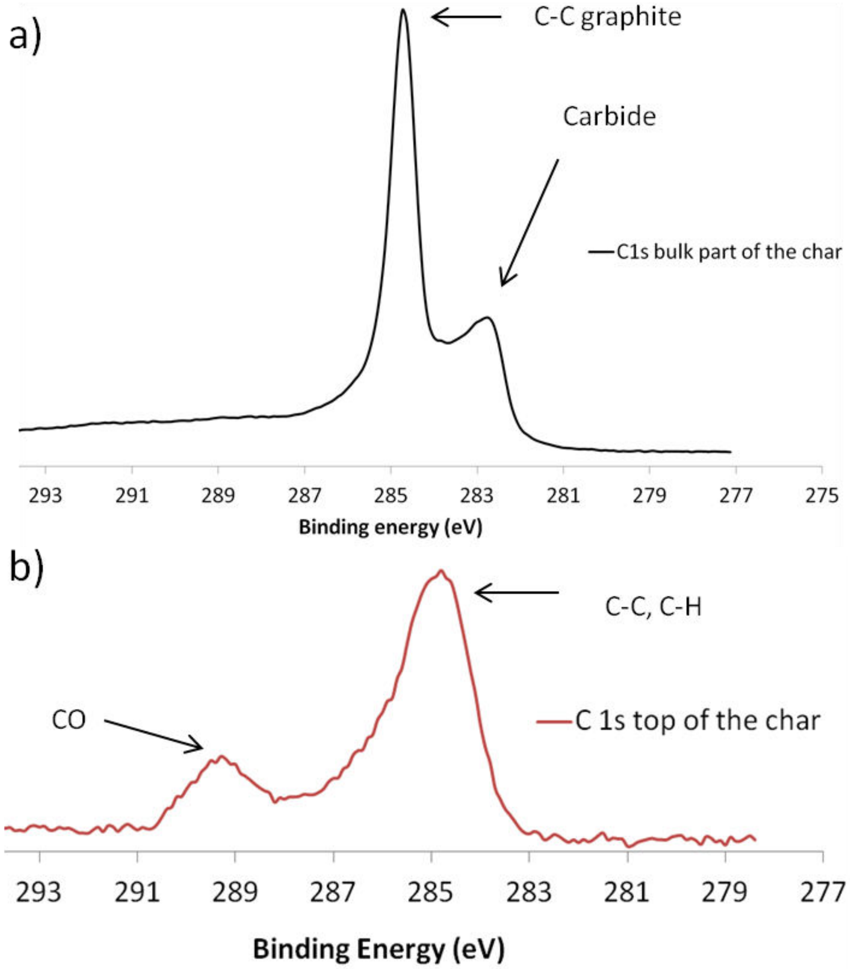

Figure 50: C1s spectrum of the bulk part and of the top of the char obtained from F3 after furnace test (ISO834)

Concerning silicon species, Si2p spectrum of the two specimens are shown in Figure 51. The results of the deconvolution are summed up in the Table 6. The Si2p XPS spectrum of the top part of the char can be decomposed into two main peaks at 101.3 ± 0.2 eV and 103.9 ± 0.2 eV. The first is assigned to calcium silicate[66] and the second to $SiO_{4/2}$ silicon structures. The Si2p XPS spectrum of the bulk part of the char exhibits a broad peak demonstrating the contribution of several silicone structures. The deconvolution of this peak gives peaks at 100.9 ± 0.2 eV, 101.9 ± 0.2 eV, 102.8 ± 0.2 eV and 103.9 ± 0.2 eV corresponding respectively to SiC, $SiO_{2/2}$ and/or calcium silicate, $SiO_{3/2}$ and $SiO_{4/2}$ silicone structures.

Table 6: Binding energy of Si 2p3/2 bands for the top and the bulk part of F3 residue after cellulosic fire testing

	SiC	**Calcium silicate**	**$SiO_{3/2}$**	**$SiO_{4/2}$**	**FWMH**
Top of the char	-	101.3 ± 0.2 eV	-	103.9 ± 0.2 eV	1.65
	SiC	**$SiO_{2/2}$**	**$SiO_{3/2}$**	**$SiO_{4/2}$**	**FWMH**
Bulk part of the char	100.9 ± 0.2 eV	101.9 ± 0.2 eV	102.8 ± 0.2 eV	103.9 ± 0.2 eV	1.39

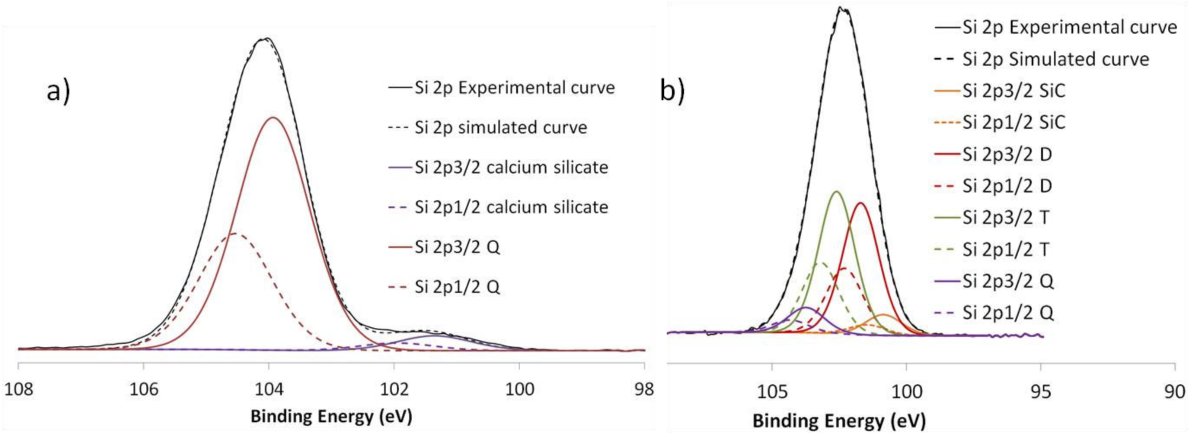

Figure 51: Si2p spectrum of a) the top and b) the bulk part of the char obtained from F3 after furnace test (ISO834)

The XPS experiments are consistent with the FTIR results obtained and demonstrate the formation of calcium silicate at high temperature on the top of the char. In order to determine the cristallinity of the species present in the bulk and in the top of the char, the two parts are analyzed by XRD. The obtained patterns are presented in Figure 52. Figure 52a) evidences the presence of graphite and calcium carbonate in the bulk part of the char whereas several peaks appear on the pattern of the top of the char demonstrating the crystallization of different calcium silicates. Indeed, the superposition of both patterns (Figure 52c) shows that other species than calcium carbonate and graphite compose the top of the char. However, the cristallinity of these species is too low to determine which kinds of calcium silicates coat the top of the char.

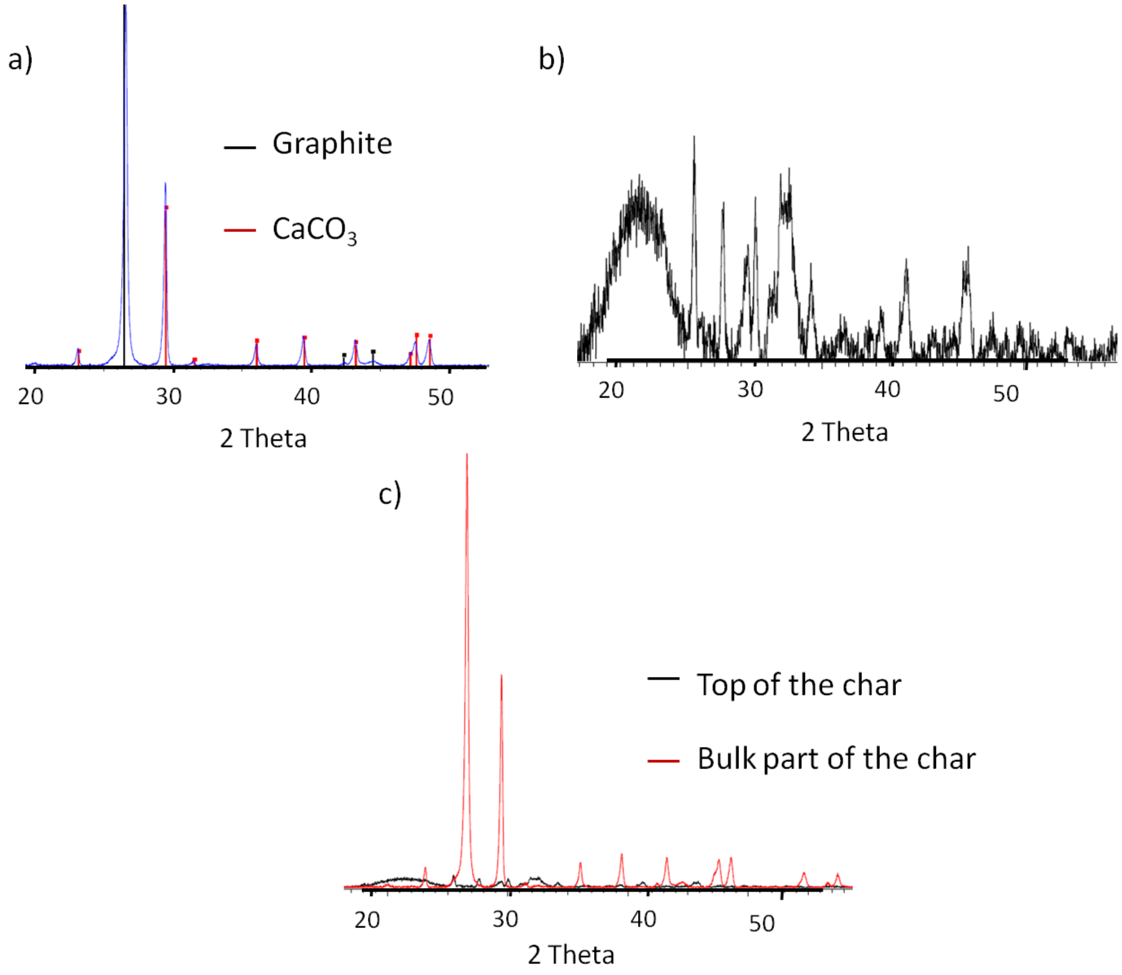

Figure 52: XRD pattern of a) the bulk part of the char, b) the top of the char and c) both part of the char obtained from F3 after furnace test (ISO834)

III- 4.2.3 Discussion

In this part, fire performance of S3/EG containing calcium carbonate and organoclay are evaluated in cellulosic fire scenario. It was shown that, intumescent silicone based coating exhibits similar fire performance as commercial intumescent paint.

It is shown that, as we reported for hydrocarbon fire scenario, the graphite platelets - composing the bulk part of the char, are embedded in complex silicone structure composed of the degradation products of the silicone matrix. The XPS and FTIR analyses demonstrate that the top of the char is composed of Q structure and calcium silicate. XRD reveals that calcium carbonate is still present in the bulk part of the char. Moreover, XPS experiments also show the formation of SiC, $SiO_{2/2}$, $SiO_{3/2}$ and $SiO_{4/2}$ structures. In the particular case of calcium silicate, it is impossible to distinguish its binding energy with that of the D structures (the main component of the formulation). The D, T and Q structures embed therefore the graphite platelets insuring the good cohesion of the char as reported previously in hydrocarbon fire scenario.

In cellulosic fire scenario, calcium carbonate reacts with the silicone matrix leading to the formation of calcium silicate and migrates to the top of the char embedding graphite platelets. This interaction between calcium carbonate and silicone matrix increases the thermal stability of the matrix and permits the formation of an additional protective ceramic layer composed of calcium silicate. Consequently, in cellulosic fire, the S3/EG/GCC based coating exhibits better fire performance than S3/EG based coating and similar insulative properties than those of a commercial intumescent paint.

III-5 Conclusion

In this chapter, we have investigated the fire performance of RTV silicone added with expandable graphite in hydrocarbon and cellulosic fire scenario.

In hydrocarbon fire scenario, silicone intumescent coating exhibits high fire performance, better than that of a commercial intumescent paint. This is explained by a high expansion - around 3400% ; a high expansion velocity - 18%/s and a low thermal conductivity at high temperature. The good cohesion of the char is due to (i) the presence of undegraded matrix; and (ii) the coating of the graphite platelets by cross-linked silicone structure. To increase the mechanical properties of the char, organoclay was added to the silicone/EG based coating. Because of specific interactions between the silicone matrix and the clay and of the good dispersion of the clay, the mechanical properties of the char are enhanced. The fire performance of the intumescent coating is also increased specially for thick coating.

In cellulosic fire scenario, calcium carbonate has to be added to the silicone matrix to reach the same fire performance as those obtained for commercial intumescent paint. In this case, calcium carbonate reacts with silicone matrix increasing its thermal stability and leading to the formation of calcium silicate which embeds the top of the char

The main conclusions obtained are summed up in the Table 7.

Table 7 : Fire performance of S3 RTV silicone based coating in two different fire scenarios

	Low loading silicone formulation (S3/EG - S3/EG/Clay)	**High loading silicone formulation (S3/EG/GCC - S3/EG/GCC/Clay)**
Applications	Hydrocarbon fire scenario	Cellulosic fire scenario
Mode of action of the intumescent silicone based coating	Better fire performance than commercial intumescent paint due to : - High expansion rate and velocity - Good mechanical properties of the char when clay is added - Low thermal conductivity at high temperature	Same fire performance as commercial intumescent paint GCC and silicone matrix reacts leading to calcium silicate increasing the thermal stability of the matrix Calcium silicate migrates at the surface and coats the top of the char leading to the formation of an additional protective ceramic

Depending on the formulation, it is thus possible to develop innovative intumescent silicone based coatings exhibiting better or similar fire performance than commercial intumescent paint for the steel protection against simulated fire (cellulosic and hydrocarbon). However, in hydrocarbon fire scenario the limited factor seems to be the mechanical properties of the char to test thick silicone intumescent coating. The next chapter will therefore deals with the development of new formulations in order to be able to test 3 mm thick coating.

Chapter IV: Resistance to fire of high cross-linked RTV silicone

IV-1 Introduction

In order to reach better fire performance in hydrocarbon fire scenario, one of the easiest ways is to increase the initial thickness of the coating. Indeed, epoxy-based intumescent coatings are usually applied with a thickness of at least 3 mm to allow reaching high time to failure in hydrocarbon fire scenario. However, one main issue associated with a high thickness, is the adhesion of the coating on the steel plate and its cohesion. Indeed, if the expansion of the coating is very high and if the cohesion of the intumescent structure is too low, it will lead the protective char to fall off during the experiment and thus the protection is lost.

Several approaches can be used to avoid it. For example, in the case of epoxy based system, a mesh is usually added in the middle of the coating to maintain the integrity of the protective char layer[63]. In the previous chapter, we demonstrated that it is possible to improve the integrity of the char using mineral fillers but this effect is limited. Thus, in this chapter another approach will be followed. In the state of the art, we reported that high cross-linked silicone matrix present a higher thermal stability and **higher char yield**. It thus appears than another way to modify the mechanical properties of the char is to play on the cross-link density of the matrix.

The aim of this chapter is to evaluate the influence of the crosslink density of the RTV silicone matrix on the mechanical properties of the char and on the fire performance of thick silicone intumescent coating in hydrocarbon fire scenario. In order to increase the crosslink density of the matrix two ways are examined. It is not possible to increase the amount of cross-linked agent since it is added in large excess. Consequently, in a first way, **hydrophilic fumed silica** (with hydroxyl function at the surface of the particle) is added to the S3 based RTV silicone matrix. The hydroxyl function of PDMS can react with fumed silica[67] and therefore increase the crosslink density of the RTV silicone. The matrix will be characterized by ^{29}Si CPMAS NMR and the fire performance of S3 added with EG/Fumed silica/clay is investigated in hydrocarbon fire scenario. In a second way, the hydroxyl contents of hydroxyl PDMS was increased and **S1** (the same as the one used in the second chapter) is used as hydroxyl PDMS. We have shown in the second chapter that, fire performance of S1 based coating is limited due to its low thermal stability and low thermal properties (high thermal diffusivity at high temperature). However, the catalyst used to make this resin crosslink was a tin based catalyst whereas it is a titanium based catalyst for S3 based RTV silicone. The influence of the catalyst used to make the RTV silicone crosslink will be therefore fully investigated.

This part is based on the following paper:

B.Gardelle, S.Duquesne, P.Vandereecken, S.Bellayer and S.Bourbigot - Resistance to fire of curable silicone/expandable graphite based coating: effect of the catalyst – **European Polymer Journal,** 2013, In press.

For the two approaches, the strategy will be to first determinate the influence of the cross-linked density on the mechanical properties of the char for silicone/25%EG based coating using the air Jet test described in the last chapter. Then, the fire performance of 3 mm based coating are evaluating for the fire protection of steel against a simulated hydrocarbon fire.

IV-2 Resistance to fire of S3/EG/fumed silica/Clay based coating in hydrocarbon fire scenario

IV-2.1 Introduction

The aim of this part is to evaluate the influence of hydrophilic fumed silica - Aerosil 200 supplied by Degussa - in the crosslink density of the matrix and on the fire performance of S3/EG/Clay based coating. In a first step, the matrix added with fumed silica is fully characterized using solid state ^{29}Si NMR. In a second step, fire performance of S3/EG/Fumed silica/Clay based coatings is evaluated in hydrocarbon fire scenario.

IV-2.2 Results and discussion

IV-2.2.1 Silicone/Fumed silica characterization

At first, fumed silica and S3 added with 1.5% of fumed silica are characterized using ^{29}Si solid state NMR. The spectra obtained are presented in Figure 53. For pure fumed silica, three peaks are observed at - 91 ppm, -100 ppm and -110 ppm corresponding to respectively Q^2, Q^3 and Q^4 structures. Q^2 and Q^3 structures highlight the presence of hydroxyl groups at the surface of the silica particle. Concerning S3/Fumed silica material, the peak at - 22 ppm, - 48 ppm, -57 ppm and -66 ppm correspond respectively to D, T^1, T^2 and T^3 structures coming from the silicone matrix (as reported previously). However, two additional peaks appear at - 100 ppm and -110 ppm corresponding to the Q^3 and Q^4 structure and no peak assigned to Q^2 structure can be distinguished.

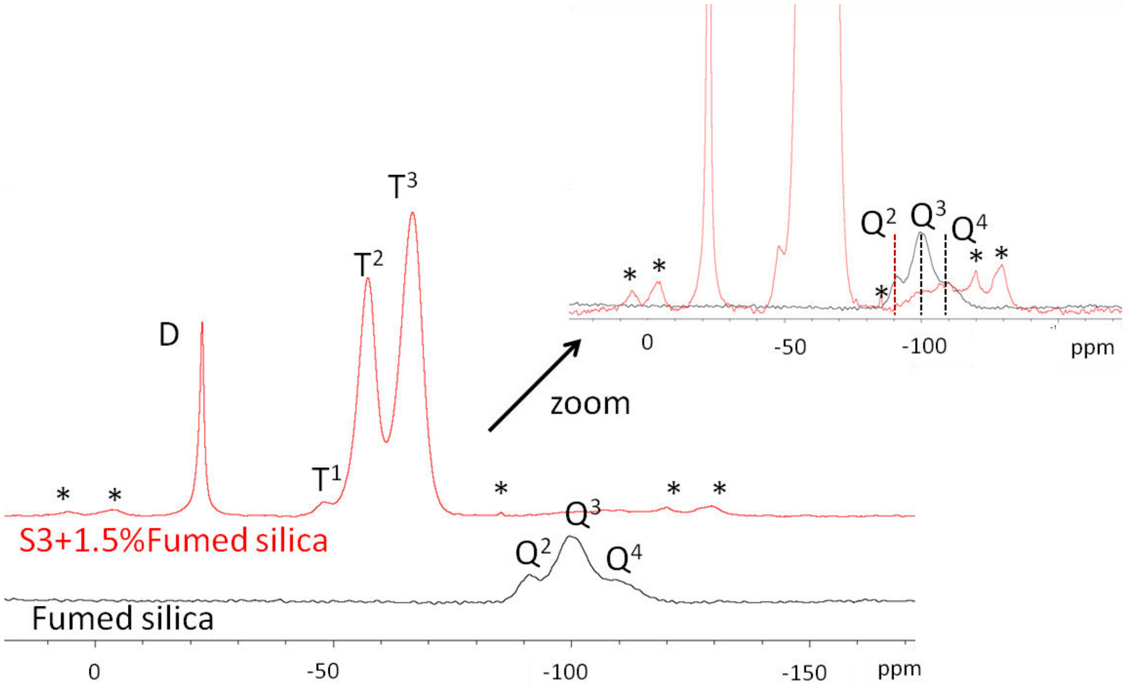

Figure 53: 29Si CPMAS NMR spectra of fumed silica and S3/Fumed silica. (*spinning side band)

It shows that there are chemical reactions between the silicone matrix and hydroxyl groups at the surface of the silica leading to the formation of high cross-linked silicone network as illustrated in Figure 54.

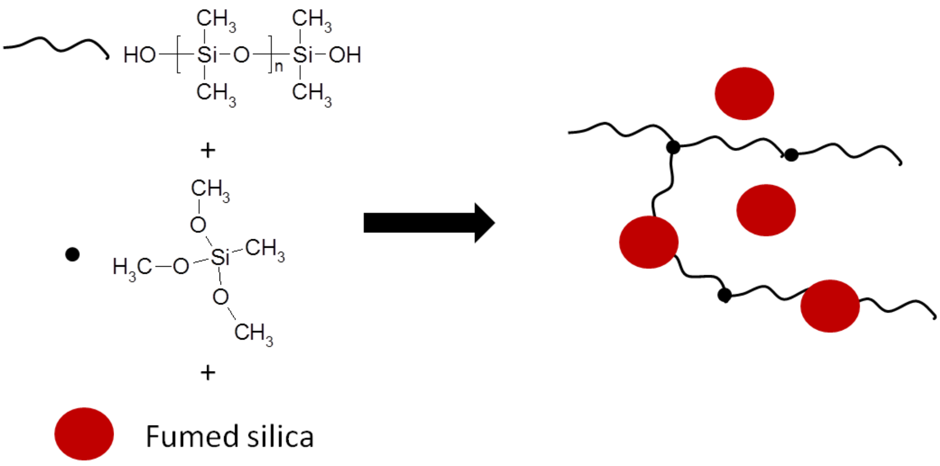

Figure 54: Illustration of the formation of a cross-linked silicone network when fumed silica is added to S3

IV-2.2.2 Mechanical properties of the char and Fire performance

The influence of the fumed silica on the mechanical properties is firstly investigated. The two matrices - S3 and S3+1%Fumed silica - containing 25% of EG were tested using the air jet test. Figure 55 illustrates the residue after the test and in both cases; the char was completely destroyed by the air impact. This suggests that fumed silica does not increase significantly the cohesion of the char.

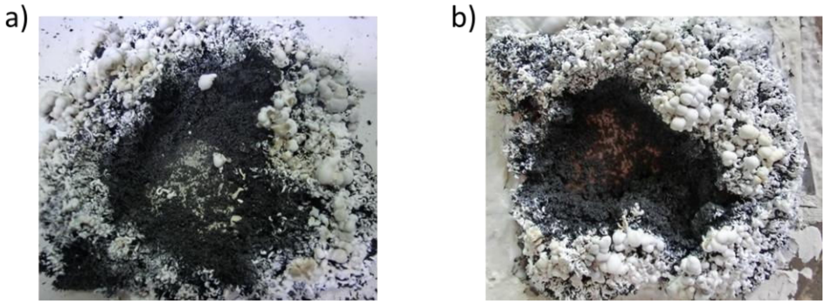

Figure 55: Residue of a) S3+1%Fumed silica+25%EG and b) S3+25%EG after Air jet test

The next step is to evaluate the fire protection of steel against hydrocarbon fire for 3 mm based coating. Figure 56 shows the temperature versus time curves. In both cases, a part of the char falls off during the fire test explaining the knee point of the temperature/time curve after 400s testing. Consequently, the insulative performance of the two formulations is similar.

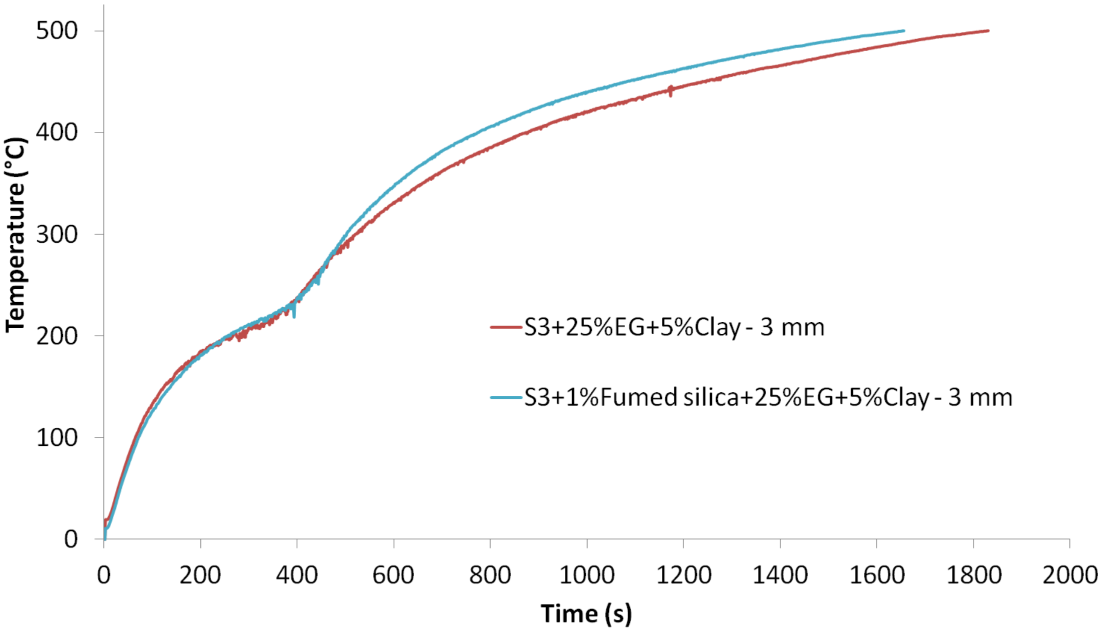

Figure 56: Temperature versus time curve of 3 mm of S3/EG/Clay and S3/EG/fumed silica/Clay in hydrocarbon fire scenario

Finally, the fact to increase the crosslink density of the silicone matrix incorporating fumed silica does not play a significant role on the mechanical properties of the char and on the fire performance of S3/EG/clay based coating. The other way to increase the cross-linked density of the matrix is to modify the hydroxyl PDMS used. That is why, in the next step, the amount of hydroxyl group of the hydroxyl PDMS is significantly increased using shorter length chain than that used for S3.

IV-3 Resistance to fire of high cross-linked RTV silicone rubber: Effect of the hydroxyl PDMS

IV-3.1 Introduction

The silicone resin used in this part is composed of an hydroxylated PDMS with a viscosity of 80 cS (viscosity is measured using cone/plate rheometer CP-52), methyltrimethoxysilane (MTM) as crosslinking agent and an organometallic catalyst- called **S1**. For this kind of RTV silicone rubber tin based catalyst is usually used. However, as we have shown in the second chapter, this RTV silicone containing calcium carbonate exhibits low insulative performance due to its low thermal stability. In this part, this silicone matrix was cross-linked with titanium-based catalyst and the influence of the catalyst used is fully investigated in hydrocarbon fire scenario. The first silicone resin cross-linked with tin based catalyst was called **S1-Sn** and that with titanium based catalyst **S1-Ti**. The cross-link density of each resin is first determined by ^{29}Si solid state NMR and then the mechanical properties of the char is characterized by air jet test

IV-3.2 Results and discussion

IV-3.2.1 S1-Sn and S1-Ti characterization

First of all, morphology of S1-Sn and S1-Ti are characterized using ^{29}Si NMR to evaluate the crosslink density of the matrix. Figure 57 shows the ^{29}Si NMR spectrum of both silicone matrices. On the S1-Sn spectrum, three peaks can be distinguished at -22 ppm, -58 ppm and -67 ppm assigned to D, T^2 and T^3 structures respectively. Concerning, S1-Ti spectrum, three peaks can be distinguished at -19 ppm, -22 ppm corresponding to D structures and an additional broad band at -67 ppm characterizing T^3 structure. The explanation of the peak at -19 ppm and why the peak at -67 ppm is broader when titanium based catalyst is used will be explained later in the chapter. The aim of this part is to evaluate the crosslink density of the matrix.

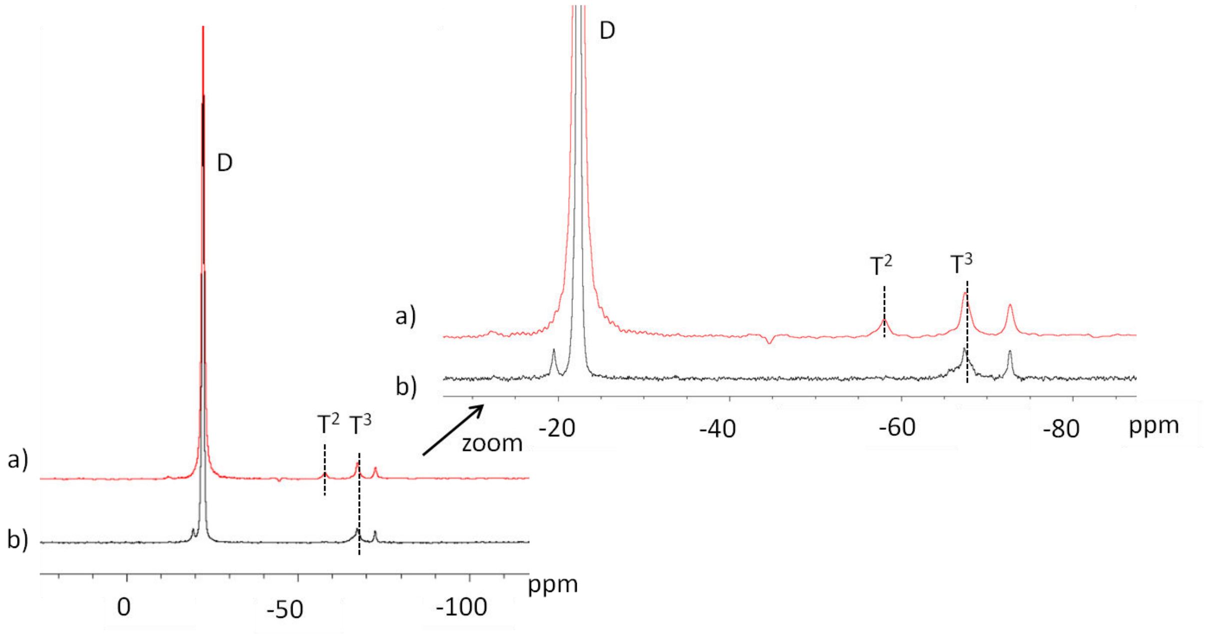

Figure 57: 29Si NMR of S1-Sn and S1-Ti silicone

The deconvolution of S1-Ti spectra using DMFIT software[68] is presented in Figure 58. The red curve represents the simulated spectrum and the black the experimental spectrum. It highlights a good fit and permits to quantify the amount of the different structures: 7% of T structures and 93% of D structures as for S1-Sn silicone matrix (presented in the chapter II).

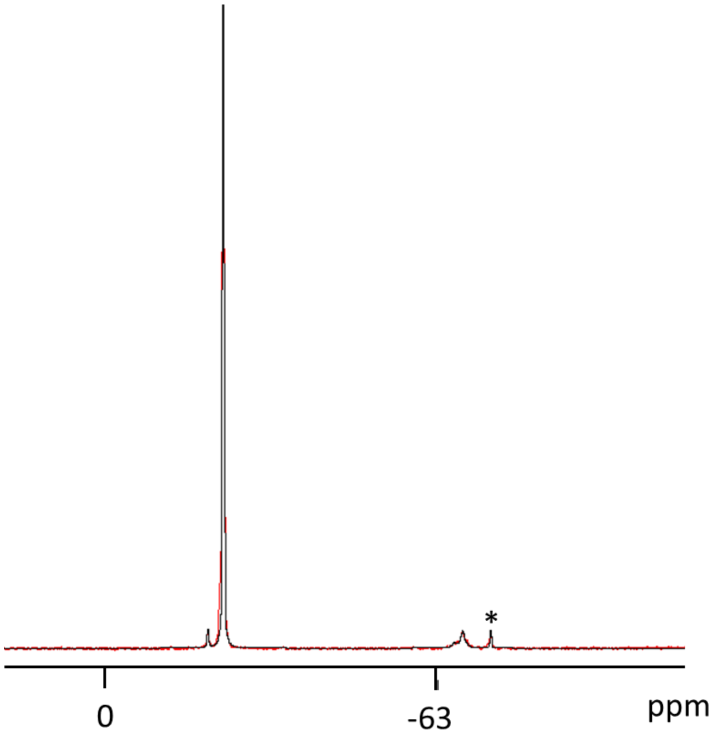

Figure 58: Deconvolution of S1-Ti matrix using DMFIT software (*spinning side band)

This shows that the crosslink density is increased compared to S3 (3% of T structure and 97% of D structure presented in the chapter III). In order to highlight its effect on the mechanical properties of the char S3/EG, S1-Ti/EG and S1-Sn/EG based formulations are tested in Air Jest fire test.

IV-3.2.2 Mechanical properties of the char

The three formulations exhibit the same behavior before switching air on. However, when the air flow is switch on, a complete destruction of the char is observed for S3/EG and for S1-Sn/EG based coating whereas when titanium based catalyst is used; there is no char destruction (Figure 59). This evidences the superior mechanical properties and the extremely good cohesion of the Ti-based formulation. This demonstrates also that the mechanical properties of the S1-Ti+25%EG char is higher than those of S3+25%EG.

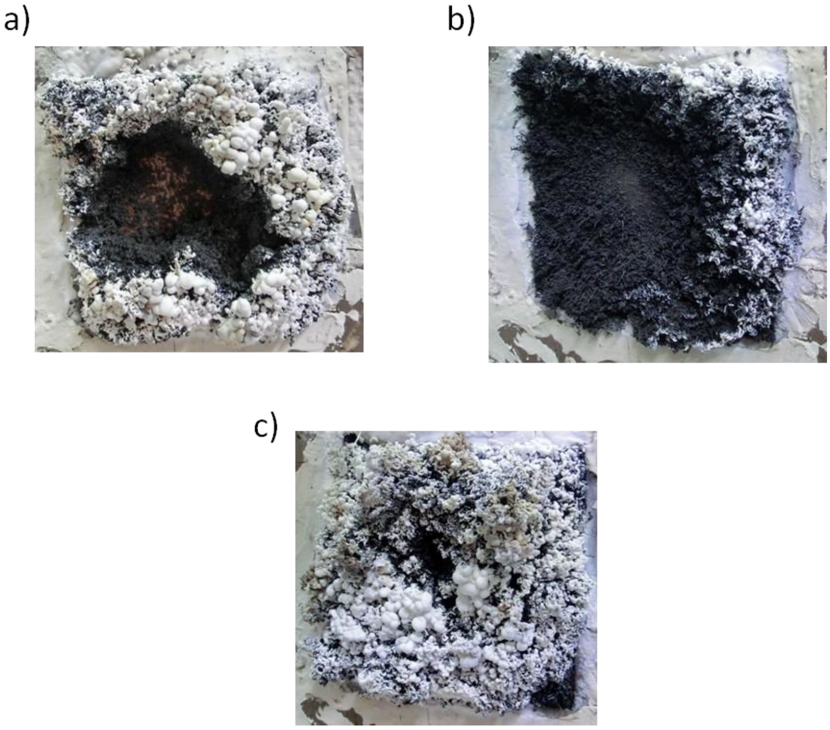

Figure 59: Residue of a)S3+25%EG, b)S1-Sn+25%EG and c)S1-Ti +25%EG after Air Jet fire testing

This part evidences two things: (i) the fact to increase the crosslink density of the matrix plays an active role on the mechanical properties of the char when 25%EG is incorporated to the silicone matrix and (ii) the catalyst used to make the resin cross-linked has a crucial influence.

The next step is therefore dedicated to study the influence of the catalyst on the fire performance of silicone/EG based coating.

IV-3.2.3 Resistance to fire of high cross-linked RTV silicone rubber: Effect of the catalyst[69]

The fire performance of 1 mm S1-Sn and S1-Ti added with 25%EG is evaluated in hydrocarbon fire. Figure 60 shows the temperature versus time curve of the two silicone intumescent coatings and highlights the fact that the used catalyst has a real influence on the fire performance of the coating. Indeed, the time to reach 500°C for S1-Sn+25%EG and S1-Ti+25%EG are respectively 860s and 1500s demonstrating the better fire performance of S1-Ti+25%EG based coating.

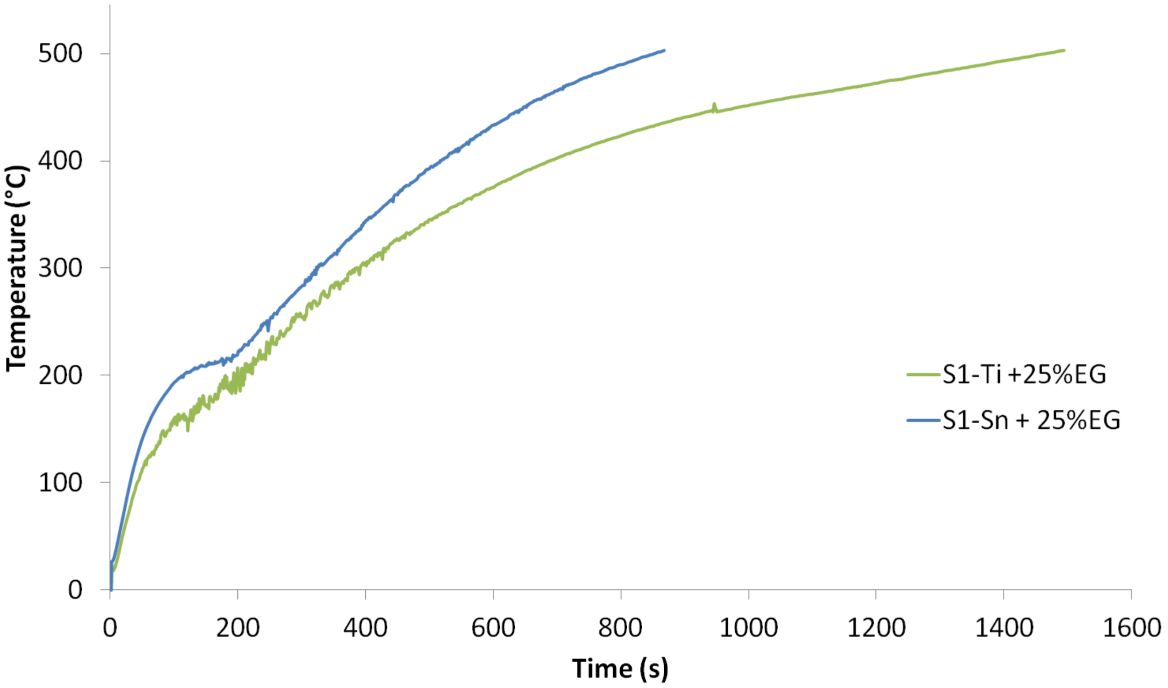

Figure 60: Temperature versus time curve of S1-Sn+25%EG and S1-Ti+25%EG based coating in hydrocarbon fire scenario

When titanium based catalyst is used, a high expansion (2100%) and a good cohesion of the char are observed whereas the main part of the char collapse during fire experiment when tin based catalyst is used. This evidences also that S1-Ti silicone matrix limits the expansion of the coating since the expansion of S1-Ti/EG and S3/EG based coating reach respectively 2100% and 3400% when exposed to a simulated hydrocarbon fire.

The chemical composition of the char after furnace testing should at least partially explain the different mechanical properties of each chars. XPS analysis on the two chars highlights that when titanium based catalyst is used, the graphite platelets are embedded in more cross-linked silicone structures than when tin based catalyst is used. This is explained by a higher thermal stability of S1-Ti silicone matrix than that of S1-Sn. It was also demonstrated using EPMA that the tin is located at the surface of the resin and catalyzes the depolymerization of the silicone matrix[69] whereas the titanium participates to the silicone network leading to the formation of Si-O-Ti bound. It explains the ^{29}Si NMR spectra presented in Figure 57. Indeed, the additional peak at -19 ppm could be attributed to Si-O-Ti bound in D structure and the peak related to T^3 structure is broader for S1-Ti matrix than that of S1-Sn. This is explained by the presence of another peak at -66ppm (the two peaks overlap) which should be assigned to Si-O-Ti bond in T^3 structure. Thanks to this study, it is possible to propose a crosslink mechanism of both resins and it is illustrated in Figure 61.

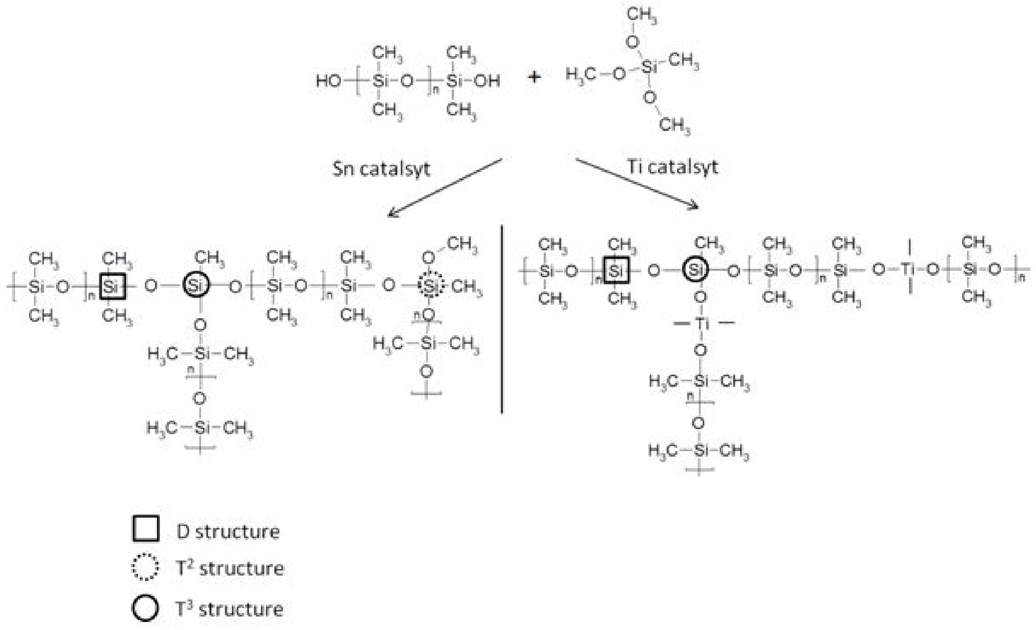

Figure 61: Chemical pathway of resin cross-linking

In the two previous parts, we have shown that the crosslink density of the RTV silicone can significantly be increased using shorter hydroxyl PDMS chain. When titanium based catalyst is used to make this resin cross-linked, it participates to the silicone network leading to an increase of the thermal stability. The char after hydrocarbon fire test is composed of graphite platelets embedded in silica network mainly composed of T structure and therefore presents high mechanical properties. This study demonstrates thus that the mechanical properties of silicone/EG based coating can significantly be increased using S1-Ti based RTV silicone matrix.

IV-3.2.4 Fire performance of 3 mm based coating using S1-Ti matrix for steel protection against hydrocarbon fire

In the previous part, we have shown that the increase of the crosslink density of the silicone matrix increases the mechanical properties of the char. The aim of this part is to compare the fire behavior of S1-Ti and S3 based coating at 3 mm. Figure 62 presents the temperature/time curve obtained. It highlights the better insulative performance when S1-Ti is used as silicone matrix since 500°C is reached in 2230s and a good cohesion of the char during the test occurs.

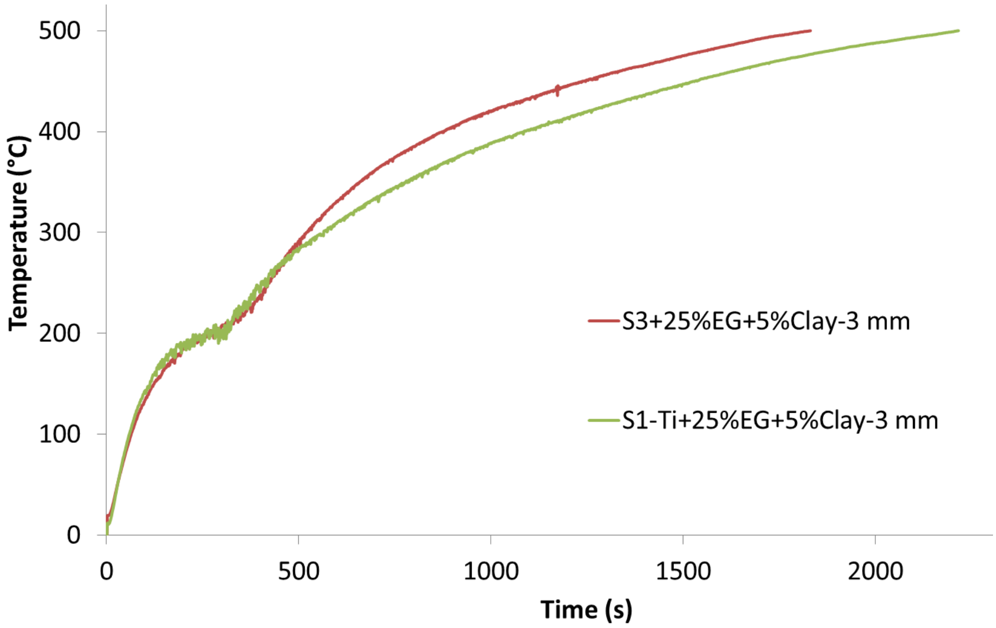

Figure 62: Temperature versus time curve of 3 mm of S3+25%EG+5%Clay and S1-Ti+25%EG+5%Clay in hydrocarbon fire

Figure 63 shows the two residues after furnace testing. Even if there is no significant modification of the expansion after testing, the top of the S1-Ti based char is covered by a larger amount of silica and its cohesion is higher (by visual observation) than S3/EG/Clay char even if it does not fall off during the fire test.

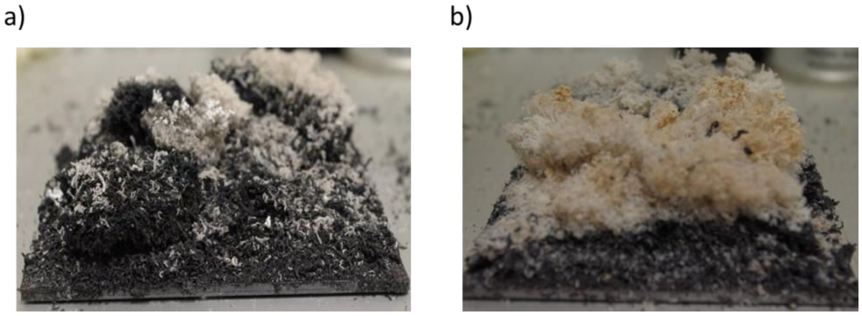

Figure 63: Residue of 3 mm based coating of a) S3+25%EG+5%clay and b) S1-Ti+25%EG+5%Clay after hydrocarbon fire test

We therefore evidenced that the fact to use S1-Ti based silicone matrix increasing the cohesion of the char and when 3 mm is tested, the char does not fall off during the test whereas it is the case for S3 based coating.

In the two previous chapters we highlight the fact that the critical parameters to be taken into account to develop efficient silicone intumescent coating for the protection of steel against fire are: (i) the use of expandable graphite to ensure the expansion behavior of the coating and its low thermal conductivity at high temperature, (ii) incorporate clay in the formulation increases the mechanical properties of the char, (iii) calcium carbonate reacts with silicone resin at high temperature leading to the formation of calcium silicate acting as a supplementary ceramic barrier at the top of the char and finally (iv) the cross-link density of the silicone has to be increased to ensure high mechanical properties of the char.

Considering all these parameter a more complex formulation at 3 mm is tested in hydrocarbon fire.

The silicone matrix is composed of S1-Ti and 5% of MQ resin (5% of S1 is substituted by 5% of MQ resin). The MQ silicone resin is composed of nanosilica comprising some hydroxyl function (reactive) and trimethylsilyl at the surface. Chemical structure of MQ silicone is presented in Figure 64.

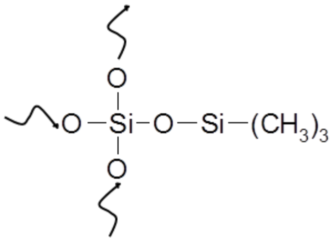

Figure 64: Chemical structure of MQ silicone resin

The formulation, called F4, is composed of 15% of expandable graphite to ensure the expansion behavior and its low thermal conductivity at high temperature, 20% of GCC and 7% of Clay to increase the mechanical properties of the char.

Figure 65 presents the temperature/time curve obtained for F4 and S1-Ti/EG/Clay at 3 mm in hydrocarbon fire.

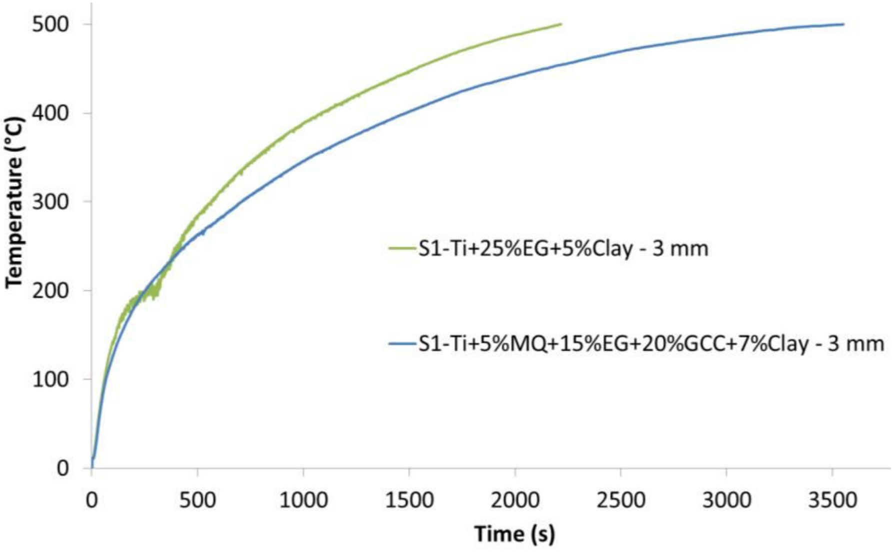

Figure 65: Temperature versus time curve of 3 mm S1-Ti/EG/Clay and S1-Ti/EG/GCC/Clay based coating in simulated hydrocarbon fire

For F4 based coating, 400°C and 500°C are reached respectively in 1500s and 3525s against 1090s and 2230s for S1-Ti/EG/Clay. It evidences the high fire performance of F4 based coating and Figure 66 highlights its good cohesion.

Figure 66: Residue of F4 based coating after hydrocarbon fire exposure

Further experiment on the F4 formulation should be carried out to explain the exact mode of action of each component. An experimental design should also be interesting to determine the optimal formulation for the fire protection of steel using thick silicone coating against hydrocarbon fire.

IV-4 Conclusion

In this chapter, the influence of the crosslink density on the fire performance of silicone/EG based coating was investigated. Two ways were followed, the first using fumed silica as additional filler and the second using another hydroxyl PDMS.

We have evidenced that the fact to use fumed silica does not play an active role neither on the fire performance of silicone based coating nor on the mechanical properties of the char.

Nevertheless, using shorter length chain of hydroxyl PDMS for the silicone matrix and a titanium based catalysts to ensure high thermal stability, the mechanical properties of the silicone/EG char was significantly increased. This is explained by the fact that the expansion is lower than that of S3/EG and the graphite platelets are embedded in high cross-linked silicone structures. Using this matrix and substituting 5% of S1 by 5% of MQ resin, incorporating expandable graphite, calcium carbonate and clay in the silicone enable to develop thick and very efficient intumescent coating for the steel protection against hydrocarbon fire.

General Conclusion

General conclusion

On the field of protection of steel structure against fire, intumescent coating is known to be very efficient. However, most of this coating are organic based and therefore exhibits some limitations. The challenge of this work was to develop silicone based coating for the fire protection of steel in two different fire scenarios: cellulosic and hydrocarbon fire. For this, different intumescent silicon based coatings have been tested and, their mode of action has been elucidated to point out their limitations and the way to improve their performances.

First of all, a high cross-linked phenyl silicone resin based coating was developed. This coating exhibits high insulative performance when exposed to an open flame but its low viscosity at high temperature limits considerably its performance in furnace tests. That is why, in a second step, fire protection properties of RTV silicone based coating added with calcium carbonate was investigated. This coating exhibits heat barrier properties in cellulosic fire scenario compared with virgin steel but its performance are limited compared with commercial intumescent paint. This low fire performance was attributed to the low expansion rate of the coating and thus in the following study, expandable graphite was thus used as blowing agent in RTV silicone matrix.

For the formulation including EG, 1 mm silicone based coatings exhibit better fire performance than commercial intumescent paint in simulated hydrocarbon fire. This high fire performance was attributed to: (i) its high expansion rate (ii) its low thermal conductivity at high temperature and (iii) the good cohesion of the char. This good cohesion was explained by strong interaction occurring between expandable graphite and silicone matrix. During the intumescent process, graphite platelets are oxidized and embedded in a complex silicone structure ensuring the good mechanical properties of the char.

The effect of clay was also investigated for the development of thicker intumescent coating. Indeed, it was shown that, the clay increases significantly the cohesion of the char in hydrocarbon fire scenario that is particularly important for thick coating. The reinforcement of the char takes place thanks to specific reactions between the clay and the silicone matrix and because the clay platelets are uniformly dispersed throughout the thickness of the char.

However, the fire protective behavior of such silicone intumescent based coating is limited in cellulosic fire scenario compared with that of commercial intumescent paint. Calcium carbonate was thus used as additional filler. It is shown that in this case, fire performance of silicone intumescent based coatings is higher than that of commercial intumescent paint. Calcium carbonate increases the thermal stability of the silicone matrix leading to the formation of calcium silicate in cellulosic fire scenario. Calcium silicate species form on the top of the char a protective ceramic-like layer increasing the insulative properties of the coating.

The influence of the cross-link density of the RTV silicone matrix used on the mechanical properties of the char was finally investigated. It was demonstrated, that the catalyst used to cross-link the silicone resin has a critical influence on the fire performance of the intumescent coating. Using high cross-linked silicone matrix and titanium based catalyst allows increasing the mechanical properties of the protective layer resulting from the degradation of RTV silicone/expandable graphite based coating.

As a conclusion, it is possible to draw general rules for the development of effective intumescent silicone coatings. The formulation has to be composed of:
(i) **High cross-linked RTV** silicone and the catalyst has to be a **titanium based catalyst.**
(ii) **Expandable graphite** to ensure the expansion of the coating and also its low thermal conductivity at high temperature.
(iii) Inorganic fillers such as **clay** and **calcium carbonate** to increase respectively the mechanical properties of the char and the thermal stability of the matrix.
Moreover, depending on the final application, the formulation have to be adapted making an experimental design to ensure high fire performance of the silicone based coating.

This work is the first highlighting the high potential to develop silicone based coatings for the fire protection of steel in various fire scenarios. The key parameters to develop high effective coatings were also determined.

All the study previously reported investigated the performance of silicone based on coating for the protection of steel. This lead us to investigate the effectiveness of such coating on the fire protection of other materials. In particular, , mainly because of their excellent mechanical properties, composite materials are more and more used in building and in aeronautic industry. In both cases, these materials have to be protected against fire. We have thus began to investigate if it is possible to protect composites against fire using the previously developed intumescent silicone coatings.

Outlook – Fire protection of composites

1. Introduction

We have shown that RTV silicone resins added with expandable graphite and fillers such as clay and calcium carbonate exhibit similar even better fire performance than commercial intumescent coating in both cellulosic and hydrocarbon fire scenarios on steel. The strong interaction between expandable graphite and silicone is responsible for this high performance. The mode of action of clay and calcium carbonate was also elucidated. However, all these coatings have been evaluated for the fire protection of steel. In this part, the feasibility of the fire protection of composite using silicone intumescent coating is examined.

The use of composites in civil engineering structural components is increasing day by day due to their light weight, high specific strength, and stiffness properties.

Moreover, because of their exceptional mechanical properties, carbon fiber reinforced polymer (CFRP) are increasingly being used in the design of aircraft and they have attracted attention of researchers and industrial manufacturers to be used in primary structural components of aircrafts such as Boeing 787 or the coming Airbus A350. For each application a specific fire test is used.

For the first, building codes and regulations require materials exhibiting low flame spread and low smoke generation. The associated test to evaluate the fire protection of composite used in building industry is the Steiner Tunnel (ASTM E-84)[70]. For this, fire performance of S3 based coating is evaluated and compared with that of Fire Tex M93 commercial intumescent paint using a small scale Steiner Tunnel test developed in our laboratory.

For the second application, when CFRPs are exposed to a jet fuel fire, the composite materials degrade and quickly ignite, releasing volatile gases, and producing char resulting in a significant reduction in structural strength. In this research we are interested in the fire behavior of CRFP undergoing jet fuel fire - about 200kW/m² heat flux- and how to protect it. For this, S1-Ti intumescent based coating is used because of the high mechanical properties of the char when this matrix is used. This part is based on the following paper:

S.Bourbigot, B.Gardelle, S.Duquesne - Intumescent silicone-based coatings for the fire protection of carbon fiber reinforced composites - **2013 - International Association for Fire Safety Science - Submitted**

2. Fire protection of composite for civil application

2.1 Material and fire testing

In this part, the composite to be tested is a polyethylene terephthalate (PET) foam block (ARMAform, Armacell Benelux SA) covered with glass woven fabrics (Gurit) impregnated by an epoxy resin (Ampreg 21FR, Gurit). These composites are used for making the ceiling of railway stations which will be built in Saudi Arabia (railway stations for high speed train).

After a screening using the S3 silicone matrix and different fillers, the intumescent silicone coating used is composed of S3 added with 22%EG, 25%GCC, 1%Aerosil and 2% of mineral fibers mainly composed of SiO_2, Al_2O_3, CaO+MgO (MS603 supplied by Lapinus company). Fire Tex M93 intumescent coating is used as reference. Both formulations are applied to the composite at 13g/cm² to obtain 1 mm based coating.

To evaluate the properties of the composites coated with intumescent coating, a 'mini' Steiner tunnel (reduction of the Steiner tunnel at 1/8 scale) has been developed[71]. The test is fully described in Figure 67. The Steiner tunnel test is the primary test method for evaluating resistance to fire of interior finish materials in the United States. The method is described in ASTM E 84. The apparatus consists of a tunnel-like enclosure measuring 8.7 × 0.45 × 0.31 m (25 × 1½ × 1 ft). The test specimen is 7.6 m (24 ft) long and 0.46 m (18 in.) wide and is mounted in the ceiling position. It is exposed at one end, designated as the burner end, to an 88-kW (5000-Btu/min) gas burner. There is a forced draft through the tunnel from the burner end with an average initial air velocity of 1.2 m/s (240 ft/min). The measurements consist of flame spread over the surface and smoke obscuration in the exhaust duct of the tunnel. Test duration is 10 minutes.

A flame spread index (FSI) is calculated on the basis of the area under the curve of flame tip location versus time. The FSI is 0 for an inert board, and is normalized to approximately 100 for red oak flooring. The FSI is determined as follow: the total area (At) under the flame spread distance-time plate is calculated. In both cases, At is less than 97.5, so the FSI = 0.515*At. A smoke developed index (SDI) is calculated on the basis of the area under the light obscuration vs. time curve, and is equal to 100 for red oak flooring. The SDI corresponds to the area under the curve %Abosrbance versus time.

The "mini" Steiner Tunnel test was developed to a scale 1/8. Small windows permit to follow the flame spread and the smoke is collected in the chimney to measure its opacity with a Smoke Density Analyzer TRDA 302 from TAURUS. Previous work showed reasonable correlation with the large scale test[72].

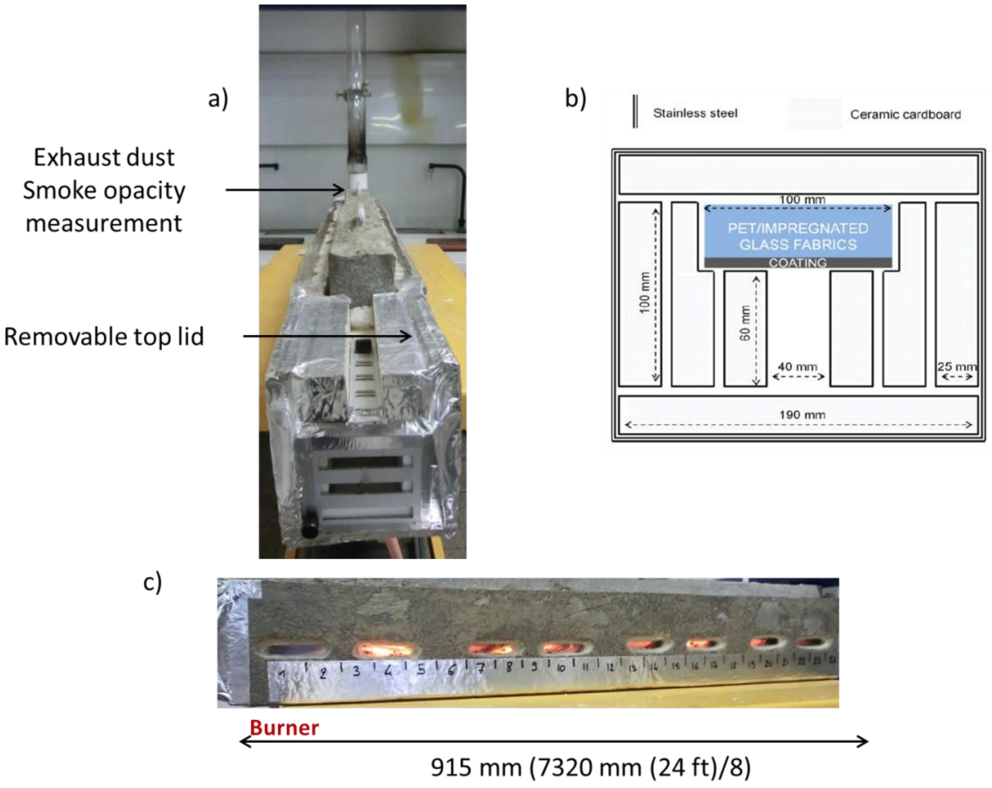

Figure 67: (a) Schematic view of the lab-scale Steiner tunnel, (b) its internal construction (side view) and c) its side for the flame spread measurement

2.2 Results and discussion

The first parameter evaluated is the flame spread during the fire test. Figure 68 shows the flame spread versus time for the M93 and S3 based coating during the test. It highlights the fact that when the composite is coated with S3 intumescent based formulation, the flame reaches only 2 feet (61 cm) after 300s and does not propagate further. While when M93 based coating is used, the flame spread reaches 2 feet after 300s fire testing and continues to propagate to finally achieve 6 feet of the composite at the end of the test. This demonstrates the lower flame spread for the composite coated with S3 intumescent based coating.

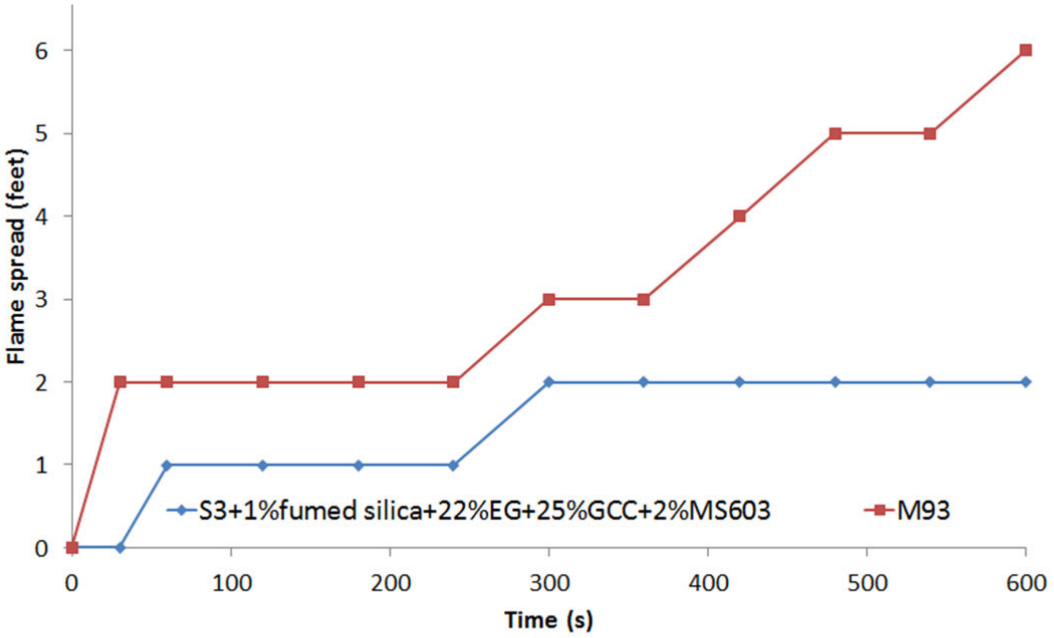

Figure 68: Flame spread for the two intumescent coatings during small scale Steiner Tunnel test

Figure 69 presents the residues of the two coated composites after Steiner Tunnel test. It shows that in both cases an expanded structure is formed. We have demonstrated in the chapter III that in case of fire (cellulosic), S3/EG/GCC based formulation swells leading to the formation of an expanded structure protecting steel against fire. We can reasonably assume that the charring pathway of silicone based coating on composite is similar. The char should therefore be composed of graphite platelets embedded in complex silicone structures. The white powder covering the top of the char should be silica and calcium silicate. This expanded structure limits therefore the heat transfer between the source and the composite. Concerning composite residue coated with M93 intumescent paint, Figure 69b) illustrates the higher flame spread than the composite coated with S3 based coating.

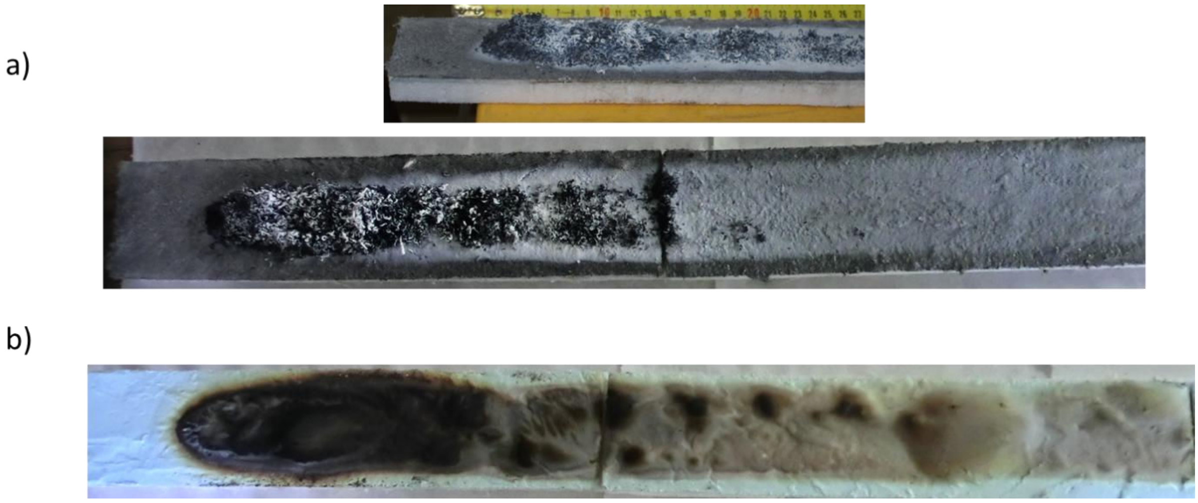

Figure 69: Residue of the composite coated with a) S3/EG/GCC and b) M93 intumescent based coating

The second parameter to take into account is the smoke opacity generated by the intumescent coating during fire testing. The absorbance versus time curve is presented in Figure 70.

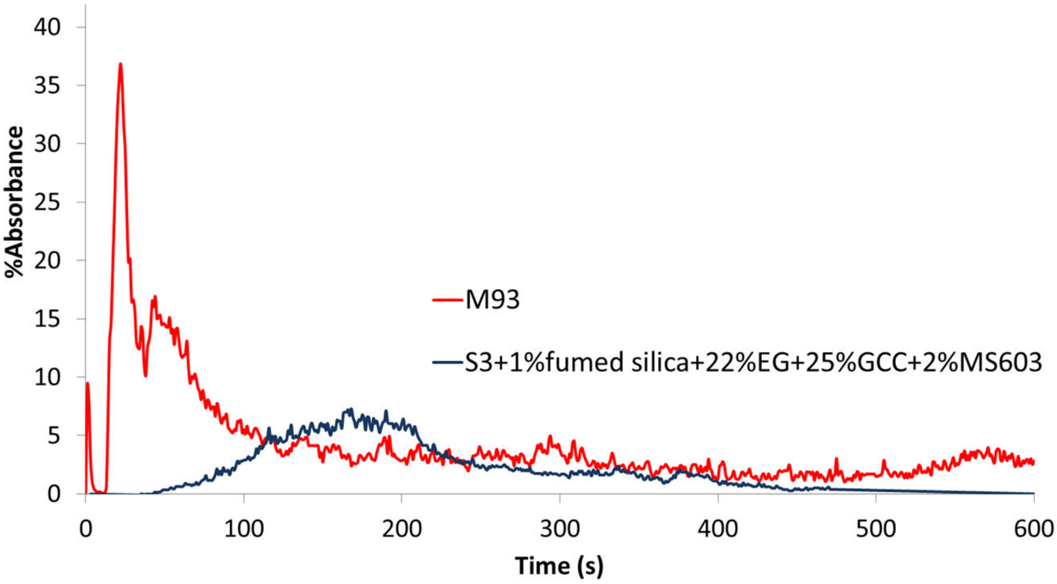

Figure 70: %Absorbance versus time of composite coated with S3+1%fumed silica +22%EG + 25%GCC +2%MS603 and M93 in small scale Steiner Tunnel test

Concerning the composite coated with M93 intumescent coating, the maximum of the absorbance of the smoke released reached 35 % whereas it reaches only 8% for the composite coated with S3 based coating. This highlights the lower smoke opacity evolved by the silicone coating compared with that of commercial epoxy-intumescent coating. The FSI and the SDI were then determined for the two composites. The results are reported in Table 8. The composite coated with S3 based coating presents lower SDI and FSI than that coated with M93 based coating.

Table 8: SDI and FSI of the two coated composite

Intumescent coating	SDI	FSI
M93	45	15
S3+1%Fumed silica+22%EG+25%GCC+2%MS603	20	5

Intumescent silicone based coating exhibits therefore higher fire performance than commercial intumescent paint using this small scale Steiner Tunnel test.

This study therefore demonstrates the good feasibility for the fire protection of composite for civil applications using intumescent coating (building applications). It also evidences the better fire performance of intumescent silicone based coating than commercial intumescent paint.

After evaluating the fire resistant properties of silicone intumescent coating on composite for civil applications, intumescent silicone are coated onto carbon fiber reinforced polymer (CFRP) for aeronautic applications and exposed to a simulated jet fuel fire.

3. Fire protection of composite for aeronautic applications[73]

3.1 Introduction

Recently Mouritz et al[74]. reported the use of conventional organic intumescent paints to protect composite structures from fire and it appeared as successful. The aim of this part is to use high cross-linked RTV silicone coating for the fire protection of CRFP. Two main systems are tested: the first, high intumescent coating with expandable graphite and the second, low intumescent coating without expandable graphite. Chemical compositions of the formulations are reported in Table 9.

Table 9: Chemical composition of the intumescent coated tested

Silicone formulation	F1 – High intumescing coating	F2- Low intumescent coating
RTV Silicone matrix	56%	56%
Expandable graphite	25%	-
Calcium carbonate	12%	37%
Clay (C30B)	7%	7%

The jet fire bench test intends to mimic, at the small-scale, a jet fuel fire which can be caused by burning jet fuel external to the aircraft as a result of fuel tank damage during the impact of an aircraft or by jet fuel fire occurring in the engine nacelle. The measurements were carried out using a constant heat flux test provided by a propane burner (10kW propane burner) delivering a heat flux of 200 kW/m² on CFRP. Thermocouples (4 K-type thermocouples) were placed on the back side of CFRP to measure the temperature as a function of time during the test. To explain the fire behavior of the two coatings, several parameters are investigated. Physical parameters of the intumescent silicone-based coating including the heat conductivity as a function of temperature and the dynamic of expansion during the test will be first investigated in order to propose a mechanism of protection.

3.2 Results and discussion

Figure 71 shows the temperature on the backside of the samples as a function of time. When the temperature raises up suddenly it indicates the ignition of the composite on the backside. For a thickness of 500 µm (Figure 71 (a)), it is clearly shown that the F1 intumescent coating provides the most efficient protection since the ignition of the composite backside occurs at 460s while it is at 260s and 100s for CFRP-F2 and virgin CFRP respectively. If 1000 µm intumescent coating is applied on CFRP (Figure 71b), the composite is well protected and no ignition at the back side of the coating occurs.

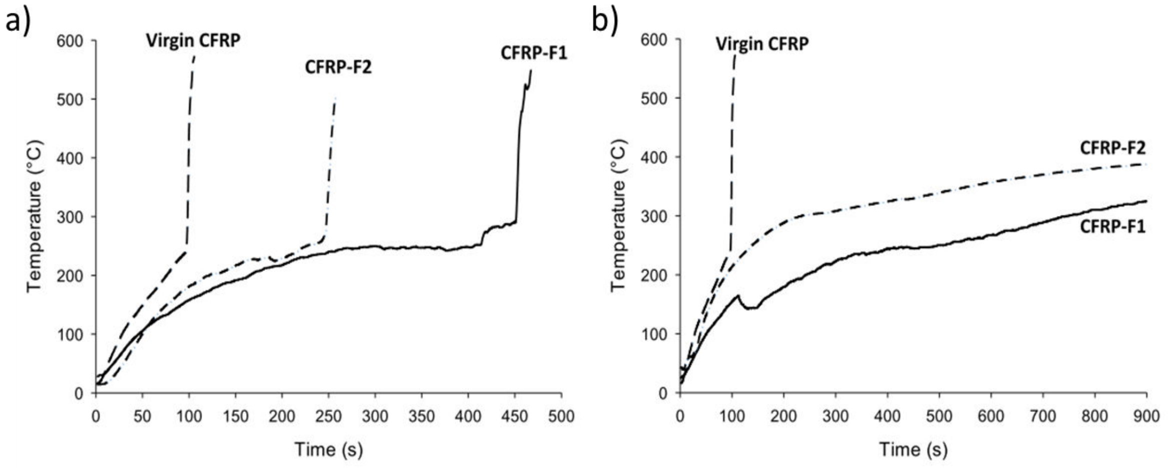

Figure 71: Temperature as a function of time of coated CFRPs compared to virgin CFRP (backside temperature) during the jet fire test at coating thickness of (a) 500 µm and of (b) 1000 µm

Concerning, the high intumescent material, due to the presence of expandable graphite there is the formation of a thick expanded structure. For the low intumescent coating, there is the formation of a not expanded porous material. In order to explain these fire performances, physical properties of the two intumescent materials are investigated: their swelling ability and thermal conductivity at high temperature. Figure 72a) highlights the high expansion rate of F1 based coating and Figure 72b) shows the low thermal conductivity at high temperature for the two silicone based coatings. For F1 based coating, during the fire experiment, there is the formation of a thick expanded material with low thermal conductivity limiting thus the heat transfer between the fire and the composite. For F2 based coating, there is the formation of a ceramic-like material characterized by a low thermal conductivity at high temperature.

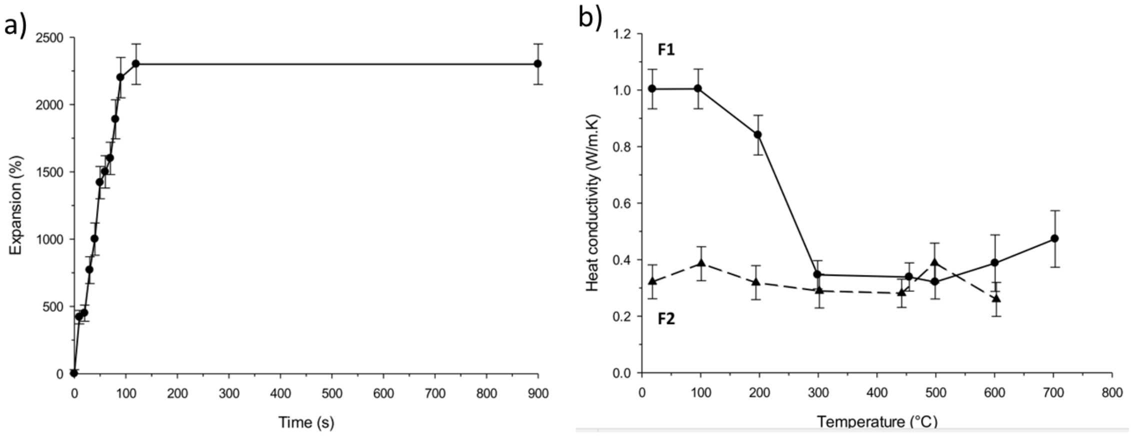

Figure 72: a) Expansion versus time curve of F1 based coating during fire test and b) thermal conductivity of F1 and F2 from ambient temperature to 600°C

In order to determine a mode of action of the fire protection using the two silicone based coating, the residue obtained after fire testing are analyzed by XPS, XRD and ^{29}SiNMR (for F2 residue). All spectra obtained for F2 are presented in Figure 73. For F2 based coating, ^{29}Si NMR evidences the formation of T and Q^4 structures and therefore the formation of a cross-linked silica network. However, the Q structure comes not only from the degradation of the silicone matrix and the presence of the clay but also by the formation of calcium silicate. Indeed, XPS spectrum highlights the formation of these structures as it was observed in the chapter III. XRD analysis shows the presence of characteristic peaks which should be attributed to calcium silicate species but their cristallinity is too low to determine the kind of calcium silicate.

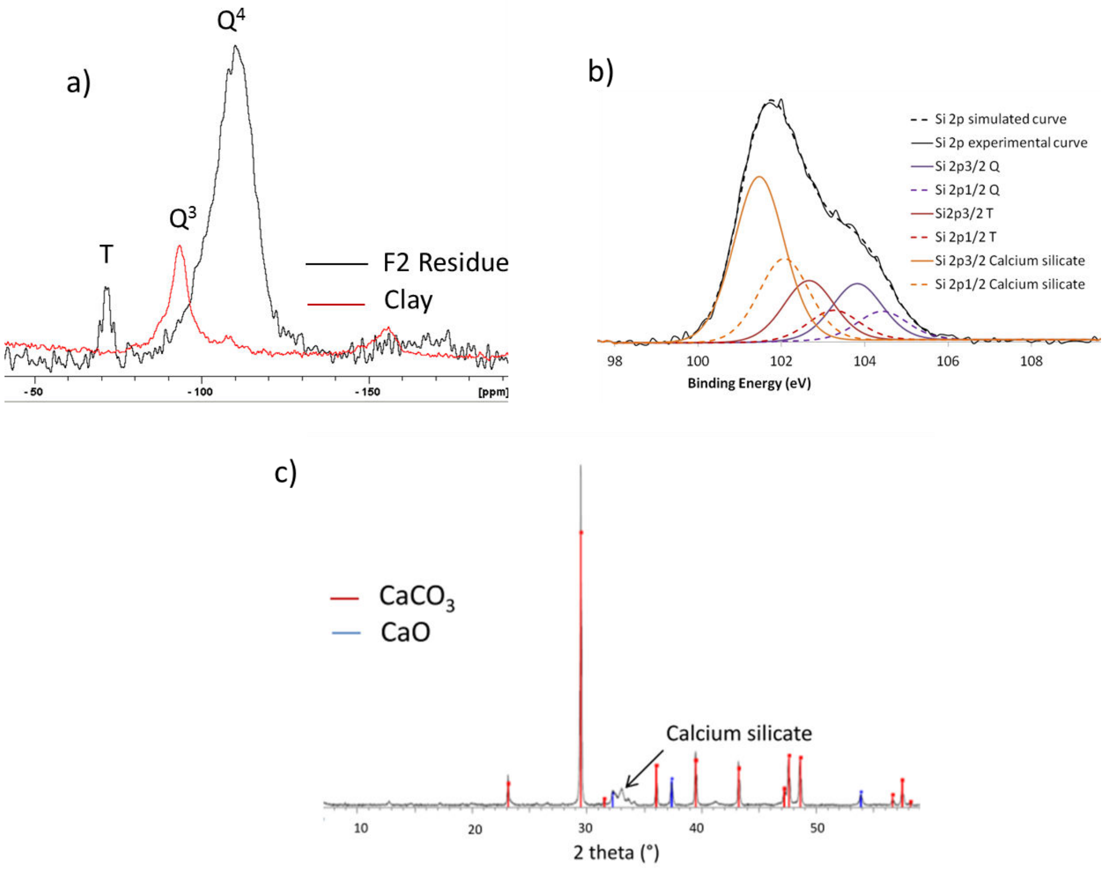

Figure 73: a) 29Si NMR spectra of Clay and F2 residue, b)Si 2p spectrum and c)XRD pattern of F2 residue

Finally, when F2 based coating is exposed to jet fuel fire there is formation of a ceramic-like porous material composed of calcium silicate and high cross-linked silicone structure. It was shown that this ceramic has a low thermal conductivity at high temperature protecting therefore the composite during the fire test.

For F1 based material, the residue was analyzed by XRD and XPS. XPS spectrum highlights the presence of SiC, D or calcium silicate, T and Q structures. The formation of SiC, T and Q structures comes from the degradation of the silicone matrix which embed the graphite platelets (as demonstrated in the chapter IV). Moreover, the XRD experiment highlights the presence of calcium silicate, calcium carbonate and calcium oxide (as for F2 based residue) and graphite. It is thus shown that the incorporation of expandable graphite in silicone permits the formation of an intumescent char upon heating composed of graphite platelets embedded in silicone structure and calcium silicate.

Finally, its high expansion rate delivers rapidly the protection of interest. Associated to its low heat conductivity, the high expanded intumescent char (2400%) limits heat transfer from the flame to CFRP. The high mechanical properties of the char is insuring by the fact that graphite platelets are embedded in high cross-linked silicone structure and calcium silicate. These points explain the high insulative properties of this coating.

4. Conclusion

We have demonstrated that the intumescent silicone coatings developed for the fire protection of steel can be applied onto composites. It is evidenced that these coatings provide high fire protection on composites for civil and aeronautic applications.

For civil application, intumescent silicone based coatings are applied on polyethylene terephthalate (PET) foam block covered with glass woven fabrics impregnated by an epoxy resin. The fire behaviors of coated composites were evaluated using small scale Steiner Tunnel test. It is shown that silicone based coating exhibits better fire performance than organic intumescent paint. The two intumescent coatings highlight good fire protection behavior due to the formation of an expanded structure protecting the composite. However, the composite coated with silicone based coating releases lower smoke opacity and lower flame spread compared to commercial organic intumescent paint.

For aeronautic applications, intumescent silicone based coating has been tested on carbon fiber reinforced composite using a small scale jet fire test. During the fire test, there is formation of a thick insulative structure (low thermal conductivity at high temperature) based on graphite platelets embedded in calcium silicate and high cross-linked silicone structures. This expanded char limits therefore the heat transfer between the fire source and the composite.

The intumescent silicone based coatings that have been developed in this study show high efficiency for both fire protection of steel and of composites. The high potential of such coatings was thus demonstrated, However, further work have to be done especially concerning the ageing of the silicone coating and its mechanical properties. As an example, for aeronautic applications, several parameters have also to be considered such as the potential delamination of the material that may occur at high temperature or the effect of oil on the fire properties of coating.

References

References

1. Gosselin, G., Stuctural fire protection, predictive methods. Proceedings of building science Insight **1987**.
2. Gardner, L.; Baddoo, N. R., Fire testing and design of stainless steel structures. Journal of Constructional Steel Research **2006,** 62 (6), 532-543.
3. Usmani, A. S.; Chung, Y. C.; Torero, J. L., How did the WTC towers collapse: a new theory. Fire Safety J. **2003,** 38 (6), 501-533.
4. Weil, E. D., Fire-Protective and Flame-Retardant Coatings - A State-of-the-Art Review. J. Fire Sci. **2011**.
5. Protection, P. T. F. http://www.promat-tunnel.com/idprt004.htm

6. UL rapid rise fire tests of protection materials for structural steel.
7. G.Elliott Fire protection, safety and security. http://www.ecuinternational.com/ihc/pdf/IHC006.pdf.
8. M.G.Goode Fire protection of structural steel in high-rise buildings. http://www.fire.nist.gov/bfrlpubs/build04/PDF/b04047.pdf.
9. Paroc http://www.paroc.dk/solutions-and-products/solutions/fire-protection/steel-structures?sc_lang=en.
10. Pandey, J. L.; Banerjee, M. K., High-temperature-resistant (slurry-based) coatings. Anti-Corrosion Methods and Materials **1997,** 44 (6), 368-375.
11. Thomson, K. W.; Rodrigo, P. D. D.; Preston, C. M.; Griffin, G. J., In the firing line: Ceramifying polymers enhance strength of intumescent coatings. European Coatings Journal **2006,** (12), 34-36+38-39.
12. Gardelle, B.; Duquesne, S.; Vu, C.; Bourbigot, S., Thermal degradation and fire performance of polysilazane-based coatings. Thermochim. Acta **2011,** 519 (1-2), 28-37.
13. Vandersall, H. L., Intumescent coating systems, their development and chemistry. J of Fire & Flammability **1970,** 1, 97-140.
14. Jimenez, M.; Duquesne, S.; Bourbigot, S., Intumescent fire protective coating: Toward a better understanding of their mechanism of action. Thermochim. Acta **2006,** 449 (1-2), 16-26.
15. Bourbigot, S.; Le Bras, M.; Delobel, R.; Decressain, R.; Amoureux, J. P., Synergistic effect of zeolite in an intumescence process: Study of the carbonaceous structures using solid-state NMR. Journal of the Chemical Society - Faraday Transactions **1996,** 92 (1), 149-158.
16. Otáhal, R.; Veselý, D.; Násadová, J.; Zíma, V.; Němec, P.; Kalenda, P., Intumescent coatings based on an organic-inorganic hybrid resin and the effect of mineral fibres on fire-resistant properties of intumescent coatings. Pigment and Resin Technology **2011,** 40 (4), 247-253.
17. Staggs, J. E. J., Thermal conductivity estimates of intumescent chars by direct numerical simulation. Fire Safety J. **2010,** 45 (4), 228-237.
18. Duquesne, S.; Magnet, S.; Jama, C.; Delobel, R., Intumescent paints: Fire protective coatings for metallic substrates. Surf. Coat. Technol. **2004,** 180-181, 302-307.
19. Camino, G.; Costa, L.; Martinasso, G., Intumescent fire-retardant systems. Polym. Degrad. Stab. **1989,** 23 (4), 359-376.
20. Wladyka-Przybylak, M.; Kozlowski, R., Thermal characteristics of different intumescent coatings. Fire and Materials **1999,** 23 (1), 33-43.
21. Anna, P.; Marosi, G.; Csontos, I.; Bourbigot, S.; Le Bras, M.; Delobel, R., Influence of modified rheology on the efficiency of intumescent flame retardant systems. Polym. Degrad. Stab. **2001,** 74 (3), 423-426.
22. Jimenez, M.; Duquesne, S.; Bourbigot, S., Characterization of the performance of an intumescent fire protective coating. Surf. Coat. Technol. **2006,** 201 (3-4), 979-987.

23. Duquesne, S.; Le Bras, M.; Bourbigot, S.; Delobel, R.; Camino, G.; Eling, B.; Lindsay, C.; Roels, T., Thermal degradation of polyurethane and polyurethane/expandable graphite coatings. Polym. Degrad. Stab. **2001,** 74 (3), 493-499.

24. Li, G.; Liang, G.; He, T.; Yang, Q.; Song, X., Effects of EG and MoSi2 on thermal degradation of intumescent coating. Polym. Degrad. Stab. **2007,** 92 (4), 569-579.

25. Wang, Z.; Han, E.; Ke, W., Influence of expandable graphite on fire resistance and water resistance of flame-retardant coatings. Corros. Sci. **2007,** 49 (5), 2237-2253.

26. Reshetnikov, I. S.; Yablokova, M. Y.; Potapova, E. V.; Khalturinskij, N. A.; Chernyh, V. Y.; Mashlyakovskii, L. N., Mechanical stability of intumescent chars. J. Appl. Polym. Sci. **1998,** 67 (10), 1827-1830.

27. Bourbigot, S.; Samyn, F.; Turf, T.; Duquesne, S., Nanomorphology and reaction to fire of polyurethane and polyamide nanocomposites containing flame retardants. Polym. Degrad. Stab. **2010,** 95 (3), 320-326.

28. Ullah, S.; Ahmad, F.; Megat-Yusoff, P. S. M., Effect of boric acid with kaolin clay on thermal degradation of intumescent fire retardant coating. Journal of Applied Sciences **2011,** 11 (21), 3645-3649.

29. Duquesne, S.; Delobel, R.; Le Bras, M.; Camino, G., A comparative study of the mechanism of action of ammonium polyphosphate and expandable graphite in polyurethane. Polym. Degrad. Stab. **2002,** 77 (2), 333-344.

30. Bourbigot, S., Quantitative approach of intumescence by numerical simulation. 243 rd American Chemical society Natioanl meeting ed.; San Diego, 2012.

31. Bourbigot, S.; Turf, T.; Bellayer, S.; Duquesne, S., Polyhedral oligomeric silsesquioxane as flame retardant for thermoplastic polyurethane. Polym. Degrad. Stab. **2009,** 94 (8), 1230-1237.

32. Muller, M.; Bourbigot, S.; Duquesne, S.; Klein, R. A.; Giannini, G.; Lindsay, C. I., Measurement and investigation of intumescent char strength: Application to polyurethanes. J. Fire Sci. **2013**.

33. Jimenez, M.; Bellayer, S.; Revel, B.; Duquesne, S.; Bourbigot, S., Comprehensive Study of the Influence of Different Aging Scenarios on the Fire Protective Behavior of an Epoxy Based Intumescent Coating. Industrial & Engineering Chemistry Research **2012,** 52 (2), 729-743.

34. Nguyen, D. T.; E.Veinot, D.; Foster, J. Inorganic intumescent fire protective coatings. 4.888.057, 1989.

35. Wang, G.; Yang, J., Influences of binder on fire protection and anticorrosion properties of intumescent fire resistive coating for steel structure. Surf. Coat. Technol. **2010,** 204 (8), 1186-1192.

36. Wade, R. J. Intumescent composition. 2012.

37. Stark, F. O.; Falender, J. R.; Wright, A. P., 9.3 - Silicones. In Comprehensive Organometallic Chemistry, Editors-in-Chief: Geoffrey, W.; Stone, F. G. A.; Edward W. AbelA2 - Editors-in-Chief: Geoffrey Wilkinson, F. G. A. S.; Edward, W. A., Eds. Pergamon: Oxford, 1982; pp 305-363.

38. Eaborn, C., Chemistry and technology of silicones : by W. Noll, Academic Press, New York, 1968, xiv+702 pages, $ 32.50. J. Organomet. Chem. **1969,** 17 (2), 359.

39. de Buyl, F., Silicone sealants and structural adhesives. Int. J. Adhes. Adhes. **2001,** 21 (5), 411-422.

40. Wolf, A., MATERIAL PROPERTIES OF CONSTRUCTION SEALANTS. KAUT GUMMI KUNSTST **1988,** 41 (2), 173-178.

41. Hshieh, F.-Y.; Buch, R. R., Controlled-atmosphere cone calorimeter studies of silicones. Fire and Materials **1997,** 21 (6), 265-270.

42. Buch, R. R., Rates of heat release and related fire parameters for silicones. Fire Safety J. **1991,** 17 (1), 1-12.

43. Zhou, W.; Yang, H.; Guo, X.; Lu, J., Thermal degradation behaviors of some branched and linear polysiloxanes. Polym. Degrad. Stab. **2006,** 91 (7), 1471-1475.

44. Genovese, A.; Shanks, R. A., Fire performance of poly(dimethyl siloxane) composites evaluated by cone calorimetry. Composites Part A: Applied Science and Manufacturing **2008,** 39 (2), 398-405.

45. Beigbeder, A.; Linares, M.; Devalckenaere, M.; Degée, P.; Claes, M.; Beljonne, D.; Lazzaroni, R.; Dubois, P., CH-π Interactions as the Driving Force for Silicone-Based Nanocomposites with Exceptional Properties. Adv. Mater. **2008,** 20 (5), 1003-1007.

46. Bonduel, D., Carbon Nanotubes/Silicone Nanocomposites for Flame Resistant Coatings In European Coatings Conference, 2010.

47. Paul, Y., EVALUATION DE LA RESISTANCE AU FEU DE REVETEMENTS POUR LA PROTECTION DE SUBSTRATS METALLIQUES - CONCEPTION DE TESTS A ECHELLE LABORATOIRE. Villeneuve d'Ascq, 2009.

48. Staggs, J. E. J., Numerical characterization of the thermal performance of static porous insulation layers on steel substrates in furnace tests. J. Fire Sci. **2011,** 29 (2), 177-192.

49. Gustafsson, S. E., Transient plane source techniques for thermal conductivity and thermal diffusivity measurements of solid materials. Rev. Sci. Instrum. **1991,** 62 (3), 797-804.

50. Gardelle, B.; Duquesne, S.; Rerat, V.; Bourbigot, S., Thermal degradation and fire performance of intumescent silicone-based coatings. Polym. Adv. Technol. **2012**.

51. Camino, G.; Lomakin, S. M.; Lazzari, M., Polydimethylsiloxane thermal degradation Part 1. Kinetic aspects. Polymer **2001,** 42 (6), 2395-2402.

52. Sanders, D. M.; Person, W. B.; Hench, L. L., QUANTITATIVE ANALYSIS OF GLASS STRUCTURE WITH THE USE OF INFRARED REFLECTION SPECTRA. Appl. Spectrosc. **1974,** 21 (3), 247-255.

53. Singh, G.; Chander, S.; Ray, A., Heat transfer characteristics of natural gas/air swirling flame impinging on a flat surface. Exp. Therm Fluid Sci. **2012,** 41 (0), 165-176.

54. Wang, Y.; Zhang, F.; Jiao, C.; Jin, Y.; Zhang, J., Convective Heat Transfer of the Bunsen Flame in the UL94 Vertical Burning Test for Polymers. J. Fire Sci. **2009**.

55. Ramaswamy, B.; Kawahara, M., Arbitrary Lagrangian–Eulerianc finite element method for unsteady, convective, incompressible viscous free surface fluid flow. Int. J. Numer. Methods Fluids **1987,** 7 (10), 1053-1075.

56. Gardelle, B.; Duquesne, S.; Rerat, V.; Bourbigot, S., Thermal degradation and fire performance of intumescent silicone-based coatings. Polym. Adv. Technol. **2013,** 24 (1), 62-69.

57. Gardelle, B.; Duquesne, S.; Vandereecken, P.; Bourbigot, S., Fire performances of curable silicone based coatings. In ACS book Fire and Polymers VI: New Advances in Flame Retardant Chemistry and Science, 2012.

58. Hamdani, S.; Longuet, C.; Perrin, D.; Lopez-cuesta, J.-M.; Ganachaud, F., Flame retardancy of silicone-based materials. Polym. Degrad. Stab. **2009,** 94 (4), 465-495.

59. Hermansson, A.; Hjertberg, T.; Sultan, B.-Å., The flame retardant mechanism of polyolefins modified with chalk and silicone elastomer. Fire and Materials **2003,** 27 (2), 51-70.

60. Koo, J. H.; Ng, P. S.; Cheung, F. B., Effect of high temperature additives in fire resistant materials. J. Fire Sci. **1997,** 15 (6), 488-504.

61. Gardelle, B.; Duquesne, S.; Vandereecken, P.; Bourbigot, S., Characterization of the carbonization process of expandable graphite/silicone formulations in a simulated fire. Polym. Degrad. Stab. **2013,** 98 (5), 1052-1063.

62. Camino, G.; Duquesne, S.; Delobel, R.; Eling, B.; Lindsay, C.; Roels, T., Mechanism of Expandable Graphite Fire Retardant Action in Polyurethanes. In Fire and Polymers, American Chemical Society: 2001; Vol. 797, pp 90-109.

63. Ciret, J. Investigation of Intumescent Coatings for Fire Protection - Application to Jet-Fire. University of Lille 1, 2010.

64. Saravanapavan, P.; Hench, L. L., Mesoporous calcium silicate glasses. I. Synthesis. J. Non-Cryst. Solids **2003,** 318 (1–2), 1-13.

65. Reig, F. B.; Adelantado, J. V. G.; Moya Moreno, M. C. M., FTIR quantitative analysis of calcium carbonate (calcite) and silica (quartz) mixtures using the constant ratio method. Application to geological samples. Talanta **2002,** 58 (4), 811-821.

66. Zhao, M.; Yang, X.; Church, T. L.; Harris, A. T., Novel CaO–SiO2 Sorbent and Bifunctional Ni/Co–CaO/SiO2 Complex for Selective H2 Synthesis from Cellulose. Environmental Science & Technology **2012,** 46 (5), 2976-2983.

67. Wheeler, P. A.; Wang, J.; Baker, J.; Mathias, L. J., Synthesis and Characterization of Covalently Functionalized Laponite Clay. Chem. Mater. **2005,** 17 (11), 3012-3018.

68. Massiot, D.; Fayon, F.; Capron, M.; King, I.; Le Calvé, S.; Alonso, B.; Durand, J.-O.; Bujoli, B.; Gan, Z.; Hoatson, G., Modelling one- and two-dimensional solid-state NMR spectra. Magn. Reson. Chem. **2002,** 40 (1), 70-76.

69. Gardelle, B.; Duquesne, S.; Vandereecken, P.; Bellayer, S.; Bourbigot, S., Resistance to fire of curable silicone/expandable graphite based coating: effect of the catalyst. Eur. Polym. J. **2013,** (0).

70. Babrauskas, V.; Lucas, D.; Eisenberg, D.; Singla, V.; Dedeo, M.; Blum, A., Flame retardants in building insulation: a case for re-evaluating building codes. Building Research & Information **2012,** 40 (6), 738-755.

71. Bourbigot, S.; Bachelet, P.; Jimenez, M.; Duquesne, S., How to keep cooler under fire. European Coatings Journal **2012,** (9), 28-33.

72. Bourbigot, S.; Bachelet, P.; Samyn, F.; Jimenez, M.; Duquesne, S., Intumescence as method for providing fire resistance to structural composites: application to poly(ethylene terephtalate) foam sandwich–structured composite. Compos. Interfaces **2013,** 20 (4), 269-277.

73. Bourbigot, S.; B, G.; S, D., Intumescent silicone-based ocatings for the fire protection of carbon fiber reinforced composites. IAFSS - Submitted **2013**.

74. Mouritz, A. P.; Feih, S.; Kandare, E.; Gibson, A. G., Thermal–mechanical modelling of laminates with fire protection coating. Composites Part B: Engineering **2013,** 48 (0), 68-78.

75. Jimenez, M.; Duquesne, S.; Bourbigot, S., High-throughput fire testing for intumescent coatings. Ind. Eng. Chem. Res. **2006,** 45 (22), 7475-7481.

Appendix 1: Material and Experimental device

Silicone matrix

The Table 10 sums up the silicone matrix used in this work.

Table 10: Silicone resin used in this work

Silicone resin	Phenyl silicone resin	S1 based on Hydroxyl PDMS 80 cs	S2 based on Hydroxyl PDMS 2000 cs	S3 based on Hydroxyl PDMS 15000 cs
Chapter II	**Yes**	**Yes**	**Yes**	No
Chapter III	No	No	No	**Yes**
Chapter IV	No	**Yes**	No	**Yes**
Chapter V	No	**Yes**	No	**Yes**

Phenyl silicone resin:

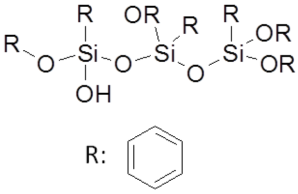

Room temperature vulcanized silicone rubber:

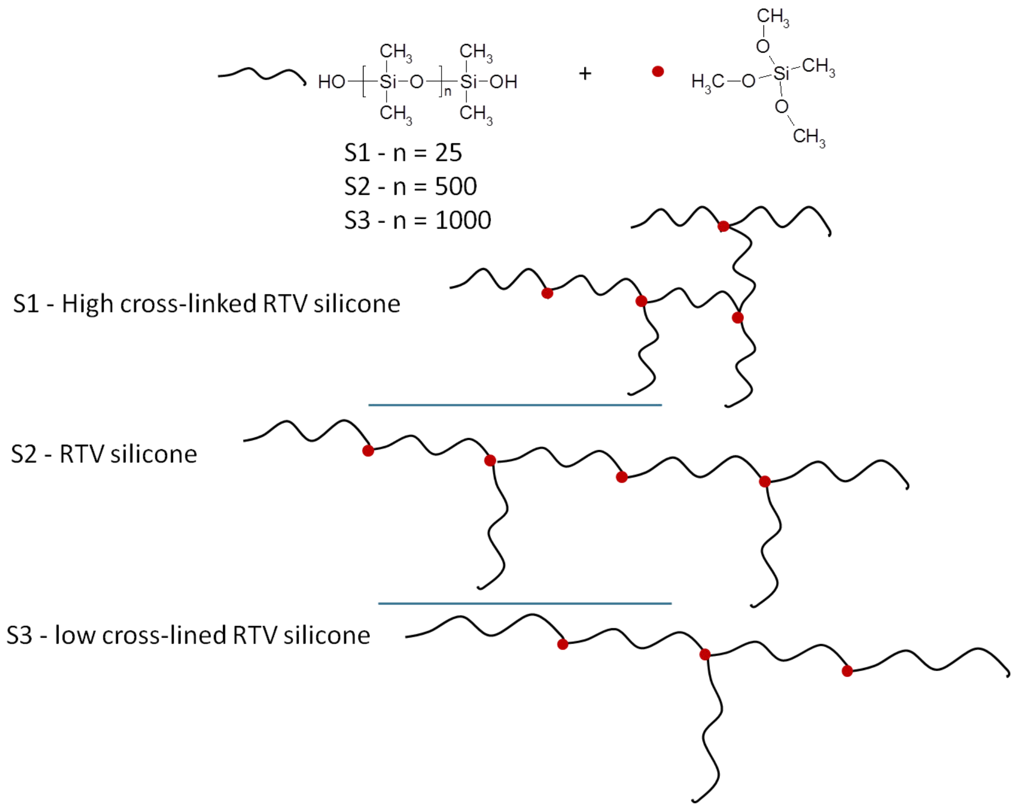

Chapter II

Fire protection test

Lab-scale fire test

For each tests, intumescent coatings are coated onto steel plate. Coatings are exposed to different temperature constraints more or less severe but the aim is to evaluate the insulative properties of the coating. The temperature at the back side of the plate is thus measured as a function of time using a pyrometer (temperature measured in the center of the plate). The backside of the plate is coated with black paint (Jeltz) having a constant emissivity (0.92) and thermally resistant up to 800°C in order to get reliable temperature measurements with the pyrometer.

In a first step, to evaluate the insulative properties of novel silicone based coating, two small lab scale tests have been used. The first – Torch test - is based on Torch Test method (American Bureau of Mines Fire Endurance, 1966) (Figure 74). The coating is exposed to an open flame (temperature of the flame around 1100°C). This test allows evaluating fire performance of an intumescent coating in radiative/convective heating scenario.

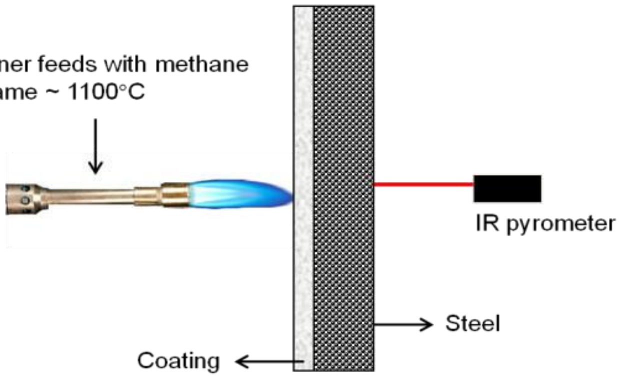

Figure 74: Schematic representation of the Torch test

The second small test used is the heat radiator test. It permits to measure the efficiency of a heat barrier [75] and shown good correlation with large scale test (industrial furnace test running according to UL-1709) in the case of intumescent paint protecting steel. In the test, the heat source is a heat radiator (Figure 75) and so, the heating is purely radiative. Steel plate is put at 4 cm under the heat source delivering a constant heat flux of 30 kW/m².

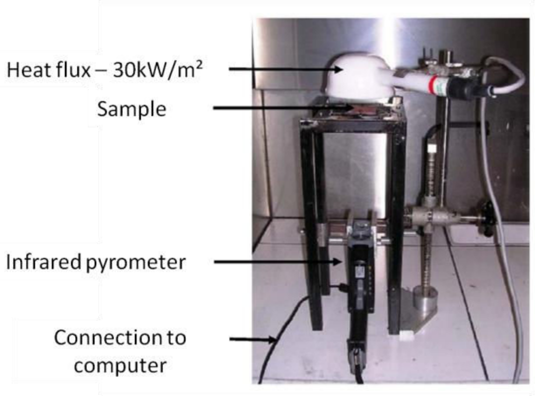

Figure 75: Heat radiator test

However, as we have shown previously, several fire scenarios can be considered. Even if the previous tests evaluate the insulative performance of intumescent coating, small furnace tests have to be developed to highlight the fire performance of intumescent coating in fire scenario.

Small scale furnace test

To evaluate the fire performances of intumescent coating in cellulosic fire scenario – standard ISO834 - a furnace test was developed (Figure 76). The lab-made furnace exhibits an internal volume of 40 dm^3. Refractory fibers (stable up to 1300°C) cover the different sides of the furnace. It is equipped with a burner of 35kW fed with propane. The gas pressure was fixed at 1.8 bars and the flow was regulated in order to mimic the ISO834 curve. The sample is put into the furnace door, with the coated side inside the furnace.

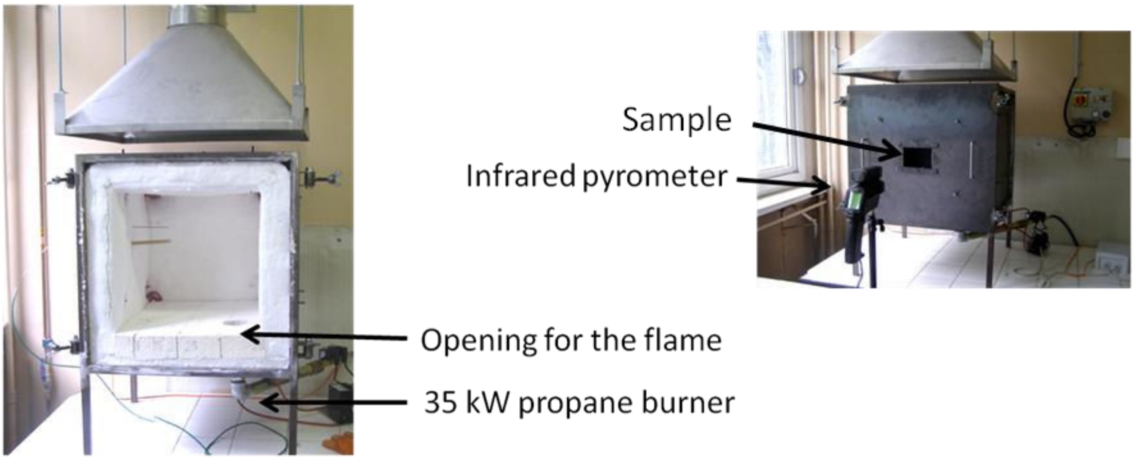

Figure 76: Furnace to evaluate fire performances of intumescent coating in cellulosic fire scenario

Figure 77 shows the evolution of the temperature versus time inside the furnace and highlights the good correlation between the standard curve and the experimental curve.

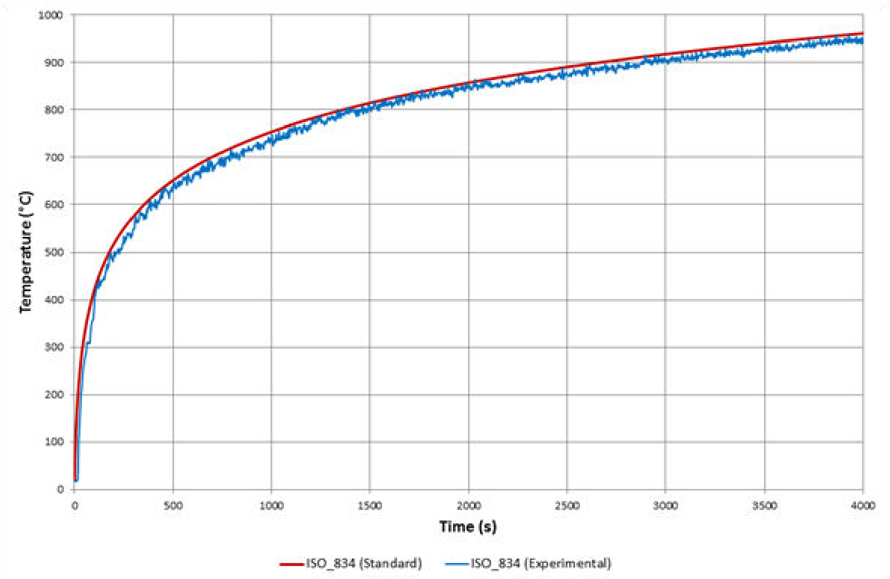

Figure 77: Temperature versus time curve inside the furnace

Rheological measurement

The rheological studies are based on the use of Thermal Scanning rheometer TSR Rheometric Scientific ARES-20A, in a parallel plate configuration. In order to measure the viscosity of material versus temperature, sample pellets (d = 25 mm, thickness = 3mm) are positioned between the two plates. Testing are carried out using a "dynamic Temperature ramp test" with a heating rate of 10°C/min in the range 25-80°C, a strain of 1% and a constant normal force of 10g.

Chapter III

Fire test

In hydrocarbon fire scenario, temperature increases is more severe and the previously described furnace is not adapted to reach 1100°C in 5 minutes. That is why another furnace equipped with two 20kW burners fed with propane was developed. This test was designed to mimic the UL1709 normalized temperature/time curve, related to hydrocarbon fire. The lab-made furnace exhibits an internal volume of 26 dm^3 (Figure 78). Refractory fibers (stable up to 1300°C) cover the different sides of the furnace. The gas pressure was fixed at 1.8 bars and the flow was regulated in order to mimic the UL1709 curve. The furnace is equipped with a quartz window in order to follow the intumescent process during the fire test.

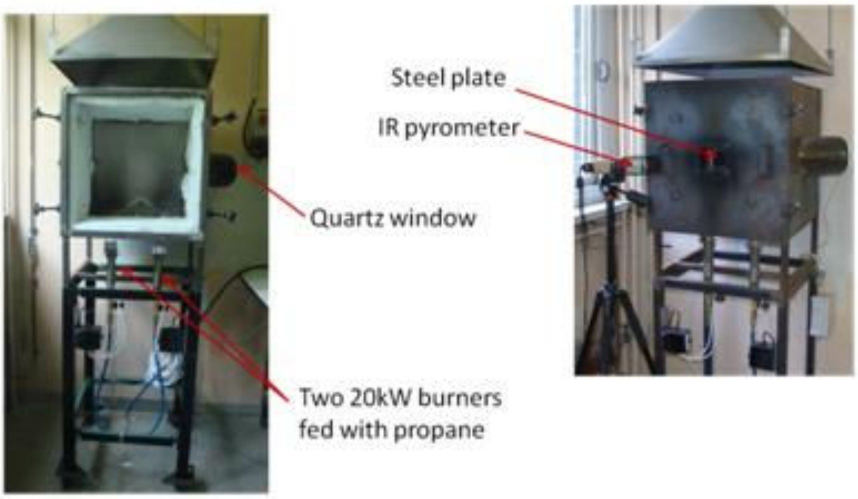

Figure 78: Furnace to evaluate fire performances of intumescent coating in hydrocarbon fire scenario

Figure 79 shows the evolution of the temperature versus time inside the furnace and highlights the good correlation between the standard curve – UL1709 - and the experimental curve.

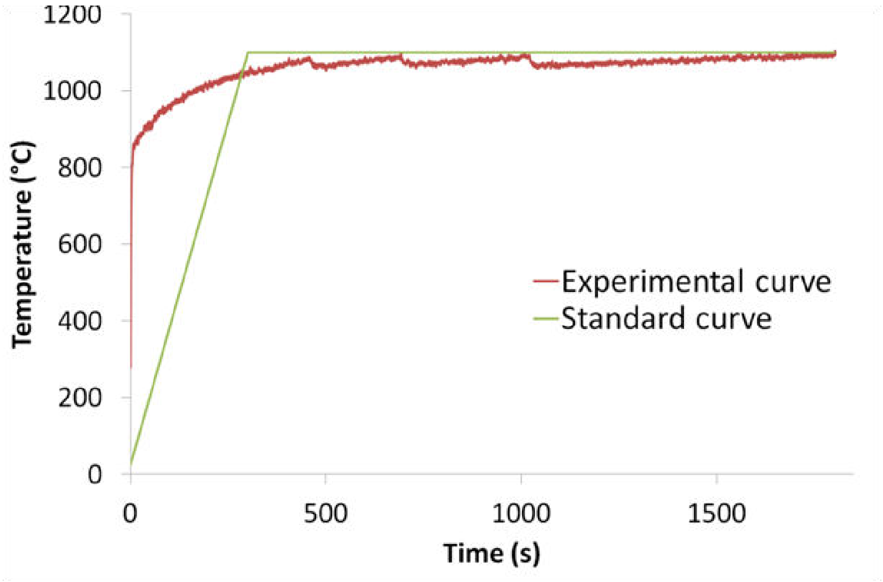

Figure 79: Temperature versus time curve inside the furnace

Expansion measurements versus temperature

The expansion versus temperature measurements are carried out using a thermal Scanning rheometer TSR Rheometric Scientific ARES-20A, in a parallel plate configuration. The samples are sample pellets (d = 25 mm, thickness = 3mm). They are positioned between the two plates, a normal force is applied and no strain are applied to the material and the gap is measured while the sample is exposed to a linear heating ramp of 10°C/min from ambient temperature to 500°C.

Chapter IV

^{29}Si NMR CPMAS

The silicone matrix added with fumed silica is characterized by 29Si NMR using CPMAS sequence. For each experiment, a delay of 5s and a contact time of 6 ms are used. The scan number for fumed silica and S3/fumed silica are respectively 13312 and 47104 to obtain an acceptable signal to noise ratio.

Appendix 2: Papers

Research article

polymers advanced technologies

Received: 9 March 2012, Revised: 1 May 2012, Accepted: 2 May 2012, Published online in Wiley Online Library: 11 June 2012

(wileyonlinelibrary.com) DOI: 10.1002/pat.3050

Thermal degradation and fire performance of intumescent silicone-based coatings

B. Gardelle[a,b,c,d], **S. Duquesne**[a,b,c,d], **V. Rerat**[e] and **S. Bourbigot**[a,b,c,d]*

This paper deals with the thermal degradation and fire performance of silicone-based coatings for protecting steel. In this study, the fire performance of silicone coatings as virgin or formulated materials is evaluated using two homemade fire testing methodologies: one similar to the "torch test" fire testing method and the other using a heat radiator test. It was shown that the performance of the silicone-based coating used as thermal barrier can be improved incorporating a modifier (a mixture of polydimethylsiloxane and silica coated by a silane). In this case, silicone-based coating swells and exhibits same fire performance as commercial intumescent coating at the torch test. It is shown that the incorporation of modifier in the silicone makes it to swell upon heating resulting in the formation of expanded material exhibiting low heat conductivity. Thermal degradation of the coating is also investigated: it occurs in three main steps leading to the formation of a tridimensional network characterized by the formation of Q^4 structure at high temperature. Copyright © 2012 John Wiley & Sons, Ltd.

Keywords: silicone; resistance to fire; intumescent coating; thermal conductivity

INTRODUCTION

The protection of metallic materials against fire has become an important issue in the construction industry. Indeed, prevention of the structural collapse of the building is paramount to ensure the safe evacuation of people from the building and is a prime requirement of building regulations in many countries. Steel usually begins to lose its structural properties above 500 °C[1], and it should be protected against fire. One of the most used systems to protect metallic structures is intumescent paint. These coatings have the properties to swell to thick insulative foam when heated above a critical temperature. Intumescent coatings are mostly based on a char-forming material, a mineral acid catalyst, a blowing agent and a binder resin.[2,3] However, these materials are typically organic-based materials and exhibit some disadvantages. First, organic additives undergo exothermic decomposition which reduces the thermal insulative value of the system. Second, the resulting carbonaceous char in some cases has a low structural integrity, and the coating cannot withstand the mechanical stress induced by a fire. Third, the coating releases organic gases (potentially toxic) which are undesirable in a closed fire environment.[4] The purpose of this work is thus to investigate and to develop a new organic–inorganic hybrid coating to protect steel against fire.

Silicones are polymers whose backbones consist of alternating Si–O bonds and have the properties to exhibit very low thermal conductivity, to be water and heat resistant and to evolve few toxic gases during their degradation.

Mechanical and thermal properties of silicone depend on their chemical structure and also on their environment. As an example, thermal degradation and char yield of polydimethyl siloxane (PDMS) depends on the heating rate and on the atmosphere.[5] Linear PDMS tend to decompose in one step in nitrogen flow without residue, whereas branched PDMS degrade in several steps and char yield increase with branched rate.[6] It indicates that branched structure benefits the formation of a network when siloxane is heated. Thermal degradation of branched silicone depends also on the phenyl content. It was shown that the polysiloxanes with phenyl side group show higher thermal stability than those with methyl groups.[6] Silicone-containing methyl and phenyl groups have already been studied as flame retardant in thermoplastic.[7] The authors show that polycarbonate (PC) containing a branch silicone with methyl and phenyl met the flame retarding standards specified by UL94 (V-0 rating). They also show that adding the silicone derivatives did not adversely affect the other properties of PC, such as strength or moldability. Moreover, Kashiwagi *et al*. evaluated the effect of silica gel and fumed silica in fire performance of polypropylene in cone calorimeter. The authors show that silica gel decreases the heat release rate of PP. Silica accumulate at the surface of the sample acting as a barrier protecting the material.[8] It is a typical case where the reaction to fire (contribution to fire growth) of polymeric material is enhanced.

In the case of fire protection or fire resistance (defined as the ability of materials to resist the passage of fire and/or gaseous products of combustion and obviously to keep the load-bearing

---

* *Correspondence to: S. Bourbigot, ENSCL, ISP-UMET, F-59652 Villeneuve d'Ascq, France: Serge Bourbigot.*
E-mail: serge.bourbigot@ensc-lille.fr

a *B. Gardelle, S. Duquesne, S. Bourbigot*
Univ Lille Nord de France, F-5900Lille, France

b *B. Gardelle, S. Duquesne, S. Bourbigot*
ENSCL, ISP-UMET, F-59652Villeneuve d'Ascq, France

c *B. Gardelle, S. Duquesne, S. Bourbigot*
USTL, ISP-UMET, F-59655Villeneuve d'Ascq, France

d *B. Gardelle, S. Duquesne, S. Bourbigot*
CNRS, UMR 8207, F-59652Villeneuve d'Ascq, France

e *V. Rerat*
Dow Corning S.A. - Seneffe, Belgium

properties of the steel), the use of silicone-based protective coating for protecting steel is very few reported in the open literature. A. Beigbeder evaluated the fire protective performance of PDMS/carbon nanotube-based coating onto aluminum plate.[9] He highlighted that in convective/radiative heating test, this coating exhibited improving properties compared to virgin aluminum. However, this coating is not intumescent.

The purpose of this paper is to investigate the fire resistance of phenyl silicone coating exhibiting an intumescent behavior upon heating using two homemade tests: one based on the torch test (radiative/convective heating scenario) and a heat radiator test (radiative heating scenario). On the other hand, it is recognized that the governing parameters for intumescent coating to get efficient heat barrier performance are the fast expansion of the coating as a function of temperature and its low thermal conductivity (formation of a dense and porous char).[10] Those parameters will thus be examined in this paper. Especially, thermal conductivities of silicone-based coating will be investigated as a function of temperature by the Hotdisk method.[11] Finally, thermal degradation of the silicone coating will then be studied characterizing the gas and condensed phases in order to explain the intumescence phenomenon and fire performance of silicone-based coatings.

EXPERIMENTAL PROCEDURE

MATERIALS

The silicone material used in this study is the resin silicone 217 supplied by Dow Corning (Senneffe, Belgium). This resin is a phenyl branched resin containing 6% of hydroxyl group. A solution of 11 g/mL is obtained dissolving the resin in absolute ethanol supplied by VWR (Fontenay sous Bois, France) so as to obtain a viscous solution. 8% of 7081 resin modifier (based on the total weight) supplied by Dow Corning (Senneffe, Belgium) was also incorporated in order to enhance the fire performance of the coating. The modifier is a mixture of polydimethylsiloxane and silica coated by a silane. Coatings were applied at a thickness of 400 +/− 50 µm on steel plates (XC38, 3 mm thick). The coatings were dried at 90 °C for 1 h.

Moreover, metallic structures are generally protected with intumescent paint. Nullifire S707-120 (Nullifire, England) is used as reference and for comparison in our study. The same thickness of Nullifire was coated on the same steel plate as above.

Fire performance

a) Torch test

Fire performance of the coatings was evaluated using a homemade fire testing method (Fig. 1) based on the torch test method (American Bureau of Mines Fire Endurance Test (4), 1966). The coating is exposed to an open flame (temperature of the flame around 1100 °C). The temperature at the back side of the plate is measured as a function of time using a pyrometer (temperature measured in the center of the plate). The backside of the plate is coated with black paint (Jeltz) having a constant emissivity (0.92) and thermally resistant up to 800 °C in order to get reliable temperature measurements with the pyrometer. This test allows evaluating fire performance of an intumescent coating in radiative/convective heating scenario.

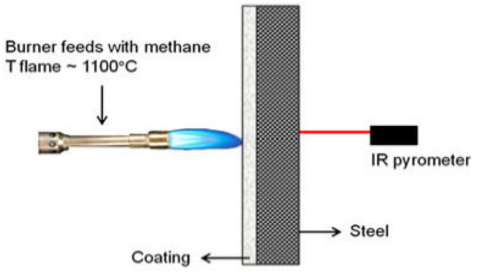

Figure 1. Schematic representation of the torch test.

b) Heat radiator test

We have developed in our laboratory a small-scale test permitting to measure the efficiency of a heat barrier.[12] The upper side of an assembly (protective material + substrate) undergoes an external heat flux and the temperature as a function of time is recorded on the backside of the substrate (material to be protected). Even if the temperatures reached in this test are less than in large-scale furnace test, this experimental setup has shown correlation with large-scale test (industrial furnace test running according to UL-1709) in the case of intumescent paint protecting steel.[12] In the test, the heat source is a heat radiator (Fig. 2), and so, the heating is purely radiative. Steel plate (used as substrate to be heat protected in this work) is put at 4 cm under the heat source delivering a constant heat flux of 30 kW/m², and its non-heated side is painted with the same black paint (Jeltz) as above. The constant emissivity of the backside of the plate allows accurate measurement of the surface temperature of the plate using an infrared pyrometer as mentioned above.

Sample characterization

Sample residues were characterized using a numerical microscope VHX-1000 supply by Keyence. The VHX-1000 creates a 3D image based on automatically captured images, and it calculates height profile data on a desired measuring line.

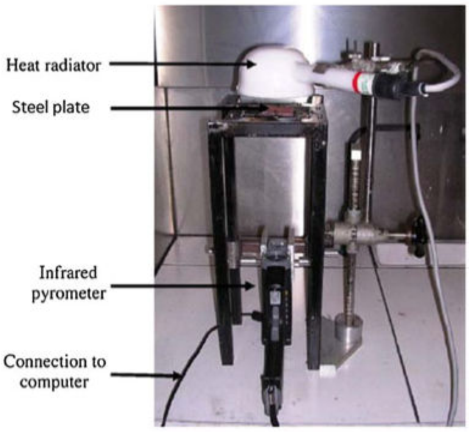

Figure 2. Heat radiator experimental setup.

Thermal degradation

a) TGA

Thermogravimetric analyses (TGA) were carried out using a TGA Q5000 from TA Instruments at 10 °C/min in a nitrogen flow (25 mL/min). For each sample, 15 mg of powder was positioned in alumina pans. Both the onset temperature (corresponding to 5% wt-% loss) and the temperature corresponding to the maximum rate of degradation have an uncertainty of 1 °C.

b) TGA/FTIR

Gases released during the degradation of the material were analyzed using a thermo gravimetric analysis (TGA Q5000, TA Instrument) connected to a Fourier transformed infrared (FTIR) spectrometer (ThermoScientific) Nicolet iS10. The IR spectra were recorded between 400 cm^{-1} and 4000 cm^{-1} (spectra recorded every 5 s). For each exeperiment, samples of 15 mg material (powder) were positioned in alumina pans. All the analyses have been carried out in nitrogen flow (100 mL/min).

a) Heat treatment and characterization of the heat treated residues

TGA experiments enable to define characteristic temperatures of degradation. Heat treatments were performed in a tubular furnace at those determined temperatures in nitrogen flow for 3 h. The collected residues were then analyzed using ^{29}Si solid state nuclear magnetic resonance (NMR).

^{29}Si NMR spectroscopy is a powerful tool for examining silicone surrounding. This technique can distinguish between several kinds of structures including M, D, T and Q structures which characterize silicone network (Fig. 3).

^{29}Si NMR spectra were recorded on a Bruker Advance II 400 operating at 9.4 T and equipped with 7 mm probe. NMR spectra were acquired with magic angle spinning (MAS) of 5 kHz. The reference used for ^{29}Si NMR was tetramethylsilane. A delay of 5 s between the pulses and a π/6 pulse length were used. For all spectra, 256 scans were accumulated.

Thermal conductivity measurement

Thermal conductivity of the silicone 217 and of the silicone 217 added with 8% of modifier 7081 were measured from 25 °C to 500 °C by a hot disk thermal constant analyzer (Hot Disk TPS 2500 S) from Thermoconcept (Bordeaux, France), which is a transient plane source technique.[11] The sensor which is warmth emitter and thermocouple is directly molded in the sample to ensure a good contact between the sample and the sensor during the experiment. The temperature is stabilized each 100 °C, and it is stable with less than 0.1 °C deviation. The conductivity measurements were made by applying a power of 0.01–0.07 W for between 5 and 40 s, depending on the thermal conductivity of the sample. Figures 4a and 4b illustrate, respectively, the furnace and the sample holder especially designed for permitting the expansion and the degradation of the coating as a function of temperature. The furnace is directly connected to nitrogen flow to prevent the oxidation of the sensor. This experimental setup allows measuring the thermal conductivity of the material as a function of the temperature.

RESULTS AND DISCUSSION

Fire performance

a) Torch test

The temperature profile obtained in the torch test for the virgin steel plate is compared with those obtained for the pure silicone coating, for the formulated silicone coatings and for the intumescent coating in Fig. 5. It is observed in all cases that the temperature increases until around 400 s, and then a steady state is reached after this time. The temperature at the steady state for the virgin plate is around 380 °C, whereas those obtained for pure silicone and for silicone/modifier-coated steel plate are, respectively, around 350 °C and 230 °C evidencing

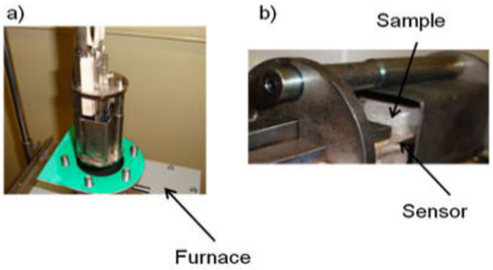

Figure 4. a) Furnace for thermal conductivity measurement. b) Sample preparation.

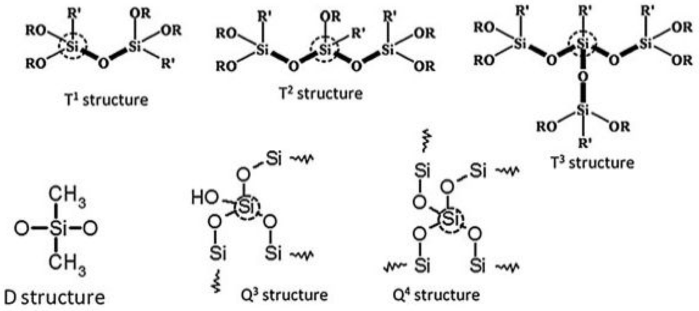

Figure 3. Schematics presentation of D, T^{i} and Q^{i} silicone structures.

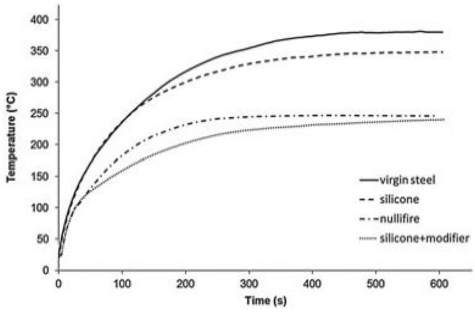

Figure 5. Time/temperature curves for the virgin steel plate and for the silicone coatings plate.

the heat barrier properties of the coatings. The temperature for the intumescent coating is around 230 °C at the steady state.

Silicone-based coating with and without modifier exhibits fire barrier properties against an open flame. In the steady state, temperature difference between the non-protected steel and the protected steel is 130 °C at the maximum, and so, when combined with the modifier, silicone-based coating reaches the same fire performance as a commercial intumescent coating. Note that during the entire test, the fire performance of silicone-based coating is better than those of intumescent paint and especially at shorter times (e.g. about 50 °C difference at 200 s). It demonstrates therefore the good fire performance of silicone/modifier-based coating in a convective/radiative heating test.

The picture of the silicone containing the modifier on its steel plate after the torch test shows a degradation and a swelling of the coating (Fig. 6a). Around the impact of the burner, the thickness of the coating is about 4 mm (corresponding to an expansion of 1000%). At the opposite, Fig. 6b shows the silicone without modifier on its steel plate after the test, the thickness around the impact is about 600 μm evidencing a very low expansion. Finally, the intumescent paint exhibits the formation of an expanded char after the test (expansion of 1500% higher than that of the silicone containing the modifier). Qualitatively and based on those observations and the literature review, the formation of an expanded coating during the test explains at least partially the fire protection delivered by the intumescent paint and the silicone-based coating containing the modifier.

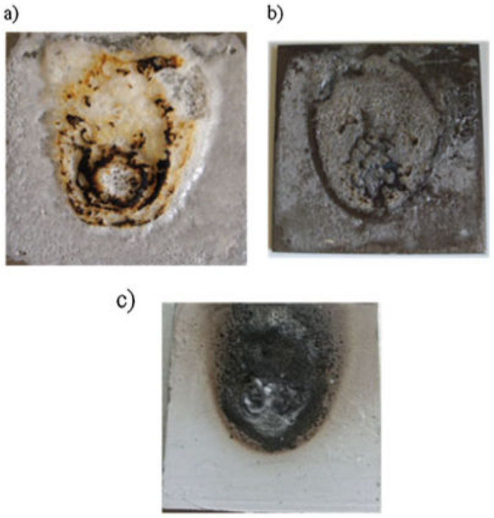

Figure 6. a) Silicone/modifier; b) Silicone and c) Nullifire steel plates after the torch test.

b) Heat radiator test

Performance of the silicone-based coatings was also evaluated in radiative fire testing conditions (Fig. 7). Similar to the results observed in the torch test, the temperature sharply increases and then reaches a steady state at around 400 s. However, for this test, it is observed that the temperature reached at the steady state is around 340 °C for the plate protected by silicone 217 containing 8% of modifier and around 360 °C for the silicone 217 steel plate compared with 400 °C for the non-coated plate. The performance obtained for the silicone-based coating is thus lower than that obtained for classical organic intumescent paint for which the temperature at the steady state is around 210 °C. Nevertheless the silicone-based coatings exhibit higher performance at shorter times (up to 200 s).

The properties obtained in radiative conditions are lower than those observed at the torch test. However, it still exhibits improved properties compared to non-coated steel and thus is considered as fire protective coating for steel applications.

The pictures of the materials after testing (Fig. 8) show a degradation of the coatings and some cracks at their surface (especially for silicone-based coatings, see Fig. 8b). It is observed the formation of white expanded foams for the silicone-based coating (expansion of 800%) while an expanded char is formed for the intumescent paint (expansion of about 800%). As discussed in the previous section, the formation of an expanded material during the test should act as an insulative barrier and explains the reduction of temperature on the backside of the steel plate.

All fire performance results and visual observations of the residue are compared and are summed up in the Table 1. It is shown that the silicone-based coating containing the modifier

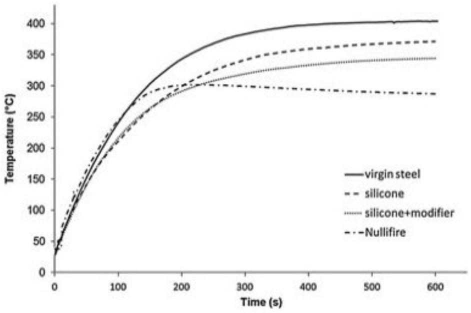

Figure 7. Time/temperature curves for silicone-based coatings in the heat radiator test.

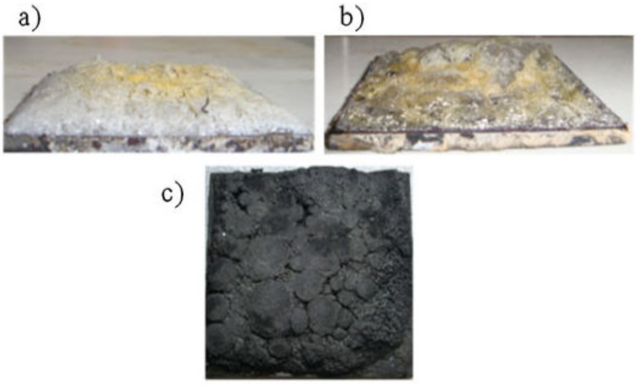

Figure 8. a)Silicone + modifier; b) Silicone and c) Nullifire steel plates after the heat radiator test.

Table 1. Summary of fire performance and visual observation of silicone-based coating

Coating	Torch test	Heat radiator
Silicone	- Low expansion 150% - Low fire performance compared to commercial intumescent paint $T_{steady\ state} = 350\,°C$	- Low expansion 200% - Several cracks - Fire performance limited due to cracks and small expansion $T_{steady\ state} = 360\,°C$
Silicone + Modifier	- Large expansion 1000% - Similar fire performance as commercial intumescent paint - $T_{steady\ state} = 230\,°C$	- Large expansion 800% - Several cracks - Fire performance limited due to cracks$T_{steady\ state} = 340\,°C$
Commercial intumescent paint(Nullifire)	- Large expansion - Good fire performance $T_{steady\ state} = 230\,°C$	- Large expansion: 800% - No cracks at the surface - Good cohesion of the char $T_{steady\ state} = 210\,°C$

is an efficient "hybrid" intumescent system. Its performance is still lower than that of a classical "organic" intumescent paint, but the concept is promising and must be further developed.

Thermal conductivity

In the two tests commented above, the silicone coatings exhibit an intumescent behavior. This expansion permits the formation of an insulative barrier reducing heat transfer from the external heating source to the substrate. Heat conductivity governs therefore the performance of the coating in terms of insulation. Very few article in the open literature deals with the measurement of thermal conductivity at high temperature of intumescent material. J.E.J Stagg determined thermal conductivities of intumescent char at high temperature by numerical simulation.[13] He evaluated thermal conductivity from ambient temperature to 1200 K and its dependence with the porosity of the material. The larger pores of the char are, the greater radiation enhancement to the effective thermal conductivity is. In function of the porosity, he demonstrated that thermal conductivity of intumescent char material varies from 0.1 W/m.K. to 0.4 W/m.K. from ambient temperature to 600 °C.

Thermal conductivity of silicone and silicone/modifier were measured from ambient temperature to 600 °C (Fig. 9). For both materials, it varies from 0.1 to 0.35 W/m.K. depending on the temperature, and they are in the same order of magnitude as values found in the literature.[10,13]

The thermal conductivity for the silicone at 20 °C and at 300 °C is, respectively, 0.35 ± 0.01 W/m.K. and 0.18 ± 0.01 W/m.K. This

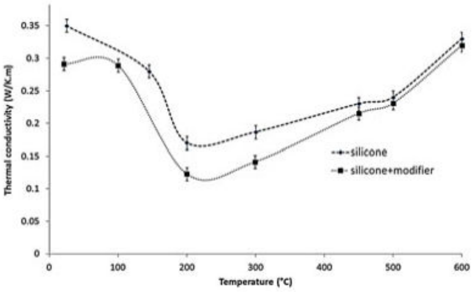

Figure 9. Thermal conductivity versus temperature curves.

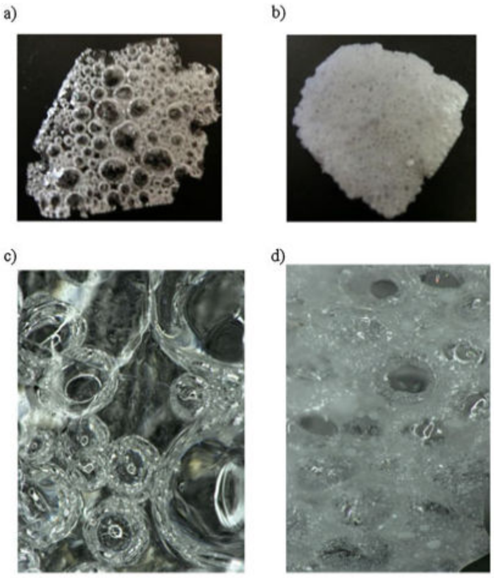

Figure 10. Picture of a) Silicone residue at 300 °C. b) Silicone/modifier residue at 300 °C and numerical picture of c) Silicone residue at 300 °C, d) Silicone/modifier residue at 300 °C.

strong decrease is due to the formation of an expanded foamed structure at 300 °C (Fig. 10a and Fig. 10c). When modifier is incorporated, the shape of the thermal conductivity curve is the same as that without modifier. However, the thermal conductivity is lower: 0.29 ± 0.01 W/m.K. at 20 °C and 0.13 ± 0.01 W/m.K. at 300 °C. This is also due to the formation of an expanded foamed structure exhibiting smaller cells than that in the case of neat silicone (Fig. 10b and Fig. 10d). At 600 °C, thermal conductivity is the same for both sample and reaches 0.32 ± 0.01 W/m.K.

For the two silicone-based coatings, thermal conductivities are very low (less than 0.3 W/m.K.), but the modifier increases the expansion of the coating during the fire test creating a thicker insulative barrier.

Thermal degradation mechanism

TGA of silicone/modifier

TG and DTG curves of the silicone and of the modifier are compared in Fig. 11.

It shows that the two materials degrade at the same temperature, but the degradation rate of the modifier is twice faster than the matrix. This result suggests that the modifier acts as blowing agent in the system silicone/modifier which permit the fast expansion of a foamed structure as observed after fire testing.

TG curves of the silicones with and without modifier are similar (Fig. 12). Both materials show an excellent thermal stability. In the two cases, degradation occurs in three main steps (second and third step overlapping). The temperatures for each step where degradation rate is maximum are, respectively, 200 °C, 500 °C and 600 °C. The weight loss of each degradation step for silicone/modifier is, respectively, 3.7 %, 10.4% and 16.8%. The total weight loss at 800 °C is only 31% demonstrating the excellent thermal stability of the silicone/modifier formulation (in TGA condition). TG curve of silicone is similar, and the weight loss of each degradation step is, respectively, 4.0%, 5.4% and 18.7%.

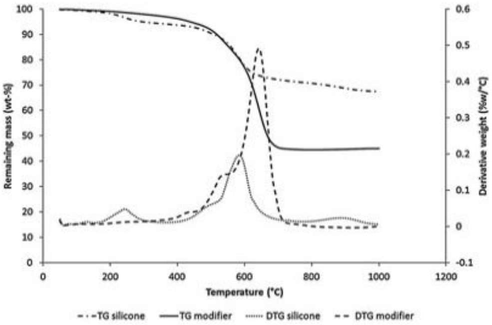

Figure 11. TGA and DTG curve of silicone and modifier in nitrogen flow.

In order to determine the degradation pathway of the silicone-based coatings, gas phase and condensed phase are analyzed. TGA coupling with FTIR is used to determine the nature of the gases released during the degradation. The two coatings have been heat treated at 250 °C and 600 °C –corresponding, respectively, to the end of the first and the third step of degradation – and the resulting residues have been characterized by ^{29}Si NMR.

Analysis of the gas phase

In order to determinate the nature of the gases evolved during each step of the degradation of silicone resin and silicone/modifier, TGA coupling with FTIR was used. Spectra are shown on Fig. 13. Band assignments have been done according to the literature.[14]

Concerning silicone resin, the first step of degradation between 50 °C and 250 °C is characterized by the release of oligomers of silicone associated to a small weight loss of 4.0wt-%. Indeed, peak at 2950 cm^{-1} corresponding to the bending vibration of CH_3 bond and peaks between 1000 and 1100 cm^{-1} corresponding to the bending vibrations of Si–O–Si bond are observed on the spectrum of the gases collected at 250 °C.

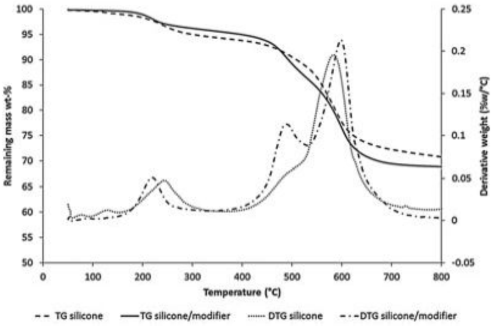

Figure 12. TGA of silicone and silicone/modifier at 10 °C/min in nitrogen flow.

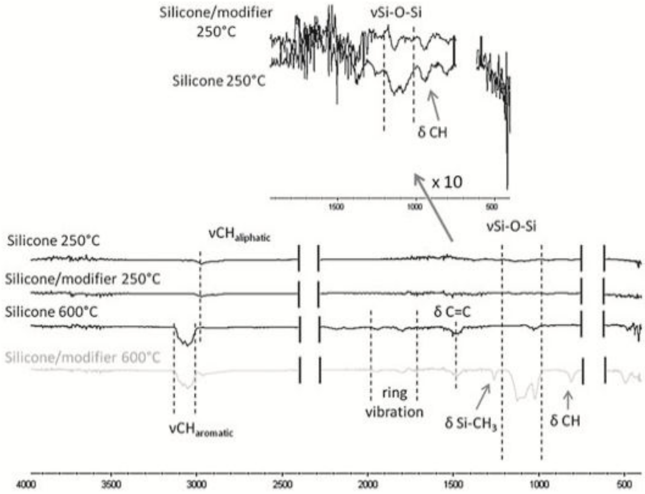

Figure 13. IR spectra of the gas evolved during the thermal degradation of the silicone resin and silicone resin + modifier at 250 °C and 600 °C.

During the second and the third step of the degradation, aromatic compounds such as benzene and biphenyl are released. Indeed, peak at 1400 cm^{-1} and between 1700 and 2000 cm^{-1} are characteristic of phenyl groups and the peaks at 3010 cm^{-1} and 1050 cm^{-1} are characteristic of respectively C–H stretching and bending vibration. It corresponds to a weight loss of 24.1%.

Concerning silicone/modifier, same gases are released during the first step of degradation. During the second and third step of degradation, aromatic compounds from the resin and silicone compound from PDMS from modifier are evolved. Camino *et al.* studied thermal degradation of PDMS and highlight that gases evolved during degradation are mainly cyclic oligomers such as cyclic hexamethylcyclotrisiloxane.[5,15] Indeed, peak at 1260 cm^{-1} corresponding to the bending vibration of Si–CH$_3$ bond and peaks between 1000 and 1100 cm^{-1} corresponding to the bending vibrations of Si–O–Si bond are observed on the spectrum of the gases collected during the degradation of silicone/modifier at 600 °C. This result suggests that there is no interaction in the gas phase since aromatic compounds from the matrix are evolved for silicone and silicone/modifier material.

Analysis of the condensed phase

After characterizing the gases released during the pyrolysis, analysis of the condensed phase has been made. Residues collected after heat treatment at the previously defined characteristic temperature (250 °C and 600 °C) have been examined by ^{29}Si solid state NMR. Note that Karrasch *et al.* used a similar approach to characterize silicate network formed during the degradation of flame retarded PC containing silicone rubber.[16] Band assignments have been done according to their work and to the literature.[16,17]

^{29}Si MAS NMR spectra of the silicone-based coatings at room temperature show two bands located at −68 ppm and −81 ppm (Fig. 14). They can be assigned to T^2 and T^3 structures. In the case

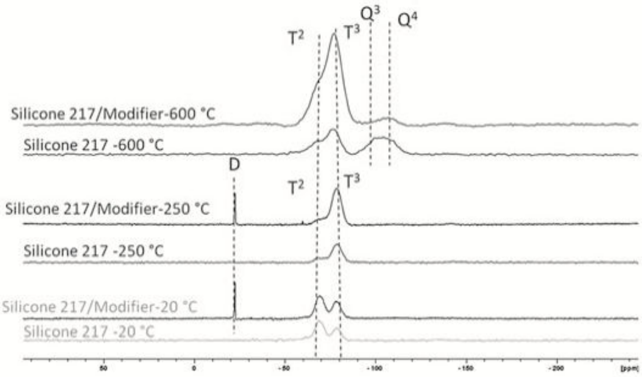

Figure 14. ^{29}Si NMR spectra of silicone and of the heat treatment residues.

Table 2. Analysis of the condensed and gas phase during the degradation coupled with thermal conductivity

	Heat thermal treatment	Mass loss %-wt	^{29}Si MAS NMR	Gas released	k (W/m.K.)
Silicone	250 °C	4.0%	T^2 and T^3 structure	Oligomers of silicone	0.18
Silicone/modifier		3.7%	D, T^2 and T^3 structures	Oligomers of silicone	0.14
Silicone	600 °C	29.0%	Tridimensional network-Q structures	Aromatic compounds such as benzene	0.33
Silicone/modifier		31.0%	Tridimensional network-Q structures	Oligomers of silicone from PDMS and aromatic compounds	0.32

of the silicone containing the modifier, one can distinguish an additional peak at −22 ppm corresponding to the D structure contained in the PDMS of the modifier (silica coated with PDMS). At 250 °C, the silicone and silicone/modifier residues contain mainly T^3 structure (band at − 81 ppm). The spectra of the silicone and silicone/modifier treated at 600 °C show the same bands as above and the formation of Q^3 and Q^4 structures which are detected at, respectively, −100 ppm and −107 ppm. The analysis of the NMR spectra shows therefore that there is no chemical interaction between the modifier and the silicone during the degradation.

Degradation mechanism

After analyzing the condensed and the gas phases during the degradation of the silicone, the degradation pathway can be established. All the results are sum up in the Table 2.

For $T < 250$ °C, oligomers of silicone are released, and the structure is composed of T^2 and T^3 sites. For $T > 250$ °C, oligomers of PDMS from modifier and aromatic compounds such as benzene from silicone are released. There is the formation of tridimensional network composed of Q^3 and Q^4 structures.

Discussion

It was clearly shown that silicone and silicone/modifier exhibit different behavior when undergoing pure radiative or radiative/convective heating. In the case of pure radiative heating, silicone-based coatings crack and so exhibit relatively low fire performance. These cracks are assumed to be due to the high vibration energy of Si–O bound in infrared field. The intumescence phenomenon observed during the fire tests (and the resulting fire protection) is attributed to rheological phenomenon: the silicone coating softens upon heating, and it is then expanded because of the fast degradation of the modifier releasing gases (Fig. 11). The network formed at high temperature can trap the gases released by the modifier and make the coating to swell. Finally, this expanded coating has a low thermal conductivity (0.32 W/m.K.) and provides the fire protection measured during the tests. Note that the heat conductivity of the intumescent structure is not changed by the modifier and so the better protection delivered by the silicone/modifier is due to the higher thickness of the protective coating.

CONCLUSION

This paper has investigated the thermal degradation and fire performance of silicone-based coatings. The fire performance of silicone coating has been evaluated using two homemade fire tests, one based on the torch test and the heat radiator test. It is shown that the performance of the silicone-based coatings can reach that of a commercial intumescent paint. Fire performance of silicone is enhanced incorporating modifier. This filler increases the expansion of the coating during fire test, but it does not modify the thermal conductivity of the protective barrier. However, the heat conductivity is quite low for the two systems.

The thermal degradation mechanism of the silicone-based coating was also investigated and has been elucidated analyzing the gas and condensed phase during the degradation; it was shown that the degradation occurs in two main steps leading to the tridimensional network formation composed of Q^4 structure at high temperature. Silicone and the modifier degrade at the same temperature, but the degradation rate of the modifier is much faster than that of the silicone. It permits the expansion of the 3D network issue from the degradation of silicone which traps the degrading gases of the modifier. It leads to the formation of an expanded thick foamed structure exhibiting low heat conductivity and ensuring fire protection.

REFERENCES

[1] L. Gardner, N. R. Baddoo. *J. Constr. Steel Res.* **2006**, *62*, 532.
[2] E. D. Weil. *J. Fire Sci.* **2011**, *29*(3), 259–296.
[3] S. Duquesne, S. Magnet, C. Jama, R. Delobel. *Surf. Coat.Technol.* **2004**, *180–181*, 302.
[4] D. T. Nguyen, D. E. Veinot, J. Foster. Patent U. S., Ed. Canada, **1989**.
[5] G. Camino, S. M. Lomakin, M. Lazzari. *Polymer* **2001**, *42*, 2395.
[6] W. Zhou, H. Yang, X. Guo, J. Lu. *Polym. Degrad. Stab.* **2006**, *91*, 1471.
[7] M. Iji, S. Serizawa. *Polym. Adv. Technol.* **1998**, *9*, 593.
[8] T. Kashiwagi, J. W. Gilman, K. M. Butler, R. H. Harris, J. R. Shields, A. Asano. *Fire and Materials* **2000**, *24*, 277.
[9] A. Beigbeder, M. Linares, M. Devalckenaere, P. Degée, M. Claes, D. Beljonne, R. Lazzaroni, P. Dubois. *Adv. Mater.* **2008**, *20*, 1003.
[10] J. E. J. Staggs. *J. Fire Sci.* **2011**, *29*, 177.
[11] S. E. Gustafsson. *Rev. Sci. Instrum.* **1991**, *62*, 797.
[12] M. Jimenez, S. Duquesne, S. Bourbigot. *Ind. Eng. Chem. Res.* **2006**, *45*, 7475.
[13] J. E. J. Staggs. *Fire Safety J.* **2010**, *45*(4), 228–237.
[14] J. T. Sun, Y. D. Huang, H. L. Cao, G. F. Gong. *Polym. Degrad. Stab.* **2004**, *85*, 725.
[15] G. Camino, S. M. Lomakin, M. Lageard. *Polymer* **2002**, *43*, 2011.
[16] A. Karrasch, E. Wawrzyn, B. Schartel, C. Jäger. *Polym. Degrad. Stab.* **2010**, *95*, 2534.
[17] F. Babonneau, N. Baccile, G. Laurent, J. Maquet, T. Azaïs, C. Gervais, C. Bonhomme. *Comptes Rendus. Chimie* **2010**, *13*, 58.

Fire Performance of curable Silicone-based coatings

B. Gardelle[1,2,3,4], S. Duquesne[1,2, 3,4], P.Vandereecken [5],
S. Bourbigot[1, 2, 3,4]*
[1] Univ Lille Nord de France, F-5900 Lille, France
[2] ENSCL, ISP-UMET, F-59652 Villeneuve d'Ascq, France
[3] USTL, ISP-UMET, F-59655 Villeneuve d'Ascq, France
[4] CNRS, UMR 8207, F-59652 Villeneuve d'Ascq, France
[5] Dow Corning S.A. - 7180 Seneffe, Belgium
*Corresponding author: Serge Bourbigot - tel: +33 (0)320434888
e-mail: serge.bourbigot@ensc-lille.fr

Abstract

Polysiloxane elastomers are widely used because of their high thermal stability and low thermal conductivity. In this study, the fire performance of silicone based coatings containing ground calcium carbonate (GCC) are evaluated using a fire testing methodology similar to the "Torch Test" fire testing method. Two kinds of room temperature vulcanized silicone resins containing 50% of GCC are used. The two resins, S1 and S2, are based on polydimethylsiloxane (PDMS) and are composed of D [$SiO_2(CH_3)_2$] and T [$CH_3Si(O_{1/2})_3$] structures. The two resins mainly differ from their chain length. It is shown that the performance of the silicone based coating used as thermal barrier are better when the coating is mainly composed of D structures and

has high crosslinking density. This is explained by its lower thermal diffusivity at high temperature and by its higher thermal stability.

Introduction

Polydimethylsiloxane (PDMS) is widely used in construction and electrical abilities because of its excellent thermal stability and fire properties including low heat of combustion and low rate of heat released compared to organic polymers[1, 2]. This polymer is available in different forms from liquid to cross-linked rubber. The rubbers can be found in two main classes[3]: one cross-linked by poly-addition, and another by poly-condensation.

For poly-addition, cross-linking of silicone rubber is achieved using vinyl endblocked polymers and reacting them with the SiH groups carried by functional oligomers. This reaction is catalyzed by Pt or Rh metal complex[3] as illustrated in Figure 1.

$$\sim\sim\sim\ OMe_2Si\text{-}CH{=}CH_2 + H\text{-}SiR_3 \xrightarrow{cat} \sim\sim\sim\ OMe_2Si\text{-}CH_2\text{-}CH_2\text{-}SiR_3$$

Figure 1 : Poly-addition reaction

Silicones prepared via the poly-condensation method are used to make sealants that find applications in original equipment manufactories for glazing sealing windows and doors for either residential or public buildings. They are also used as building component providing a barrier against severe environments such as humidity or dust[4]. These products are ready to use and require no mixing : cross-linking starts when the product is exposed to moisture. Most silicone sealants are formulated from a reactive polymer prepared from an hydroxy-polydimethylsiloxane and a large excess of methyltrimetoxysilane. The poly-condensation reaction is illustrated in Figure 2.

$$\mathrm{HO{-}(Me_2SiO)}_x\mathrm{{-}H} \quad + \mathrm{exc.\ MeSi(OAc)_3}$$

$$\xrightarrow{-2\mathrm{AcOH}} \mathrm{(AcO)_2MeSiO(Me_2SiO)}_x\mathrm{OSiMe(OAc)_2}$$

Figure 2 : Poly-condensation reaction

On the other hand, calcium carbonates have attracted more and more interest due to the availability of these raw materials and to its low cost. This filler is mainly used in PDMS to improve its mechanical[3] and flame retardant properties[5, 6]. Calcium carbonate also enhances thermal stability of PDMS. Upon heating silicone containing calcium carbonate form ceramic-like calcium silicate residue[6]. When incorporated in thermoplastics, the formation of this type of residue acts as a protective barrier which provides significant flame retardancy.

In this work, passive fire protection of steel using silicone-based coating is investigated. The protection of metallic materials against fire has become an important issue in the construction industry. Steel begins to lose its structural properties above 500 °C and it must be therefore protected against fire[7]. Prevention of the structural collapse of the building is paramount to ensure the safe evacuation of people from the building, and is a prime requirement of building regulations in many countries.

In that field, the use of silicone-based protective coating is very few reported in the literature. Beigbeder et al. evaluated the fire protective performance of PDMS/Carbone nanotube based coating onto aluminium plate. They highlighted that in convective/radiative heating test, this coating exhibited improved properties compared to virgin aluminum.

In this paper, fire performance of two silicone sealants containing calcium carbonate is investigated using an homemade fire test based on the Torch test. Since the formation of protective coating at the surface of steel will be involved, thermal parameters including heat conductivity and thermal diffusivity should be low in order to limit heat transfer. These parameters will be measured as a function of temperature using the Hotdisk method and will be commented[8]. The structure formed by the silicone based-coatings upon heating will be then investigated by ^{29}Si solid state NMR and potential correlation between the structure and the thermal properties will be examined.

2- Experimental

2.1- Materials

The two curable PDMS were formed from three main components: an hydroxyl PDMS, methyltrimethoxysilane as cross-linking agent and an organometallic catalyst such as tin and titanium catalyst. All the materials were supplied by Dow Corning, Seneffe (Belgium).

The first resin, hereafter called silicone 1 (S1), was composed of an hydroxylated PDMS with a viscosity of 80 cS (viscosity is measured using cone/plate rheometer CP-52), a large excess of methyltrimethoxysilane (MTM) and a tin catalyst.

The second, hereafter called silicone 2 (S2), was composed of a hydroxylated PDMS with a viscosity of 2000 cS (viscosity is measured using cone/plate rheometer CP-52), a large excess of MTM and a titanium catalyst. S1 and S2 mainly differ from their chain length; S2 having a longer chain length than S1.

50% of ground calcium carbonate (GCC) stearic acid coated with an average particle size of 4.5µm supplied by Dow Corning is incorporated into the matrix to enhance the fire performance of the coating. Both formulations were applied on a 10 cm x 10 cm x 3 mm steel plate to obtain 400 ± 40 µm coating. Steel plates were cleaned before application with ethanol and a primer (Primer 1200 from Dow Corning) was applied to enhance the coating adhesion.

2.2- Solid state NMR

^{29}Si NMR spectroscopy is a powerful tool for examining silicon surrounding. This technique can distinguish between several kinds of structures including D and T structures which characterize silicone network (Figure 3).

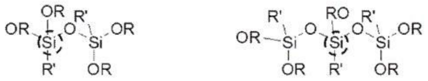

T^1 structure

T^2 structure

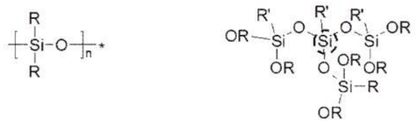

D structure

T^3 structure

Figure 3 : Schematics presentation of D, T^i silicone structures

^{29}Si NMR spectra were recorded on a Bruker Advance II 400 operating at 9.4T and equipped with 7 mm probe. NMR spectra were acquired with MAS (magic angle spinning) of 5 kHz. The reference used for ^{29}Si NMR was tetramethylsilane (TMS). A delay of 180s between the pulses and a $\pi/2$ pulse length were used. For S1 and S1/GCC materials respectively 64 scans and 784 scans were accumulated. For S2 and S2/GCC materials respectively 1250 scans and 7620 scans were accumulated. In order to quantify the amount of D and T structure within each resin, simulation of ^{29}Si NMR spectra were obtained using DMfit99 software[9].

2.3 -Fire performance

Fire performance of the coatings were evaluated using an homemade fire testing method (Figure 4) based on Torch Test method (American Bureau of Mines Fire Endurance Test (4), 1966). The coating is exposed to an open flame (temperature of the flame around 1100°C).

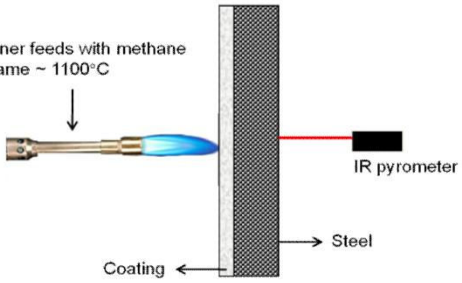

Figure 4: Schematic representation of the Torch Test

The temperature at the back side of the plate is measured as a function of time using a pyrometer (temperature measured in the center of the plate). The backside of the plate is coated with black paint (Jeltz) having a constant emissivity (0.92) and thermally resistant up to 800°C in order to get reliable temperature measurements with the pyrometer. This test allows evaluating the fire performance of a coating in radiative/convective heating scenario.

2.4 Thermal properties

Thermogravimetric analyses (TGA) were carried out using a TGA Q5000 from TA Instruments at 10 °C/min in a nitrogen flow (25 mL/min). For each sample, 15 mg of sample were positioned in alumina pans. Gases released during the degradation of the material were analyzed using a thermo gravimetric analysis (TGA Q5000, TA Instrument) connected to a Fourier transformed infrared (FTIR) spectrometer (ThermoScientific) Nicolet iS10. The IR spectra were recorded between 400 cm^{-1} and 4000 cm^{-1} (spectra recorded every 11 s). For each experiment, samples of 15mg material (powder) were positioned in alumina pans. All the analyses have been carried out in nitrogen flow (75 mL/min).

Thermal conductivity and diffusivity of both formulations: S1 + 50%GCC and S2 + 50%GCC were measured from 25°C to 500°C using a hot disk thermal constant analyzer (Hot Disk TPS 2500 S) from Thermoconcept (Bordeaux, France), which is a transient plane source technique[8]. The sensor which is warmth emitter and thermocouple is directly molded in the sample to ensure a good contact between the sample and the sensor during the experiment. The temperature is stabilized each 100°C with less than 0.1°C deviation. The conductivity measurements were made by applying a power of 0.03–0.15 W for between 5 and 60 s, depending on the thermal conductivity of the sample. The furnace is directly connected to nitrogen flow and all experiments are carried out in inert atmosphere to prevent the oxidation of the sensor. For each sample, two experiments are carried out to evaluate the uncertainty of measurement. This experimental set up allows measuring the thermal conductivity and diffusivity of the material versus the temperature.

3- Results and Discussion

3.1- Resin characterization

Figure 5 illustrates chemical reactions which occur during the cross-linking of the hydroxylated PDMS[3]. Exposed to moisture, hydroxyl group reacts with the methoxy group of MTM which lead mainly to T^1 and T^2 structures. Without any fillers, the crosslinking is complete and no silanol group are remaining.

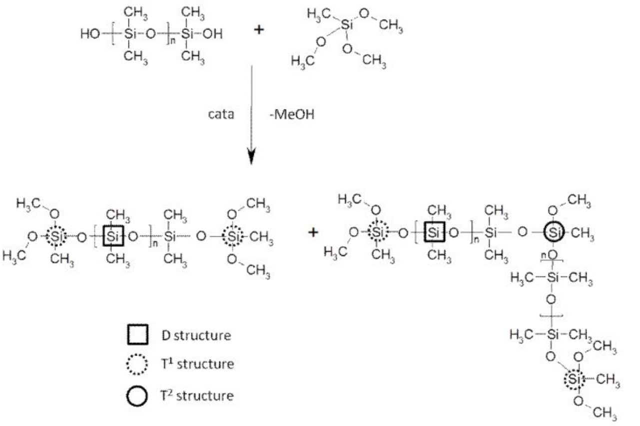

Figure 5 : Chemical pathway of resin cross-linking

Figure 6 shows ^{29}Si NMR spectra of resins S1 and S2. Band assignments have been made according to the literature[10].

Three bands appear in both spectra at -22 ppm, -58 ppm and -67 ppm corresponding to respectively D, T^1 and T^2 structures. It demonstrates that the two resins have similar chemical structure composed of D, T^1 and T^2 units.

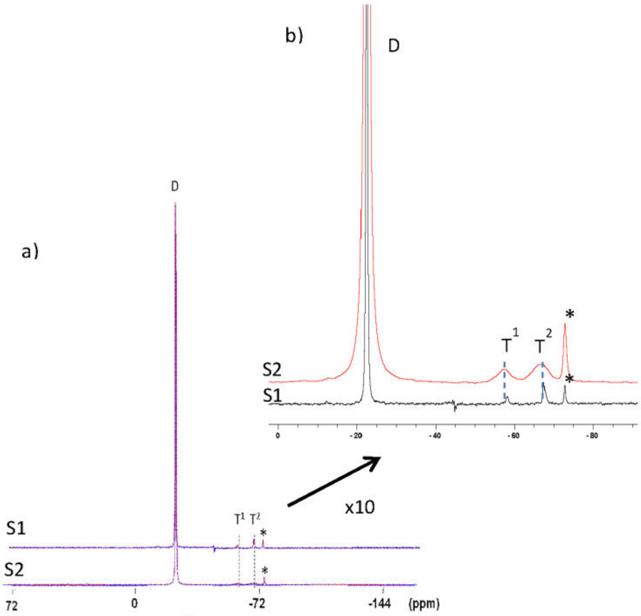

Figure 6 : a) blue line- ^{29}Si solide state MAS NMR spectra / red line - calculated spectra with DMFIT software b)zoom of T bands

It is noteworthy that handling S1 compared with S2, S2 is more rigid than S1 rubber that could be due to a different crosslinking degree of the two resins. Indeed, it is well known that that the crosslinking degree of polymers is directly linked with its mechanical properties[11] (in particular highly cross-linked elastomers exhibit high modulus).

Deconvolution of the spectra allows quantifying the ratio between D and T in each siloxane resin and so, it allows evaluating the crosslinking density of each resin. Results are summarized in Table I.

It is shown that S1 contains more T structure than S2. For S1, polymeric chains are shorter than those of S2 and so, there are more reactive hydroxyl group in S1. Consequently, the amount of MTM in S1 is higher than in S2 to make the resin cross-linked. The crosslink density of S1 is thus higher than S2.

Table I: Deconvolution results of S1 and S2 resin

Material	D	T
S1	93%	7%
S2	95%	5%

The next step of the study is to evaluate the influence of T structure and of the silicone network on fire performances of S1 and S2 based coating containing GCC.

3.2- Fire Performances

The temperature profiles obtained in the Torch Test of the silicone-based coatings on steel plate are compared with that of the uncoated steel plate (Figure 7). It is observed in all cases that the temperature increases until around 400 s and then a steady state is reached. The temperature at the steady state for the uncoated steel plate is around 380°C whereas those obtained for S1/GCC and S2/GCC coated steel plate are respectively around 320°C and 295°C evidencing the heat barrier properties of the coatings.

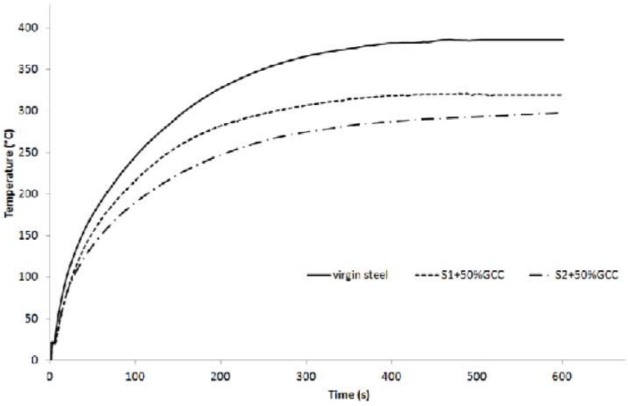

Figure 7 : Time/temperature curves for the virgin steel plate and for the silicone coatings plate

Figure 8 illustrates S1/GCC and S2/GCC based coating after torch test experiment. It shows that no swelling of the coating occurs during experiment and that some cracks are visible for S2 based coating.

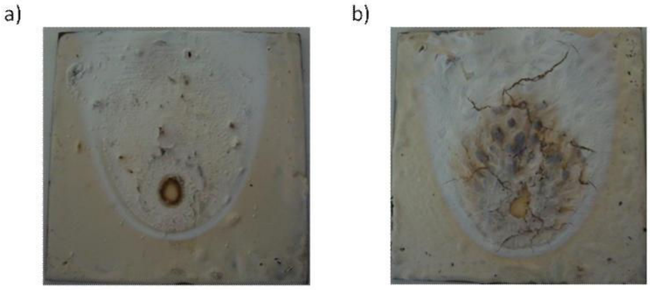

Figure 8: a) S1+50%GCC b) S2 + 50%GCC steel plate after torch test

To explain the fire performance of coatings several parameters have to be taken into account. J.E.J Stagg demonstrates that the fire performance of intumescent coatings are governing by their thickness (their expansion during the fire test) and their thermal properties such as heat conductivity[12]. In this last case, fire protection is due to the formation of thick insulative foam with low thermal conductivity at high temperature. In the present work, silicone based coating do not swell during fire experiment and we can reasonably assume that the main parameters governing fire performance are their thermal properties at high temperature such as thermal conductivity and diffusivity.

3.3- Thermal properties

In this section, thermal diffusivity and thermal conductivity are thus investigated from ambient temperature to 500°C using the hot disk technology.

Heat conductivity is one of the parameters governing the performance of the coating in terms of insulation. Very few article in the literature deals with the measurement of thermal conductivity at high temperature of material. J.E.J Stagg determined thermal conductivities of intumescent char at high temperature by numerical simulation[13]. He evaluated thermal conductivity from ambient temperature to 1200K and its dependence with the porosity of the material. He calculated that thermal conductivity of intumescent char material varies from 0.1 W/m.K. to 0.4 W/m.K. from ambient temperature to 600°C suggesting the heat insulative properties of these materials.

Thermal conductivity of S1/GCC and S2/GCC are measured from ambient temperature to 500°C (Figure 9).

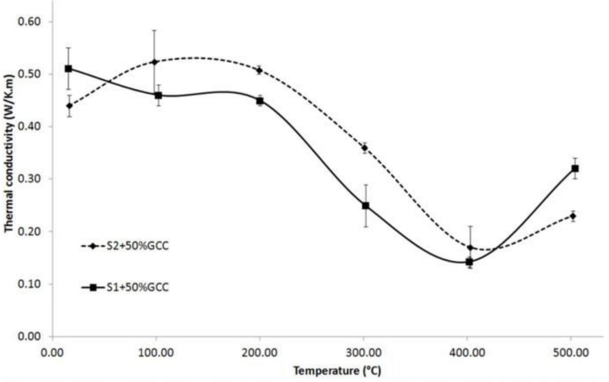

Figure 9 : Thermal conductivity versus temperature curve for S1/GCC and S2/GCC adding with GCC

For the two materials, heat conductivity decreases from 25°C to 400°C due to the formation of some alveolus inside the material (Figure 10). Indeed, the heating rate in the furnace is very low compared to that in the fire test and therefore, it allows the material to encapsulate gases evolved during the matrix degradation. During the torch test, the coating is directly exposed to an open flame and the temperature of the coating reaches 800°C in few seconds. Because of this high heating rate, the coating does not swell and just cracks appear on the coating after testing (Figure 8).

Figure 10 : Picture of S2/GCC residue at 500°C

For S1 and S2 based material, thermal conductivities are similar and reach respectively 0.32 ± 0.02 W/K.m and 0.23 ± 0.01 W/K.m at 500°C.

The other important parameter when dealing with heat transfer is the thermal diffusivity α (eq. 1) which depends on the thermal conductivity k, the density ρ, and the specific heat capacity C_p.

Equation 1 : Thermal diffusivity Eq.1

$$\alpha = \frac{k}{\rho.c_p} \qquad \text{Eq. 1}$$

Figure 11 shows the thermal diffusivity versus temperature for S1/GCC and S2/GCC material. When S2/GCC material is heated, thermal diffusivity varies from 0.05 ± 0.03 mm²/s to 0.15 ± 0.01 mm²/s. According to the errors on the measurement, we may say there are no significant changes of the thermal diffusivity as a function of temperature. However, thermal diffusivity of S1/GCC material increased significantly when heated to 500°C. At ambient temperature, thermal diffusivity is 0.04 ± 0.02 mm²/s (as that of S2 based material) and reach 0.45 ± 0.04 mm²/s at 500°C which is 4 times higher than that of S2/GCC.

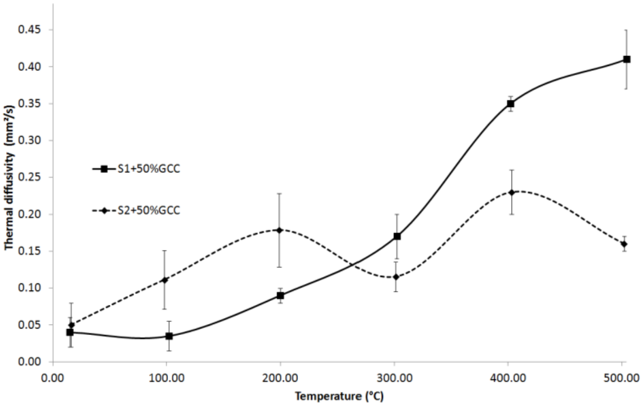

Figure 11 : Thermal diffusivity versus temperature curve for S1 and S2 adding with GCC

Thermal diffusivity describes the ability of a material to conduct heat (k) compared to store the heat ($\rho.c_p$). In a material with high thermal diffusivity, heat moves rapidly through. Heat diffuses therefore more rapidly in S1/GCC matrix than in S2/GCC. Since k of the two materials are similar, the change of thermal diffusivity is explained by the changes of $\rho.c_p$, i.e. by the heating storage (lower heating storage of S1 compared to that of S2).

This strong difference of heat diffusivity of the two materials should be due to different thermal stability. Depending on its degradation pathway, the resin exhibits morphological modification and hence modification of its thermal properties.

Thermal stability of the two materials is thus investigated (Figure 12).

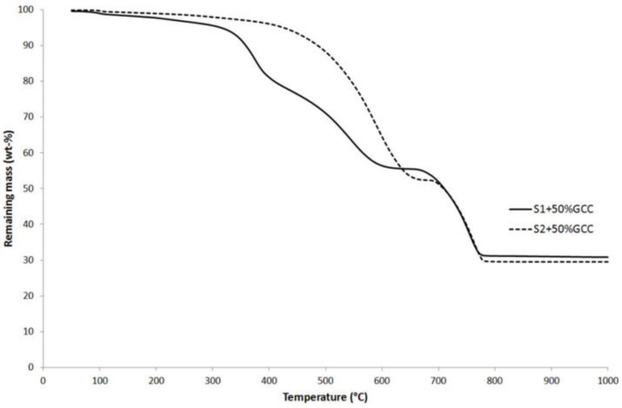

Figure 12 : TG curve of S1/GCC and S2/GCC in nitrogen flow at 10°C/min

It is observed that S2/GCC is more stable than S1/GCC. Thermal degradation of S1/GCC occurs in three main steps (the last step corresponding to the degradation of calcium carbonate). The temperatures for each step where degradation rate is maximum, are respectively 376°C, 540°C and 760°C. The weight loss of each degradation step for S1/GCC is respectively 20%, 24% and 25%. Concerning S2 based material, thermal degradation occurs in two main steps (the last corresponding to the degradation of calcium carbonate). The temperatures for each step where degradation rate is maximum, are respectively 590°C and 760°C and the weight loss of each degradation step are 47% and 23%. The two resins contain 50% of calcium carbonate. The thermal degradation of calcium carbonate is well known and lead to the formation of CaO releasing carbon dioxide[5]. Theoretically, the amount of CO_2

released by the calcium carbonate is 22%. This demonstrates that the last step of degradation of each material is mainly due to calcium carbonate and the gas released should be carbon dioxide. This will be confirmed by TGA-FTIR experiment.

To explain the lower thermal stability of S1/GCC compared to S2/GCC, the chemical structure of the two materials is examined by solid state ^{29}Si NMR (Figure 13). As for the pure resin, three main bands appears in ^{29}Si NMR spectra at -22 ppm, -58 ppm and -67 ppm corresponding to respectively D, T^1 and T^2 structures.

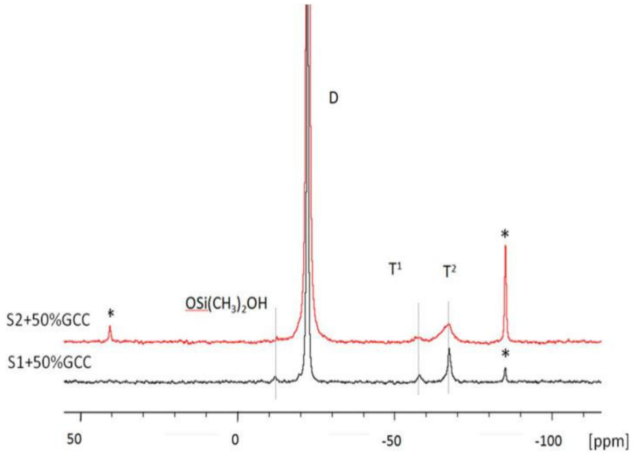

Figure 5 : ^{29}Si NMR spectra of S1/GCC and S2/GCC materials

Deconvolution of the bands allows determining the ratio D/T in each resin and so, to evaluate the crosslinking degree of the material. The results are reported in Table II. This evidences that S1 based resin is more cross-linked (it contains more T structure) when calcium carbonate is incorporated. On the contrary, there is no modification of the crosslinking density of S2 when calcium carbonate is incorporated.

Moreover, for S1/GCC, an additional band appears at -12 ppm corresponding to silanol site. The presence of this residual silanol could explain the lower thermal stability of S1/GCC compare to S2/GCC.

Table II : Deconvolution results of S1 ; S2 ; S1/GCC and S2/GCC

Resin	**$OSi(CH_3)_2OH$**	**D**	**T**
S1	-	93%	7%
S1/GCC	1%	87%	12%
S2	-	95%	5%
S2/GCC	<1%	95%	5%

Indeed, the silanol function is known to induce depolymerization by "un-zipping reaction" and to lead to the formation of cyclic silicone compounds[5] that evolved in the gas phase. This reaction is due to intramolecular interaction and is illustrated in Figure 14.

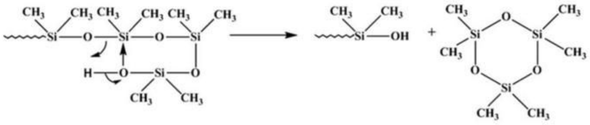

Figure 14 : Schematic illustration of "un-zipping" reaction

In order to verify the un-zipping reaction due to silanol group, TGA coupled with FTIR was used. Figure 15 and Figure 16 respectively show the infrared spectra of gases released during the degradation of S1/GCC and S2/GCC material. For both material, the same gases are released and are composed of cyclic silicone oligomers and carbon dioxide at high temperature. Peak at 2950 cm^{-1} corresponding to the bending vibration of CH_3 bond ; peaks between 1000-1100 cm^{-1} corresponding to the bending vibrations of Si-O-Si bond and peak at 1260 cm^{-1} assigning to the bending vibration of Si-CH_3 bond are observed. From 200°C to 650°C, cyclic oligomers are thus released from the two materials. However, Figure 15a illustrates the intensity of the peak at 1080 cm^{-1} (corresponding to the bending vibration of Si-O-Si) versus time during TG analysis. It shows that cyclic oligomers are released in two steps when S1/GCC is heated whereas only one is observed for S2/GCC (Figure 16a).

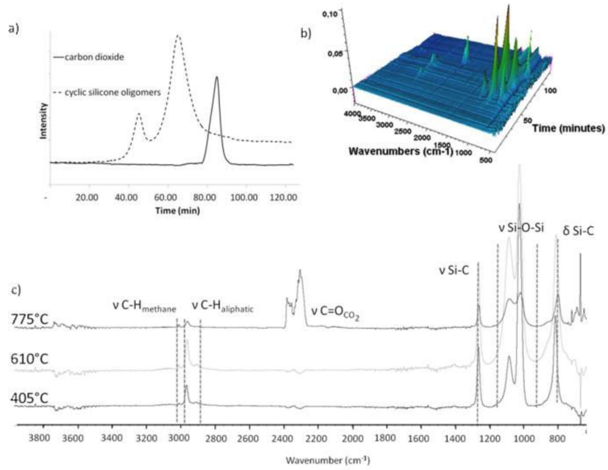

Figure 15 : a) Intensity of the band at 1080 cm^{-1} versus time b) IR spectra of the gas released during TG experiment c)IR spectra of the gas evolved during the thermal degradation of the S1/GCC at 405°C, 610°C and 775°C

During the last step of degradation (for T>700°C), carbon dioxide from calcium carbonate is released.

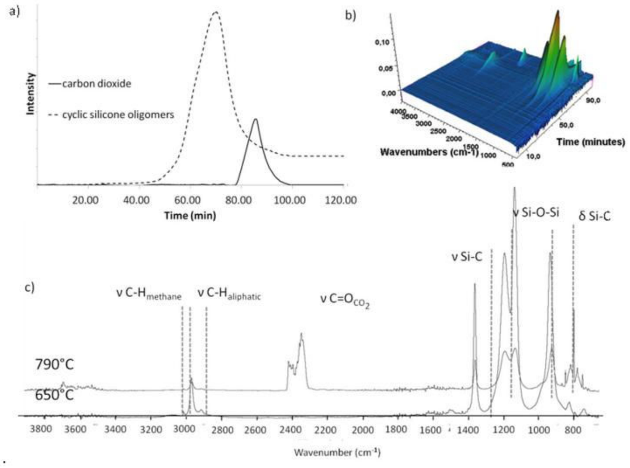

Figure 16 : a) Intensity of the band at 1080 cm^{-1} versus time b) IR spectra of the gas released during TG experiment c)IR spectra of the gas evolved during the thermal degradation of the S2/GCC at 650°C, 790°C

The analysis of the gas phase during the degradation of each material confirms that the lower thermal stability of S1/GCC is due to the remaining silanol group in the coating. Indeed, upon heating, the remaining silanol promotes the depolymerization of the polymer evolving cyclic oligomers at lower temperature and in two steps. The resulting residue exhibits therefore different thermal properties at high temperature.

3.4- Discussion and Conclusion

In this study, fire performance of two silicone resins containing GCC have been evaluated in convective/radiative heating source. The two silicone resins exhibit heat barrier properties. When GCC is incorporated in the silicone resins, remaining silanol group are present in S1/GCC based material. This leads to a lower thermal stability due to depolymerization reaction occurring at lower temperature (250°C). Because of this lower thermal stability (and also because of different degradation pathway), S1/GCC has a higher thermal diffusivity than S2/GCC as a function of temperature explaining its lower fire performance compared to S2/GCC.

This work has evidenced that in the field of resistance to fire, methyl-silicone based coatings have to be composed of mainly D structure and no silanol group to ensure a high thermal stability combined with appropriate thermal parameters (low heat conductivity and thermal diffusivity).

References

1. Genovese, A.; Shanks, R. A., Fire performance of poly(dimethyl siloxane) composites evaluated by cone calorimetry. *Composites Part A: Applied Science and Manufacturing* **2008,** *39* (2), 398-405.
2. Buch, R. R., Rates of heat release and related fire parameters for silicones. *Fire Safety J.* **1991,** *17* (1), 1-12.
3. de Buyl, F., Silicone sealants and structural adhesives. *Int. J. Adhes. Adhes.* **2001,** *21* (5), 411-422.
4. Wolf, A., MATERIAL PROPERTIES OF CONSTRUCTION SEALANTS. *Kautschuk und Gummi, Kunststoffe* **1988,** *41* (2), 173-178.

5. Hamdani, S.; Longuet, C.; Perrin, D.; Lopez-cuesta, J.-M.; Ganachaud, F., Flame retardancy of silicone-based materials. *Polym. Degrad. Stab.* **2009,** *94* (4), 465-495.
6. Hermansson, A.; Hjertberg, T.; Sultan, B.-Å., The flame retardant mechanism of polyolefins modified with chalk and silicone elastomer. *Fire and Materials* **2003,** *27* (2), 51-70.
7. Gardner, L.; Baddoo, N. R., Fire testing and design of stainless steel structures. *Journal of Constructional Steel Research* **2006,** *62* (6), 532-543.
8. Gustafsson, S. E., Transient plane source techniques for thermal conductivity and thermal diffusivity measurements of solid materials. *Rev. Sci. Instrum.* **1991,** *62* (3), 797-804.
9. Massiot, D.; Fayon, F.; Capron, M.; King, I.; Le Calvé, S.; Alonso, B.; Durand, J.-O.; Bujoli, B.; Gan, Z.; Hoatson, G., Modelling one- and two-dimensional solid-state NMR spectra. *Magn. Reson. Chem.* **2002,** *40* (1), 70-76.
10. Babonneau, F.; Baccile, N.; Laurent, G.; Maquet, J.; Azaïs, T.; Gervais, C.; Bonhomme, C., Solid-state nuclear magnetic resonance: A valuable tool to explore organic-inorganic interfaces in silica-based hybrid materials. *Comptes Rendus Chimie* **2010,** *13* (1-2), 58-68.
11. Kim, D. J.; Park, Y. J.; Kim, H. J.; Park, H. J.; Lee, B. W., Mechanical properties of alkoxy type silicone sealants. *Journal of Industrial and Engineering Chemistry* **2002,** *8* (3), 241-246.
12. Staggs, J. E. J., Thermal conductivity estimates of intumescent chars by direct numerical simulation. *Fire Safety J.* **2010,** *45* (4), 228-237.
13. J.E.J, S., Thermal conductivity estimates of intumescent chars by direct numerical simulation. *Fire Safety J.* **2010,** *45* (4), 228-237.

Polymer Degradation and Stability 98 (2013) 1052–1063

Contents lists available at SciVerse ScienceDirect

Polymer Degradation and Stability

journal homepage: www.elsevier.com/locate/polydegstab

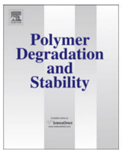

Characterization of the carbonization process of expandable graphite/silicone formulations in a simulated fire

B. Gardelle [a], S. Duquesne [a,*], P. Vandereecken [b], S. Bourbigot [a]

[a] *ISP/UMET – UMR/CNRS 8207, Ecole Nationale Supérieure de Chimie de Lille (ENSCL), Avenue Dimitri Mendeleïev – Bât. C7a, BP 90108, 59652 Villeneuve d'Ascq Cedex, France*
[b] *Dow Corning S.A., High Performance Building Solutions, Rue Jules Bordet, 8-7180 Seneffe, Belgium*

ARTICLE INFO

Article history:
Received 5 November 2012
Received in revised form
8 January 2013
Accepted 2 February 2013
Available online 20 February 2013

Keywords:
Silicone
Resistance to fire
Expandable graphite
Thermal conductivity

ABSTRACT

The fire performance of curable-silicone based coatings containing expandable graphite (EG) is evaluated in hydrocarbon fire scenario (standard UL1709) using a lab-scale furnace test. From 5% to 25% of expandable graphite is incorporated in the silicone matrix to make the coating swell during the fire experiment. Fire performance of 25%EG/silicone-based coating is better than that of commercial intumescent paint used as reference. This is explained by a high swelling velocity (18%/s), a high expansion (3400%), an impressive cohesion of the char and a low heat conductivity at high temperature (0.35 W/K m at 500 °C). To elucidate this way of charring, the residue after fire testing was analyzed by scanning electron microscopy, transmission electron microscopy, energy dispersive spectrometry, X-ray photo-electron spectroscopy and X-ray diffraction. It is shown that the char is composed of two main parts: the top is composed of quartz and amorphous silica which coat graphite flakes and the heart of the char is composed of graphite flakes embedded in degraded silicone forming a complex structure. It is shown that, the good cohesion of the char is due to: (i) the presence of the undegraded silicone matrix; and (ii) the coating of graphite pellets by silicone.

1. Introduction

Polydimethylsiloxane (PDMS) is widely used in construction and electrical abilities because of its excellent thermal stability and fire properties including low heat of combustion and low rate of heat release compared to conventional organic polymers [1,2]. This polymer is available in different forms from liquid to cross-linked rubber. The rubbers can be found in two main classes [3]: one cross-linked by polyaddition, and another by polycondensation.

Silicones prepared via the polycondensation method are used to make sealants that find applications in original equipment manufactories for glazing sealing windows and doors for either residential or public buildings. They are also used as a building component providing a barrier against severe environments such as humidity or dust [4]. These products are ready to use and require no mixing: cross-linking starts when the product is exposed to moisture. Most silicone sealants are formulated from a reactive polymer prepared from a hydroxy-polydimethylsiloxane and a large excess of cross-linked agent such as tri-acetoxysilane. The polycondensation reaction is illustrated in Equation (1).

$$HO-(Me_2SiO)_x-H \quad + exc.\ MeSi(OAc)_3 \xrightarrow{-2AcOH} (AcO)_2MeSiO(Me_2SiO)_xOSiMe(OAc)_2$$

Equation (1). Polycondensation reaction of hydroxy-PDMS.

The protection of metallic materials against fire has become an important issue in the construction industry. Indeed, steel begins to lose its structural properties above 500 °C and it must be therefore protected against fire [5]. Prevention of the structural collapse of the building is paramount to ensure the safe evacuation of people from the building, and is a prime requirement of building regulations in many countries. One of the most used systems to protect metallic structures is intumescent paint. These coatings have the properties to swell to thick insulative foam when heated above a critical temperature. Intumescent coatings are mostly based on a combination of a char-forming material, a mineral acid catalyst, a blowing agent and a binder resin [6,7]. However, these materials are typically organic-based materials and exhibit some disadvantages. Firstly, organic additives undergo exothermic decomposition which reduces the thermal insulative value of the system. Secondly,

---

* Corresponding author. Tel.: +33 320337236; fax: +33 320436584.
E-mail address: sophie.duquesne@ensc-lille.fr (S. Duquesne).

0141-3910/$ – see front matter © 2013 Elsevier Ltd. All rights reserved.
http://dx.doi.org/10.1016/j.polymdegradstab.2013.02.001

the resulting carbonaceous char in some cases has a low structural integrity and the coating cannot withstand the mechanical stress induced by a fire. Thirdly, the coating releases organic gases (potentially toxic) which are undesirable in a closed fire environment [8].

Currently, some alternative to organic intumescent coating has been studied. We recently reported the use of ceramic precursor – polysilazane – based coating as a heat barrier on steel plate. The purpose of this work was to form a ceramic at high temperature which could protect a substrate in fire scenario [9]. The performance of the polysilazane coating can be improved incorporating some fire retardant such as aluminum trihydroxide but it is limited compared to commercial intumescent paint. The use of silicone-based protective coating is very few reported in the literature. We recently evaluated the fire performance of an intumescent silicone-based coating. In this study, fire performance of a phenyl silicone resin added with modifier silica was evaluated in pure radiative and convective/radiative heating source condition [10]. We highlighted the good heat barrier properties of this intumescent based coating in radiative/convective heating source whereas fire performance of this coating is rather limited in the case of pure radiative heating source and therefore in real fire scenario. Indeed, in pure radiative heating source, silicone-based coatings cracks due to the high vibration of Si–O bound in infrared field and so exhibits low fire performances.

Expandable graphite (EG) is a "particular" intumescent additive known to impart fire retardancy to various materials [11]. EG is a graphite intercalation compound in which sulfuric acid and/or nitric acid is inserted between the carbon layers of graphite. Upon heating, exfoliation of the graphite occurs, i.e. expansion along *c*-axis of the crystal structure by about hundred times. The material generated in that way is a puffed-up material of low density with a "worm" like structure. In recent decades, more and more papers reported the use of expandable graphite in intumescent based coating. This intumescent additive increases the fire performance and anti-oxidant properties of intumescent based coating [6,12,13]. However, in the above mentioned studies, expandable graphite is only incorporated into complex organic intumescent based formulations. It is noteworthy that in organic-based coating, EG decreased considerably the cohesion of the char [13].

The use of EG in silicone-based coating to protect material against fire is not reported in the literature. Beigbeder et al. highlight the high adsorption of the PDMS chains onto carbon nanotube mostly triggered by CH–π interactions between the methyl group from PDMS and the π-electron-rich surface of the carbon nanotube [14] and evaluated the fire protective performance of PDMS/Carbone nanotube based coating onto aluminum plate. They showed that in convective/radiative heating test, this coating exhibited improved properties compared to virgin aluminum. However, this silicone-based coating is clearly not intumescent. In this work, passive fire protection of steel using silicone-based coating from polycondensation is investigated using expandable graphite as blowing agent.

The purpose of this paper is to investigate the heat barrier properties of curable-silicone/expandable graphite based coating in hydrocarbon fire scenario (standard UL1709). It is recognized that the governing parameters for intumescent coating to get efficient heat barrier performance are the fast expansion of the coating as a function of temperature and its low thermal conductivity (formation of a dense and porous char) [15]. Those parameters will thus be examined in this paper. The charring process and the expansion of the coating occurring during the fire scenario will be then fully investigated.

2. Experimental

2.1. Materials

The silicone resin called silicone 1 (S1), was composed of a hydroxylated PDMS with a viscosity of 15,000 cS (viscosity is measured using cone/plate rheometer CP-52), methyltrimethoxysilane as a cross-linking agent and a titanium catalyst. All the materials were supplied by Dow Corning, Seneffe (Belgium).

From 5% to 25% of expandable graphite ES350F5 from Graphitwerk Kropfmuehl (Germany) with an average grain size of 300 μm was added to the silicone matrix. Each formulation was applied on a 10 cm × 10 cm × 3 mm steel plate to obtain 1.0 ± 0.1 mm coating. Steel plates were cleaned before application with ethanol and a primer (Primer 1200 from Dow Corning) was applied to enhance the coating adhesion.

Metallic structures are generally protected with intumescent paint. Epoxy based intumescent paint Fire Tex M93 (M93) from Leigh's Paint, England, was used as reference and for comparison in our study. The same thickness of M93 was coated on the same steel plate as above.

2.2. ^{29}Si solid state NMR resin characterization

^{29}Si NMR spectroscopy is a powerful tool for examining silicon surrounding. This technique can distinguish between several kinds of structures including D $[SiO_2(CH_3)_2]$, T $[CH_3Si(O_{1/2})_3]$ and Q $[Si(O_{1/2})_4]$ structures which characterize silicone network. ^{29}Si NMR spectra were recorded on a Bruker Advance II 400 operating at 9.4T and using a 7 mm probe. NMR spectra were acquired with MAS (magic angle spinning) of 5 kHz. The reference used for ^{29}Si NMR was tetramethylsilane (TMS). A delay of 180 s between the pulses and a $\pi/2$ pulse length were used. 288 scans were accumulated to get an acceptable signal to noise ratio. In order to quantify the amount of D and T structure within the resin, simulation of ^{29}Si NMR spectra was obtained using DMfit99 software [16].

2.3. Fire testing methods

The small scale furnace test was developed in our laboratory to evaluate the fire performance of intumescent coatings in fire scenario (cellulosic and hydrocarbon).

This test was designed to mimic the ISO834 (or ASTME119) and the UL1709 normalized temperature/time curve, respectively related to cellulosic fire and to hydrocarbon fire.

The lab-made furnace exhibits an internal volume of 40 dm^3 (Fig. 1). Refractory fibers (stable up to 1300 °C) cover the different

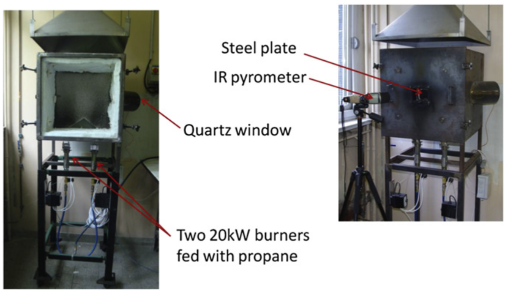

Fig. 1. Furnace set up to mimic hydrocarbon fire scenario.

faces of the furnace. The furnace was equipped with two gas burners (20 kW propane burners). The gas pressure was fixed at 1.8 bars and the flow was regulated in order to mimic the UL1709 curve (in this study). A temperature probe inside the furnace regulates the temperature and a K-type thermocouple allows the furnace temperature profile to be registered. In this study fire protection of silicone-based coating was evaluated under a hydrocarbon fire scenario (standard UL179).

The temperature at the backside of the plate is measured as a function of time using a pyrometer (temperature measured in the center of the plate). The backside of the plate is coated with black paint (Jeltz) having a constant emissivity (0.92) and thermally resistant up to 800 °C in order to get reliable temperature measurements with the pyrometer. The critical temperature of steel is defined as the temperature at which only 60% of the original strength remains, point at which failure is imminent under full design loads. The temperature of 500 °C has been officially adopted as a standard for normally loaded structural components whereas 400 °C is often used for heavily loaded structure [17]. In this study, the time to reach the two temperatures is taken into account to evaluate the heat barrier properties of intumescent coatings.

2.4. Charring characterization

2.4.1. Swelling

In order to measure the swelling of intumescent coating in fire scenario, conical electrical heater at 50 kW/m^2 (corresponding to common heat flux in a mild fire scenario) is used and the development of the char was monitored by an infrared camera. Pictures obtained from the film are analyzed by Image J software (NIH, Bethesda, MD) and the thickness of the coating is measured. Using this set up, the swelling of intumescent coating is measured versus time.

2.4.2. X-ray photoelectron spectroscopy (XPS)

XPS experiments were carried out on an ultra-high vacuum KRATOS Axis Ultra spectrometer using the monochromatized Al Kα (1486.6 eV) source. Constant analyzer pass energy of 40 eV was used. The full width at half maximum (FWHM) was restrained to be equal in both peaks, and the area of the peak assigned to Si2p$_{1/2}$ was restrained to be half the area of the Si2p$_{3/2}$. The energy separation between the Si2p$_{3/2}$ and Si2p$_{1/2}$ doublet is constant and is 0.6 eV. Simulation of the experimental peaks was carried out using the Gaussian–Lorentzian mixture from CasaXPS software.

2.4.3. Electron microscopy

Scanning electron microscopy (SEM) and transmission electron microscopy (TEM) were used. For SEM, the samples were analyzed with a Hitachi S4700 microscope. Secondary electron SEM images were obtained at 6 kV, 10 mA. For TEM, sample was dissolved in THF and transferred to Cu grids of 400 meshes. Bright-field TEM images of sample were obtained at 200 kV under low dose conditions with a FEI TECNAI 62 20 electron microscope, using a Gatan CCD camera. EDS EDAX experiment was carried out to determine the chemical composition of each material.

2.4.4. Numerical microscopy

Sample residues were characterized using a numerical microscope VHX-1000 supplied by Keyence. The VHX-1000 creates a 3D image based on automatically captured images, and it calculates height profile data on a desired measuring line.

2.4.5. X-ray diffraction

XRD spectra were recorded in the 10°–80° 2θ range using a Bruker Advanced D8 diffractometer ($\lambda_{(\mathrm{Cu\ K\alpha})} = 1.5418$ Å) in configuration $\theta/2\theta$. The acquisition parameters were as follows: a step of 0.02°, a step time of 2 s. The data are analyzed using the diffraction, patterns of inorganic crystal structure database.

2.4.6. Thermal conductivity

Thermal conductivity material was measured from 25 °C to 500 °C using a hot disk thermal constant analyzer (Hot Disk TPS 2500 S) from Thermoconcept (Bordeaux, France), which is a transient plane source technique [18]. The sensor which is warmth

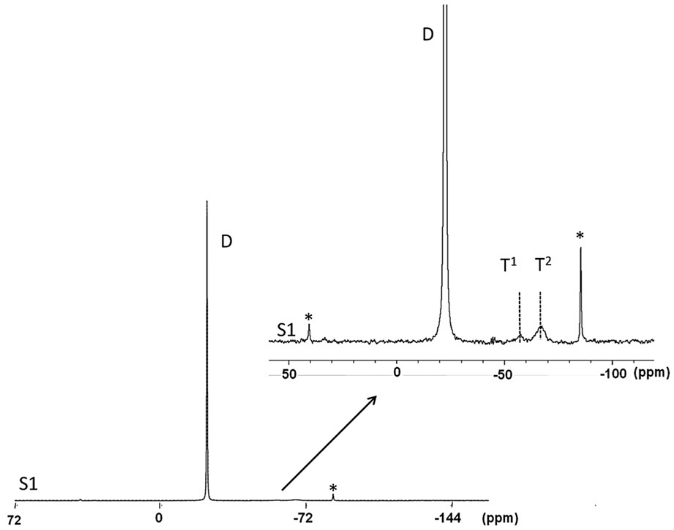

Fig. 2. S1 ^{29}Si NMR spectra.

emitter and thermocouple is directly molded in the sample to ensure a good contact between the sample and the sensor during the experiment. The temperature is stabilized each 100.0 °C with less than 0.1 °C deviation. The conductivity measurements were made by applying a power of 0.03–0.15 W for between 5 and 60 s, depending on the thermal conductivity of the sample. The furnace is directly connected to nitrogen flow and all experiments are carried out in inert atmosphere to prevent the oxidation of the sensor. This experimental set up allows measuring the thermal conductivity of the material versus the temperature.

3. Results

3.1. ^{29}Si NMR resin characterization

Fig. 2 shows ^{29}Si NMR spectrum of resins S1. Three bands can be distinguished at −22 ppm, −58 ppm and −67 ppm assigned to D, T^2 and T^3 structures respectively [19,20].

Deconvolution of the spectra allows quantifying the ratio between D and T. It shows that S1 siloxane resin is composed of 97% of D structure and 3% of T structure. A cross-linking mechanism is involved in the formation of the matrix. Fig. 3 illustrates chemical reactions which occur during the cross-linking of the hydroxyl terminated PDMS [3]. Exposed to moisture, hydroxyl group reacts with the methoxy group of MTM which lead mainly to T^2 and T^3 structures.

3.2. Fire protection

Fig. 4 shows the evolution of temperature as a function of time on the backside of the steel plates coated with the different formulations during hydrocarbon fire scenario. The influence of the amount of EG on the heat barrier properties of silicone-based coating is investigated and compared with those of the virgin steel plate. For each formulation, the shape of the curves is similar. During the first 200 s, the temperature increases to 200 °C and then the temperature rises at different rates depending on the amount of graphite.

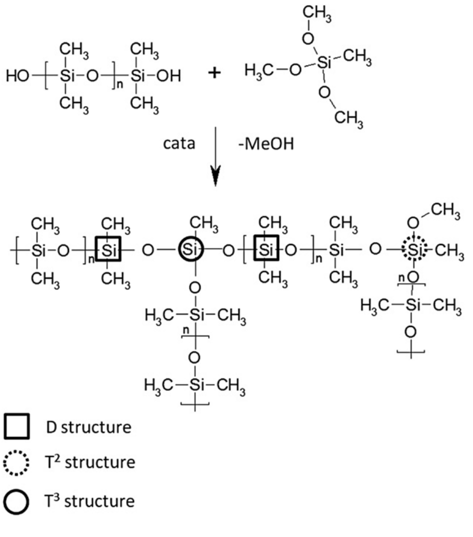

Fig. 3. Chemical pathway of resin cross-linking.

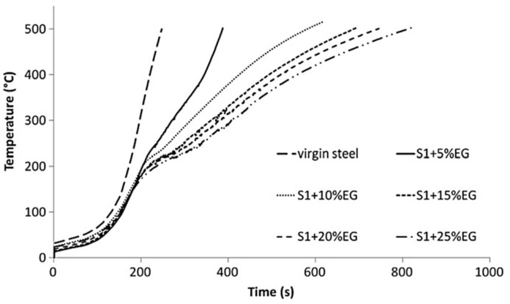

Fig. 4. Temperature versus time curves in hydrocarbon fire scenario.

The times to reach both 400 °C and 500 °C as a function of EG loading are summarized in Table 1. The time to reach 500 °C for S1 + 5%EG, S1 + 10%EG, S1 + 15%EG, S1 + 20%EG, S1 + 25%EG is respectively 385 s, 580 s, 690 s, 740 s and 810 s. Consequently, the time to reach critical temperatures of each formulation increases with the percent of graphite added compared with virgin steel. This evidences that the quantity of graphite enhances greatly the heat barrier properties of silicone-based coatings and from 10% to 25% EG adding, a surprisingly cohesion of the char is highlighted. Although there is a high expansion of the coating, the char adheres to the steel plate.

Fig. 5 compares the residue of S1 containing 5%, 10% and 25% EG. When 5% of expandable graphite is added to S1 (Fig. 5a), the top of the coating falls off from the plate explaining the rapid change of slope at 400 °C. From 10% to 25% of graphite, the expansion rate rises from 1500% to 3400% explaining partially that the time to reach critical temperature increases significantly.

These results demonstrate that the fire protection properties of silicone-based coatings increase with the amount of expandable graphite. The expansion rate increases with the amount of expandable graphite (Table 1) and hence the insulative properties of the coating.

However, when 25% of EG is added, a low adhesion of the char at the top of the plate occurs and a quiet low mechanical property is observed (the char can be easily removed from the plate after fire testing). Despite this fact, critical temperatures for S1 + 25% are reached in 560 s and 810 s respectively for 400 °C and 500 °C whereas they are reached in 500 s and 680 s for the conventional organic intumescent paint (M93) steel plate. This evidences that fire protection of S1 + 25%EG can reach superior performance than commercial intumescent paint.

Fig. 6 illustrates the behavior of S1 + 25%EG coating during fire experiment. Fig. 6a shows the coating ignition during the first minute testing. After 250 s (Fig. 6b), it shows the charring process is achieved after 250 s a formation of high expanded structure and an expanded "worms" like structure embedded by white powder is visible.

In the next step of the study, fire performance and charring process of S1 + 25%EG will be investigated since it provides the best performance. The expansion rate and the final expansion of the coating have been identified as governing parameters in the fire protection and they will be therefore evaluated in the following. In addition to this, heat conductivity cannot be ignored because it will govern the insulative properties of the intumescent coating: this parameter will also be measured and it will be associated to the swelling rate and to the expansion to explain the mechanism of protection.

Table 1
Time to reach failure temperature of each formulation.

	Virgin steel	S1 + 5%EG	S1 + 10%EG	S1 + 15%EG	S1 + 20%EG	S1 + 25%EG	M93
Time to reach 400 °C	220 s	345 s	380 s	492 s	520 s	560 s	500 s
Time to reach 500 °C	248 s	385 s	580 s	690 s	740 s	810 s	680 s
Expansion rate	–	Expansion: 1000%	Expansion: 1500%	Expansion: 2000%	Expansion: 3000%	Expansion: 3400%	Expansion: 1500%
Experimental observation		Loss of adherence of the char from the plate	Good cohesion of the char	Good cohesion of the char	Good cohesion of the char	Low adhesion of the char at the top of the plate	Good cohesion

3.3. Swelling measurements

In the previous section, it has been shown that when 25% of expandable graphite is added to silicone matrix, the expansion reaches 3400% which is more than twice higher than commercial intumescent paint. The rate of expansion has also to be considered. Indeed, to ensure a fast and efficient protection of the substrate, the coating has to expand quickly [21].

To quantify the expansion velocity of the coating two methods were used. For the first one – static state – the furnace test was stopped after different times and the thickness of the coating was measured. Fig. 7 shows the obtained residues after different time and illustrates the high expansion rate. After 250 s testing, the expansion reaches 2500% a white powder is observed on the top of the char. It is assumed that this white powder corresponds to silica. After 300 s fire testing, the expansion reaches 3000% and increases to 3400% at the end of the test. Secondly, the development of the char was monitored by an infrared camera during cone calorimetry (50 kW/m^2). This allowed measuring the swelling versus time of intumescent coating during the expansion in dynamic (Fig. 7). The expansion after 30 s, 60 s, 120 s and 180 s reaches respectively 330%, 1500%, 2350% and 3200%. Using these two methods swelling versus time curve could be plotted (Fig. 7) and the velocity of expansion can be calculated from the slope of the curve during the expansion step. It reaches 18%/s in static method and 19%/s in dynamic method.

The curves of swelling as a function of time evidence that the expansion rate in the case of our system does not depend on the heating condition. The charring phenomenon is mainly due to the expansion of graphite layers and no chemical reaction between siloxane chains and graphite is expected. Thus, it could reasonably explain why the expansion rate is not affected by the fire scenario since the expansion is only due to a temperature increase. When the temperature reaches the critical temperature of expansion of EG (around 250 °C), the coating swells. In this study, high expansion rate (3400%) and velocity (18%/s) permit the formation of an

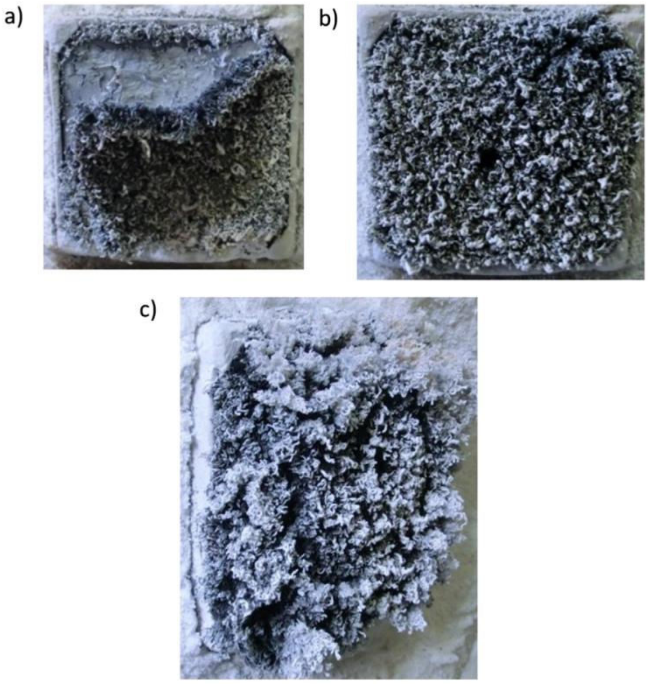

Fig. 5. a) S1 + 5%EG residue, b) S1 + 10%EG residue, c) S1 + 25%EG residue after testing in hydrocarbon fire scenario.

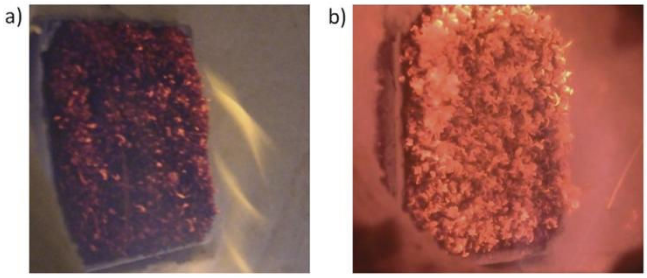

Fig. 6. S1 + 25%EG after a) 150 s and b) 250 s fire testing.

insulative barrier reducing heat transfer from the external heating source to the substrate.

3.4. Thermal conductivity

In this section, thermal conductivity of S1 + 25%EG is studied from ambient temperature to 500 °C. Heat conductivity is one of the parameters governing the performance of the coating in terms of insulation. Very few papers deal with the measurement of thermal conductivity at high temperature of material. J.E.J Stagg determined thermal conductivities of intumescent char at high temperature by numerical simulation [22]. He evaluated thermal conductivity from ambient temperature to 1200 K and its dependence with the porosity of the material. He calculated that thermal conductivity of intumescent char material varies from 0.1 W/K m to 0.4 W/K m from ambient temperature to 600 °C suggesting the heat insulative properties of these materials.

Silicone matrix is known to have insulative properties and to have low thermal conductivity at ambient temperature [23]. At ambient temperature, heat conductivity of virgin S1 matrix reaches 0.16 ± 0.02 W/K m. When 25% of EG is added to silicone matrix, it increases to 0.50 ± 0.02 W/K m due to the high thermal conductivity of graphite. Thermal conductivity of S1 + 25%EG is then measured from ambient temperature to 500 °C (Fig. 8).

Heat conductivity decreases from 0.5 ± 0.02 W/K m to 0.21 ± 0.02 W/K m at 400 °C due to the formation of an expanded structure which should be composed of several alveoli (Fig. 8). At higher temperature, the material is expanded and no significant morphology modification is expected. Thermal conductivity thus increases up to 0.35 W/K m at 500 °C. In our study, thermal conductivity decreases when the EG/S1 is heated due to the foaming of the material and heat conductivities are in the same order of magnitude as values found in the literature for classical intumescent char [15,22]. Consequently, the low heat conductivity of this system ensures insulative properties of the coating.

In fire scenario, expandable graphite/silicone system exhibits high expansion rate. This expanded structure has a low thermal conductivity and, the combination of these two parameters explains the excellent fire performance of this intumescent silicone-based coating. It is noteworthy that in organic-based coating, when more than 20% of expandable graphite is added in the matrix, there is low cohesion of the char and so the coating exhibits low fire protection properties [24,25]. This bad cohesion could be explained by the mode of action of EG. Indeed, in general, no reaction

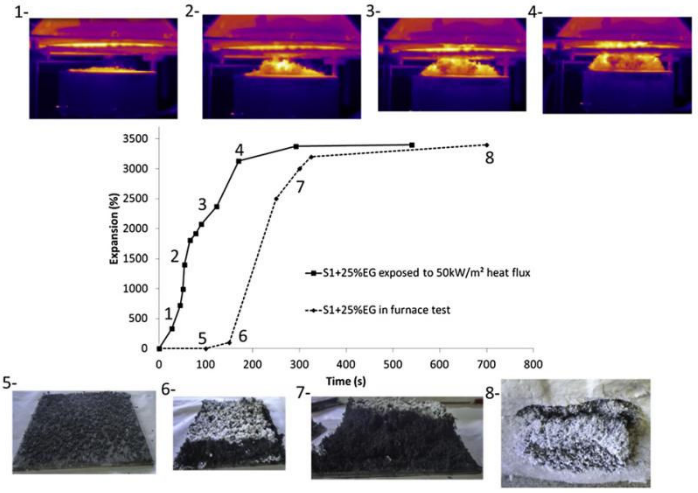

Fig. 7. Swelling versus time curve in static and dynamic state.

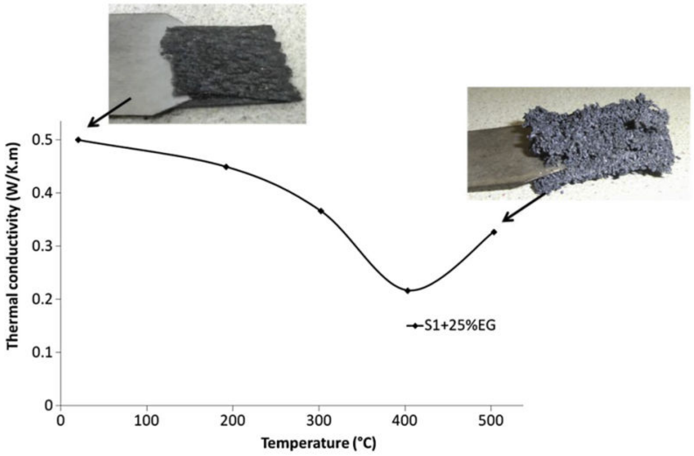

Fig. 8. Thermal conductivity of S1 + 25%EG from ambient temperature to 500 °C.

between EG and the other components of a formulation is observed. Thus after expansion, there is no "link" between the expanded graphite particles and the cohesion of the char residue is poor. In this case, 25% of EG was added to silicone matrix and a good cohesion of the char was observed. It allows the char remaining on the steel plate during the fire test and thus high insulative properties were obtained. In the next step of this study, the development of the char was thus investigated to determine a pathway of charring and to explain this unexpected cohesion of the char.

3.5. Residue characterization

In order to determine a pathway of charring, the first step was to analyze the residue after the furnace step. Fig. 7 illustrates that the char is made in two main parts: the top which is composed of white friable solid and the interior (black) which is composed of expanded graphite vermicule embedded in an inorganic matrix.

3.5.1. Characterization of the top layer of the char

SEM pictures of the top of the char are presented in Fig. 9. It shows that this part of the char is composed of few micrometer spheres and exhibiting homogenous diameter (around 200/300 nm).

Because a silicone matrix is used in this study it suggests the formation of amorphous or crystallized silica at the top of the char during the test. In order to confirm this hypothesis, the white residue was analyzed using ^{29}Si NMR. The spectrum is presented in Fig. 10a and it exhibits a single band at −110 ppm corresponding to Q^4 structure in a silica network [10]. Balls characterized by SEM are thus composed of silica.

XRD experiment was also carried out to determine the crystallinity of the silica and X-ray diffractogram is presented in Fig. 10b. Broad band from 17° to 26° is observed and it is assigned to amorphous silica; two other sharp peaks at 26.5° and 26.6° correspond to respectively graphite and quartz [26,27].

As a consequence, these analyzes have demonstrated that at the top of the char, amorphous silica and quartz embed graphite flake constitute the first insulative layer. Fig. 11 clearly shows that at the interface between the top and the bulk part of the char, some worms from expandable graphite are coated with silica while other remains black.

3.5.2. Bulk char characterization

SEM pictures of the "heart" of the char are presented in Fig. 12. Fig. 12a shows a classical worm from expanded graphite while Fig. 12b corresponds to graphite flake at higher magnification. It highlights the presence of some particles between and on the graphite layer.

Because of high paramagnetic field of expandable graphite, it was not possible to perform solid state NMR experiment. X-ray

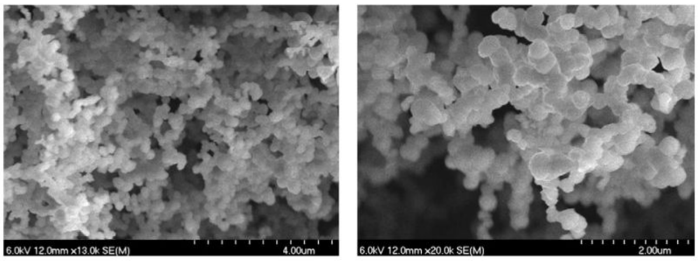

Fig. 9. SEM pictures of the top of the char.

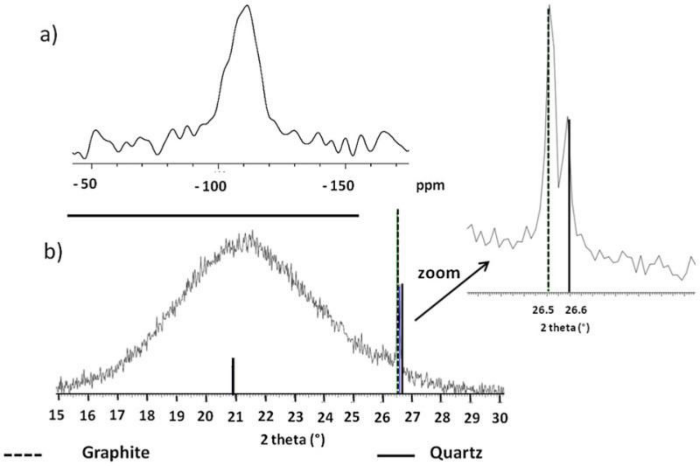

Fig. 10. a) ^{29}Si NMR and b) X-ray diffractogram of the top of the char.

photoelectron spectroscopy (XPS) was thus carried out as an alternative technique to characterize the charred silicone structures. Indeed, O'Hare et al. studied the D, T and Q structures in pure silicone using XPS experiment and obtained good correlation with ^{29}Si NMR experiment [28]. Based on their work, a similar approach has been followed.

Fig. 13 shows XPS Si2p spectrum of S1 + 25%EG before and after fire testing. After fire testing Si2p spectrum shows a broad peak (from 100 eV to 106 eV) revealing the contribution of several components.

Deconvolution of each spectrum is presented in Fig. 13. Band positions of each structure are summarized in Table 2 and were attributed according to the literature [28,29].

Before fire testing, two Si2p$_{3/2}$ are shown at 101.7 ± 0.2 eV and 102.6 ± 0.2 eV assigned to respectively D and T structures of the silicone matrix as we showed by ^{29}Si NMR on the matrix without graphite.

After fire testing, several structures are detected in the bulk part of the char. Peaks at 100.9 ± 0.2 eV, 101.7 ± 0.2 eV, 102.6 ± 0.2 eV and 103.6 ± 0.2 eV correspond respectively to SiC, D, T and Q silicone structure. It points out reduction and oxidation of the silicone during fire test.

When exposed to hydrocarbon fire scenario, there is the formation of several structures: (i) the oxidation of the silicone due to the high temperature and to the oxidizing atmosphere in the furnace lead to the formation of Q structures and (ii) concurrently to the oxidation, reduction due to the presence of graphite, it leads to the formation of few amount of silicon carbide. The presence of D structure demonstrates that at the end of the fire test the silicone matrix is not completely degraded.

As a consequence, it can be concluded that the heart of the char is mainly composed of amorphous silica and graphite. Morphology study by TEM of graphite platelets from the bulk of the char and of virgin graphite shows no modification.

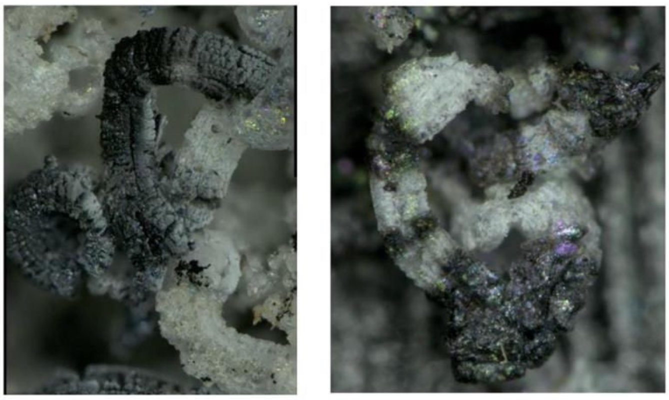

Fig. 11. 3D microscope pictures of the char after furnace testing.

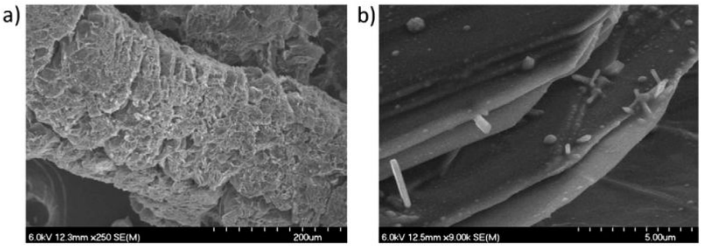

Fig. 12. SEM pictures of the interior of the char.

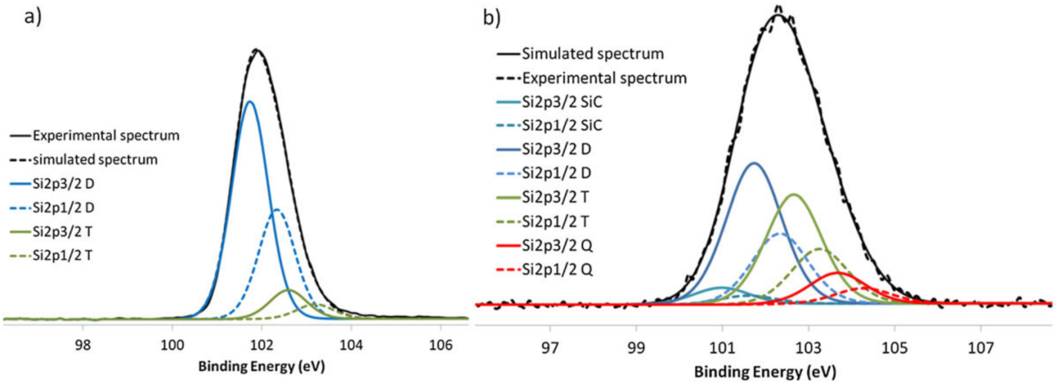

Fig. 13. XPS Si2p spectrum of a) S1 + 25%EG before furnace testing and b) bulk of the char after testing.

EDS experiment was also carried out to determine the chemical composition of the graphite platelet. Fig. 14a) highlights, as expected, that virgin graphite is composed of carbon. Fig. 14b) shows that after burning, the expanded graphite platelets are composed of silica and carbon. This demonstrates that the graphite platelets present in the char are coated with silica and Si–O–C based compound. The peak intensity of carbon in the EDS spectrum is too low to affirm that silicone carbide coat the graphite flakes. Consequently, it is reasonable to assume that the low amount of silicon carbide is observed between the graphite flakes.

In this part, chemical composition of the char has been investigated. Silicone combined with expandable graphite exhibits high heat barrier properties. The char obtained after hydrocarbon fire testing is composed of two main parts. The top of the char is composed of a white and friable powder. At high temperature, silicone leads to the formation of quartz and amorphous silica. Because of the polar properties of Si–O bound, graphite adsorbs siloxane chain and therefore amorphous silica and quartz coat graphite. It constitutes the first insulative layer. Concerning the heart of the char, only oxidation of the silicone with the formation of silica was expected but, we have clearly shown that: (i) silicone matrix is not completely degraded (D structure has been evidenced by XPS experiment), (ii) T and Q silicone structures coat graphite flake and (iii) graphite and silicone react together to yield silicon carbide which should be located between graphite flakes. This silicone coating on graphite flake permits the good cohesion of the char during fire and it avoids its delamination like in the case of conventional intumescent systems. The next step of this work consists to explain the char formation process analyzing its chemical composition during fire experiment so as to elucidate the formation of this complex structure composed of graphite embedded in silicone structures.

3.6. *Charring mechanism*

To determine a pathway of charring, S1 + 25%EG steel plate has been tested in hydrocarbon fire scenario and the residue has been collected after 200 s, 225 s and 250 s fire testing. At these times, the expansion rate is maximal and reaches 18%/s. We can so assume that the charring phenomenon occurs during this step. The residues were analyzed by XPS to determine the chemical composition of the heart of the char. C1s XPS spectra are shown in Fig. 15.

Table 2
Binding energy of various silicone structures present in both material.

Sample	Si2p$_{3/2}$ SiC	Si2p$_{3/2}$ D	Si2p$_{3/2}$ T	Si2p$_{3/2}$ Q	FHMW
S1 + 25%EG before testing	–	101.7 ± 0.2 eV	102.6 ± 0.2 eV	–	0.96
Interior of the char	100.9 ± 0.2 eV	101.7 ± 0.2 eV	102.6 ± 0.2 eV	103.6 ± 0.2 eV	1.58

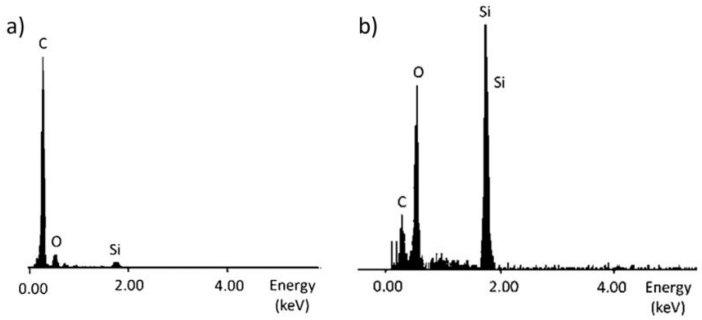

Fig. 14. EDS spectra of a) virgin graphite and b) interior of the char.

C1s spectrum before fire testing shows three different binding energy at 284.2 ± 0.2 eV, 284.9 ± 0.2 eV and 285.7 ± 0.2 eV assigned to respectively Si–**C**H$_3$, C–C$_{sp2\ graphite}$ and **C**–O–Si functional groups. After 200 s there is partial oxidation of graphite platelets since two other peaks with a binding energy of 286.9 ± 0.2 eV and 288.8 ± 0.2 eV appears corresponding to respectively carbonyl and carboxylic acid function [12]. The band at 286.0 ± 0.2 eV is assigned to C–O which should come from C–O–Si but it is not possible to exclude the possibility of forming C–O–C epoxy-bridge present in graphite oxide [30] and C–OH from oxidation of graphite platelets. After 225 s, the main oxidized function is the carbonyl and no or few carboxyl functions are observed. However, the carboxyl peak exhibits a low intensity at $t = 200$ s and because of the partial oxidation of the graphite this function should be not homogenous on the residue. It explains why in the spectra after 225 s fire testing no peak corresponding to

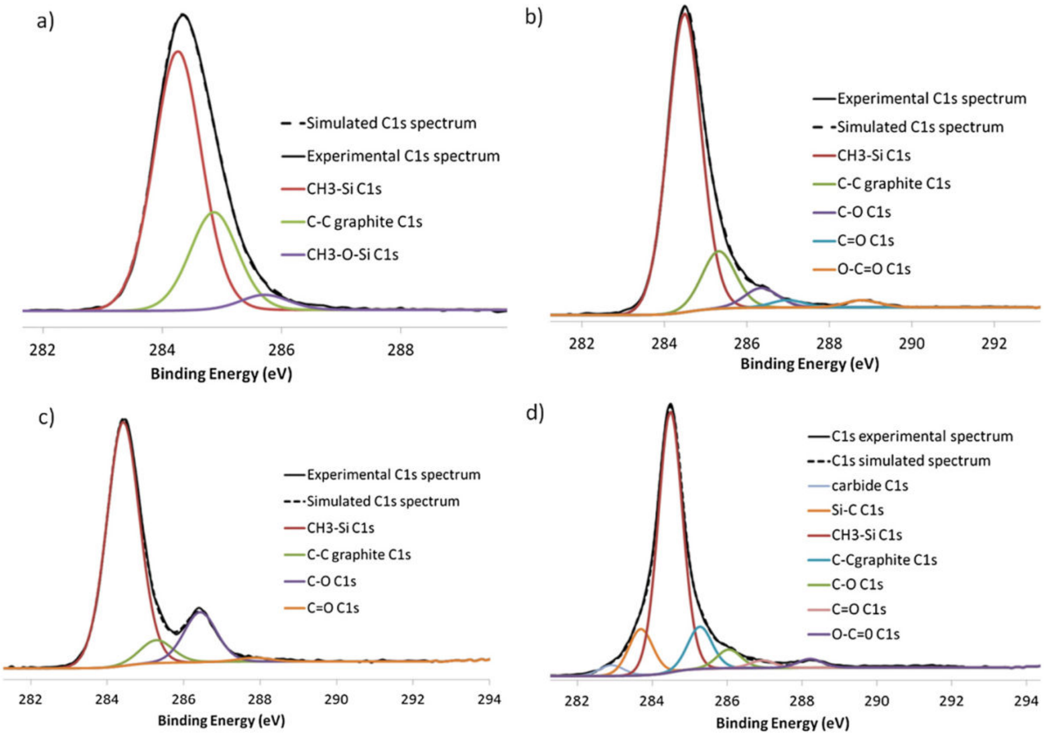

Fig. 15. C1s XPS spectra of S1 + 25%EG a) before fire testing and after b) 200 s and c) 225 s fire testing d) 250 s fire testing.

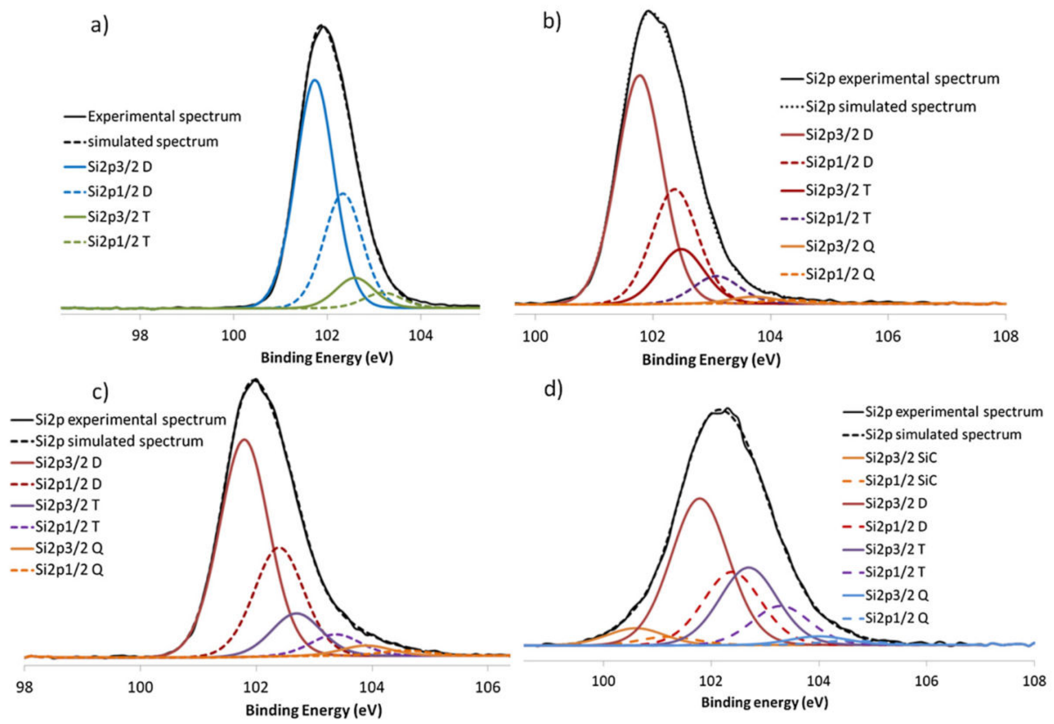

Fig. 16. Si2p XPS spectra of S1 + 25%EG a) before fire testing and after b) 200 s c) 225 s fire testing d) 250 s fire testing.

carboxyl function is detected whereas the peak attributed to O–C=O appears again after 250 s fire testing. After 250 s fire testing, C1s spectrum shows the formation of silicon carbide characterized by a peak at 283.6 ± 0.2 eV and another carbide at 282.9 ± 0.2 eV which is assumed to be titanium carbide resulting from a reaction of the catalyst. As mentioned previously, there is a partial oxidation of the graphite flake explaining the formation of carbonyl and carboxyl functions.

Concerning silicon environment, XPS Si2p spectra of the residue obtained after the furnace test at characteristic times are presented in Fig. 16.

As shown above, the sample is composed of D and T structure before fire testing with two $Si2p_{3/2}$ binding energies at 101.7 ± 0.2 eV and 102.6 ± 0.2 eV. After 200 s and 225 s fire testing, there is the formation of Q structure characterized by $Si2p_{3/2}$ binding energy at 103.7 ± 0.2 eV. After 250 s fire testing, Si2p spectrum shows the formation of silicon carbide with a $Si2p_{3/2}$ binding energy of 100.6 ± 0.2 eV and the same silicon structure as after 200 s fire testing (D, T and Q).

Based on the different results, it is thus possible to draw mechanism of formation of the charred residue. During fire scenario, the partial oxidation of the graphite platelets occurs due to the release of sulfuric and/or nitric acid and to the high temperature. There is the formation of reactive group such as carbonyl, carboxylic acid and/or hydroxyl function. The oxygen and hydroxyl groups can be located randomly above and/or below the carbon basal plane, and the carboxyl groups are at the edge of the graphite flake [30].

Due to the formation of such reactive groups, silicone could react with this function leading to the formation of Si–O–C (such as siloxane chains) and Si–C bridge between the graphite platelets resulting in the formation of a cohesive residue.

To conclude with, when EG/silicone-based coatings are tested in fire scenario, there is an intumescent phenomenon characterized by a high expansion rate of the coating, high insulative properties and a good cohesion of the char. The intumescence process has been investigated; a partial oxidation of the graphite flake at high temperature occurs leading to the formation of reactive functions (carbonyl, hydroxyl and carboxyl). At high temperature, the silicone matrix reacts with this function leading to the formation of silicon carbide and Si–O–C structure. Because of the polar properties of Si–O bond, graphite adsorbs siloxane chain/silica which coat graphite flake at high temperature. The good cohesion of the interior of the char is thus due to: (i) the presence of undegraded matrix; and (ii) the formation of a coating of the graphite pellets with silicone compound due to the high affinity between siloxane chain and graphite flakes.

4. Conclusion

This paper has investigated the fire performance and the charring process of expandable graphite/curable-silicone based coatings. Heat barrier efficiency of the silicone-based coating was evaluated in hydrocarbon fire scenario – standard UL1709 – using a lab-scale furnace test. Fire performance of this system was increased with the amount of expandable graphite. When 25% of

EG was added to siloxane matrix, heat insulative properties were better than those obtained in the case of a commercial intumescent based coating. This performance is explained by the formation of an expanded insulative char (3400% expansion) formed with a high expansion velocity (18%/s) and exhibiting a low thermal conductivity (0.35 W/K m at 500 °C). The good cohesion of the char is attributed to interaction occurring between the resin and the graphite platelets at high temperature. During fire testing, there is oxidation of graphite platelets and formation of silicon carbide, as well as formation of T and Q structures. TEM and EDS experiment on the residue at the end of the test have allowed demonstrating that the graphite is coated by silicone compound. The matrix in the bulk of the char and the formation of a complex silicone/graphite structures at high temperature are responsible to the surprisingly good cohesion of the char in fire scenario. This elucidates the excellent fire performance of this silicone-based coating and highlights a promising concept using expandable graphite/silicone in the field of fire protection.

Acknowledgments

The authors gratefully acknowledge Mr. Revel for his skillful experimental assistance and his expertise in NMR and Dr. Bellayer for her experimental assistance and her expertise in electron microscopy.

References

[1] Genovese A, Shanks RA. Fire performance of poly(dimethyl siloxane) composites evaluated by cone calorimetry. Compos Part A Appl Sci Manuf 2008;39:398–405.
[2] Buch RR. Rates of heat release and related fire parameters for silicones. Fire Saf J 1991;17:1–12.
[3] de Buyl F. Silicone sealants and structural adhesives. Int J Adhes Adhes 2001; 21:411–22.
[4] Wolf A. Material properties of construction sealants. Kaut Gummi Kunstst 1988;41:173–8.
[5] Gardner L, Baddoo NR. Fire testing and design of stainless steel structures. J Constr Steel Res 2006;62:532–43.
[6] Weil ED. Fire-protective and flame-retardant coatings – a state-of-the-art review. J Fire Sci 2011;29:259–98.
[7] Duquesne S, Magnet S, Jama C, Delobel R. Intumescent paints: fire protective coatings for metallic substrates. Surf Coat Technol 2004;180-181:302–7.
[8] Nguyen DT, Veinot DE, Foster J. Inorganic intumescent fire protective coatings. In: Patent US, editor. Canada: 1989.
[9] Gardelle B, Duquesne S, Vu C, Bourbigot S. Thermal degradation and fire performance of polysilazane-based coatings. Thermochim Acta 2011;519:28–37.
[10] Gardelle B, Duquesne S, Rerat V, Bourbigot S. Thermal degradation and fire performance of intumescent silicone-based coatings. Polym Adv Technol 2013;24:62–9.
[11] Duquesne S, Le Bras M, Bourbigot S, Delobel R, Camino G, Eling B, et al. Thermal degradation of polyurethane and polyurethane/expandable graphite coatings. Polym Degrad Stab 2001;74:493–9.
[12] Li G, Liang G, He T, Yang Q, Song X. Effects of EG and $MoSi_2$ on thermal degradation of intumescent coating. Polym Degrad Stab 2007;92:569–79.
[13] Wang Z, Han E, Ke W. Influence of expandable graphite on fire resistance and water resistance of flame-retardant coatings. Corros Sci 2007;49:2237–53.
[14] Beigbeder A, Linares M, Devalckenaere M, Degée P, Claes M, Beljonne D, et al. CH-π interactions as the driving force for silicone-based nanocomposites with exceptional properties. Adv Mater 2008;20:1003–7.
[15] Staggs JEJ. Numerical characterization of the thermal performance of static porous insulation layers on steel substrates in furnace tests. J Fire Sci 2011;29: 177–92.
[16] Massiot D, Fayon F, Capron M, King I, Le Calvé S, Alonso B, et al. Modelling one- and two-dimensional solid-state NMR spectra. Magn Reson Chem 2002; 40:70–6.
[17] Gosselin G. Structural fire protection, predictive methods. In: Proceedings of building science insight; 1987.
[18] Gustafsson SE. Transient plane source techniques for thermal conductivity and thermal diffusivity measurements of solid materials. Rev Sci Instrum 1991;62:797–804.
[19] Babonneau F, Baccile N, Laurent G, Maquet J, Azaïs T, Gervais C, et al. Solid-state nuclear magnetic resonance: a valuable tool to explore organic-inorganic interfaces in silica-based hybrid materials. Comptes Rendus Chim 2010;13:58–68.
[20] Karrasch A, Wawrzyn E, Schartel B, Jäger C. Solid-state NMR on thermal and fire residues of bisphenol A polycarbonate/silicone acrylate rubber/bisphenol A bis(diphenyl-phosphate) (PC/SiR/BDP) and PC/SiR/BDP/zinc borate (PC/SiR/BDP/ZnB) – part II: the influence of SiR. Polym Degrad Stab 2010;95:2534–40.
[21] Bourbigot S. Quantitative approach of intumescence by numerical simulation. In: 243 rd American Chemical Society National meeting, editor. San Diego: 2012.
[22] S JEJ. Thermal conductivity estimates of intumescent chars by direct numerical simulation. Fire Saf J 2010;45:228–37.
[23] Raza MA, Westwood A, Brown A, Hondow N, Stirling C. Characterisation of graphite nanoplatelets and the physical properties of graphite nanoplatelet/silicone composites for thermal interface applications. Carbon 2011;49: 4269–79.
[24] Wang Z, Han E, Ke W. Thermal degradation of expandable graphite modified APP/PER/EN flame retardant coating. Acta Materiae Compositae Sinica 2005; 22:52–9.
[25] Ullah S, Ahmad F, Megat-Yusoff PSM, Azm NHB. A study of bonding mechanism of expandable graphite based intumescent coating on steel substrate. J Appl Sci 2011;11:1630–5.
[26] Sharif M, Faghihi-Sani MA, Golestani-Fard F, Saberi A, Soltani AK. Coating of graphite flakes with MgO/carbon nanocomposite via gas state reaction. J Alloys Compd 2010;500:74–7.
[27] Hurst JA. Determination of quartz in bulk materials from workplace environments using X-ray diffractometry and the absorption diffraction method. Talanta 2012;93:392–7.
[28] O'Hare LA, Parbhoo B, Leadley SR. Development of a methodology for XPS curve-fitting of the Si 2p core level of siloxane materials. Surf Interface Anal 2004;36:1427–34.
[29] Contarini S, Howlett SP, Rizzo C, De Angelis BA. XPS study on the dispersion of carbon additives in silicon carbide powders. Appl Surf Sci 1991;51:177–83.
[30] Dreyer DR, Park S, Bielawski CW, Ruoff RS. The chemistry of graphene oxide. Chem Soc Rev 2010;39:228–40.

Resistance to fire of intumescent silicone based coating: the role of organoclay

B. Gardelle[1], S. Duquesne[1], P.Vandereecken[2], S.Bellayer[3], S. Bourbigot[1*]

[1]ISP/UMET – UMR/CNRS 8207, Ecole Nationale Supérieure de Chimie de Lille (ENSCL), Avenue Dimitri Mendeleïev – Bât. C7a, BP 90108, 59652 Villeneuve d'Ascq Cedex, France

[2] Dow Corning S.A., High Performance Building solutions, Rue Jules Bordet, 8 - 7180 Seneffe, Belgium

[3] Ecole Nationale Supérieure de Chimie de Lille (ENSCL), Avenue Dimitri Mendeleïev – Bât. C7a, CS 90108, 59652 Villeneuve d'Ascq Cedex, France

[*]Corresponding author - tel: +33 (0)3 20 43 48 88 - mail: serge.bourbigot@ensc-lille.fr

Abstract

The fire performance of a curable-silicone based coatings containing expandable graphite (EG) and an organoclay is evaluated in hydrocarbon fire scenario (standard UL1709) using a lab-scale furnace test. It is shown that the use of organoclay allows achieving better performance. The influence of the clay as additional filler is investigated on the fire performance and on the mechanical properties of the char. It is shown that the clay increases significantly the mechanical properties of the char and hence, the fire performance of the silicone based coating. In a next part, the silicone/clay material was characterized by electron microscopy, wide-angle X-ray scattering and solid state ^{29}Si nuclear magnetic resonance (NMR). It evidences the nanodispersion of the clay into the silicone matrix and two main interactions: (i) intercalation of some silicate layers and (ii) chemical reactions between the hydroxyl groups of the clay and the silicone matrix. Finally, X-ray fluorescence of the residue after fire testing shows the organoclay is present uniformly throughout the thickness of the char, due to the previous interaction, and hence increasing the cohesion of the char.

Keyword: Resistance to fire; intumescent silicone; organoclay; char strength

Introduction

The protection of metallic materials against fire has become an important issue in the offshore platform industry. Indeed, steel begins to lose its structural properties above 500 °C and it must be therefore protected against fire [1]. Prevention of the structural collapse of building is paramount to ensure the safe evacuation of people from the building, and is a prime requirement of building regulations in many countries. One of the most used systems to protect metallic structures is intumescent paint. These coatings have the properties to swell when exposed to fire and thus make a thick insulative foam. Intumescent coatings are mostly based on a combination of a char-forming material, a mineral acid catalyst, a blowing agent and a binder resin [2, 3]. However, these materials are typically organic-based materials and exhibit some disadvantages. First, organic additives undergo exothermic decomposition which reduces the thermal insulative value of the system. Second, the resulting carbonaceous char in some cases has a low structural integrity and the coating cannot withstand the mechanical stress induced by a fire and/or by other external constraints. And third, the coating releases organic gases (potentially toxic) which are undesirable in a closed fire environment [4].

Currently, some alternative to organic intumescent coating have been studied [5-7] in our lab, we recently evaluated the fire performance of an intumescent silicone based coating[5]. In this study, the fire performance of a phenyl silicone resin containing silica-based modifier was evaluated in pure radiative and in convective/radiative heating conditions[5]. We reported the good heat barrier properties of this intumescent silicone based coating in radiative/convective heating whereas fire performance of this coating is rather limited in the case of pure radiative heating. Indeed, in pure radiative heating source, silicone based coatings cracks due to the high vibration of Si-O bond in infrared field and so, it exhibits low fire performances.

On the other hand, expandable graphite (EG) is a ‘‘particular’’ intumescent additive known to impart fire retardancy to various materials [8]. EG is a graphite intercalation compound in which sulfuric acid and/or nitric acid is inserted between the carbon layers of graphite. Upon heating, exfoliation of the graphite occurs, i.e. expansion along c-axis of the crystal structure by about hundred times. The material generates in that way is a puffed-up material of low density with a ‘‘worm’’ like structure. In recent decades, more and more papers reported the use of expandable graphite in intumescent based coating. This intumescent additive increases the fire performance and anti-oxidant properties of traditionnal intumescent based coating [2, 9, 10]. However, in the above mentioned studies, expandable graphite is incorporated into complex organic intumescent based formulations. It is noteworthy that in organic based coating, EG decreases considerably the cohesion of the char [10].

We recently reported the used of silicone based coating containing EG for the fire protection of steel[11]. We reported high fire performance of silicone containing 25% of EG in curable silicone resin cross linked with titanium-based catalyst. The good performances were explained by the formation of an expanded insulative char (3400% expansion) formed at a high expansion velocity (18%/s) and exhibiting a low thermal conductivity (0.35 W/K.m at 500°C). It was shown that the formation of a complex silicone/graphite structure at high temperature is responsible of the good cohesion of the char in fire scenario. Mechanical strength of the char is a key parameter to ensure its integrity in fire scenario. This factor is significant because in fire scenario, char destruction can proceed not only by means of ablation and heterogeneous surface burning but also by means of an external influence such as wind, mechanical action of the fire or convective air flows. To ensure the good cohesion of the char, several additives are added to the intumescent formulation such as mineral fibres [12], organo-clay [13, 14], ceramic precursor[15]. In this study, organoclay are used to increase mechanical properties of the char.

The purpose of this paper is to investigate the heat barrier properties of curable silicone/expandable graphite based coating using organoclay as filler in hydrocarbon fire scenario (standard UL1709). The effect of the organoclay on the mechanical properties of the char will be carefully investigated. To explain the influence of the clay on the fire performance and mechanical properties of the resulting char, silicone matrix containing organoclay and residues obtained after furnace test will be characterized.

2. Experimental

2.1 Materials

The silicone resin called silicone 1 (S1), is composed of a hydroxylated PDMS with a viscosity of 15000 cS (viscosity is measured using cone/plate rheometer CP-52), methyltrimethoxysilane (MTM) as crosslinking agent and a titanium catalyst. All the materials were supplied by Dow Corning, Seneffe (Belgium).

25% of expandable graphite (ES350F5 from Graphitwerk Kropfmuehl (Germany)) with an average grain size of 300µm was incorporated in the silicone matrix. 5% of Cloisite 30B ((C30B) – organoclay mineral from Southern Clay) are incorporated and dispersed manually with a spatula in the formulations to increase the fire performances of the coating. Each formulation was applied with a spatula on a 10 cm x 10 cm x 3 mm steel plate to obtain 1.0 ± 0.15 mm and 1.5 ± 0.15 mm coatings. Steel plates were first cleaned before application with ethanol and a primer (Primer 1200 from Dow Corning) was applied to enhance the coating adhesion. To characterize the silicone/clay material, the ratio S1/clay was kept constant and so, S1+6% clay material is characterized.

2.2 Fire Testing Methods

The small scale furnace test was developed in our laboratory to evaluate the fire performance of intumescent coatings in fire scenario. This test was designed to mimic the UL1709 normalized temperature/time curve, referred to hydrocarbon fire. The lab-made furnace exhibits an internal volume of 26 dm^3 (Figure 1). Refractory fibers (stable up to 1300°C) cover the different sides of the furnace. The furnace is equipped with two gas burners (20kW propane burners). The gas pressure was fixed at 1.8 bars and the flow was regulated in order to mimic the UL1709 curve. A temperature probe inside the furnace regulates the temperature and a K-type thermocouple allows the furnace temperature profile to be registered. The furnace is equipped with a quartz window allowing following the intumescent process taking place during the test.

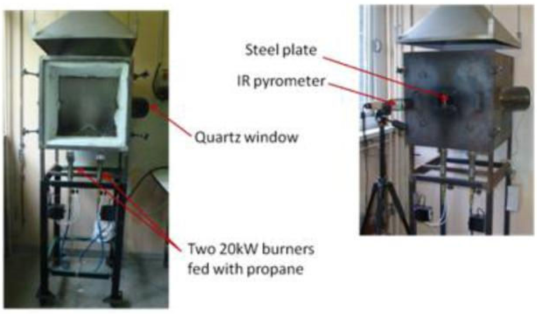

Figure 1: Furnace set up to mimic hydrocarbon fire scenario

The temperature at the back side of the plate is measured as a function of time using a pyrometer (temperature measured in the center of the plate). The plate is not insulated. The backside of the plate is coated with a black paint (Jeltz) having a constant emissivity (0.92) and thermally resistant up to 800°C in order to get reliable temperature measurements with the pyrometer. The critical temperature of steel defined as the temperature at which only 60% of the original strength remains, point at which failure is imminent under full design loads were obtained. The temperature of 500°C has been adopted as a standard for normally loaded structural components whereas 400°C is often used for heavily loaded structure [16]. In this study, the time to reach the two temperatures is taken into account to evaluate the heat barrier properties of the intumescent coatings.

2.3 Air Jet Test

To evaluate the mechanical properties of an intumescent material few experimental setup are reported in the literature [17, 18]. In the lab, we have developed an approach involving a rheometer in which the intumescent structure is developed at a given temperature (for example 500°C) without any constrain. After the steady state was obtained, the upper plate of the rheometer is brought into contact with the intumesced material and the gap between the plates is reduced linearly (0.02 mm/s). The compression force is thus followed as a function of the gap [17]. However, this technique is limited for experimental reason to 500°C and the silicone based formulation are not degraded at this temperature and its expansion is not maximum, so this technique is not appropriate. Another method was developed by Reshetnikov et al. [18] using a "Structurometer ST-1", developed at the Moscow State Food Academy. They measure the force required to destroy a char. The samples were first pyrolysed and then a destructive force was applied to the sample. Mechanical properties of the char are investigated at ambient temperature which may not be representative of its behaviour at high temperature.

Based on the above considerations, we have designed a new lab scale test to evaluate the mechanical properties and the cohesion of the char obtained from intumescent coatings. Its set up is illustrated in Figure 2.

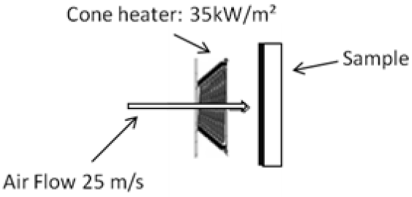

Figure 2: Schematic experimental set up used to determinate the cohesion properties of the char

The coating is directly exposed to an electrical cone heater providing pure radiative heat (in this study, 35kW/m²). When the expansion of the coating is maximal (after 5 min testing), an air flow (25 m/s) impacts the char. The air flow was measured using an anemometer Testo 425. By visual observation, it is possible to have an idea of the mechanical properties of the char. Indeed, if the char is fragile, it will be destroyed by the air impact whereas a strong char will not or only slightly be affected by the air jet. The advantage of this test is to evaluate the mechanical properties in a fire scenario.

2.4 ^{29}Si solid state NMR

^{29}Si nuclear magnetic resonance (NMR) spectroscopy is a powerful tool for examining silicon surrounding. This technique can distinguish several kinds of structures including D, T and Q structures which characterize silicone network (Figure 3).

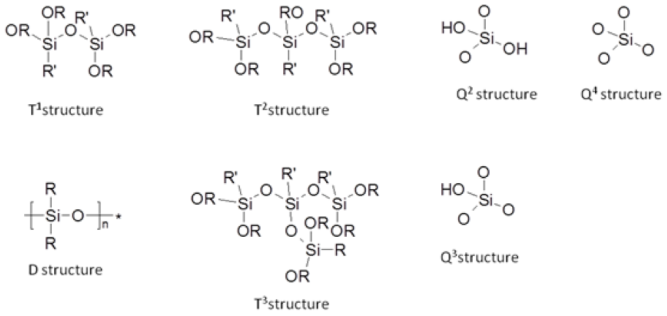

Figure 3: Schematics presentation of D, $T^1$and Q^1 silicone structures

^{29}Si NMR spectra were recorded on a Bruker Advance II 400 operating at 9.4T and using a 7 mm probe. Zirconia rotor and caps are used. NMR spectra were acquired with MAS (magic angle spinning) of 5 kHz. The reference used for ^{29}Si NMR was tetramethylsilane (TMS). For the pure clay sample, a delay of 30s between the pulses and a $\pi/2$ pulse length for 6 ms were used and 2560 scans were accumulated. For S1 and S1/clay samples a delay of 180s was used. Respectively 288 scans and 2267 scans were accumulated to get an acceptable signal to noise ratio.

2.5 X-ray Fluorescence (XRF)

Residue after fire testing were analyzed by X-ray fluorescence to determine its chemical composition. Measurements were performed on a Bruker S2-RANGER spectrometer equipped with a Pd X-ray tube and a XFLASHTM Silicon Drift Detector (SDD).

2.6 Wide-angle X-ray scattering (WAXS)

Measurements were performed by wide-angle X-ray scattering (WAXS) at room temperature. The X-ray source was generated by a 1.5 kW sealed tube with Cu target (λ = 1.54 Å), operated at 20 mA and 40 kV. The sample-to-detector distance was 20 cm. 2D-WAXS patterns were recorded on a CCD camera from Photonic Science Ltd.

2.7 Transmission Electron Microscopy (TEM)

Ultramicrotomy was used to prepare the sample. Bright-field TEM images of sample were obtained at 200 kV under low dose conditions with a FEI TECNAI 62 20 electron microscope, using a Gatan CCD camera.

3. Results

3.1 Fire protection

Figure 4 shows temperature profils as a function of time on the backside of the steel plates coated with the different formulations during hydrocarbon fire scenario. The influence of the clay on the heat barrier properties of silicone based coating is clearly shown: the paint prepared with 5% of clay exhibits a better behavior for 1 mm and particularly for 1.5 mm thick intumescent coatings. The reproducibility of measurement is acceptable and an error of 10% about the time to reach critical temperature is obtained.

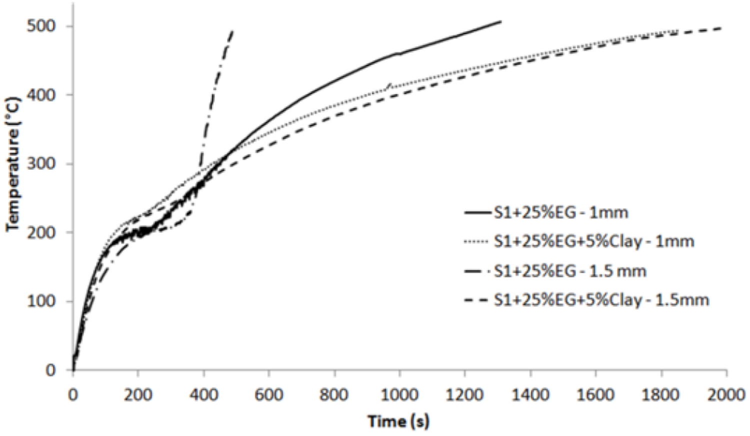

Figure 4: Temperature versus time curve of S1/EG and S1/EG/clay based coating in hydrocarbon fire scenario

For 1 mm based coating, 500°C is reached in 1300 ± 130s and 1860 ± 180s respectively for S1/EG and S1/EG/clay (table 1) demonstrating the better fire performance of silicone based coating when organoclay is used. Similar results are obtained at 400°C since the time to reach this temperature increases from 715 ± 70s for S1/EG to 900 ± 90s for S1/EG/clay. For the two formulations, the expansion rate reaches 3400%. Both residue are presented in Figure 5a) and 5b) and they exhibits same morphology. The two char are covered by a white powder.

Table 1: Time to reach critical temperature

	S1/EG - 1 mm	S1/EG/clay - 1 mm	S1/EG - 1.5 mm	S1/EG/clay - 1.5 mm
Time to reach 400°C	715 ± 70s	900 ± 90s	428± 40s	1000 ± 100s
Time to reach 500°C	1300 ± 130s	1860 ± 180s	490 ± 40s	2050 ± 200s

Fire tests carried out on 1.5 mm based coatings also evidence the better cohesion of the char when clay is used as additional filler. Indeed, when just 25% EG is added to silicone matrix there is a complete loss of adhesion of the char from the plate after 400s (Figure 5 c) leading to the loss of the insulative properties. The temperature thus sharply increases to reach 500°C in 490 ± 40s. However, when 5% of clay is incorporated in the S1/EG formulation, there is good cohesion of the char (Figure 5d) and so, the silicone based coating remains stuck on the plate providing high insulative properties. For the two formulations, critical temperature (500°C) is reached in only 490 ± 40s for S1/EG while 2050 ± 200 s is needed for S1/EG/clay based coatings.

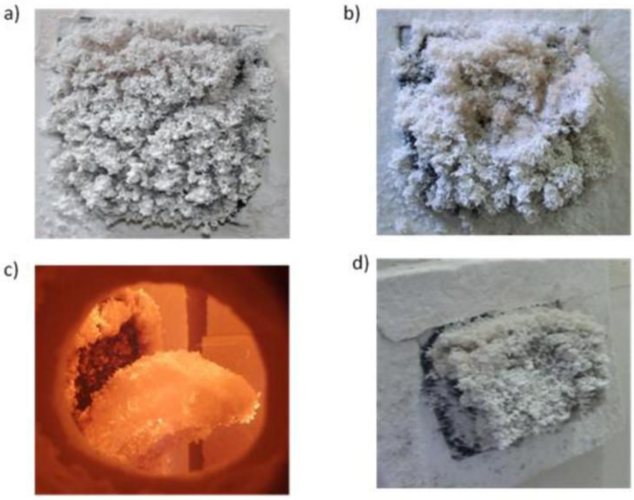

Figure 5: a)S1/EG 1 mm based coating residue, b)S1/EG/C30B 1 mm based coating residue, c)S1/EG 1.5mm based coating during fire experiment, d)S1/EG/C30B 1.5 mm based coating residue

3.2 Mechanical properties of the char

In order to investigate the mechanical properties of the intumescent chars and the influence of the clay on it, the S1/EG and S1/EG/clay formulations were tested using the air jet test. The coatings exhibit similar behavior (Figure 6a and 6b) during the first step of the test (when the air does not impact the coating). During the first minute, the coatings begin to swell; after 2 minutes, the coatings ignite and a white powder covers the expanded graphite. The residues of the two formulations after air jet testing are shown in Figure 6b and Figure 6c. It could be observed that, when the air flow is switch on, a complete destruction of the char occurs for S1/EG based coating while there is no complete char destruction when the clay is incorporated into the formulation.

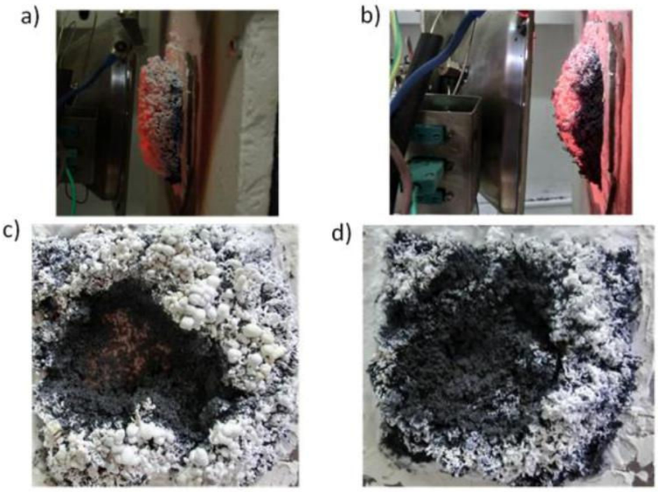

Figure 6: a) S1/EG b) S1/EG/C30B during air jet test before air impact, c)S1/EG residue after air impact, d)S1/EG/C30B after air impact

This evidences the superior mechanical properties and the extremely good cohesion of the char when organoclay is used as filler. We have thus demonstrated that the organoclay has a very significant influence on the cohesion and the mechanical properties of the intumescent char and, hence, on the fire performance of silicone based coating. In the next step of this study, the mode of action of the organoclay is evaluated. First of all, the morphology of the resin added with the clay is characterized.

3.3 Silicone/Organoclay characterization

In order to highlight possible interaction between the silicone matrix and the clay, the system without expandable graphite is studied. And, we can reasonably assume that the addition of expandable graphite should not affect significantly the dispersion of the clay in the material.

Figure 7 shows the TEM pictures of S1/clay sample at different magnitude. Some aggregates and tactoids of 3-10 layers in size can be distinguished and individual platelets can be distinguish on the pictures. Even if the dispersion of the organoclay is not completely, it is acceptable and we can conclude that a nanodispersion is achieved.

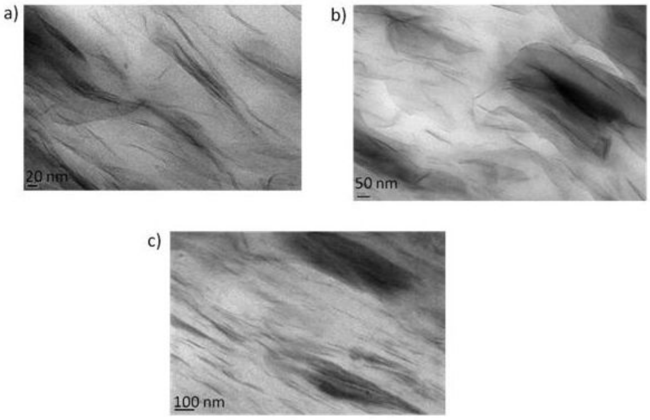

Figure 7: TEM pictures of S1/clay

WAXS patterns of the organoclay, silicone matrix and silicone/clay are presented in Figure 8. For pure polymer, no cristallinity peak in the diffraction pattern. Concerning, pure organoclay, a single peak at $2\theta = 5.0°$ corresponding to a distance between the silicate layer of about 18 Å[19] is observed. This value is consistent with the value found in the literature. When the clay is added to the silicone matrix, there is an increase of the interlayer distance of the silicate evidenced by a shift of the peak corresponding to the clay from 5.0° to 3.0°. The interlayer increases from 18 Å to 30 Å.

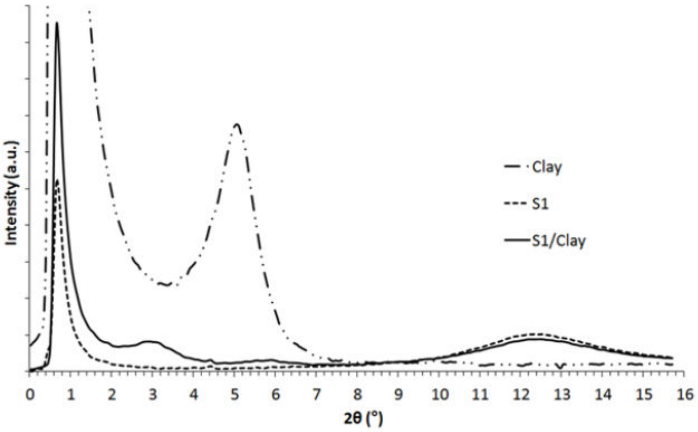

Figure 8: WAXS pattern of clay, silicone matrix and silicone/clay composite

TEM images indicate the nanodispersion of the organoclay and the WAXS analysis evidences a decrease of the peak in 2θ attributed to an intercalation into the galleries of the clay. The next step was to point out if potential interactions could occur between the clay and the silicone matrix. For this, ^{29}Si NMR spectroscopy experiments are carried out. Figure 9 presents the NMR spectra of the clay, S1 and S1/clay materials. Three sites are observed: D (-22ppm), T^2 (-57 ppm) and T^3 (-66 ppm) for the pure silicone. The T structures come from the reaction between the hydroxyl function of the PDMS and the methoxy groups of the MTM as we previously reported [11]. For the organoclay spectrum, three peaks appear at -89 ppm, -94 ppm and -108 ppm corresponding respectively to Q^2, Q^3 and Q^4 structures [20]. The presence of Q^2 and Q^3 structure indicates the presence of reactive hydroxyl groups at the surface or on the edges of the silicate layer.

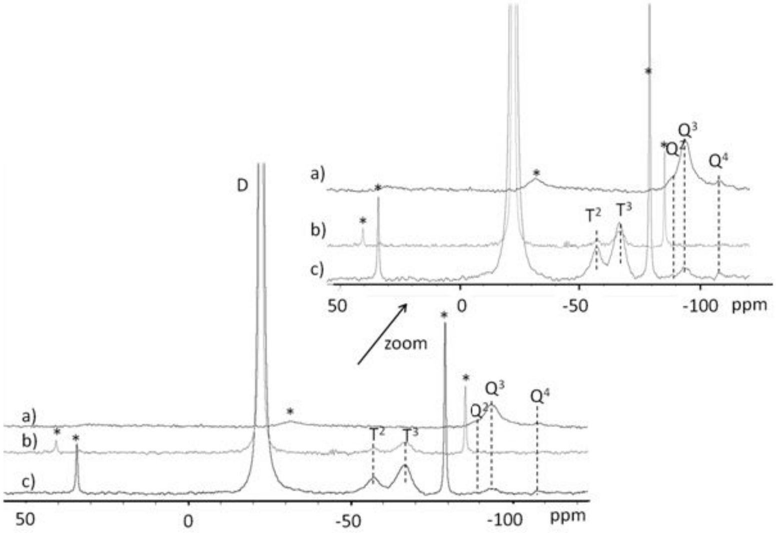

Figure 9: ^{29}Si NMR spectra of a) clay ; b) S1 and c) S1/clay

Concerning S1/clay spectrum, the three peaks corresponding to the matrix are observed at -22 ppm, -57 ppm, -66 ppm corresponding respectively to D, T^2 and T^3 structure. The peaks corresponding to the clay (Q^3 and Q^4) at -94 ppm and -108 ppm also show up. However, there is no peak (or with low intensity) corresponding to Q^2 structure at -89 ppm. A possible explanation of this observation is the chemical reaction between the hydroxyl groups of the organoclay and the silicone matrix. This reaction should occur between the ethoxy groups from the MTM and the hydroxyl groups of the clay [21].

This study evidences three main conclusions: (i) the organoclay are nanodispersed in the silicone matrix, (ii) there is an intercalation of silicone chains into the galleries of the clay and (iii) chemical interaction between organoclay and silicone could be suspected.

3.3 X-Ray Fluorescence (XRF) of the residues

A good dispersion of the clay in the char should be necessary to ensure its good cohesion during fire testing[22, 23]. To examine this, different parts of the residue of S1/EG/clay were analyzed by X-Ray fluorescence. The final expansion of the char is about 3.4 cm. To have an idea of the dispersion of the clay in the char, four parts were analyzed by XRF: the top, 1.5 cm from the top, 2.5 cm from the top and the bottom of the char. Organoclay are alumino-silicate and thus if aluminium is detected in the sample it will evidence the presence of the organoclay. Figure 10 shows the XRF spectrum of the four parts of the char.

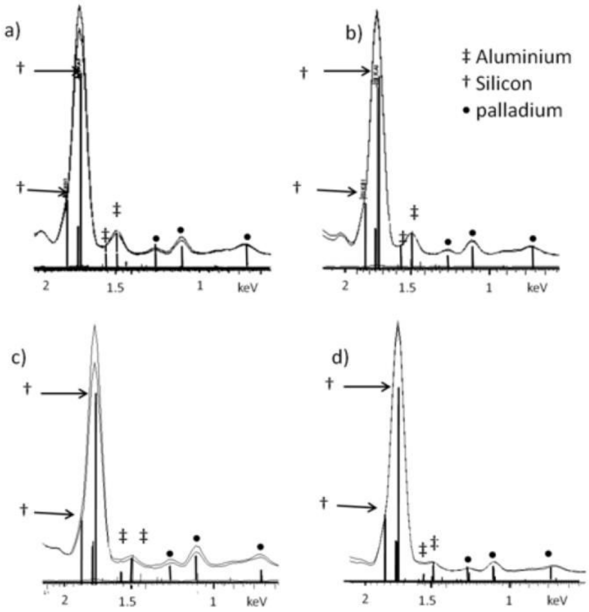

Figure 10: XRF spectrum of : a) the top of the char, b) 1.5cm from the top of the char, c) 2.5cm from the top of the char and d) the bottom of the char.

For all samples the same peaks are observed. The main peak at 1.75 keV, 1.5 keV and 1.1 keV correspond to respectively silicon, aluminium and palladium. Palladium comes from the experimental device (the source). These analyses evidence the fact that the organoclay is detected in all parts of the char.

3.5 Discussion

The fire performance of silicone/expandable graphite based coating has been investigated in hydrocarbon fire scenario for two different thicknesses: 1 mm and 1.5 mm. For thick intumescent based coating, when 25% of EG is added to the silicone matrix there is a complete loss of adherence of the char from the plate. This is explained by a low cohesion of the char and by the impressive expansion of the system (around 3000%). In order to avoid the collapse of the structure for thick coating, organoclay was incorporated in the formulation. In this case, S1/EG/clay exhibits excellent fire performances at 1 mm and 1.5 mm thick coating. The mechanical properties of the char have been investigated using air jet test and evidence the better mechanical properties of the char when organoclay is added to the S1/EG. The characterization of the silicone/organoclay composite shows the nanodispersion of the clay in individual platelets and intercalation of the silicone chains into the galleries of the clay. Moreover, ^{29}Si NMR lets us to propose chemical reaction between the clay and the silicone matrix leading to a strong cohesion between the clay platelets and the silicone matrix. This is illustrated in Figure 11. During the cross-link step of the resin/clay material, there is formation of a three dimensional network based on T structures and some Q structures due to the chemical reaction between the silicone and the clay.

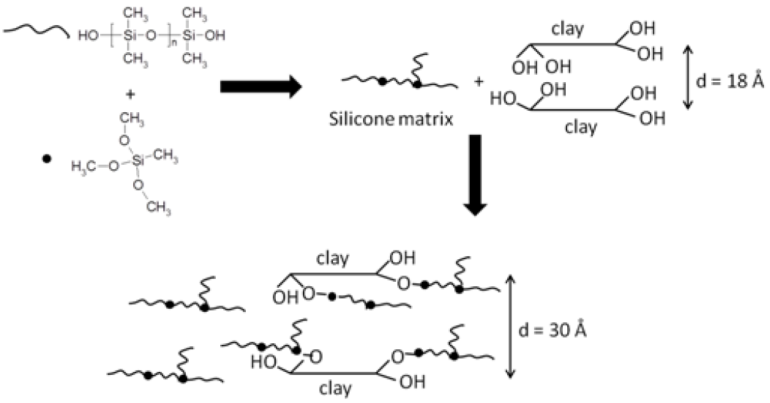

Figure 11: Schematic intercalation of the organoclay in the silicone matrix

In hydrocarbon fire scenario, there is expansion of the coating and the graphite platelets are embedded in complex silicone structure [11].

The residue after furnace testing was analyzed by x-ray fluorescence and shows the presence of the clay in the whole. As a consequence, it may be proposed that the good interaction between the matrix and the clay platelets lead when the material degrade to the formation of a cohesive structure that will embedded the expanded graphite platelets. The clay platelets will thus be present uniformly throughout the thickness of the char and no decantation or surface migration is observed. The char thus presents high mechanical properties and, therefore, high fire protective behavior. These are illustrated in the figure 12.

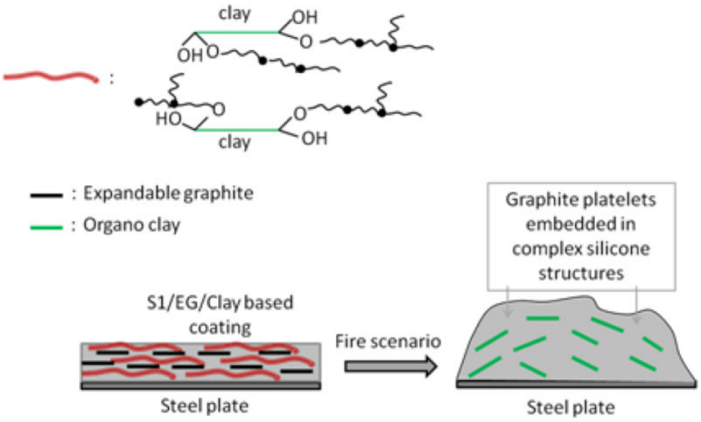

Figure 12: Mode of action of the clay in hydrocarbon fire scenario

Conclusion

In this paper we have investigated the fire performance of silicone/expandable graphite/clay in hydrocarbon fire scenario. We demonstrated that the organoclay increases significantly the mechanical properties of the char and therefore its cohesion during fire testing. This will result in high fire protective behavior. This phenomenon was explained reasonably by the characterization of the material by TEM, WAXS and ^{29}Si NMR evidencing a nanodispersion of the fillers and two main interactions: (i) the intercalation of some silicate platelets and (ii) a chemical reaction between the hydroxyl groups from the clay with the silicone matrix.

Acknowledgements

The authors gratefully acknowledge Mr. Revel for his skillful experimental assistance and his expertise in NMR and Dr. Stoclet for his experimental assistance and his expertise in Wide-angle X-ray scattering.

References

[1] L. Gardner, N.R. Baddoo, Fire testing and design of stainless steel structures, Journal of Constructional Steel Research, 62 (2006) 532-543.

[2] E.D. Weil, Fire-Protective and Flame-Retardant Coatings - A State-of-the-Art Review, J. Fire Sci., (2011).

[3] S. Duquesne, S. Magnet, C. Jama, R. Delobel, Intumescent paints: Fire protective coatings for metallic substrates, Surf. Coat. Technol., 180-181 (2004) 302-307.

[4] D.T. Nguyen, D. E.Veinot, J. Foster, Inorganic intumescent fire protective coatings, in: U.S. Patent (Ed.), Canada, 1989.

[5] B. Gardelle, S. Duquesne, V. Rerat, S. Bourbigot, Thermal degradation and fire performance of intumescent silicone-based coatings, Polym. Adv. Technol., 24 (2013) 62-69.

[6] B. Gardelle, S. Duquesne, P. Vandereecken, S. Bourbigot, Fire performances of curable silicone based coatings, in: ACS book Fire and Polymers VI: New Advances in Flame Retardant Chemistry and Science, 2012.

[7] B. Gardelle, S. Duquesne, C. Vu, S. Bourbigot, Thermal degradation and fire performance of polysilazane-based coatings, Thermochim. Acta, 519 (2011) 28-37.

[8] S. Duquesne, M. Le Bras, S. Bourbigot, R. Delobel, G. Camino, B. Eling, C. Lindsay, T. Roels, Thermal degradation of polyurethane and polyurethane/expandable graphite coatings, Polym. Degrad. Stab., 74 (2001) 493-499.

[9] G. Li, G. Liang, T. He, Q. Yang, X. Song, Effects of EG and MoSi2 on thermal degradation of intumescent coating, Polym. Degrad. Stab., 92 (2007) 569-579.

[10] Z. Wang, E. Han, W. Ke, Influence of expandable graphite on fire resistance and water resistance of flame-retardant coatings, Corros. Sci., 49 (2007) 2237-2253.

[11] B. Gardelle, S. Duquesne, P. Vandereecken, S. Bourbigot, Characterization of the carbonization process of expandable graphite/silicone formulations in a simulated fire, Polym. Degrad. Stab., Accepted (2013).

[12] R. Otáhal, D. Veselý, J. Násadová, V. Zíma, P. Němec, P. Kalenda, Intumescent coatings based on an organic-inorganic hybrid resin and the effect of mineral fibres on fire-resistant properties of intumescent coatings, Pigment and Resin Technology, 40 (2011) 247-253.

[13] S. Bourbigot, F. Samyn, T. Turf, S. Duquesne, Nanomorphology and reaction to fire of polyurethane and polyamide nanocomposites containing flame retardants, Polym. Degrad. Stab., 95 (2010) 320-326.

[14] S. Ullah, F. Ahmad, P.S.M. Megat-Yusoff, Effect of boric acid with kaolin clay on thermal degradation of intumescent fire retardant coating, Journal of Applied Sciences, 11 (2011) 3645-3649.

[15] J.H. Koo, P.S. Ng, F.B. Cheung, Effect of high temperature additives in fire resistant materials, J. Fire Sci., 15 (1997) 488-504.

[16] G. Gosselin, Stuctural fire protection, predictive methods, Proceedings of building science Insight, (1987).

[17] M. Jimenez, S. Duquesne, S. Bourbigot, Characterization of the performance of an intumescent fire protective coating, Surf. Coat. Technol., 201 (2006) 979-987.

[18] I.S. Reshetnikov, M.Y. Yablokova, E.V. Potapova, N.A. Khalturinskij, V.Y. Chernyh, L.N. Mashlyakovskii, Mechanical stability of intumescent chars, J. Appl. Polym. Sci., 67 (1998) 1827-1830.

[19] S. Filippi, M. Paci, G. Polacco, N.T. Dintcheva, P. Magagnini, On the interlayer spacing collapse of Cloisite® 30B organoclay, Polym. Degrad. Stab., 96 (2011) 823-832.

[20] F. Babonneau, N. Baccile, G. Laurent, J. Maquet, T. Azaïs, C. Gervais, C. Bonhomme, Solid-state nuclear magnetic resonance: A valuable tool to explore organic-inorganic interfaces in silica-based hybrid materials, Comptes Rendus Chimie, 13 (2010) 58-68.

[21] P.A. Wheeler, J. Wang, J. Baker, L.J. Mathias, Synthesis and Characterization of Covalently Functionalized Laponite Clay, Chem. Mater., 17 (2005) 3012-3018.

[22] S. Bourbigot, M.L. Bras, F. Dabrowski, J.W. Gilman, T. Kashiwagi, PA-6 clay nanocomposite hybrid as char forming agent in intumescent formulations, Fire and Materials, 24 (2000) 201-208.

[23] S. Duquesne, C. Jama, M. Le Bras, R. Delobel, P. Recourt, J.M. Gloaguen, Elaboration of EVA-nanoclay systems - Characterization, thermal behaviour and fire performance, Compos. Sci. Technol., 63 (2003) 1141-1148.

ARTICLE IN PRESS

European Polymer Journal xxx (2013) xxx–xxx

Contents lists available at SciVerse ScienceDirect

European Polymer Journal

journal homepage: www.elsevier.com/locate/europolj

Macromolecular Nanotechnology

Resistance to fire of curable silicone/expandable graphite based coating: Effect of the catalyst

B. Gardelle [a], S. Duquesne [a,*], P. Vandereecken [b], S. Bellayer [c], S. Bourbigot [a]

[a] *ISP/UMET – UMR/CNRS 8207, Ecole Nationale Supérieure de Chimie de Lille (ENSCL), Avenue Dimitri Mendeleïev – Bât. C7a, BP 90108, 59652 Villeneuve d'Ascq Cedex, France*

[b] *Dow Corning S.A., High Performance Building Solutions, Rue Jules Bordet, 8 – 7180 Seneffe, Belgium*

[c] *Ecole Nationale Supérieure de Chimie de Lille (ENSCL), Avenue Dimitri Mendeleïev – Bât. C7a, CS 90108, 59652 Villeneuve d'Ascq Cedex, France*

ARTICLE INFO

Article history:
Received 2 April 2013
Received in revised form 12 April 2013
Accepted 23 April 2013
Available online xxxx

Keywords:
Fire protection
Catalyst
Silicone coating
Expandable graphite
Intumescent coating

ABSTRACT

The fire performance of two curable-silicone based coatings containing 25% expandable graphite (EG) are evaluated in hydrocarbon fire scenario (standard UL1709) using a lab-scale furnace test. In this paper, the influence of the catalyst on the fire performance are investigated. Two organometallic titanium based- and tin based catalyst are used to make the curable silicone crosslink. When titanium based catalyst is used, the fire performance are higher and the mechanical properties of the char is better than that when tin is used as catalyst. To explain this surprising different fire behavior, the two residues after the furnace test were analyzed by X-ray photospectroscopy. It has been demonstrated that in the case of titanium based catalyst, the char is composed of graphite embedded by cross-linked silicone structure compare to linear silicone structure in the case of tin based catalyst. The two silicone resins were characterized by Fourier Transform Infrared spectroscopy, ^{29}Si NMR, thermogravimetric analyses, EPMA (electron probe microanalyses). It was highlighted that the tin migrates into the surface during the crosslinking of the matrix leading to a low thermal stability and, thus, low fire performances. Whereas, when titanium based catalyst is used, it participates to the silicone network with the formation of Si–O–Ti bounds increasing the thermal stability of the matrix and so enhancing the fire performance of the silicone/EG based coating.

1. Introduction

The protection of metallic materials against fire has become an important issue in the construction industry. Indeed, steel begins to lose its structural properties above 500 °C and it must be therefore protected against fire [1]. Prevention of the structural collapse of the building is paramount to ensure the safe evacuation of people from the building, and is a prime requirement of building regulations in many countries. One of the most used systems to protect metallic structures is intumescent paint. These coatings have the properties to swell to thick insulative foam when heated above a critical temperature. Intumescent coatings are mostly based on a combination of a char-forming material, a mineral acid catalyst, a blowing agent and a binder resin [2,3]. However, these materials are typically organic-based materials and exhibit some disadvantages. First, organic additives undergo exothermic decomposition which reduces the thermal insulative value of the system. Second, the resulting carbonaceous char in some cases has a low structural integrity and the coating cannot withstand the mechanical stress induced by a fire and/or by other external constraints. And third, the coating releases organic gases (potentially toxic) which are undesirable in a closed fire environment [4].

Currently, some alternative to organic intumescent coating have been studied [5–7]. The use of silicone-based

---

* Corresponding author. Tel.: +33 (0)3 20 33 72 36.
E-mail address: sophie.duquesne@ensc-lille.fr (S. Duquesne).

0014-3057/$ - see front matter © 2013 Elsevier Ltd. All rights reserved.
http://dx.doi.org/10.1016/j.eurpolymj.2013.04.021

Please cite this article in press as: Gardelle B et al. Resistance to fire of curable silicone/expandable graphite based coating: Effect of the catalyst. Eur Polym J (2013), http://dx.doi.org/10.1016/j.eurpolymj.2013.04.021

protective coating is poorly reported in the literature. We recently evaluated the fire performance of an intumescent silicone based coating [6]. In this study, the fire performance of a phenyl silicone resin containing silica-based modifier was evaluated in pure radiative and convective/radiative heating conditions [6]. We reported the good heat barrier properties of this intumescent silicone based coating in radiative/convective heating whereas fire performance of this coating is rather limited in the case of pure radiative heating. Indeed, in pure radiative heating source, silicone based coatings cracks due to the high vibration of Si–O bond in infrared field and so, it exhibits low fire performances.

Polydimethylsiloxane (PDMS) is widely used in the construction industry and electrical equipments because of its excellent thermal stability and fire properties including low heat of combustion and low rate of heat release compared to conventional organic polymers [8,9]. This polymer is available in different forms from liquid to cross-linked rubber. The rubbers can be found in two main classes [10]: one cross-linked by polyaddition, and another by polycondensation. Silicones prepared via the polycondensation method are used to make sealants that find applications in original equipment manufactories providing a barrier against severe environments such as humidity or dust [11]. These products are ready to use and they require no additional mixing: cross-linking starts when the product is exposed to moisture. Most silicone sealants are formulated from a reactive polymer prepared from an hydroxy-polydimethylsiloxane and a large excess of cross-linker such as tri-acetoxysilane. Organometallic catalysts have to be used to make the resin crosslink. The two most used catalysts are tin and titanium based catalysts. The polycondensation reaction is illustrated in Eq. (1).

$$\mathrm{HO}-(\mathrm{Me_2SiO})_x-\mathrm{H}+\mathrm{exc.\ MeSi(OAc)_3}$$
$$\times \xrightarrow{-2\mathrm{AcOH}} \mathrm{(AcO)_2MeSiO(Me_2SiO)_xOSiMe(OAc)_2} \qquad (1)$$

On the other hand, expandable graphite (EG) is a "particular" intumescent additive known to impart fire retardancy to various materials [12]. EG is a graphite intercalation compound in which sulfuric acid and/or nitric acid is inserted between the carbon layers of graphite. Upon heating, exfoliation of the graphite occurs, i.e. expansion along *c*-axis of the crystal structure by about hundred times. The material generates in that way is a puffed-up material of low density with a "worm" like structure. In recent decades, more and more papers reported the use of expandable graphite in intumescent based coatings. This intumescent additive increases the fire performance and anti-oxidant properties of intumescent based coatings [2,13,14]. However, in the above mentioned studies, expandable graphite is only incorporated into complex organic intumescent based formulations. It is noteworthy that in organic based coating, EG decreases considerably the cohesion of the char [14].

We recently reported the used of silicone based coating containing EG for the fire protection of steel [7]. We reported high fire performance of silicone added with 25% of EG in curable silicone resin cross linked with titanium catalyst. The good performances were explained by the formation of an expanded insulative char (3400% expansion) formed with a high expansion velocity (18%/s) and exhibiting a low thermal conductivity (0.35 W/K m at 500 °C). It was shown that the formation of a complex silicone/graphite structures at high temperature is responsible to the extremely high cohesion of the char in fire scenario.

The purpose of this paper is to investigate the heat barrier properties of curable silicone/expandable graphite based coating in hydrocarbon fire scenario (standard UL1709). The effect of two different organometallic catalysts on the mechanical properties of the char will be carefully investigated. To explain the influence of the catalyst on the fire performance, residues obtained after furnace test will be fully characterized. The structure and thermal stability of the silicone resins will be finally studied for the two catalysts.

2. Experimental

2.1. Materials

The first resin, hereafter called S1–Sn, was composed of 83% of an hydroxylated PDMS with a viscosity of 80 cS (viscosity is measured using cone/plate rheometer CP-52), 15.1% of methyltrimethoxysilane (MTM) as crosslinking agent and 1.9% of a tin based catalyst. The tin based catalyst is a di-alkyl alkanoate (alkyl: methyl, butyl, octyl and alkanoate: laurate, decanoate, etc.). The second, hereafter called S1–Ti, was composed of 77% of an hydroxylated PDMS with a viscosity of 80 cS (viscosity is measured using cone/plate rheometer CP-52), 15% of MTM and 8% of a titanium based catalyst. The titanium based catalyst is a tetra alkoxy titanates (alkoxy: n-propoxy, i-propoxy, n-butoxy, t-butoxy).

25% of expandable graphite ES350F5 from Graphitwerk Kropfmuehl (Germany) with an average grain size of 300 μm was added to the silicone matrix. Both formulations were applied on a 10 cm × 10 cm × 3 mm steel plate to obtain 1.0 ± 0.1 mm coating. Steel plates were cleaned before application with ethanol and a primer (Primer 1200 from Dow Corning) was applied to enhance the coating adhesion.

2.2. Fire testing methods

The small scale furnace test was developed in our laboratory to evaluate the fire performance of intumescent coatings in fire scenario. This test was designed to mimic the UL1709 normalized temperature/time curve, related to hydrocarbon fire. The lab-made furnace exhibits an internal volume of 26 dm^3 (Fig. 1). Refractory fibers (stable up to 1300 °C) cover the different sides of the furnace. The furnace was equipped with two gas burners (20 kW propane burners). The gas pressure was fixed at 1.8 bars and the flow was regulated in order to mimic the UL1709 curve. A temperature probe inside the furnace regulates the temperature and a K-type thermocouple allows the furnace temperature profile to be registered. The furnace is equipped with a quartz window allowing to follow the intumescent process taking place during the test.

Please cite this article in press as: Gardelle B et al. Resistance to fire of curable silicone/expandable graphite based coating: Effect of the catalyst. Eur Polym J (2013), http://dx.doi.org/10.1016/j.eurpolymj.2013.04.021

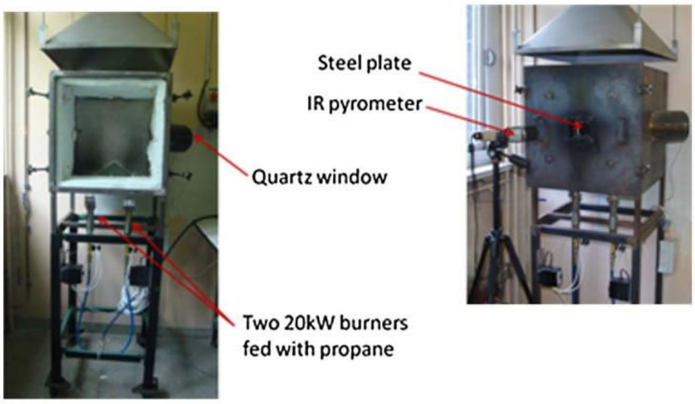

Fig. 1. Furnace set up to mimic hydrocarbon fire scenario.

The temperature at the back side of the plate is measured as a function of time using a pyrometer (temperature measured in the center of the plate). The backside of the plate is coated with black paint (Jeltz) having a constant emissivity (0.92) and thermally resistant up to 800 °C in order to get reliable temperature measurements with the pyrometer. The critical temperature of steel is defined as the temperature at which only 60% of the original strength remains, point at which failure is imminent under full design loads. The temperature of 500 °C has been officially adopted as a standard for normally loaded structural components whereas 400 °C is often used for heavily loaded structure [15]. In this study, the time to reach the two temperatures is taken into account to evaluate the heat barrier properties of the intumescent coatings.

2.3. Air jet test

To evaluate the mechanical properties of an intumescent material few experimental setup are reported in the open literature [16,17]. For the example, the intumescent structure could be developed at 500 °C in a rheometer device without any constrain. At 500 °C, the upper plate of the rheometer is brought into contact with the intumesced material and the gap between the plates is reduced linearly (0.02 mm/s). The compression force is thus followed as a function of the gap [16]. However, at 500 °C, silicone based formulation are not degraded and so the expansion is not maximum, so this technic cannot be used. In another method, Reshetnikov et al. [17] used a “Structurometer ST-1”, developed at the Moscow State Food Academy, to measure the force required to destroy a char. The samples were first pyrolyzed and then a destructive force was applied to the sample. Mechanical properties of the char are investigated at ambient temperature which may not be representative of its behavior at high temperature.

That is why, to evaluate the mechanical properties and the cohesion of the char from intumescent silicone based coating, a lab scale test was developed in the laboratory. Its set up is illustrated in Fig. 2.

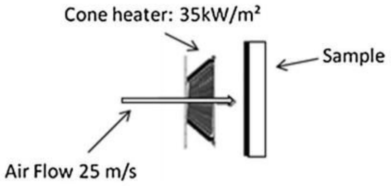

Fig. 2. Schematic experimental set up to determinate cohesion properties of the char.

The coating is directly exposed to an electrical cone heater providing pure radiative heat (in this study, 35 kW/m^2). When the expansion of the coating is maximal (after 5 min testing), air flow (25 m/s) impacts the char. By visual observation, it is possible to have an idea of the mechanical properties of the char. Indeed, if the char is fragile, it will be destroyed by the air impact whereas a strong char will not or only slightly be affected by the air jet. The advantage of this test is to evaluate the mechanical properties during a fire test.

2.4. X-ray photoelectron spectroscopy (XPS)

XPS experiments were carried out on an ultra-high vacuum KRATOS Axis Ultra spectrometer using the monochromatized Al Kα (1486.6 eV) source. Constant analyzer pass energy of 40 eV was used. The full width at half maximum (FWHM) was restrained to be equal for both Si2p$_{1/2}$ and Si2p$_{3/2}$, and the area of the peak assigned to Si2p$_{1/2}$ was restrained to be half the area of the Si2p$_{3/2}$. The energy separation between the Si2p$_{3/2}$ and Si2p$_{1/2}$ doublet was considered constant and equal to 0.6 eV. Simulation of the experimental peaks was carried out using the Gaussian–Lorentzian mixture from CasaXPS software.

2.5. Thermal properties

Thermogravimetric analyses (TGA) were carried out using a TGA Q5000 from TA Instruments at 10 °C/min in

Please cite this article in press as: Gardelle B et al. Resistance to fire of curable silicone/expandable graphite based coating: Effect of the catalyst. Eur Polym J (2013), http://dx.doi.org/10.1016/j.eurpolymj.2013.04.021

a nitrogen flow (25 mL/min). For each sample, 15 mg of sample were positioned in alumina pans.

2.6. Electron probe microanalysis (EPMA)

The samples were embedded into an epoxy resin, polished and carbon coated with a Bal-Tec SCD005 sputter coater. A Cameca SX100 electron probe microanalyser (EPMA) was used to perform elemental analysis. X-ray mappings and profiles were carried out at 15 kV, 40 μA. The crystals used to detect the K_a of Ti, Si and Sn were PET, TAP and PET respectively.

2.7. Fourier Transform Infrared spectroscopy

The infrared (IR) spectra were recorded between 400 cm^{-1} and 4000 cm^{-1} using a Fourier transformed infrared (FTIR) spectrometer (ThermoScientific) Nicolet 400D using ATR module (Dura SampIIR II).

2.8. ^{29}Si solid state NMR

^{29}Si nuclear magnetic resonance (NMR) spectroscopy is a powerful tool for examining silicon surrounding. This technique can distinguish several kinds of structures including D, T and Q structures which characterize silicone network (Fig. 3).

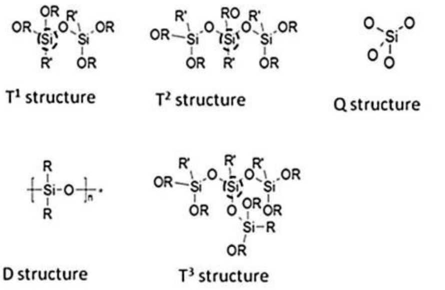

Fig. 3. Schematics presentation of D, T^i and Q silicone structures.

^{29}Si NMR spectra were recorded on a Bruker Advance II 400 operating at 9.4 T and using a 7 mm probe. NMR spectra were acquired with MAS (magic angle spinning) of 5 kHz. The reference used for ^{29}Si NMR was tetramethylsilane (TMS). A delay of 180 s between the pulses and a $\pi/2$ pulse length were used. 128 scans and 64 scans were accumulated for respectively S1–Sn and S1–Ti materials to get an acceptable signal to noise ratio.

3. Results

3.1. Fire protection

Fig. 4 shows temperature changes as a function of time on the backside of the steel plates coated with the different formulations during hydrocarbon fire scenario. The influence of the catalyst on the heat barrier properties of silicone based coating is clearly shown: the paint prepared with Ti based catalyst exhibits a better behavior than that prepared with Sn based catalyst.

For virgin steel, critical temperature is reached in only 150 s. The time to reach 500 °C for S1–Sn/EG and S1–Ti/EG are respectively 860 s and 1500 s demonstrating the better fire performance of S1–Ti/EG based coating (Table 1). After 200 s, a knee point is visible for S1–Sn/EG based coating assigned to the low cohesion of the char during the fire experiment leading to decreasing insulative properties.

Fig. 5 shows the fire behavior of the two formulations during the hydrocarbon fire test. As we reported in our previous work [7], both chars are composed of two main parts.

Table 1
Time to reach failure temperature of each formulation.

	Virgin steel	S1–Sn/25% EG	S1–Ti/25% EG
Time to reach 400 °C	100 s	524 s	685 s
Time to reach 500 °C	150 s	850 s	1460 s

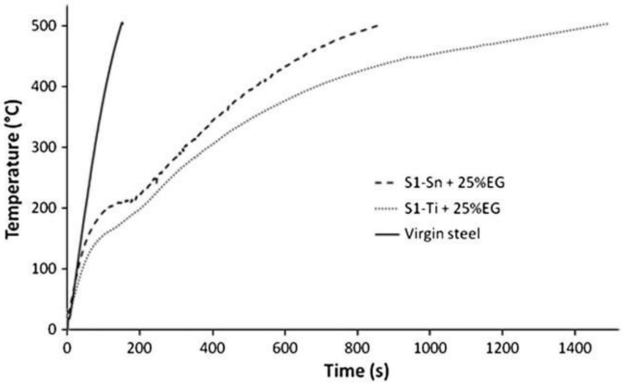

Fig. 4. Temperature versus time curves in hydrocarbon fire scenario.

Please cite this article in press as: Gardelle B et al. Resistance to fire of curable silicone/expandable graphite based coating: Effect of the catalyst. Eur Polym J (2013), http://dx.doi.org/10.1016/j.eurpolymj.2013.04.021

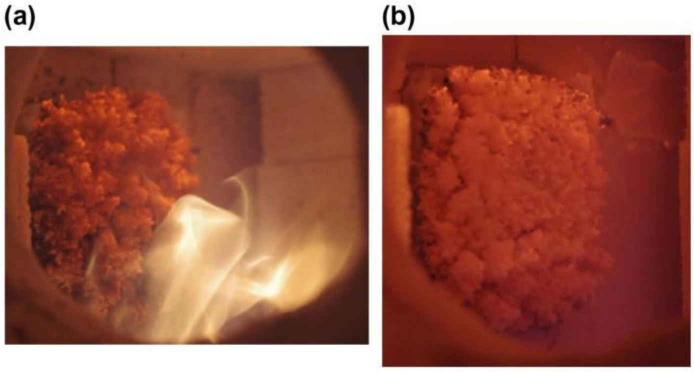

Fig. 5. Fire behavior of (a) S1–Sn/EG and (b) S1–Ti/EG based coating in hydrocarbon fire scenario.

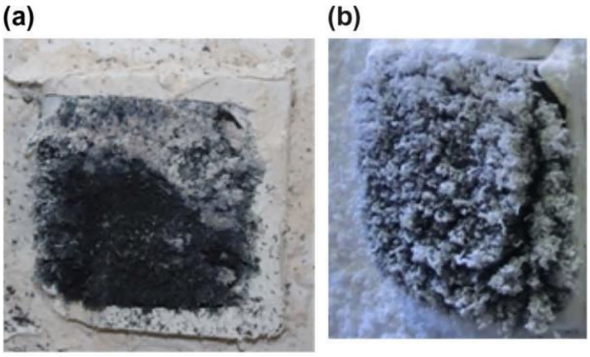

Fig. 6. Residue of S1–Sn/EG (a) and (b) of S1–Ti/EG based coating after fire testing.

Fig. 7. Fire behavior of (a)S1–Sn/EG and (b)S1–Ti/EG based coating in air jet.

Please cite this article in press as: Gardelle B et al. Resistance to fire of curable silicone/expandable graphite based coating: Effect of the catalyst. Eur Polym J (2013), http://dx.doi.org/10.1016/j.eurpolymj.2013.04.021

The top is composed of white powder which is mainly silica and the bulk of the char is composed of graphite embedded in complex silicone structures.

Fig. 6 shows the two residues obtained at the end of the test. A partial decohesion of the char formulation with the tin-based catalyst is observed while that prepared with the titanium based catalyst still 'sticks' well on the plate. When titanium based catalyst is used (Fig. 6b), a high expansion (2100%) and a good cohesion of the char are observed. It can explain why this formulation exhibits high fire performance.

In order to highlight the better mechanical properties when titanium is used as catalyst, the two formulations were tested using the air jet test. The behavior of the two formulations is shown in Fig. 7. The formulations exhibit similar behavior during the first step of the test (when the air does not impact the coating): during the first minute, the coatings begin to swell; after 2 min, the coatings ignite and a white powder covers the expanded graphite. However, when the air flow is switch on, a complete destruction of the char is observed for S1–Sn/EG based coating whereas when titanium based catalyst is used, there is no char destruction. This evidences the superior mechanical properties and the extremely good cohesion of the Ti-based formulation.

We have thus demonstrated that the catalyst has a very significant influence on the cohesion and the mechanical properties of the intumescent char and, therefore, on the fire performance of silicone based coating. The composition of the intumescent char should at least partially be responsible of this good cohesion and so, of the good fire performance of the coating. Consequently, the chemical composition of both chars after fire test is investigated in the following part.

3.2. XPS analysis

Because of high paramagnetism of expandable graphite, it was not possible to perform solid state NMR experiment (high broadening of the NMR signal) on our materials. X-ray photoelectron spectroscopy (XPS) was thus carried out as an alternative technique to characterize the charred

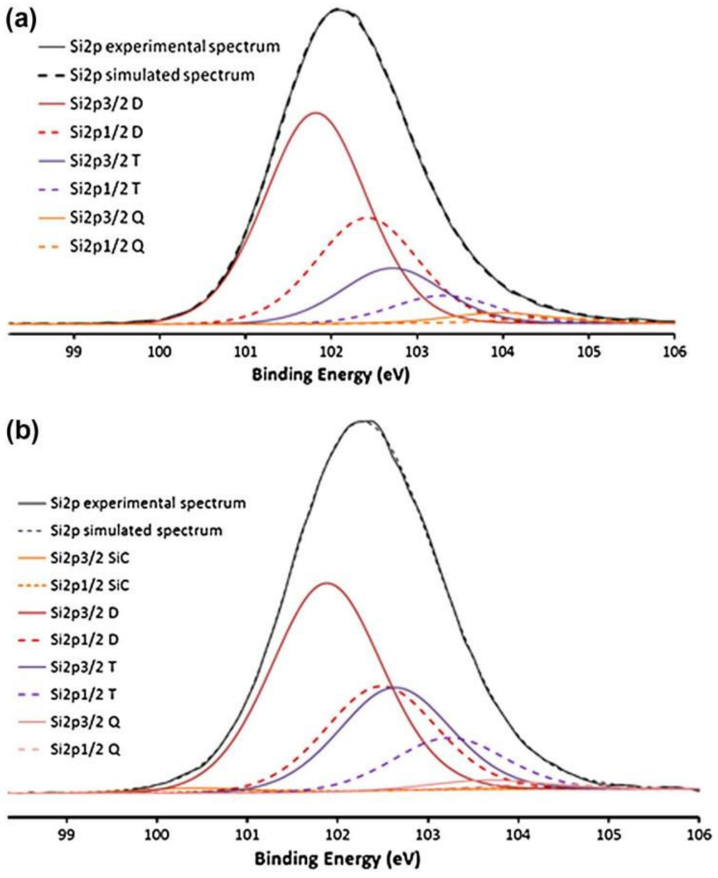

Fig. 8. Si2p spectra of (a) S1–Sn/EG and (b) S1–Ti/EG after fire test in hydrocarbon fire scenario.

Please cite this article in press as: Gardelle B et al. Resistance to fire of curable silicone/expandable graphite based coating: Effect of the catalyst. Eur Polym J (2013), http://dx.doi.org/10.1016/j.eurpolymj.2013.04.021

silicone structures. Indeed, O'Hare et al. studied the D, T and Q structures in pure silicone using XPS experiment and obtained good correlation with ^{29}Si NMR experiment [18]. Based on their work, a similar approach has been followed. XPS spectra of S1–Sn/EG and S1–Ti/EG residue are shown in Fig. 8.

The Si_{2p} XPS of S1–Ti/EG residue exhibits a broad peak revealing the contribution of several silicone structures. The decomposition of this band gives peaks at 100.4 ± 0.2 eV, 101.8 ± 0.2 eV, 102.6 ± 0.2 eV and 103.6 ± 0.2 eV corresponding respectively to SiC, D, T and Q silicone structure. The Si2p XPS band of S1–Sn/EG can be decomposed into three peaks at 101.8 ± 0.2 eV, 102.6 ± 0.2 eV and 103.6 ± 0.2 eV corresponding to respectively D, T and Q silicon structures. It demonstrates that the bulk part of the chars is composed of graphite platelets embedded in complex silicone structure. Even if the silicone structures are mainly composed of D, T and Q (few SiC are formed when titanium based catalyst is used) the amounts of each structures are different (Table 2) and it highlights that the char of S1–Ti/EG contains more T structure and less D structures than that of S1–Sn/EG.

When titanium based catalyst is used, the graphite is thus embedded in a more cross linked silicon structure whereas when tin-based catalyst is used, expanded graphite worms are embedded in a linear silicon structure and so exhibits low cohesion and low mechanical properties. This could, at least partially, explain the better cohesion of the char at high temperature and, therefore the better fire performance of S1–Ti/EG based coating when titanium based catalyst is used.

Table 2
Quantity of each silicone structure in the two residues.

	SiC (%)	D structure (%)	T structure (%)	Q structure (%)
S1–Sn/EG residue	–	78	19	3
S1–sTi/EG residue	2	64	32	2

This difference in the amount of silicone structure formed at high temperature suggests different thermal degradation pathways of the two silicone matrices. Thus, the degradation mechanism of both matrices is further investigated in the following part of this paper.

3.3. Thermal analysis of the two silicone matrices

TG curves of the two materials are presented in Fig. 9.

It is observed that the two materials exhibit different thermal stability. When tin-based catalyst is used, the degradation occurs in one main step with no residue at 800 °C. The temperature where the degradation rate is maximum is 380 °C. When titanium based catalyst is used, the degradation occurs in two main steps. The first occurs between 375 °C and 600 °C and the second between 600 °C and 700 °C. This material exhibits 5% residue at 800 °C. Moreover, DTG curves of the two materials evidence that S1–Sn degrades twice faster (1.2%/°C) than S1–Ti (0.6%/°C). Thus, we demonstrated that titanium based catalyst increases significantly the thermal stability of the matrix whereas tin based catalyst catalyzes the depolymerization of the resin. Indeed, silicones can be degraded, by substances capable of acting as depolymerisation catalysts, such as metals salts [10].

To explain this thermal stabilization, chemical analysis of the two silicone matrices are carried out, using EPMA and ^{29}Si solid state NMR.

3.4. EPMA analysis of S1–Ti and S1–Sn based materials

Chemical mapping and profiles of S1–Sn obtained by EPMA is presented in Fig. 10.

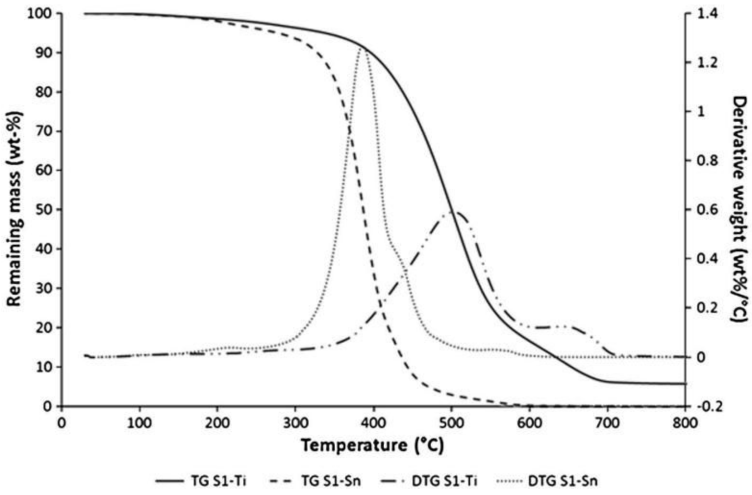

Fig. 9. TG and DTG curve of S1–Ti and S1–Sn in nitrogen flow at 10 °C/min.

Please cite this article in press as: Gardelle B et al. Resistance to fire of curable silicone/expandable graphite based coating: Effect of the catalyst. Eur Polym J (2013), http://dx.doi.org/10.1016/j.eurpolymj.2013.04.021

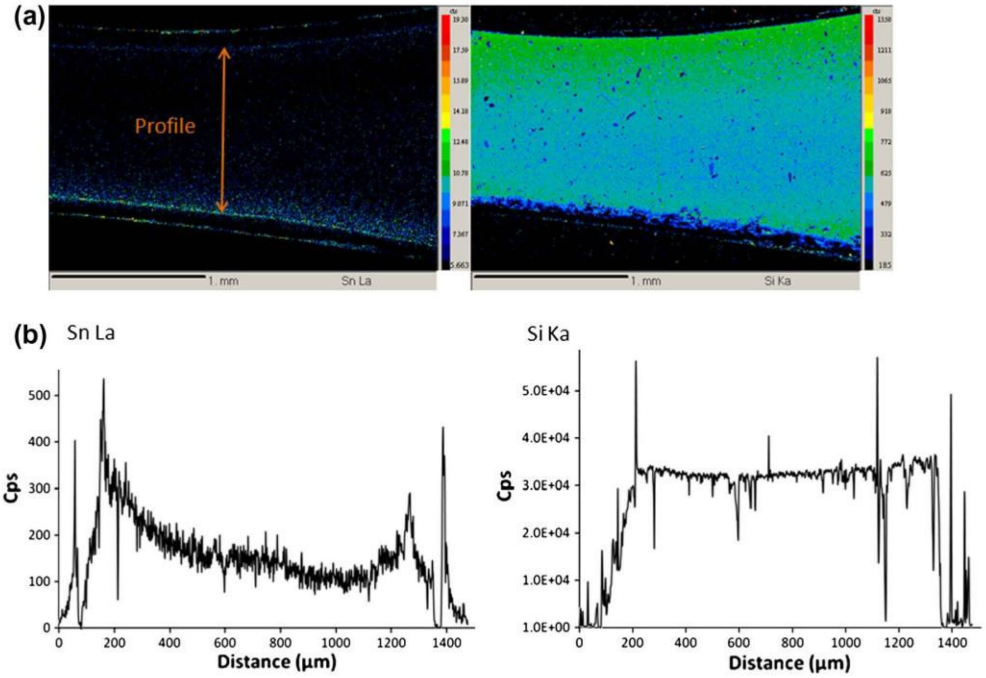

Fig. 10. Chemical mapping (a) and chemical profile (b) across S1–Sn materials.

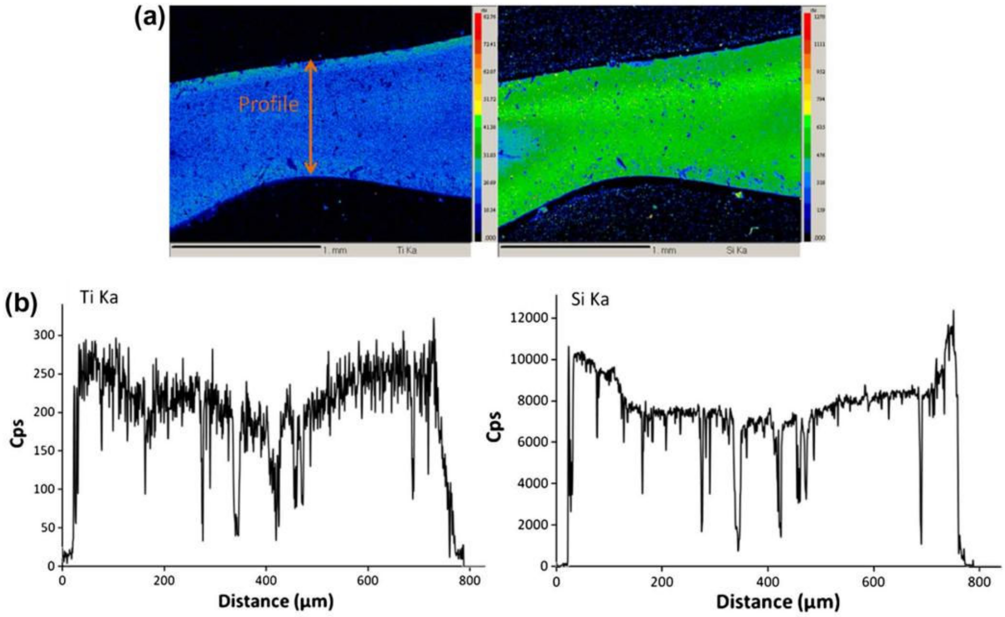

Fig. 11. Chemical mapping (a) and chemical profile (b) across S1–Ti materials.

Please cite this article in press as: Gardelle B et al. Resistance to fire of curable silicone/expandable graphite based coating: Effect of the catalyst. Eur Polym J (2013), http://dx.doi.org/10.1016/j.eurpolymj.2013.04.021

Fig. 10a) evidences that silicon is homogeneously distributed in the material whereas tin based catalyst migrates to the surface of the sample since higher intensity are observed on the top and on the bottom of the sample. Fig. 10b) shows the tin amount profile across the sample. This highlights that the maximum intensity is at the surface of the sample demonstrating the migration of the tin during the matrix crosslinking.

Concerning S1–Ti material, chemical mapping is presented in Fig. 11a) for titanium and silicone. It shows that both are homogeneously distributed in the whole material. Fig. 11b) shows that titanium and silicone exhibit exactly the same profile and, therefore, it suggests that titanium participates to the silicone network.

In order to confirm this hypothesis, ^{29}Si solid state NMR and FTIR/ATR experiments were carried out.

3.5. FTIR and ^{29}Si solid state NMR

Fig. 12 shows the infrared spectra of S1–Sn and S1–Ti silicone matrices. For the two resins, the same peaks are observed: peak at 2950 cm^{-1} corresponding to the bending vibration of CH$_3$ bond; peaks between 1000 and 1100 cm^{-1} corresponding to the bending vibrations of Si–O–Si bond and peak at 1260 cm^{-1} assigning to the bending vibration of Si–CH$_3$ bond.

When titanium is used as catalyst, an additional peak appears at 960 cm^{-1} corresponding to Si–O–Ti bond [19]. In order to confirm the presence of Si–O–Ti, the two resins were analyzed by solid state NMR. Fig. 13 shows ^{29}Si NMR spectrum of resins S1–Ti and S1–Sn. On the S1–Sn spectrum, three peaks can be distinguished at −22 ppm, −58 ppm and −67 ppm assigned to D, T^2 and T^3 structures respectively [20].

On the S1–Ti spectrum, D and T^3 structures are observed (peaks at −22 and −67 ppm). An additional peak at −19 ppm is observed. This additional peak at −19 ppm should thus correspond to Si–O–Ti bond in D structure. However, according to our knowledge, there is no reference for ^{29}Si NMR of Si–O–Ti structure reported in the open literature. Since, FTIR/ATR experiments highlighted the presence of Si–O–Ti bound, the attribution of the peak at −19 ppm to Si–O–Ti is reasonable. On the other hand, the peak related to T^3 structure is broader for S1–Ti matrix than that of S1–Sn. This is explained by the presence of an-

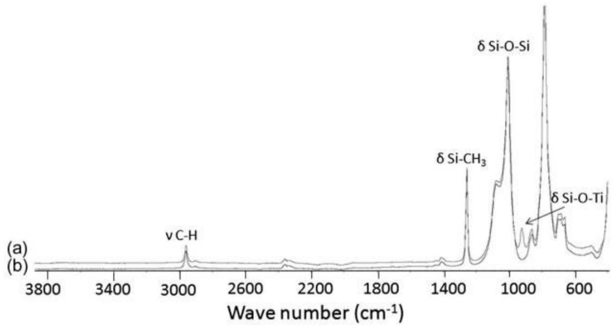

Fig. 12. FTIR spectra of (a) S1–Ti and (b) S1–Sn silicone matrix.

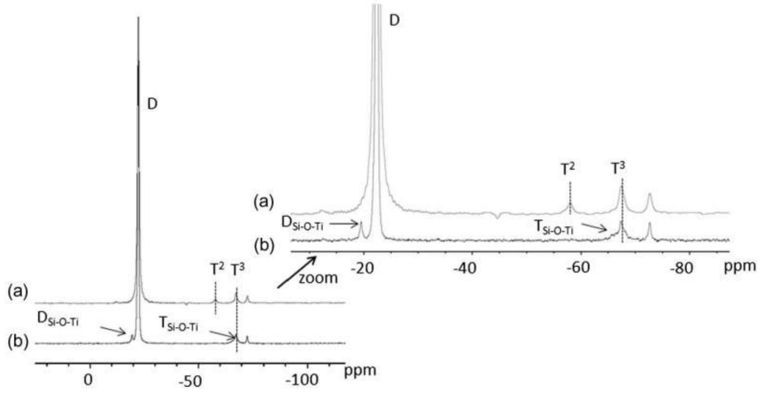

Fig. 13. 29Si NMR spectra of (a) S1–Sn and (b) S1–Ti silicone matrix.

Please cite this article in press as: Gardelle B et al. Resistance to fire of curable silicone/expandable graphite based coating: Effect of the catalyst. Eur Polym J (2013), http://dx.doi.org/10.1016/j.eurpolymj.2013.04.021

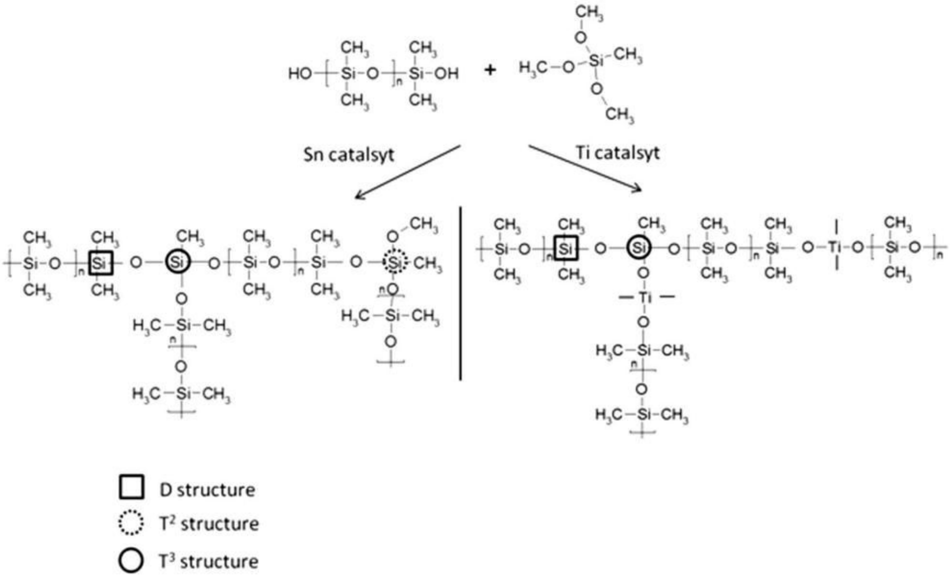

Fig. 14. Chemical pathway of resin cross-linking.

other peak at -66 ppm (the two peaks overlap) which should be assigned to Si–O–Ti bond in T^3 structure.

For each organometallic catalyst, there is the formation of T structure during the crosslinking of the silicone matrix due to the chemical reaction between the hydroxyl function from the PDMS and the methoxy groupment of MTM. However, when titanium based catalyst is used, it participates to the silicone network. The proposed crosslink mechanism of both resins is thus illustrated in Fig. 14.

4. Discussion

In this work, the fire performance of curable silicone added with expandable graphite are investigated. The chemical composition of both resin are very cloth and just the organometallic catalyst used (tin based and titanium based) differs. NMR study for the resin demonstrated that they are composed of D and T structures. However, when titanium based catalyst is used, it participates in the silicone network of the matrix via the formation of Si–O–Ti whereas tin migrates to the surface of the matrix during the crosslinking. The formation of Si–O–Ti bound leads to increase significantly the thermal stability of the resin whereas tin catalyzes the depolymerisation of the matrix and so exhibits low thermal stability. Consequently, when 25% of expandable graphite is added in the two resins, they exhibit different heat barrier properties. S1–Ti/EG based coating has better fire performance and the char has better mechanical properties than S1–Sn/EG based coating. XPS analysis on the S1–Ti/EG based residue highlights the formation of a high cross-linked silicone network (T structure) which coats the graphite platelets present in the bulk part of the char. It evidences the presence of a large amount of T structures compared with those when tin based catalyst is used. Indeed, when tin based catalyst is used the char is mainly composed of linear silicone structure and so the resulting char has low mechanical properties.

It is recognized that the main governing parameters for intumescent coating to get efficient heat barrier performance are low thermal conductivity (formation of a porous char) and high mechanical properties of the char [21]. In our last study, we highlighted the low thermal conductivity at high temperature of silicone/EG based coating [7]. We assume that the organometallic catalyst used should not play an active role on the thermal conductivity of the silicone/EG intumescent based coating since, in both cases, there is formation of an expanded structure based on graphite embedded in complex silicone structures. However, the catalyst modifies significantly the cohesion and the mechanical properties of the char.

As a consequence, the catalyst has a real influence on the silicone structure embedding the graphite platelets, so on the mechanical properties of the char and therefore on the fire performance of the silicone based coating.

5. Conclusion

In this paper, the effect of catalysts – tin and titanium based catalysts – on the fire performance of silicone/expandable graphite based coating has been investigated. It was shown that fire performance of S1–Ti/EG based coating was better than that of S1–Sn/EG based coating in hydrocarbon fire scenario. For the two materials, XPS anal-

Please cite this article in press as: Gardelle B et al. Resistance to fire of curable silicone/expandable graphite based coating: Effect of the catalyst. Eur Polym J (2013), http://dx.doi.org/10.1016/j.eurpolymj.2013.04.021

ysis on the char have demonstrated the presence of complex silicone structure embedding the expanded graphite platelets. When titanium is used as catalyst, there is a larger amount of T structures than for tin based catalyst. The char is, thus, composed of graphite embedded in high cross-linked silicone structures which should be responsible for the good cohesion and high mechanical properties of the char. This difference was attributed to the better thermal stability of S1–Ti resin than that of S1–Sn resin because titanium participates to the silicone network.

References

[1] Gardner L, Baddoo NR. Fire testing and design of stainless steel structures. J Constr Steel Res 2006;62(6):532–43.

[2] Weil ED. Fire-protective and flame-retardant coatings – a state-of-the-art review. J Fire Sci 2011.

[3] Duquesne S, Magnet S, Jama C, Delobel R. Intumescent paints: fire protective coatings for metallic substrates. Surf Coat Technol 2004;180–181:302–7.

[4] Nguyen DT, Veinot DE, Foster J. Inorganic intumescent fire protective coatings. In: Patent US, editor. Canada 1989.

[5] Gardelle B, Duquesne S, Vu C, Bourbigot S. Thermal degradation and fire performance of polysilazane-based coatings. Thermochim Acta 2011;519(1–2):28–37.

[6] Gardelle B, Duquesne S, Rerat V, Bourbigot S. Thermal degradation and fire performance of intumescent silicone-based coatings. Polym Adv Technol 2012.

[7] Gardelle B, Duquesne S, Vandereecken P, Bourbigot S. Characterization of the carbonization process of expandable graphite/silicone formulations in a simulated fire. Polym Degrad Stab 2013.

[8] Genovese A, Shanks RA. Fire performance of poly(dimethyl siloxane) composites evaluated by cone calorimetry. Compos Part A: Appl Sci Manuf 2008;39(2):398–405.

[9] Buch RR. Rates of heat release and related fire parameters for silicones. Fire Safety J 1991;17(1):1–12.

[10] de Buyl F. Silicone sealants and structural adhesives. Int J Adhes Adhes 2001;21(5):411–22.

[11] Wolf A. Material properties of construction sealants. Kaut Gummi Kunstst 1988;41(2):173–8.

[12] Duquesne S, Le Bras M, Bourbigot S, Delobel R, Camino G, Eling B, et al. Thermal degradation of polyurethane and polyurethane/expandable graphite coatings. Polym Degrad Stab 2001;74(3):493–9.

[13] Li G, Liang G, He T, Yang Q, Song X. Effects of EG and $MoSi_2$ on thermal degradation of intumescent coating. Polym Degrad Stab 2007;92(4):569–79.

[14] Wang Z, Han E, Ke W. Influence of expandable graphite on fire resistance and water resistance of flame-retardant coatings. Corros Sci 2007;49(5):2237–53.

[15] Gosselin G. Stuctural fire protection, predictive methods. Proc Buil Sci, Insight 1987.

[16] Jimenez M, Duquesne S, Bourbigot S. Characterization of the performance of an intumescent fire protective coating. Surf Coat Technol 2006;201(3–4):979–87.

[17] Reshetnikov IS, Yablokova MY, Potapova EV, Khalturinskij NA, Chernyh VY, Mashlyakovskii LN. Mechanical stability of intumescent chars. J Appl Polym Sci 1998;67(10):1827–30.

[18] O'Hare LA, Parbhoo B, Leadley SR. Development of a methodology for XPS curve-fitting of the Si2p core level of siloxane materials. Surf Interface Anal 2004;36(10):1427–34.

[19] Yagi O, Iwamiya Y, Suzuki K, Funane R, Ohishi F. Improvement in tensile strength and water repellency of paper after treatment with methyltrimethoxysilane oligomer using titanium butoxide as a catalyst. J Sol–Gel Sci Technol 2005;36(1):69–75.

[20] Babonneau F, Baccile N, Laurent G, Maquet J, Azaïs T, Gervais C, et al. Solid-state nuclear magnetic resonance: a valuable tool to explore organic-inorganic interfaces in silica-based hybrid materials. Comptes Rendus Chimie 2010;13(1–2):58–68.

[21] Staggs JEJ. Numerical characterization of the thermal performance of static porous insulation layers on steel substrates in furnace tests. J Fire Sci 2011;29(2):177–92.

Please cite this article in press as: Gardelle B et al. Resistance to fire of curable silicone/expandable graphite based coating: Effect of the catalyst. Eur Polym J (2013), http://dx.doi.org/10.1016/j.eurpolymj.2013.04.021

Intumescent silicone-based coatings for the fire protection of carbon fiber reinforced composites

SERGE BOURBIGOT, BASTIEN GARDELLE AND SOPHIE DUQUESNE
ISP/UMET UMR 8207
Ecole Nationale Supérieure de Chimie de Lille, University of Lille
Av. Mendeleïev, CS 90108
59652 Villeneuve d'Ascq, France
serge.bourbigot@ensc-lille.fr

ABSTRACT

The application of carbon fiber reinforced polymer (CFRP) in aircraft structure has introduced potential fire threats and fire protection must be provided. In this paper, intumescent silicone based-coatings (low and high intumescing coatings) are evaluated on CFRP using a bench developed in the lab mimicking jet fuel fire occurring at high heat flux (200 kW/m²). It is shown the development of large intumescence (high intumescing coating) associated with appropriate thermal properties of the coating (heat conductivity measured as low as 0.3 W/m.K) provides efficient protection for the CFRP at the jet fire test. On the other hand, the formation of cohesive ceramic (low intumescing coating) with low heat conductivity (constant heat conductivity as a function of temperature of 0.35 W/m.K) also provides protection but its efficiency is lower than that of intumescent char. It is evidenced intumescent silicone-based coatings are materials of choice for protecting CFRP in the case of jet fuel fire.

KEYWORDS: intumescence, fire chemistry, protection of composite, silicone-based coating

INTRODUCTION

Energy efficient mobility is now conducting the use and consumption of fiber-reinforced structural polymeric materials to reduce weight in transportation (aircraft, train, truck and car). In particular, carbon fiber reinforced composites are becoming materials of choice because of their superior mechanical performance and fatigue resistance (Tavares, Camanho and De Castro, 2013). Composite materials are increasingly being used in the design of aircraft and they have attracted attention of researchers and industrial manufacturers to be used in primary structural components of aircrafts such as Boeing 787 or the coming Airbus A350. However, this recent application of carbon fiber reinforced polymer (CFRP) in aircraft structure has introduced potential fire threats and it raises concerns regarding fire safety in both the in-flight and post-crash environments (Sikoutris, Vlachos, Kostopoulos, Jagger and Ledin, 2012, La Delfa, Luinge and Gibson, 2009). The fire hazard has then led to the enforcement of stringent fire safety regulations by aviation authorities on the use of composites.

When CFRPs are exposed to a jet fuel fire, the composite materials degrade and quickly ignite, releasing volatile gases, and producing char resulting in a significant reduction in structural strength. It is common practice by fire scientists to quantify the intensity of a fire by the radiant heat flux rather than flame temperature (La Delfa, Luinge and Gibson, 2009). There is an approximate relationship between fire type and heat flux, and examples are: (i) small smoldering fire: 2-10 kW/m²; (ii) trash can fire: 10-50 kW/m²; (iii) cabin fire: 50-100 kW/m²; (iv) post-flashover cabin fire: >100 kW/m² and (v) jet fuel fire: 150-200 kW/m². In this research we are interested in the fire behavior of CRFP undergoing jet fuel fire and how to protect it.

The main issue with CFRP is its susceptibility to softening and failure in the event of fire. They decompose in high temperature environments such as those created by fire and so, it leads to distortion and weakening of the composite structure which can ultimately cause failure. For this reason, CFRP must be thermally insulated especially when engine compartments (where fuel leakage can occur) or the fuselage (in the case of post-crash fire) are concerned. The fire protection of CFRPs can be achieved with reactive insulation coatings which react when exposed to fire increasing their thermal insulation properties, thereby protecting the underlying substrate. It happens with intumescent coatings which expand and form an insulative layer at the surface of the substrate upon heating. The intumescence process results from a combination of charring and foaming at the surface of the substrate (Bourbigot, Le Bras, Duquesne and Rochery, 2004). The result of this process is the formation of a multicellular (alveolar) barrier, thick and non-flammable, which likely to protect the substrate or residual material from heat or flame action. The charred layer acts as a physical barrier which slows down heat and mass transfer between gas and condensed phase. The formation of an intumescent char is a complicated process involving several critical aspects: rheology (expansion phase, viscoelasticity of char), chemistry (charring) and thermophysics (limitation of heat and mass transfer) (Jimenez, Duquesne and Bourbigot, 2006). This approach will be considered in this paper.

Recently Mouritz et al (Kandare, Griffin, Feih, Gibson, Lattimer and Mouritz, 2012, Mouritz, Feih, Kandare and Gibson, 2013) reported the use of conventional organic intumescent paints to protect composite structures from fire and it appeared as successful. In previous work, we have shown that intumescent silicone based-coating is very efficient to protect steel in the case of hydrocarbon fire scenarios (Gardelle, Duquesne, Rerat and Bourbigot, 2013, Gardelle, Duquesne, Vandereecken and Bourbigot, 2013). As far as we know, this type of coating has never been evaluated for the fire protection of composites while exhibiting numerous advantages compared to the conventional organic intumescent paints. Silicones have the properties to exhibit low thermal conductivity, to be water and heat resistant, to evolve few toxic gases during their degradation and to have high durability: they are therefore materials of choice for aircraft applications. The main goal of this paper is to investigate the performance of intumescent silicone-based coatings for the fire protection of CFRP in the case of jet fuel fire. The first part of the paper will present the fire behavior of the materials using a bench developed in the lab mimicking jet fire occurring at high heat flux (200 kW/m²). The second part will evaluate physical parameters of the intumescent silicone-based coating including the heat conductivity as a function of temperature and the dynamic of expansion during the test. The third part will investigate the fire degradation of the intumescent coating protecting the composite from a chemical point of view and finally, a mechanism of protection will be discussed.

EXPERIMENTAL

Materials

The silicone resin was composed of a hydroxylated PDMS with a viscosity of 80 cS (viscosity was measured using cone/plate rheometer CP-52), methyltrimethoxysilane (MTM) as crosslinking agent and a titanium catalyst. All the materials were supplied by Dow Corning, Seneffe (Belgium). Several fillers were incorporated in the silicone resin: expandable graphite (ES350F5 from Graphitwerk Kropfmuehl (Germany)) with an average particle size of 300 µm; an organo-clay (Cloisite 30B; C30B) supplied by Southern Clay Products, San Antonio-TX (USA); a ground calcium carbonate (GCC) stearic acid coated with an average particle size of 4.5µm supplied by Dow Corning Seneffe (Belgium). The composition of the formulations is shown in Table 1.

Table 1. Composition of the intumescent silicone-based coatings

Silicone formulation	**F1 – High intumescing coating**	**F2- Low intumescing coating**
Silicone matrix	56%	56%
Expandable graphite	25%	-
Calcium carbonate	12%	37%
Clay	7%	7%

Formulations were coated onto CFRP (carbon fiber reinforced epoxy resin supplied by Goodfellow) having the dimensions of 150 x 150 x 35 mm^3. Two thicknesses of silicone-based coating were tested: 500 ± 100 µm and 1000 ± 100 µm.

Jet fire bench

The jet fire bench intends to mimic at the small-scale jet fuel fire which can be caused by burning jet fuel external to the aircraft as a result of fuel tank damage during the impact of an aircraft or by jet fuel fire occurring in the engine nacelle. The measurements were carried out using a constant heat flux test provided by a propane burner (10kW propane burner) delivering a heat flux of 200 kW/m² on CFRP. The heat flux was calibrated with a water cooled calorimeter TG 1000-1A from Vatell Corporation. 150 mm square CFRP were placed in a vermiculite ‘picture frame’ that enabled a 100 mm square central region to be exposed to the heat flux. The purpose of the frame was to minimize effects due to the burning of volatiles around the edge of the sample. CFRP was lightly clamped on vermiculite frame with screws on the edges insulated with silica wool. Thermocouples (4 K-type thermocouples) were placed on the back side of CFRP to measure the temperature as a function temperature during the test. The set-up is shown Fig. 1.

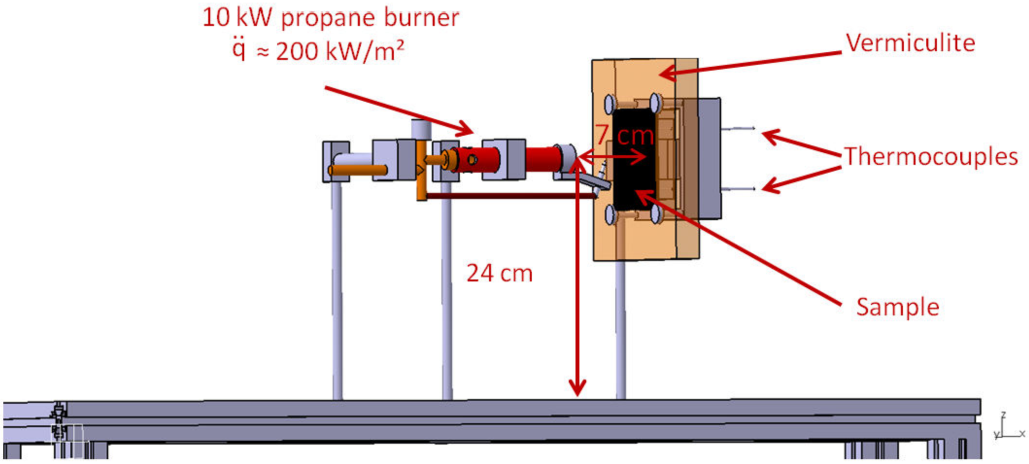

Fig. 1. Schematic view of the jet fire bench

Expansion measurement

In order to determine the expansion rate of the intumescent coating, the development of the char was monitored by an infrared camera (FLIR System A40) during the fire test. The advantage of infrared camera is to give high contrast to make image analysis. Using image analysis in dynamic conditions (from the movie), expansion of the intumescent coating can be measured and quantified. The pictures captured from the movie were analyzed by Image J software (NIH, Bethesda, MD) and the expansion of the coating was measured. In this approach, it is assumed for the calculation on images that the expansion is homogeneous and occurs in one dimension (which is reasonable, see Fig. 2).

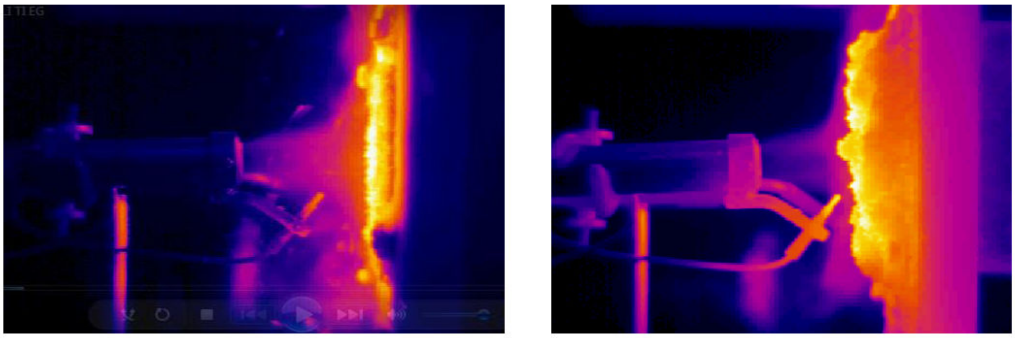

(a) (b)

Fig. 2. Infrared images of CFRP protected by the intumescent silicone-based coating during the jet fire test at (a) 40s and at (b) 900s

Thermal conductivity

Thermal conductivity material was measured from 25°C to 700°C using a hot disk thermal constant analyzer (Hot Disk TPS 2500 S) from Thermoconcept (Bordeaux, France), which is a transient plane source technique (Gustavsson and Gustafsson, 2008). The sensor which is warmth emitter and thermocouple is directly molded in the coating disk to ensure a good contact between the sample and the sensor during the experiment. The temperature is stabilized each 100.0°C with less than 0.1°C deviation. The conductivity measurements were made by applying a power of 0.03–0.15 W for between 5 and 60 s, depending on the thermal conductivity of the sample. The experimental set up is illustrated in Fig. 3. All experiments were carried out in inert atmosphere to prevent the oxidation of the sensor.

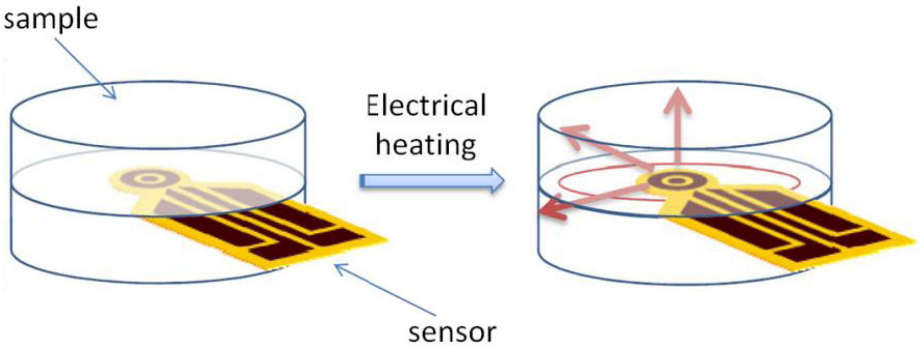

Fig. 3. Hot disk technology set up

Spectroscopic analyses

X-ray photoelectron spectroscopy (XPS) experiments were carried out on an ultra-high vacuum KRATOS Axis Ultra spectrometer using the mono-chromatized Al Kα (1486.6 eV) source. Constant analyzer pass energy of 40 eV was used. The full width at half maximum (FWHM) was restrained to be equal in both $Si_{2p3/2}$ and $Si_{2p1/2}$ peaks, and the area of the peak assigned to $Si_{2p1/2}$ was restrained to be half the area of the $Si_{2p3/2}$. The energy separation between the $Si_{2p3/2}$ and $Si_{2p1/2}$ doublet is constant and is 0.6 eV. Simulation of the experimental peaks was carried out using the Gaussian-Lorentzian mixture from CasaXPS software.

X-ray diffraction (XRD) patterns were recorded in the 10° - 80° 2θ range using a Bruker Advanced D8 diffractometer ($\lambda_{Cu\text{-}K\alpha}$ = 1.5418 Å) in configuration θ/2θ. The acquisition parameters were as follows: a step of 0.02°, a step time of 2 s. The data are analyzed using the diffraction, patterns of inorganic crystal structure database.

RESULTS AND DISCUSSION

Evaluation of the fire protection

Two types of fire protective coating (thickness = 500 µm) were applied on CFRP. The formulation F1 corresponds to formulation containing expandable graphite and so, it exhibits high expansion when undergoing high thermal constraint (Gardelle, Duquesne, Rerat and Bourbigot, 2013). On the contrary, the composition of the F2 formulation only contains GCC acting as intumescent ingredient releasing CO_2 at high temperature (T>600°C) and its expansion is quite low even if we have shown this formulation provides significant protection of steel in the case of cellulosic fire (Gardelle, Duquesne, Vandereecken and Bourbigot, 2012). The formulations were evaluated at the jet fuel fire test and the fire behavior of the two coatings at different times is shown in Table 2. The virgin CFRP burns with high flames when applying the burner and is completely pierced after 100s. CFRP-F1 exhibits an intumescent behavior which provides an efficient protection while CRFP-F2 wraps up and the coating does not expand.

Table 2. Fire behavior of virgin CFRP compared to fire protected CFRP as a function of time during the jet fuel fire test (thickness of the coating = 500 µm)

Material/Time	Starting	10 min	15 min
Virgin CFRP		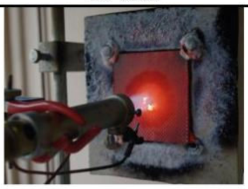	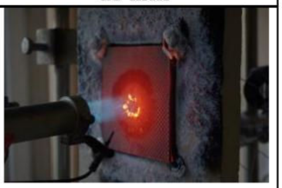
CFRP-F1			
CFRP-F2			

Fig. 4 shows the temperature on the backside of the samples as a function of time. When temperature raises up suddenly it indicates the ignition of the composite on the backside. For a thickness of 500 µm (Fig. 4-(a)), it is clearly shown that the F1 intumescent coating provides the most efficient protection since the ignition of the composite backside occurs at 460s while it is at 260s and 100s for CFRP-F2 and virgin CFRP respectively. If 1000 µm intumescent coating is applied on CFRP, the composite is well protected: its backside is not pierced and it does not ignite (Fig. 4-(b)). It is also noteworthy the F1 formulation provides higher protection compared to the F2 formulation since temperature on the backside of CFRP-F1 is always lower than that of CFRP-F2 with an average temperature difference of about 70°C (Fig. 4-(b)).

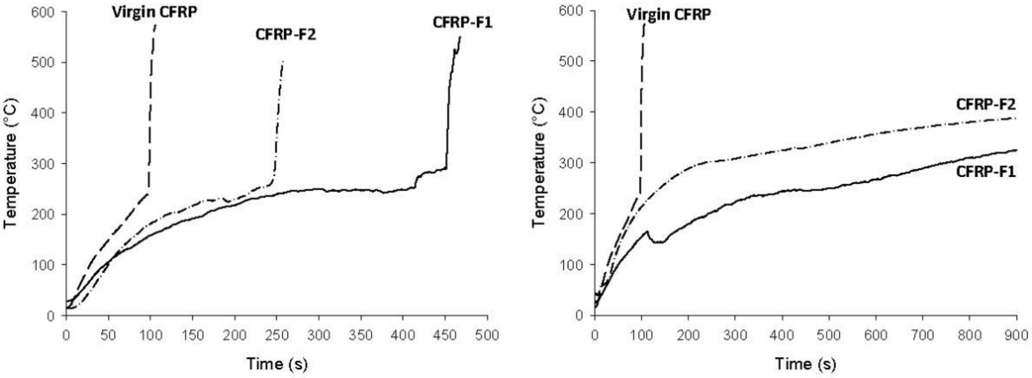

(a) (b)

Fig. 4. Temperature as a function of time of intumescent CFRPs compared to virgin CFRP (backside temperature) during the jet fire test at coating thickness of (a) 500 µm and of (b) 1000 µm

The observation of the residues after the jet fuel fire test gives information on the mode of protection of the intumescent coatings (Table 3). The virgin CFRP leaves the woven carbon fibers and epoxy resin is completely degraded. High expansion (about 2400%) of the intumescent coating is observed in the case of CFRP-F1. With 500µm of coating thickness, epoxy resin is almost completely degraded and the residue is constituted by carbon fiber plies and the expanded char. At higher coating thickness (1000µm), the intumescent char is cohesive (no destruction due to the impact of the flame) and the epoxy resin is only partially degraded evidencing the efficiency of the protection. For CFRP-F2, partial decohesion of the coating (not expanded) is observed with the complete degradation of the epoxy resin (500µm thick coating). With a 1000µm thick coating, the residue is a porous not expanded char which has partially protected the epoxy resin (not complete degradation of epoxy resin).

Table 3. Residues of the samples after 900s at the jet fire test

Material/Thickness	Coating of 500µm thick	Coating of 1000µm thick
Virgin CFRP	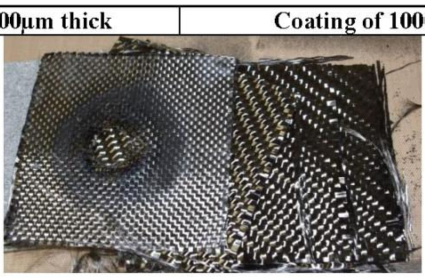	
CFRP-F1		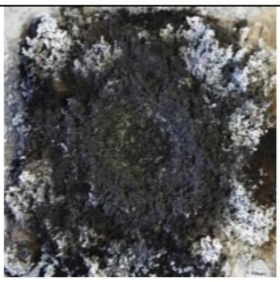
CFRP-F2	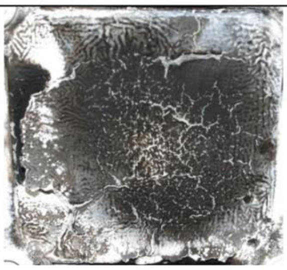	

Physical parameters of the intumescent coatings

An intumescent material reacts upon heating to produce gases that are partially trapped in a viscoelastic matrix. The matrix expands as gases are produced (the blowing agent and/or the degradation products of the polymeric matrix) and at the same time, cross-linking reactions and charring cause the matrix to harden thereby producing a coherent highly porous char. The porosity of the char is generally extremely high that the resulting structure has extremely low thermal conductivity. The most important parameters of the expanded char affecting its thermal insulation performance are its heat conductivity and its ability to swell rapidly (Bourbigot, Turf, Bellayer and Duquesne, 2009). Those two parameters are then measured in the following.

No significant expansion is observed in the case of CFRP-F2 and so, only the expansion of CFRP-F1 as a function of time was measured (Fig. 5). The intumescent coating expands rapidly up to 2400% at the beginning of the experiment and reaches a stationary state at 120s. Its expansion rate is measured at 23%/s (average value).

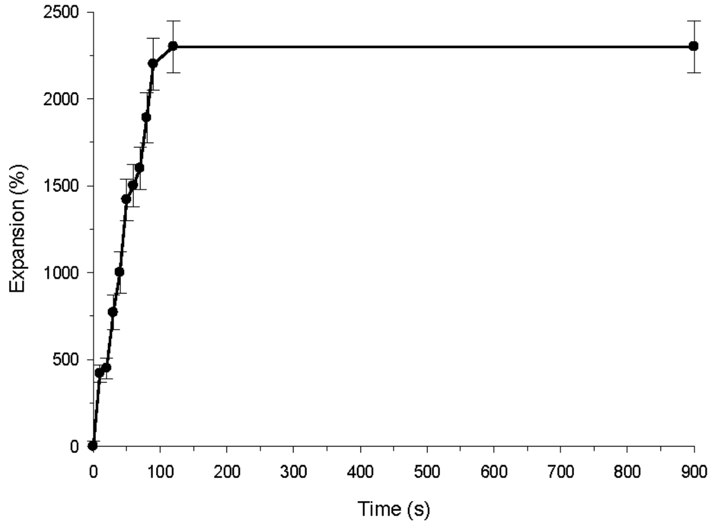

Fig. 5. Expansion as a function of time of CFRP-F1 measured during the jet fire test

Very few article in the literature deals with the measurement of thermal conductivity at high temperature of intumescent material. J.E.J Staggs determined thermal conductivities of intumescent char at high temperature by numerical simulation (Staggs, 2010). He reported that thermal conductivity of intumescent char material varies from 0.1W/m.K. to 0.4 W/m.K. from ambient temperature to 600°C. In previous work, we measured similar values on intumescent coatings (Gardelle, Duquesne, Rerat and Bourbigot, 2013, Gardelle, Duquesne, Vandereecken and Bourbigot, 2013). In the case of the intumescent formulations F1 and F2 (measurement done on the coatings without CFRP), heat conductivity is as low as 0.3 W/m.K (Fig. 6) and is in the range of values already reported for intumescent coatings. Nevertheless two distinct behaviors are observed. Heat conductivity of F2 is constant as a function of temperature (average value of 0.35 W/m.K) while that of F1 decreases when temperature increases (heat conductivity drops down from 1 W/m.K to 0.35 W/m.K between 20 to 300°C). This last behavior is characteristic of intumescent material: when temperature goes up the material expands and forms an alveolar structure of low heat conductivity. The low expansion of F2 does not permit to lower heat conductivity while the high expansion of F1 associated to the formation of multicellular reduces heat conductivity. It is also noteworthy that the heat conductivity of F1 is much higher than that of F2 (1 W/m.K vs. 0.3 W/m.K) probably because of the high loading of expandable graphite in the F1 formulation. The heat conductivity of bulk graphite is indeed as high as 1000 W/m.K (Nika and Balandin, 2012).

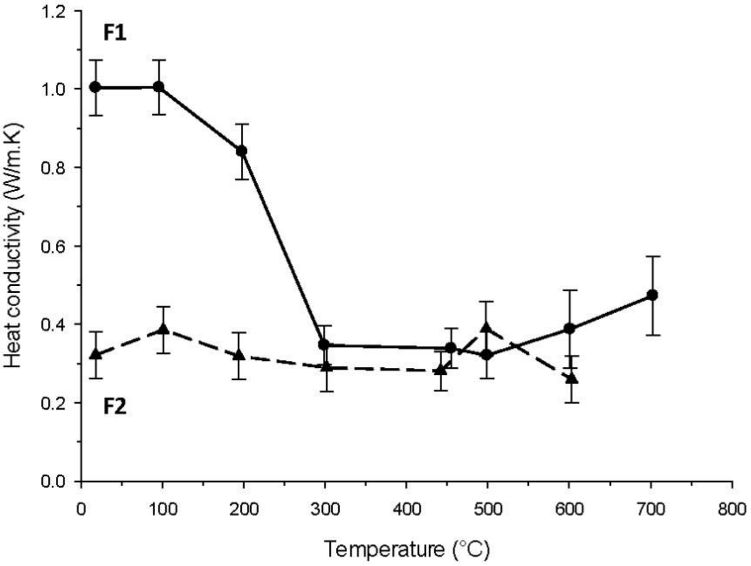

Fig. 6. Heat conductivity as a function of temperature of the formulations F1 and F2

Chemical characterization of the intumescent residues

The residues of the two formulations were analyzed in order to determine the mechanism of charring during the jet fire test. The two residues exhibit two different structures (Fig. 7). The residue of the F1 formulation is composed of worm-like pieces embedded in white coating. The worms come from expandable graphite. Expandable graphite is a graphite intercalation compound in which sulfuric acid and/or nitric acid is inserted between the carbon layers of graphite. Upon heating, exfoliation of the graphite occurs, i.e. expansion along c-axis of the crystal structure by about hundred times (Duquesne, Le Bras, Bourbigot, Delobel, Camino, Eling, Lindsay and Roels, 2001). The material generated in that way is a puffed-up material of low density with a ‘‘worm’’ like structure. According to previous work (Gardelle, Duquesne, Vandereecken and Bourbigot, 2013), the white part could be due to the adsorption of silica at the surface of the graphite worm. It will be discussed in the following. The F2 formulation does not contain expandable graphite and the residue exhibits a coral-like structure which is porous.

(a) (b)

Fig. 7. Numerical pictures (magnification x200) of the residues of (a) formulation F1 and of (b) formulation F2 after the jet fire test

The residues were further characterized by XPS. Fig. 8 shows Si_{2p} spectra of the residues of the F1 and F2 formulations after the jet fire test. They exhibit a broad band between 98 and 106 eV suggesting the presence of several components. After deconvoluting the two spectra, the resulting bands were assigned according to the literature (O'Hare, Parbhoo and Leadley, 2004, Contarini, Howlett, Rizzo and De Angelis, 1991) using the usual nomenclature of D, T and Q structures (Table 4). The two residues are composed of D and T structures (those structures are also detected in the samples before testing (Gardelle, Duquesne, Vandereecken and Bourbigot, 2013)) characterized by two $Si_{2p3/2}$ binding energies at 101.7 eV and 102.6 eV. The formation of silicon carbide (SiC) is also observed characterized by the band at a $Si_{2p3/2}$ binding energy of 100.6. Q structure is only detected in the case of F1 residue characterized by $Si_{2p3/2}$ binding energy at 103.7 eV. It is due to interactions between graphite and silicone during the fire degradation which leads to the formation of coated graphite flakes reinforcing the cohesion of the structure (see Fig. 7) (Gardelle, Duquesne, Vandereecken and Bourbigot, 2013). No Q structure is detected on XPS spectrum of F2 residue while clay contains SiO_4 in tetrahedral structure. As Al was not detected on the survey XPS spectrum, it is assumed the quantity of clay is too low to be detected.

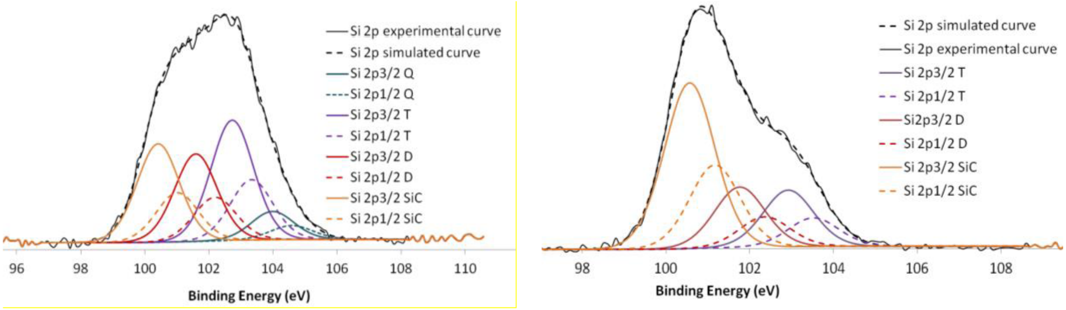

(a) (b)

Fig. 8. Si_{2p} XPS spectra of the residues of (a) formulation F1 and of (b) formulation F2 after the jet fire test

Table 4. Binding energy and assignment of the species characterized in the intumescent residues after the jet fire test

Silicone structure	SiC	D (SiO_2)	T (SiO_3)	Q (SiO_4)
F1 Residue	100.4 ± 0.2 eV	101.6 ± 0.2 eV	102.7± 0.2 eV	103.9 ± 0.2 eV
F2 Residue	100.5 ± 0.2 eV	101.7 ± 0.2 eV	102.9 ± 0.2 eV	-

Additional characterization by XRD was done on the residues to examine the changes of $CaCO_3$ in the formulations and the XRD patterns of the two residues are shown on Fig. 9. They evidence the partial decarbonation of calcium carbonate into calcium oxide and it suggests the formation of calcium silicate. Because of the high content and the high crystallinity of graphite, the intensities of the peaks related to Ca-based compounds are much lower than that of graphite (Fig. 9-(a)). Note the formation of calcium silicate was not detected by XPS (it should be characterized by Q structure on Fig. 8-(b) for the F2 residue and the Q structure of F1 residue (Fig. 8-(a)) results mainly from the formation of cross-linked silica network). The explanation is for silicates with SiO_4 tetrahedra of various polymerization types the resulting Si_{2p} XPS binding energies varied from 101.3 eV to 103.4 eV (Okada, Kameshima and Yasumori, 1998). In the particular case of calcium silicate (wollastonite-type), the binding energy is 102.2 eV and it is therefore impossible to distinguish on Fig. 8 between the T structure due to the degraded silicone (the main component of the formulation) and the Q structure of calcium silicate.

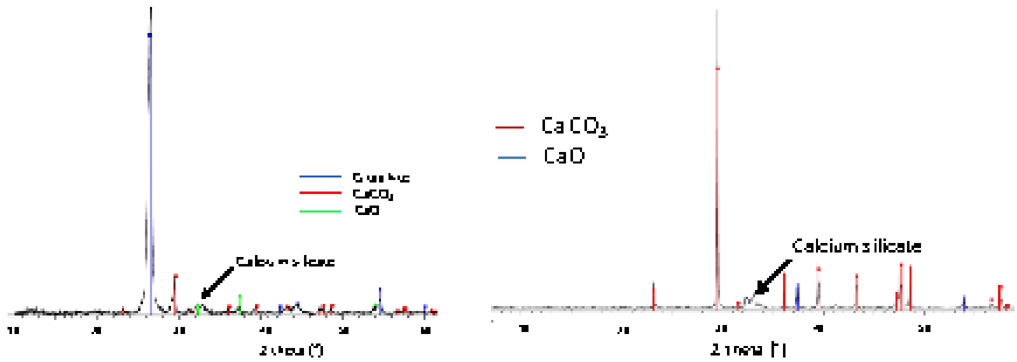

(a) (b)

Fig. 9 . XRD Characterization of the F1 (a) and F2 (b) residues

Mechanism of protection

F1 and F2 formulations applied on CFRP provide an efficient protection at the jet fire test when the coating is thick enough (1000 µm). Visual observation of the fire behavior at the jet fire reveals two modes of protection. F1 formulation produces a high expanded char while F2 formulation does not expand and forms a compact residue. The incorporation of expandable graphite in silicone permits the formation of an intumescent char upon heating. Its high expansion rate delivers rapidly the protection of interest. Associated to its low heat conductivity, the high expanded intumescent char (2400 %) limits heat transfer from the flame to CFRP. In terms of chemistry, the analyses have shown Q structures which indicate the formation of cross-linked silica network. This silica network coats the graphite worms and provides superior cohesion to the intumescent layer. Recent work done in our group has shown this cohesion was reinforced by the presence of clay in the formulation (Gardelle, Duquesne, Vandereecken, Bellayer and Bourbigot, 2013). This reinforcement takes place thanks to specific reactions between the hydroxyl groups of the clay and the silicone and also, with intercalation of the silicone chains into the galleries of the clay leading to the presence of the clay in the whole part of the char. The role of $CaCO_3$ is not completely elucidated but we may assume it permits the formation of an additional protective ceramic formed by calcium silicate, calcium oxide and non decarbonated calcium carbonate.

F2 formulation does not contain expandable graphite and its expansion upon heating is thus limited. The degradation of the silicone does not yield any cross-linked silica structure but to a ceramic constituted by calcium silicate, calcium oxide and non decarbonated calcium carbonate. The degraded silicone can act as a binder which can provide cohesion to the coating. This coating has good insulative properties exhibiting low heat conductivity even at high temperature (0.3 W/m.K at 600°C).

CONCLUSION

This paper has investigated the fire protection of CFRP using novel intumescent silicone-based coatings. A small scale test mimicking jet fuel fire was developed for examining the fire behavior of intumescent coated CFRPs. It is shown the development of large intumescence associated with appropriate thermal properties of the coating (low heat conductivity) provides efficient protection at the jet fire test. The formation of cohesive ceramic with low heat conductivity also provides protection but its efficiency is lower than that of intumescent char. It is therefore evidenced intumescent silicone-based coatings are materials of choice for protecting CFRP in the case of jet fuel fire.

REFERENCES

[1] Tavares, S. M. O., Camanho, P., and De Castro, P. M. S. T. (2013) Assessment of materials for fuselage panels considering fatigue behavior. 265-270

[2] Sikoutris, D. E., Vlachos, D. E., Kostopoulos, V., Jagger, S., and Ledin, S., (2012) Fire burnthrough response of CFRP aerostructures. Numerical investigation and experimental verification. Applied Composite Materials, 19(2):141-159, doi:10.1007/s10443-011-9187-x
[3] La Delfa, G., Luinge, J. W., and Gibson, A. G., (2009) Integrity of composite aircraft fuselage materials under crash fire conditions. Plastics, Rubber and Composites, 38(2-4):111-117, doi:10.1179/174328909X387900
[4] Bourbigot, S., Le Bras, M., Duquesne, S., and Rochery, M., (2004) Recent advances for intumescent polymers. Macromolecular Materials and Engineering, 289(6):499-511, doi:10.1002/mame.200400007
[5] Jimenez, M., Duquesne, S., and Bourbigot, S., (2006) Multiscale experimental approach for developing high-performance intumescent coatings. Industrial and Engineering Chemistry Research, 45(13):4500-4508, doi:10.1021/ie060040x
[6] Kandare, E., Griffin, G. J., Feih, S., Gibson, A. G., Lattimer, B. Y., and Mouritz, A. P., (2012) Fire structural modelling of fibre-polymer laminates protected with an intumescent coating. Composites Part A: Applied Science and Manufacturing, 43(5):793-802, doi:10.1016/j.compositesa.2011.05.012
[7] Mouritz, A. P., Feih, S., Kandare, E., and Gibson, A. G., (2013) Thermal-mechanical modelling of laminates with fire protection coating. Composites Part B: Engineering, 48:68-78, doi:10.1016/j.compositesb.2012.12.001
[8] Gardelle, B., Duquesne, S., Rerat, V., and Bourbigot, S., (2013) Thermal degradation and fire performance of intumescent silicone-based coatings. Polymers for Advanced Technologies, 24(1):62-69, doi:10.1002/pat.3050
[9] Gardelle, B., Duquesne, S., Vandereecken, P., and Bourbigot, S., (2013) Characterization of the carbonization process of expandable graphite/silicone formulations in a simulated fire. Polymer Degradation and Stability, 98(5):1052-1063, doi:10.1016/j.polymdegradstab.2013.02.001
[10] Gustavsson, M. K., and Gustafsson, S. E. (2008) Different ways of evaluating thermal transport properties from measurements with the transient plane source (hot disk) method. 397-402
[11] Gardelle, B., Duquesne, S., Vandereecken, P., and Bourbigot, S. (2012). "Fire performance of curable silicone-based coatings." *ACS Symposium Series: Fire and Polymer*, C. A. Wilkie, A. B. Morgan, and G. L. Nelson, eds., American Chemical Society, Washington, 205-221.
[12] Bourbigot, S., Turf, T., Bellayer, S., and Duquesne, S., (2009) Polyhedral oligomeric silsesquioxane as flame retardant for thermoplastic polyurethane. Polymer Degradation and Stability, 94(8):1230-1237, doi:10.1016/j.polymdegradstab.2009.04.016
[13] Staggs, J. E. J., (2010) Thermal conductivity estimates of intumescent chars by direct numerical simulation. Fire Safety Journal, 45(4):228-237, doi:10.1016/j.firesaf.2010.03.004
[14] Nika, D. L., and Balandin, A. A., (2012) Two-dimensional phonon transport in graphene. Journal of Physics Condensed Matter, 24(23), doi:10.1088/0953-8984/24/23/233203
[15] Duquesne, S., Le Bras, M., Bourbigot, S., Delobel, R., Camino, G., Eling, B., Lindsay, C., and Roels, T., (2001) Thermal degradation of polyurethane and polyurethane/expandable graphite coatings. Polymer Degradation and Stability, 74(3):493-499, doi:10.1016/S0141-3910(01)00177-X
[16] O'Hare, L. A., Parbhoo, B., and Leadley, S. R., (2004) Development of a methodology for XPS curve-fitting of the Si 2p core level of siloxane materials. Surface and Interface Analysis, 36(10):1427-1434, doi:10.1002/sia.1917
[17] Contarini, S., Howlett, S. P., Rizzo, C., and De Angelis, B. A., (1991) XPS study on the dispersion of carbon additives in silicon carbide powders. Applied Surface Science, 51(3-4):177-183, doi:10.1016/0169-4332(91)90400-E
[18] Okada, K., Kameshima, Y., and Yasumori, A., (1998) Chemical shifts of silicon X-ray photoelectron spectra by polymerization structures of silicates. Journal of the American Ceramic Society, 81(7):1970-1972,
[19] Gardelle, B., Duquesne, S., Vandereecken, P., Bellayer, S., and Bourbigot, S., (2013) Mode of action of organoclay on the fire performance of intumescent silicone based coating. Progress in Organic Coatings, submitted,

Abstract - The purpose of this Ph.D work is to develop intumescent coatings for the protection of steel against fire in two different scenarios: hydrocarbon and cellulosic fires. The aim of this coating is to ensure the integrity of steel structure exposed to fire since steel loses more than 50% of its load capacity above 550°C. Intumescent coatings expand in case of fire leading to the formation of an insulative barrier limiting the heat transfer from the heat source to the substrate. Most of these coatings are organic based and thus exhibit some limitations. Thus, in this work, hybrid organic-inorganic coatings based on silicone resins were developed. In a first step, it is shown that room temperature vulcanized (RTV) silicone rubber is the silicone matrix exhibiting the best insulative properties in fire scenarios. Expandable graphite is then used as blowing agent to make the silicone swell when exposed to fire. Due to several interactions between silicone and expandable graphite at high temperature, the coating exhibits excellent fire performance. This performance was attributed to the swelling properties, the low thermal conductivity at high temperature and the good cohesion of the developed char. Additional fillers such as calcium carbonate and organoclay are incorporated in the formulation to increase the mechanical properties of the char. Finally, the critical parameters governing the insulative properties of intumescent silicone coatings have been determined. Moreover, it was pointed out that it is possible to develop silicone coatings exhibiting better fire performance than commercial intumescent paint for the protection of steel against fire in both hydrocarbon and cellulosic fire scenarios.

Key words: intumescent coating, silicone, fire protection, hydrocarbon fire, cellulosic fire

Résumé - L'objectif de ce travail de thèse est de développer des revêtements intumescents à base de résines de silicone pour la protection de l'acier en cas d'incendie - de type hydrocarbure et cellulosique. Les revêtements intumescents ont pour fonction d'assurer l'intégrité des structures en acier exposées au feu, ce métal perdant une grande partie de ses propriétés mécaniques au-dessus de 550°C. Les revêtements intumescents classiquement utilisés sont formulés à partir de résines organiques (acrylique, epoxy…) ce qui conduit à certaines limitations. Dans ce travail, des revêtements intumescents hybrides organiques-inorganiques à base de résines de silicone ont donc été développés. Dans un premier temps, il est montré que les résines silicones de types RTV (room temperature vulcanized) présentent les meilleures propriétés de barrière thermique. Par la suite, du graphite expansible a été incorporé en tant qu'agent gonflant à la résine silicone, pour permettre l'expansion du revêtement à haute température. Grâce à des interactions spécifiques entre le silicone et le graphite expansé, le revêtement obtenu présente d'excellentes propriétés de protection thermique. Ces résultats ont été attribués à ses propriétés de gonflement, à sa faible conductivité thermique à haute température et à la bonne cohésion du char développé. Des charges minérales supplémentaires telles que le carbonate de calcium et l'argile organo-modifiée ont ensuite été incorporées dans la formulation afin d'augmenter les propriétés mécaniques du char. Enfin, les paramètres essentiels régissant les propriétés de barrières thermiques des revêtements siliconés ont été mises en évidence. En jouant sur ces paramètres, il est possible de formuler des revêtements présentant de meilleures propriétés que des peintures intumescentes commerciales pour la protection de l'acier au cours d'un incendie de type hydrocarbure ou cellulosique. Cette étude démontre donc la faisabilité du développement de revêtement intumescent à base de silicone pour la protection de l'acier en cas d'incendie.

Mots clés: Résistance au feu, intumescence, silicones, protection contre l'incendie